TOUGHNESS IMPROVEMENT OF EPOXY THERMOSETS BY ADDING DENDRITIC STRUCTURES

Marjorie Yusneiry Flores Guillen

Dipòsit Legal: T. 60-2014

UNIVERSITAT ROVIRA I VIRGILI

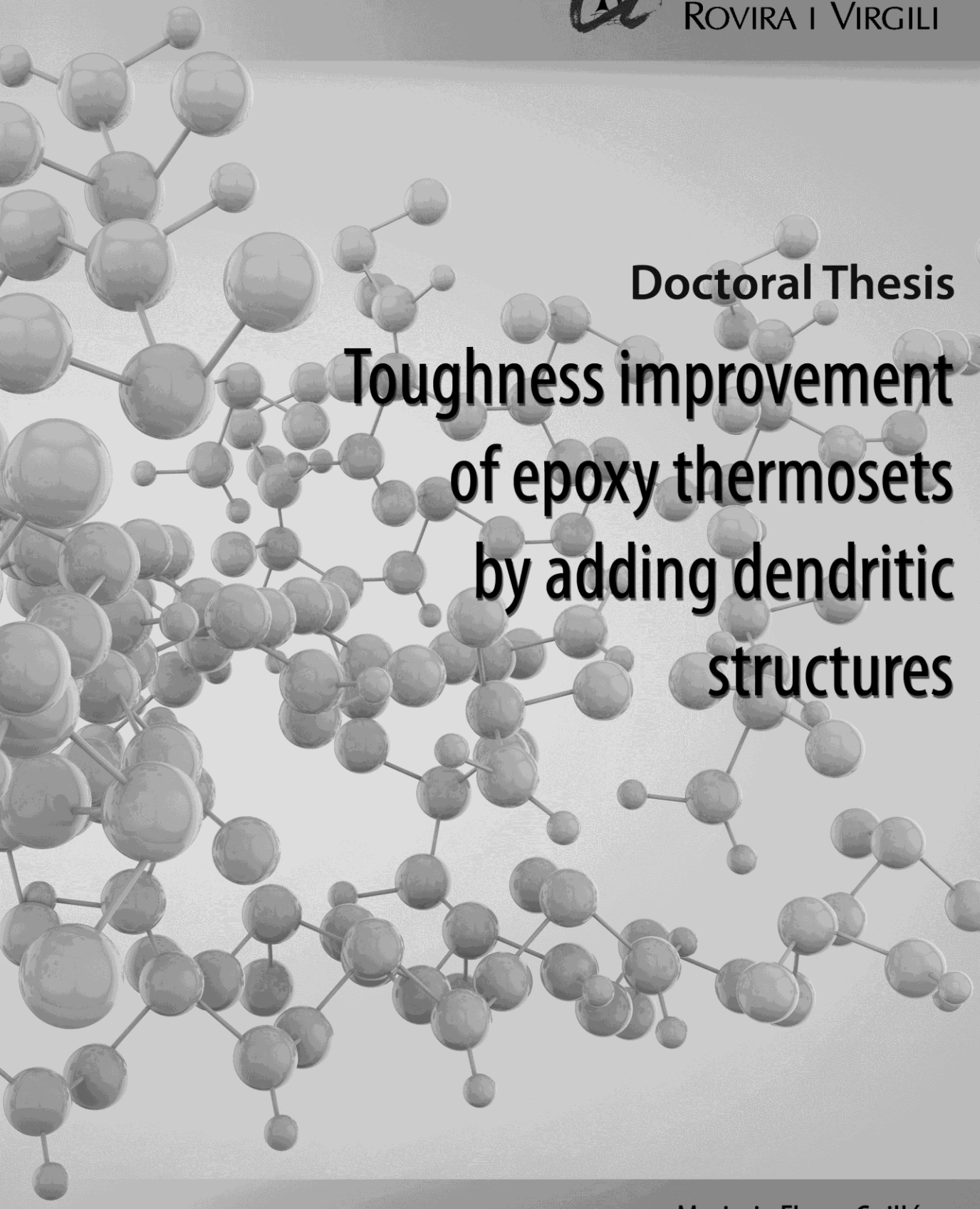

Doctoral Thesis

Toughness improvement of epoxy thermosets by adding dendritic structures

Marjorie Flores Guillén

October 2013

Marjorie Yusneiry Flores Guillén

Toughness improvement of epoxy thermosets by adding dendritic structures

Doctoral Thesis

Supervised by Prof. Àngels Serra i Albet

and Prof. Xavier Ramis Juan

Department of

Analytical Chemistry and Organic Chemistry

UNIVERSITAT ROVIRA I VIRGILI

Tarragona, Spain

2013

DEPARTAMENT DE QUÍMICA ANALÍTICA i QUÍMICA ORGÀNICA
Campus Sescelades
Carrer Marcel·lí Domingo s/n
43007 Tarragona

Professor Àngels Serra i Albet of the Department of Analytical Chemistry and Organic Chemistry at the Universitat Rovira i Virgili and Professor Xavier Ramis Juan of the Department of Heat Engines at ETSEIB, University Politècnica de Catalunya,

CERTIFY:

That the Doctoral Thesis entitled: "Toughness improvement of epoxy thermosets by adding dendritic structures", presented by Marjorie Yusneiry Flores Guillén in order to obtain the Doctor degree, has been carried out under our supervision, at the Department of Analytical Chemistry and Organic Chemistry at the Universitat Rovira i Virgili and at the Department of Heat Engines at ETSEIB, University Politècnica de Catalunya, and all the results reported in this Thesis were obtained from experiments performed by the above mentioned Doctoral student.

Tarragona, June 17th, 2013

Prof. Àngels Serra i Albet

Prof. Xavier Ramis Juan

Agradecimientos

Antes de agradecer a las personas que han colaborado en la realización de este trabajo me gustaría dar gracias a Dios y a La Virgen del Carmen que día a día nos colocan pruebas que serán los pequeños detalles que forjaran nuestro carácter.

Me gustaría expresar mi más sincera gratitud a la *Dra. Àngels Serra*, por haberme dado la oportunidad de realizar este trabajo en su grupo de investigación así como también por la ayuda prestada en la realización de la misma, mostrándose siempre disponible para cualquier discusión, brindándome su apoyo y dando su sabio consejo. Así mismo, quisiera extender estos agradecimientos al *Dr. Xavier Ramis*, por la ayuda prestada, la paciencia y la disposición de ayudarme en todo momento.

Dar gracias, al *Dr. Xavier Fernández Francos*, guía y compañero con el cual tuve largas charlas y discusiones académicas que siempre me enriquecieron un poco más dentro del mundo científico.

Agradecer al *Dr. David Foix*, que desde el primer momento me ofreció su ayuda y conocimientos enseñándome todo lo que él sabía. Horas de discusión, charlas y gratos momentos, buen amigo y compañero que siempre tuvo palabras de aliento.

Al *Dr. Francesc Ferrando* del Departamento de Ingeniería Mecánica de la URV, por la ayuda y colaboración, por siempre estar dispuesto a encontrar soluciones a los problemas que le planteaba.

Al *Dr. Marco Sangermano* por haberme dado la oportunidad de trabajar en su grupo de investigación y recibirme como si fuera una más de su grupo, agradecerle por toda su disposición, ayuda y consejos siempre que se presentaban dificultades. Además, quiero extender este agradecimiento a todas las personas que conocí y con las que compartí durante mi trabajo en el Politecnico de Turín: Ignazio, Sophie, Julia, Florence, Alessandra, Gio a todos gracias por hacerme parte del grupo de trabajo.

Los técnicos del servicio de recursos científicos de la URV: Ramón, Mercè, Mariana, Rita, Lukas y al técnico del departamento de Ingeniería Mecánica, José, a todos ustedes gracias por su ayuda y colaboración. También quiero agradecer a Dunia, Avelina, y Olga, por la ayuda prestada cuando de papeles se trataba.

Agradecer con especial aprecio a *Cristina Mas y Asta Sakalyte*, amigas, compañeras, confidentes gracias a ambas por brindarme su amistad incondicional, por siempre escucharme y tener palabras de ánimos cuando las he necesitado.

A mis compañeros de laboratorio los que aún continúan y los que ya han buscado nuevos horizontes Cristina Acebo, Surya, Adrian, Mireia, Silvana. A los chicos Suspol Maryluz, Camilo, Zeynep, Alev, Rodolfo, Cristina LLuch, Mercè, Marc a todos gracias por los buenos momentos y por hacer los días de trabajo más agradables.

A mis padres *Jesús y Flor,* seres especiales, excelentes ejemplos de vida a seguir. Gracias por siempre creer en mí, apoyos incondicionales, impulsores de mis éxitos, sin ellos este logro probablemente no hubiera sido alcanzado, el camino ha sido duro y he estado lejos de

ustedes pero siempre los he sentido conmigo. A mi hermano Walter por ser parte importante de mi vida, a su manera siempre ha estado ahí para mí.

A las familias *Flores, Guillén y Parra-Arnó*, a todos gracias por todo el cariño y el apoyo brindado.

A mis amigos de siempre Angélica, Luz Mary, Johana, Vanessa, Eveleidy, Deicy, Karina, Yuri, Yusmar, Eloy, a todos ¡gracias! desde la distancia siempre he contado con ellos demostrándome su cariño y apoyo.

A *Paulo, Sandra y Sebastian* familia que me abrió las puertas de su hogar haciéndome sentir como en casa, gracias por el cariño.

Por último a mi compañero de Vida *Enrique Parra,* no encuentro palabras para expresarte todo mi agradecimiento. Has sido mi apoyo constante y amor incondicional mi amigo y compañero inseparable, a ti simplemente gracias.

Finalmente, agradecer a la Universitat Rovira i Virgili y al Ministerio de Ciencia e Innovación por la financiación a través de su programa de ayuda Predoctoral de Formación de Personal Investigador de referencia BES-2009-025226 asociada al proyecto de investigación MAT2008-06284-C03-01 para la realización de este doctorado.

UNIVERSITAT ROVIRA I VIRGILI
TOUGHNESS IMPROVEMENT OF EPOXY THERMOSETS BY ADDING DENDRITIC STRUCTURES
Marjorie Yusneiry Flores Guillen
Dipòsit Legal: T. 60-2014

"Es más importante viajar con esperanza en el corazón que llegar sano y salvo… Debemos celebrar el fracaso de hoy porque es una clara señal de que nuestro viaje de descubrimiento aún no ha terminado. El día que el experimento sea un éxito será el día de su fin. Y no puedo evitar pensar que la tristeza del final es mayor que la alegría del éxito."

Jacqueline Kelly, La Evolucion de Calpurnia Tate.

Table of content

1.1. Historical background to epoxy resins

The term “epoxy resin” is commonly applied to a wide range of materials, both prepolymers, which contain reactive epoxy groups and cured polymers, which are still called epoxy resin although all of the reactive groups may have reacted during the polymerization process.

Historically, the first products which would now be called epoxy resin were synthesized in 1891 [1], but their commercialization did not come until much later following the work of two researchers: Pierre Castan [2] in Switzerland and Sylvan Greenlee in the United States. In fact, Castan discovered the resin forming reaction between the diglycidyl ether of bisphenol-A (DGEBA) and cyclic dicarboxylic anhydrides.

In the late1940s, the research on bisphenol-A based epoxy resins began. In the 1960s, a number of multifunctional epoxy resins were developed for higher temperature applications. In the 1970s, the development of two breakthrough waterborne coating technologies based on epoxy resins helped establish the dominant position of epoxies.

While epoxy resins are known for their excellent chemical resistance, the development and commercialization of epoxy vinyl ester resins in the 1970s offered enhanced resistance properties for hard-to-hold, corrosive chemicals such as acids, bases, and organic solvents. In conjunction with the development of the structural composites industry, epoxy vinyl ester resin composites found applications in demanding environments. Increasing requirements in the composite industries for aerospace and defence applications in the 1980s led to the development of new, high performance multifunctional epoxy resins based on complex amine and phenolic structures.

The development of the electronics and computer industries in the 1980s demanded higher performance epoxy resins. Faster speeds and more densely packed semiconductors required epoxy encapsulants with higher thermal stability, better moisture resistance, and higher device reliability. Significant advances in the manufacturing processes of epoxy resins led to the development of electronic-grade materials with lower ionic and chloride impurities and improved electrical properties.

In the 1990s, radiation-curable epoxy–acrylates and cycloaliphatic epoxies showed tremendous growth in radiation-curable applications. These include important and new uses of epoxy resins such as the photoresists and lithographic inks for the electronics industry. The continuing trend of device miniaturization demanded new, high performance resins. This has led to the development of new epoxies and epoxy hybrid systems having lower dielectric constants, higher glass-transition temperatures, and higher thermal decomposition temperatures.

Significant efforts have been directed toward performance enhancements of epoxy structural composites and some advances have been made in the epoxy-toughening area. Epoxy resins modified with hyperbranched polymers have been studied and are claimed to bring exceptional thermal, chemical, and mechanical improvements. However, commercialization has not yet materialized [3].

1.2. Epoxy resin

The term epoxy or epoxide refers to compounds characterized by the presence of an oxirane or epoxy ring, a three-member ring containing an oxygen atom that is bonded with two carbon atoms as shown in Figure. 1.1.

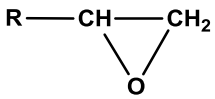

Figure 1.1. The epoxy or oxirane ring structure.

An epoxy resin can be any compound containing more than one of these epoxy groups. Once the resins are cured, the epoxy polymers have a densely crosslinked, thermosetting structure with high cohesive strength and adhesion properties. By strict definition, epoxy resins refer only to uncross-linked monomers or oligomers containing epoxy groups. However, in practice, the term epoxy resins are loosely used to include cured epoxy systems [3].

Epoxy resins display a unique combination of properties such [4]: the low pressure needed for fabrication of products; cure shrinkage is lower than unsaturated polyester resins; good control over the degree of crosslinking which depends on the adequate selection of curing agents; availability of the resin ranging from low viscous liquid to tack-free solids; compatibility with a great number of materials; adhesion; strength, durability; electrical insulation and corrosion and chemical resistance.

Furthermore, epoxy resin systems are capable of curing under almost any conditions of temperature and pressure even under adverse conditions including outdoors. These properties provide great added value in many industries [5].

The applications for epoxy-based materials are extensive and include coatings, adhesives and composite materials, being coatings one of the most important applications. Due to the fact that epoxy resins can be cross-linked with a wide variety of curing agents a huge number of coating materials with excellent adhesion properties, chemical resistance, thermal stability and exceptional mechanic properties can be obtained [6-8]. The addition of toughness modifiers, fillers, adhesion promoters, co-monomers, etc., helps to improve the characteristics of these materials.

Basically, two main types of resins are used for coatings, the glycidylic and the cycloaliphatic epoxy resins [8], having different properties such oxirane ring position and its reactivity, because the availability of epoxy group and the electronic surrounding of the oxirane oxygen [9].

Among glycidylic resins the more used are those derived from bisphenol A (DGEBA) which are obtained by the reaction of the bisphenol A with epichlorohydrin in presence of a strong base media such as NaOH. Depending on the ratio between reactants the resulting molecular weight can be tuned in order to have different resins being possible to obtain liquid, waxy or solid DGEBA resin. In Figure 1.2 the conventional process to obtain DGEBA resins is depicted [8].

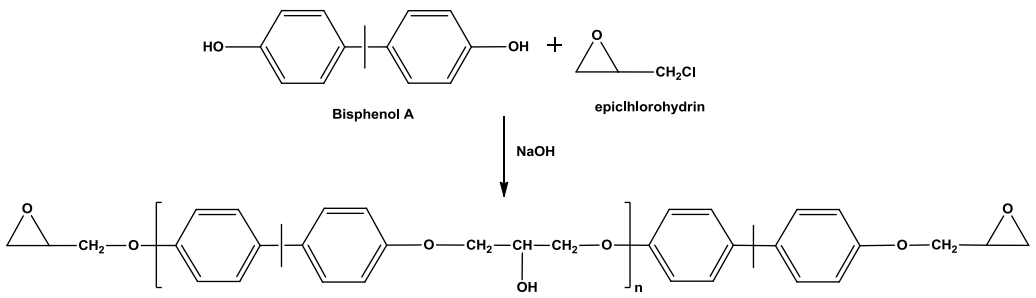

Figure 1.2. Scheme of the synthesis of DGEBA.

In addition to the DGEBA resins, there are several other epoxy resins of commercial significance. Some of the most important are collected in Figure 1.3. Since epoxy resins can be applied in many fields, depending on the final use of the resin (coatings, sealant, adhesives, etc) or the way of carrying out the polymerization, a different monomer may be chosen [5].

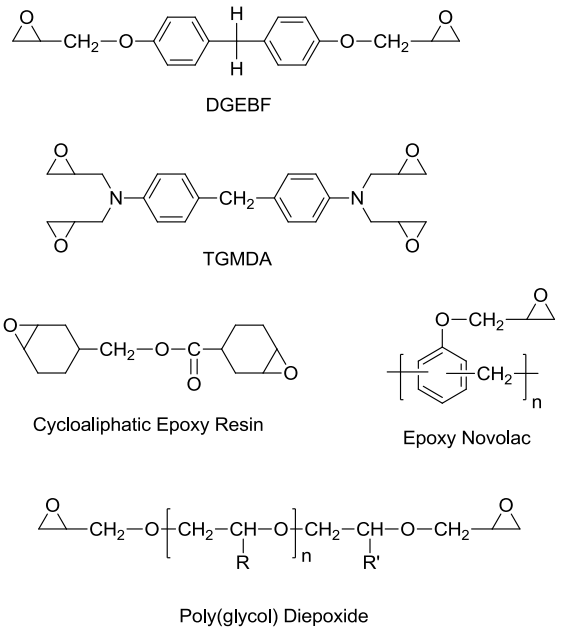

Figure 1.3. Chemical structure of most common epoxy resins.

On the other hand, cycloaliphatic epoxy resins are produced by the epoxidation of cyclic olefinic compounds. This process involves the use of diolefinic or polyolefinic compounds and an oxidizing substance [10].

Cycloaliphatic epoxies offer an interesting combination of properties. These epoxy resins are characterized by the saturated ring in their chemical structure. They are almost water-white and very low-viscosity liquids. They provide excellent electrical properties such as low dissipation factor and good arc-track resistance, good weathering, and high heat distortion temperature [1, 5, 9]. However, cycloaliphatic epoxies have not achieved general importance in adhesive

formulations because of relatively low tensile strength and because they do not cure well at room temperature and the few number of curing agents available One major application for cycloaliphatic epoxies, however, is for adhesives and coatings that can be cationically cured by exposure to UV light.

In general, the epoxy resins are capable of reacting with various curing agents or with themselves (via an initiator) to form solid, crosslinked materials. This transformation is generally referred to as curing or hardening [9]. Depending on the particular details of the epoxy formulation, curing may be accomplished at room temperature, with the application of external heat, or with the application of an external source of energy other than heat such as ultraviolet irradiation (UV) or electron beam (EB) [5].

Besides, the curing agents are selected depending of processes or properties desired. The most commonly used are diamines, polyamides, phenolic resins and anhydrides and to a lesser extent di or polyisocyanates and polymercaptans [11]. The kinetics of the curing process, the glass transition temperature and the properties of the obtained materials depend not only on the type of resin but also on the identity of the curing agent and curing conditions. Moreover, in case of stoichiometric agents, the epoxy-curing agent ratio is also of the main importance.

Apart from stoichiometric curing agents, initiators can be used for homopolymerization of epoxy resins. These initiators can be anionic, such tertiary amines, or cationic, such borontrifluoride monoethyl amine (BF_3-MEA) and rare earth triflates on thermocuring systems and triarylsulfonium or diaryliodonium salts on photocuring processes [10].

1.3. Curing processes

1.3.1. Thermal curing process

The curing of epoxy resins is a fast process which depending on the curing agent used the required curing temperature can vary from room temperature to more than 200 ºC. These systems are known as thermal systems, and two different types can be distinguished: (a) the stoichiometric systems, which require a certain amount of a compound with active functional groups and (b) the catalytic systems where homopolymerization takes place initiated either under anionic or cationic conditions.

1.3.2. Stoichiometric systems

Amines are the most common type of curing agents for epoxy resins. Primary and secondary aliphatic amines, such diethylenetriamine and triethylenetetramine, were the first curing agents used. Both, primary and secondary amines react relatively rapidly with epoxy groups at room temperature in order to form three-dimensional crosslinked structures. Nevertheless, primary and secondary aromatic amines can also be used to cure at elevated temperatures providing more densely crosslinked structures with better mechanical properties, elevated-temperature performance and chemical resistance. Among them 4,4'-diamino diphenylmethane, 1,3-phenylenediamine or 4,4'-diamino diphenylsulfone are some of the most extensively used.

Primary amines are able to react with epoxides as depicted in Figure 1.4. In this case the reaction consists of a polycondensation in two steps between the amines and the epoxide

groups [5]. In the first step of the reaction the primary amine is converted into a secondary β-amino alcohol which further reacts to form a tertiary β-amino hydroxyl group.

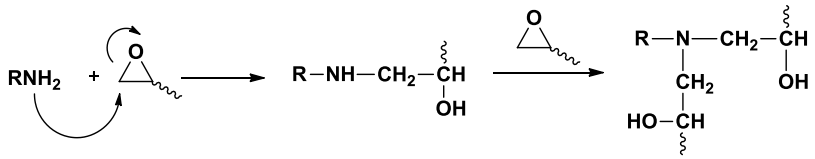

Figure 1.4. Mechanism of reaction between epoxides and primary and secondary amines.

To reach crosslinked networks from diepoxides, primary diamines are required. In this type of curing process, diepoxy resins act with a functionality of two (each epoxide with a functionality of one), whereas primary diamines act with a functionality of four (each active hydrogen with a functionality of one). It should be commented that the global functionality needed to cure epoxy resins should be at least four.

After amines, acid anhydrides are the second most used group of curing agents. Several anhydrides can be used and some of them are illustrated in Figure 1.5. However, these compounds do not react with epoxy resins except in presence of water, alcohol or acids and bases, named accelerators. Among the most used accelerators are the tertiary amines, metallic salts and imidazoles.

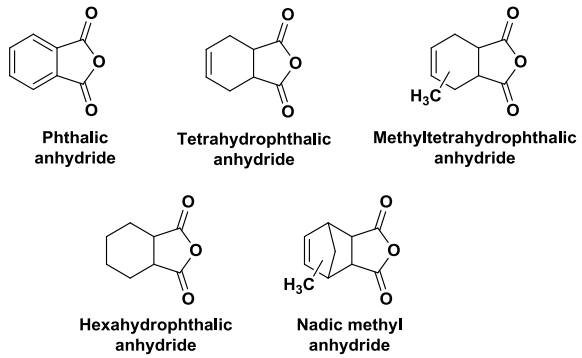

Figure 1.5. Chemical structures of acid anhydrides used as curing agents.

The reaction between anhydrides and epoxy groups is quite complex [12-14], with many side reactions competing for taking place. The most significant reactions are the opening of the anhydride ring with a hydroxyl group forming the monoester followed by the reaction between the nascent carboxylic group and the epoxy in order to provide an ester linkage [5]. The reaction of the anhydride with epoxy resins is illustrated in Figure 1.6.

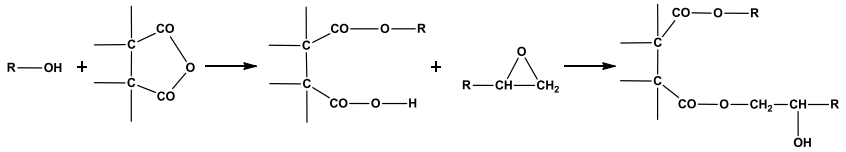

Figure 1.6. Anhydride epoxy reaction.

Finally, either aromatic or aliphatic isocyanates may also be used as curing agents for epoxy resins providing very good curing at low temperature, good flexibility, impact and abrasion resistance as well as good adhesion.

Since the isocyanate reactivity is high, different side-reactions can take place when they react with epoxy resins. One of these reactions is the formation of isocyanurate structures by the trimerization of isocyanate groups which is favoured in the presence of basic catalysts such tertiary amines or triphenylphosphines [15]. The presence of isocyanurate rings enhances the mechanical properties. Another reaction which can take place is the formation of oxazolidones as the result of the cycloaddition of isocyanate groups with epoxides and they are characterized for having high thermal stability (Figure 1.7) [15].

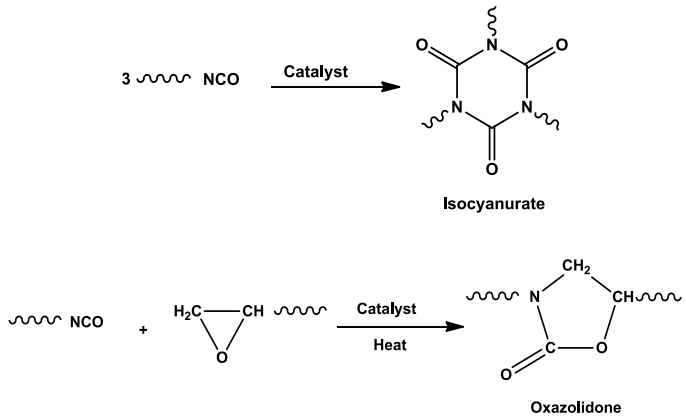

Figure 1.7. Isocyanurate and oxazolidone formation reactions.

1.3.3. Catalytic systems

Another group of curing agents to be used under thermal conditions are initiators. These curing agents, used in catalytic amounts, promote the homopolymerization of epoxides via ring opening mechanism. This ring-opening mechanism is similar in terms of kinetics to polyaddition since presents an initiation step, a propagation and finally a termination. In general, depending on the propagation mechanism there are three types of reactions: anionic, cationic and ionic-coordinative [16].

In all these curing systems the functionality of the epoxide group is two and therefore the global functionality of a diepoxy resin is four. Thus, from a diepoxide crosslinked structures can be obtained by the use of the adequate initiator.

An anionic polymerization takes place when initiators with high nucleophylic character or strong basic characteristics are involved. In the field of epoxy thermosets the most extended anionic initiators are tertiary amines [9], such 4-(N,N-dimethylamine)pyridine (DMAP) or 1-methyl imidazole (MI) [17, 18]. The curing mechanism using tertiary amines is depicted in Figure 1.8. As can be seen, the opening of the epoxide by the nucleophylic attack of the amine forming an alkoxide is the first step. The presence of species which can coordinate with epoxides (such as hydroxyl groups) promotes the initiation step speeding up the reaction. In following steps this

alkoxide propagates the polymerization by opening another epoxide, finally forming the crosslinked network, constituted by polyether structures [19].

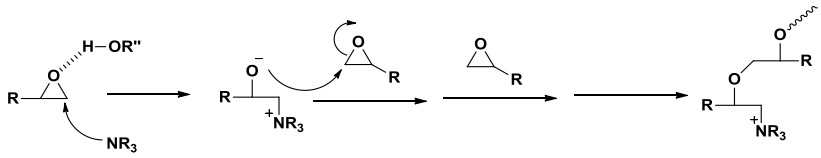

Figure 1.8. Mechanism of polymerization of epoxides catalyzed by amines.

If the initiation step is catalyzed by Brönsted or Lewis acids, the propagation takes place via a cationic mechanism [9]. The most extended Lewis acid is BF_3/amine [20, 21]. In recent years also lanthanide triflates have demonstrated to be good cationic initiators [22-24].

Figure 1.9 shows the mechanism of propagation for cationic polymerization of epoxide, which is more complex than the anionic one. There are two co-existent propagation mechanisms: the activated chain end and the active monomer [25]. In both mechanisms the ring opening is promoted. The activated chain end (ACE) is the reaction between the activated epoxide and another, being the activated epoxide linked to the end of the growing chain. On the other hand, in the activated monomer mechanism (AM) a hydroxyl group is required to open an activated epoxide, and then an intermolecular interchange of protons with one activated epoxide takes place. On that way the monomer is always the activated epoxide.

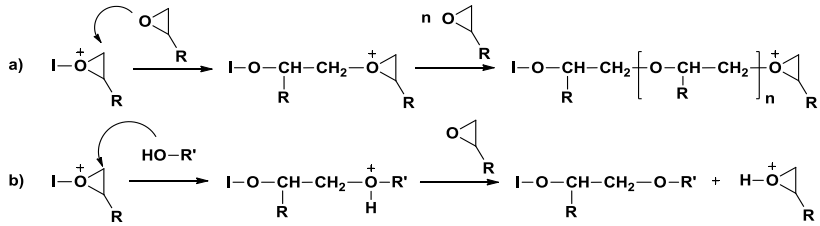

Figure 1.9. Mechanism of propagation of the cationic ring opening polymerization of epoxides: a) activated chain end and b) activated monomer.

1.4. UV curing process

Radiation induced polymerization (photopolymerization) is an efficient method for fast generation of highly cross-linked polymer networks from liquid resin systems. Various types of radiation such as ultraviolet (UV) radiation [26], γ-irradiation [27], and electron beam [28] can be used for initiation of polymerization reactions. Photocuring of resins by means of irradiation in the UV shows several potential advantages compared to thermal curing. In photocuring processes, the chain polymerization occurs through a photochemical event, in which propagating active centres are generated, typically cations. Additionally, since no heating is required, the energy consumption in UV curing is typically lower [29]. Radiation curing is found to be an efficient, fast curing technique [30]. However, radiation curing of resins cannot be used for closed mould processes unlike thermal curing processes. In addition, there are some drawbacks as the high initial economical investment to work under UV conditions required and the transparency of the substrates needed to the radiation.

Usually, the irradiation affects the photoinitiator, which on decomposing generates species able to initiate the curing of the epoxy resin, as schematized in Figure 1.10 [31].

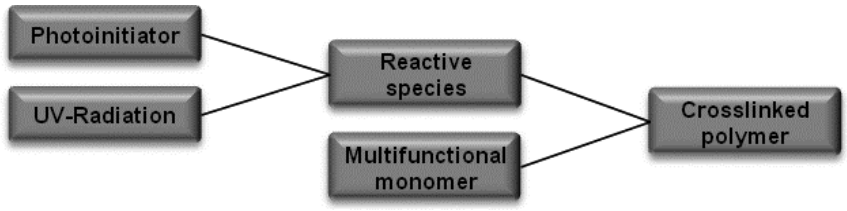

Figure 1.10. Schematic representation of radiation curing processes.

Cationic polymerization is a chain-wise polymerization with the three stages: *initiation*, *propagation*, and *termination*. On irradiation, the photoinitiator is ionized. Active centres are formed by reaction of the resulting positive charges (electrophiles) with monomers. A polymer chain is then generated by the addition of monomers to the active centre. Growth of the chains is terminated most commonly either by reaction of negative and positive charges on the chain or by chain transfer. It should be remembered, that polymerization includes monomer activation and active chain end as competitive propagation steps [25].

Cationic polymerizations proceed long after the irradiation has ceased, in addition the cationic reactions progressively penetrate into parts of the component that are not directly exposed to UV radiation [32], consuming nearly all of the monomer. These processes, known as “dark reaction” and “shadow curing”, are the result of the ability of the acid specie formed by irradiation of the photoinitiator to continue the polymerization [33]. The steric hindrance and vitrification may cause premature ending of the polymerization process. The mobility of cations, which are occluded in the glassy polymer network, can be recovered by heating (thermal postcuring). The reaction will resume until the polymer is fully cured [31].

Resin systems, which can be cured via cationic polymerization, typically consist of two basic components: diepoxy monomers, which form the backbone of the polymer network and photoinitiator, which forms protonic acids on photolysis (as represented in Figure 1.11). Thus, triarylsulfonium and diaryliodonium salts are the most widely used types of cationic photo initiators [34]. Crivello introduced the diaryliodonium salts for the first time as photoinitiators in UV curing [34]. Their properties such as high thermal stability and inactivity towards monomers at room temperature made these salts very attractive for practical applications.

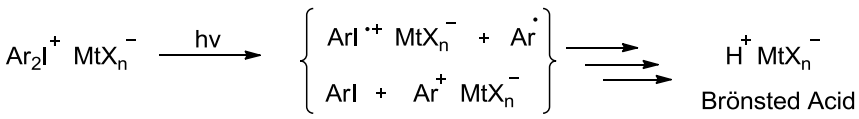

Figure 1.11. Schematic mechanism of formation of Brönsted acids from diaryl iodonium salts.

1.5. Transitions during the formation of polymeric networks

During the formation of the polymer network two main transitions can take place: gelation and vitrification. Gelation is a critical transition defined by the conversion at which the mass-average molar mass becomes infinite and vitrification is characterized by the conversion at

which the polymer begins to show the typical properties of a glass and its glass transition temperature (T_g) is the same than the temperature of curing [11].

Significant transformations of the physical properties occur during gelation and vitrification. The system will be transformed from a liquid into a crosslinked gel during the gelation process. Whilst, when vitrification takes place, the system will be transformed from a liquid or gel (if gelation has already taken place) into a glass. The vitrification is due to the reduction of mobility because the formation of covalent bonds, up to a point where the cooperative movements, which are characteristics of rubbery and liquid states, are no longer possible.

The curing temperature, affects both transitions in different ways. It has been shown that the gel conversion does not depend on the temperature for ideal step-wise polymerizations but can show a small dependence when the reactivity of functional groups or substitution effects vary with temperature. For chain-wise polymerization the temperature can change the ratios of reaction rates of the different elementary steps, which finally affects the conversion at the gelation.

For the vitrification the situation is completely different. Increasing the temperature also increases the possibility of producing cooperative movements of fragments of the thermosetting polymer. Thereby, the conversion at which vitrification takes place increases with the cure temperature. However, in the glassy state relaxation times become longer, making difficult the completion of the polymerization reaction. Moreover, once in the glassy state, small advances in the conversion of functional groups produce a further increase in the already long relaxation times. Thus, the reaction becomes autoretarded and stops. Only with an increase of the temperature in the curing process it is possible to restart the polymerization reaction by devitrification

Gelation and vitrification have very different implications in the curing process. Thus, whereas vitrification is a physical phenomenon with reversible characteristics, gelation is a chemical feature, non-reversible, which implies that the material cannot be processed anymore after reaching this point. Because vitrification can occur at the curing temperature, post-curing of the obtained samples at higher temperature is always highly recommended.

1.6. Epoxy thermosets properties

The main reason for the widespread and growing use of epoxy resin in the industry is not only the good electrical and mechanical properties, but the peculiar processing characteristics. These characteristics are absence of volatile matter on curing and good adhesion to other materials. In addition, epoxy resins also have high modulus and failure strength, low creep, and good performance at elevated temperatures. However, the tight structure of such thermosetting polymers also implies some drawbacks such as relative brittleness, which confers low impact resistance and the shrinkage that undergoes during the curing process, that finally leads to the apparition of stresses and defects in the material, also reducing adhesion to the substrates Thus, new strategies to overcome these drawbacks are needed, but these strategies should not compromise others resins' properties.

1.6.1 Toughness

The major complaint against the use of epoxies is their brittleness, which is due to their high crosslinked character. Several methods have been tried to improve toughness. These

include: inter-dispersed particles, thermoplastic blends, the increasing of the flexibility of the network, the lowering of the crosslink density and/or the decreasing of the functionality of curing agents [35].

However, the incorporation of a second dispersed phase, which allows to dissipate energy in a most efficient way, has been the most promising strategy for lowering the toughness of epoxy thermosets. Among the second phases used, rubbers, thermoplastics, core-shell particles and hard inclusions can be considered. However, the addition of these modifiers usually leads to a reduction of Young modulus and thermomechanical characteristics and to an increased viscosity [35].

In recent years, hyperbranched polymers (HBPs) have been used as toughness modifiers of epoxy thermosets [36, 37]. The incorporation of HBPs into the network structure introduces higher flexibility and increases the impact resistance without affecting others properties, such hardness, modulus or glass transition temperature [38]. These improvements are attributed either to the flexibilizing effect or reduction of the crosslinking densities because the homogeneous incorporation of HBPs or to local heterogeneities within the crosslinked network due to the formation of phase separated particles [39].

Furthermore, the possibility of tune the HBP structure allows obtaining different degrees of compatibility with the resin and homogeneous or phase-separate materials can be prepared in this way [40]. Therefore, different mechanical properties can be expected depending on the HBPs used [41]. Since the interaction between phases is an important factor related with fracture mechanism, the structure of the HBP must be tailored in order to improve interfacial adhesion between phases.

Finally, the most recent strategy for improving toughness has been the preparation of nanostructured materials. The formation of nanostructures in multi-component thermosets can further optimize the interactions between the thermosetting matrix and the modifiers and thus the mechanical properties of materials can be significantly improved. This is known as “toughening by nanostructures” [42]. For instance, it has been reported the modification of epoxy resin blocks of copolymers based on poly(ε-caprolactone) [43]. In fact, by incorporation of a small amount of the copolymer a significant increase in toughness was obtained. Other kind of block copolymers are structures based on star-shaped polymers. These polymers have been used and phase separation in DGEBA matrices with increased T_g have been obtained [44].

Both HBPs and multiarm star polymers are very advantageous as modifiers for epoxy formulations because the lower viscosities, which allow to maintain their good processabilities. This characteristic is in contrast to the observed when thermoplastics or rubbers are used as toughness modifiers [45].

1.6.2. Shrinkage

Shrinkage is another critical point of epoxy thermosets that lead to the appearance of internal stresses and consequently to defects in the materials, such as microvoids, microcracks or warping [46].

It is possible to distinguish between shrinkage in the liquid stage and shrinkage in the gel or solid state, but also it is necessary to distinguish between thermal and chemical shrinkage.

Thermal shrinkage occurs during the thermal curing because after curing the thermosets obtained at high temperature should be cooled down until room temperature and therefore it is hard to avoid it. However, it can be avoided in UV curing since it is performed at room temperature and scarce thermal shrinkage can be originated. On the other hand, chemical shrinkage occurs because the formation of new covalent bonding in the reactions taking place during the curing process. Many approaches have been attended in order to solve the shrinkage issue related with the chemical reactions during the curing process. Among these approaches can be mentioned the introduction of inorganic inert charges such as silica, quartz or mica. Also it is possible to use polymeric charges, as for example PVC or polystyrene. However, the lowering of T_g, reduced toughness, increased viscosity, worsening of the material properties and the loss of transparency make this strategy not adequate for all the applications [1].

Another approach addressed to reduce the shrinkage effect is the use of expanding monomers [47-50]. These monomers lead to zero shrinkage or even positive expansion during polymerization and they are generally bicyclics that opens with the conversion of covalent bonds to van der Waals distances. Expanding monomers can be added to epoxy formulations or obtained *in situ* during curing from the reaction between epoxides and cyclic lactones or carbonates [51, 52].

Recently, new strategies as the incorporation of HBPs as modifiers [53] have been applied with good results in reducing shrinkage without affecting others properties of the resin.

1.7. Dendritic polymers

1.7.1. Topology

Dendritic polymers are tree-like and highly branched macromolecules with three-dimensional architectures [54]. They are polymers with densely branched structure and a large number of end groups. Dendritic molecules are composed of repeating units emanating from a central core or a focal point. When the structure of the molecule is perfectly symmetric around the core, and adopts a spherical three-dimensional morphology, a dendrimer is formed. In contrast, the presence of some imperfections and degrees of branching lower than one will result in a hyperbranched polymer structure (HBPs). A schematic representation of dendrimers and HBPs is presented in Figure 1.12.

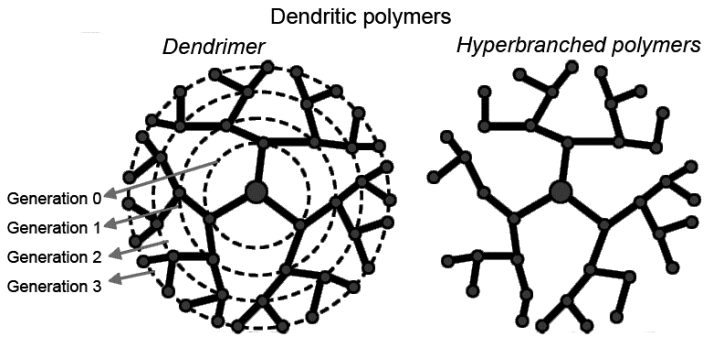

Figure 1.12. Schematic configuration of a tri-functional dendrimer of generation 3 and an example of a hyperbranched polymer molecule.

For a given number of monomers and generation, there is only one dendrimer structure possible but a large number of isomeric hyperbranched structures because of the different ways of distributing the branched and unbranched monomers [55-59].

The structural parameter used to characterize the topology of HBPs is the degree of branching, defined as:

$$DB = \frac{2D}{(2D + L)} \qquad (1)$$

where *D* is the number of fully branched units and *L* is the number of partially reacted units [60]. The value of the degree of branching varies from 0 for linear polymers to 1 for dendrimers, being around 0.5 for HBPs.

The complexity on the dendrimers multi-step synthesis turns them into a very expensive material for industrial applications. Nonetheless, if perfect structures are not needed, HBPs would avoid this major drawback of dendrimers, since HBPs can be synthetized in one single-step reactions and their synthesis can be scaled-up for industrial applications. Companies such as the Perstorp Group (Perstorp, Sweden), DSM Fine Chemicals (Geleen, Netherlands), BASF AG (Ludwigshafen, Germany), and Hyperpolymers GmbH (Freiburg, Germany) already produce commercially available hyperbranched polymers on a large-scale.

Since the polarity of hyperbranched macromolecules can be adjusted by controlled functionalization of the end groups, their compatibility with other compounds can be tailored. The remarkable selectivities and capacities of HBPs in combination with their low melt viscosity, high solubility and thermal stability can be used for the optimization of a number of processes.

1.7.2. History of HBPs

The history of HBPs started in the late 19th century when the formation of a resin from tartaric acid (A_2B_2 monomer) and glycerol (B_3 monomer) was reported. Subsequently, the report of the reaction between phthalic anhydride (latent A_2 monomer) or phthalic acid (A_2 monomer) and glycerol (B_3 monomer) in 1901 was made [61]. Kienle et al. [61-63] found out that the specific viscosity of samples of phthalic anhydride and glycerol was low in comparison with that of other synthetic linear polymers. In 1909, the first commercial synthetic polymers, phenolic resins, were introduced [64]. Just prior to gelation, these polymers are the so called random hyperbranched materials. In 1952, Flory [65] reported that highly branched polymers can be synthesized without gelation by polycondensation of an AB_n monomer ($n \geq 2$) in which A and B functional groups can react one with each other. It was not until 1978 that the first synthesis of branched systems was reported by Vögtle and co-workers [66]. In 1988, the first HBP was finally synthesized in the form of soluble polyphenylene by Kim and Webster [67, 68]. Since then, HBPs have gained considerable attention from both academia and industry due to their unique properties and ease of preparation.

1.7.3. Synthesis and structural characterization of hyperbranched polymers

The tedious step-wise synthetic procedure for dendrimers often results in expensive products with limited availability. On the contrary, HBPs are prepared in one-step procedures,

most common by polycondensation of AB_n monomers [67, 69-71]. If n≥2 and the functionality A will react only with functionalities B of another molecule, the polymerization of AB_n monomers results in highly branched polymers [71].

For example, in terms of AB_2 synthesized HBPs, generally three different units can be observed: lineal (L), dendritic (D) and terminal (T) (Figure 1.13). Moreover, knowing the synthetic mechanism another unit can be observed, the focal or initial group (I) or the core which are the starting points of HBP formation.

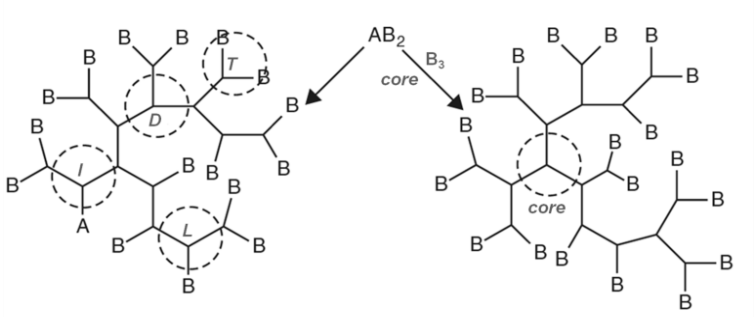

Figura 1.13. Schematic structure of HBPs obtained by AB_2.

Otherwise, the synthetic techniques for HBPs can be divided into two major categories. The first category was described above and it is named as single-monomer methodology (SMM), where hyperbranched macromolecules are synthesized by polymerization of an AB_n, AB* or a latent AB_n monomer. The second category contains examples of the double-monomer methodology (DMM) in which direct polymerization of two types of monomers or a monomer pair generates HBPs [54].

According to the reaction mechanism, the SMM category includes at least four specific approaches [54, 72]: (I) step-growth polycondensation of AB_n monomers method is used to prepare polyphenylenes, polyesters, polyamides and polycarbonates, among others; (II) self-condensing vinyl polymerization (SCVP) of AB* monomers technique is applied to synthesize poly(styrene)s, poly(methacrylate)s or poly(acrylate)s, as examples; (III) multi-branching ring-opening polymerization (SCROP) can be used to obtain for example, polyamines, polyethers and polyesters; and (IV) proton-transfer polymerization (PTP) has been applied to the formation of hyperbranched polysiloxanes or polyesters with epoxy or hydroxyl end groups.

On the other hand, DDM category includes two main subclasses based on the selected monomer pairs and different reaction pathways: (I) "A_2 + B_3" methodology has been applied to synthesize some polymer architectures including polyamides, polycarbonates and polyureas [72]; and (II) couple-monomer methodology (CMM), which is the combination of the basic SMM and "A_2 + B_3" and it is used to prepare many types of HBPs such as poly(sulfone amine)s, poly(ester amine)s, poly(urea urethane)s, etc. [54].

1.7.4. Properties of HBPs

HBPs have special properties which are the key to their industrial applications. One of the most interesting physical properties is their different viscosity characteristics in comparison with their linear analogues [72], which is a consequence of the architecture of the molecules. Hyperbranched macromolecules in solution reach a maximum of intrinsic viscosity as a function of molecular weight as their shape changes from an extended to a more compact globular structure, especially at high molecular weights [58]. Other interesting characteristics of HBPs are their conformation and degree of branching. X-ray and small-angle neutron scattering experiments show that dendrimers have spherical conformations, whilst HBPs have globular structures [73]. The degree of branching is reflected in the flexibility of the branching components. Polymers with a higher degree of branching have lower viscosities [72].

Besides, HBPs have high chemical reactivity and enhanced solubility when compared to their linear analogues. They also exhibit enhanced compatibility with other polymers as has been demonstrated by blending studies [72].

Hyperbranched materials also have outstanding mechanical properties such as modulus, tensile strength and compressive moduli which reflect the compact highly branched structures [72]. The addition of an all-aromatic hyperbranched polyester to a linear Bisphenol A polycarbonate resulted in increased tensile and compressive moduli and decreased strain-to-break and toughness [74].

1.7.5. Applications of HBPs

On the basis of their unique structures and properties and easy synthesis, HBPs are promising materials and have a wide range of potential applications. Thus, it is not hard to imagine the amount of different possible applications [75]. Because of the low cost and well-defined architecture HBPs have increasingly attracted attention in the biomaterials field [54]. Most of the HBPs applications are based on the nature and the large number of functional groups within a molecule [76-79], which allows the tailoring of their thermal, rheological, and solution properties and thus provides a powerful tool to design HBPs for a wide variety of applications. Moreover, modification of the number and type of functional groups on HBPs is essential to control their solubility, compatibility, reactivity, adhesion to various surfaces, self-assembly, chemical recognition, and electrochemical and luminescence properties. Figure 1.14 gives an overview of the investigated applications for HBPs [54, 72].

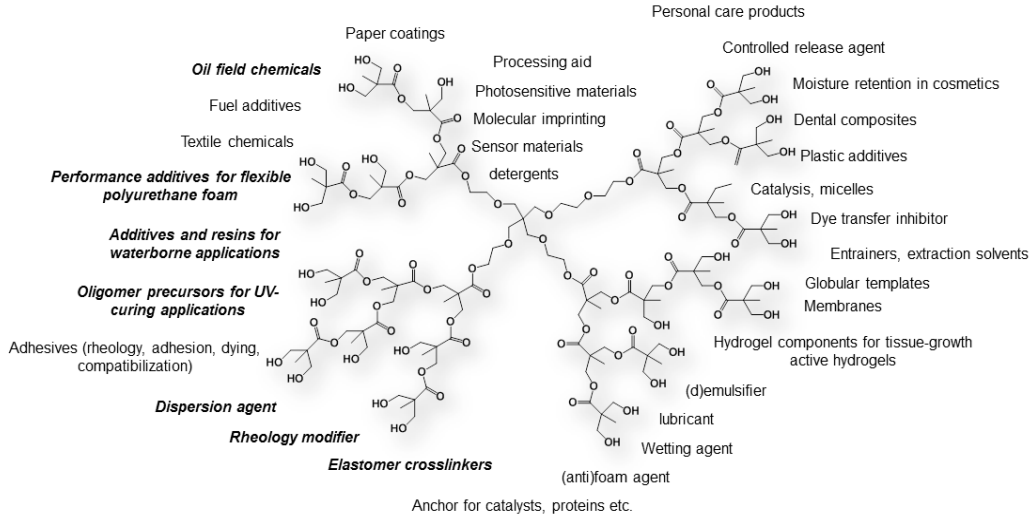

Figure 1.14. Industrial applications of HBPs

On the other hand, owing to those special properties, HBPs have been used as rheology modifiers or blend components [68, 80], toughening agents for thermosets [37, 81] and cross-linking or adhesive agents [82]. Also, HBPs have been used as the base for various coating resins [54], including powder coatings [83], flame retardant coatings [84] and barrier coatings for flexible packaging [85].

1.7.6. Star polymers

Dendritic polymers with a single branch point and all arms exhibiting low degrees of compositional heterogeneity with respect to composition, molecular weight and molecular weight distribution are named star-branched polymers [86]. However, if star polymers have arms with different in either molecular weight or composition are known as heteroarm star-branched polymers or mikto-arm star polymers [87, 88].

Star polymers resemble more closely the hard sphere model, especially when the numbers of arms in the star polymer is high. The hard sphere character of star polymer is directly correlated to the degree of dynamic crosslinking. If the number of arm is high the dynamic crosslinking decreases and it is lower than in linear polymers, causing lower intrinsic viscosity of star polymers as compared to linear polymers of same molecular weight [89]. Basically, star polymers consist of linear polymeric chains radiating from one single branched point, called “core” or central nodule, and which can itself be polymeric. One of the main feature of star polymers is their compact structure and the multiple functionality when comparing with their linear analogues with identical molar masses [90].

1.7.7. Synthesis of star polymers

Star polymers can be obtained mainly by two methods: (I) the core-first approach where the polymerization is conducted from either a well defined initiator with a known number of initiating groups or a less defined multifunctional macromolecule or HBP [91], and (II) arm-first where two approaches are possible: one is where a linear polymer, previously synthesized, with a

reactive chain end is directly attached to a multifunctional core. The other, is the direct copolymerization of a macromonomer with a di or multifunctional monomer in the presence of an initiator [90] (Figure 1.15).

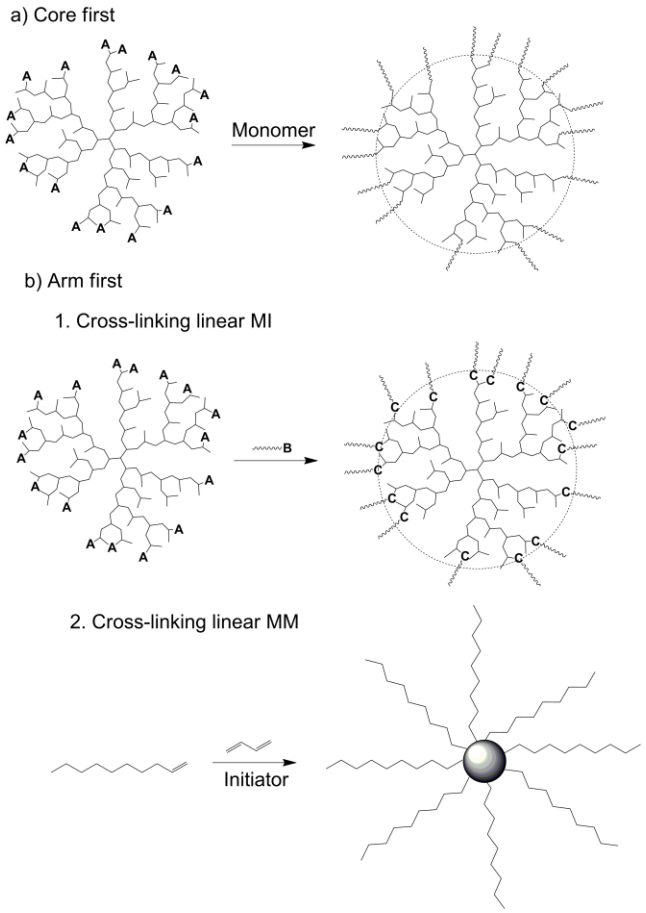

Figure 1.15. Synthesis of star polymers by different methods

The core-first approach allows obtaining well defined star polymers with a known number of arms. High yields are achieved with only simple purification methods. On the other hand, arm-first approach is much more complex since it is difficult to control the arm incorporation being the number of arm unknown in most cases. In addition, the purification procedures are much more complex. Despite of the approach used, obtaining star polymer with more than 30 arms is a tough task since a macroinitiator is needed (i.e. HBP) and the molecular weight of the arms can be only determined by indirect methods. Moreover, if radical polymerization methods are used, the reaction conditions have to be controlled in order to avoid star-star coupling [92]. In most of the core-first syntheses, HBPs can be used as macroinitiator. Some of the most used HBPs are polyesters [93, 94], polyethers [95] and polyethyleneimine [96].

1.7.8. Properties of star polymers

It has been found that not only the chemical structure of the star has influence on the properties of this type of polymers, but also the length of arms.

From the literature is known that the increase of the number of arms usually lowers the melting and crystallization temperatures of the stars [90]. Anyway, star polymers have lower melting and crystallization temperatures, depending on the length and number of arms, than their linear analogs with similar molar masses.

Star polymers with amphiphilic character could change their conformation with solvent polarity because their hydrophilic segments extend in more polar solvents and hydrophobic segments in less polar media. Additionally, the large polyfunctionality in some cases may be advantageous because it leads to a good water solubility and biocompatibility [97].

1.7.9. Applications of star polymers

Nowadays, the exploitation of star biocompatible and biodegradable polymers is receiving considerable attention. Incorporating biocompatible segments on the star copolymers structures are of particular interest to biomedical applications. Polyethylene glycol (PEG) and its conjugates are used in wide areas of small molecule encapsulation, drug formulation, modification of proteins and pharmaceutical molecules, cosmetics, biomedical coatings, and other surface modifications. In conclusion, star polymers have potential applications as components of different types of complexes, hydrogels, networks, ultrathin coatings, and thermoset modifiers, etc. [98-102].

1.8. HBPs and star polymers as modifiers for epoxy thermosets

The lower cost makes HBPs a real commercial alternative when comparing with dendrimers. One of the firsts HBP used as modifier for epoxy resins was a hyperbranched polyester aliphatic based on 2,2-bis(hydroxymethyl)propionic acid (BHMPA) [103], this polymer was commercialized by Perstorp as Boltorn HXX (where XX can be 20, 30 and/or 40) (see structures in Figure 1.16).

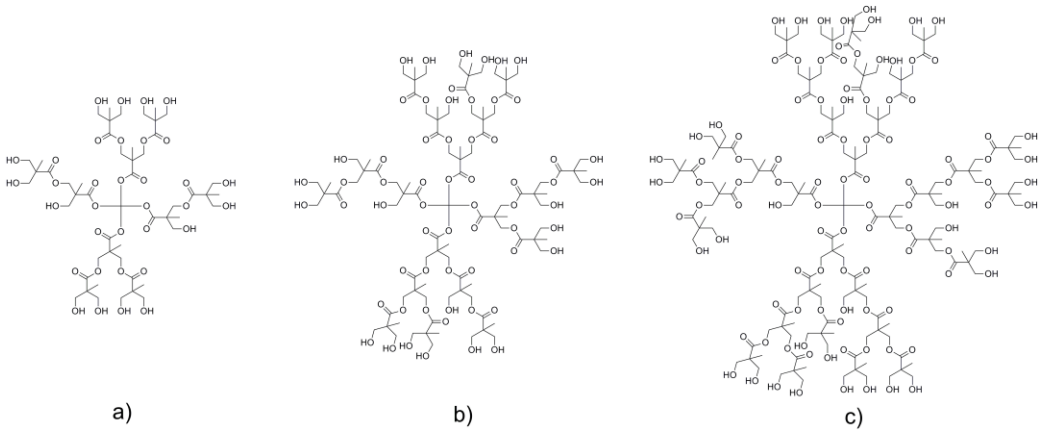

Figure 1.16. Idealized chemical structures of Boltorn (a) H20, (b) H30 and (c) H40.

The reaction to obtain the Boltorn polymers is a polycondensation of AB_2 of the dihydroxymethyl propionic acid (MHMPA). This polymerization starts from an ethoxylated pentaerythritol core (PP50) and is carried out at 140 ºC using p-toluenesulfonic acid as catalyst (see Figure 1.17). The monomer addition is performed in a pseudo-one step, where the monomer is added in stoichiometric amounts in order to obtain the corresponding generation [103].

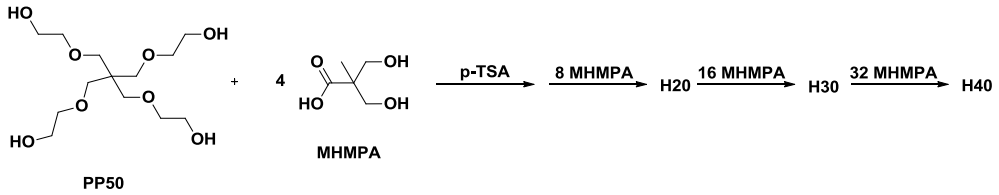

Figure 1.17. Synthesis of Boltorn HX polymers in a pseudo-one pot reaction.

This HBP family has been extensively studied and nowadays their characteristics, such molecular weight, molecular weight dispersity and branching degree, are well described (Table 1.1).

Table 1.1 Characterization of Boltorn HX polymers.

HBP	Molar ratio (PP50:MHMPA)	$\overline{M_w}$ (g/mol)	$\overline{M_n}$ (g/mol)	$Đ_M$	DB (%)
H20	1:12	1860	920	2.01	43.5
H30	1:28	3340	1410	2.38	43.0
H40	1:60	6640	2580	2.57	43.0

Using middle-up approaches, which consist on using a known HBP structure as precursor, several polymers based on Boltorn HXX have been synthesized. For example, Boltorn U3000 and Boltorn W3000, commercialized by Perstop, which comes from the esterification of terminal OH groups with different fatty acids and from the combined esterification with fatty acid and hydrophilic chains, respectively.

Not only commercial products have been described. In fact, there are many reports of different modifications of Boltorn-like polymers. Few examples such the incorporation of methacrylic groups to reduce shrinkage in thermosets [104], trimethyl silyl groups to tune the porosity of coatings [105], and benzoyl groups to study the formation of self-assembly structures induced by π-π stacking [106] have been described. On the field of thermosets, the incorporation of long aliphatic chains at the hydroxylic chain ends leads to phase separation of the HBP within the epoxy matrix, due to the difference in polarity between the core and the shell [107].

Other example of this kind of structures is the hyperbranched polyglycidol. Due to its good properties, hyperbranched polyglycidol polymer has many applications on biomedical and technology fields. What is more, it has a well-defined structure, high content of polar groups, high structural flexibility and high amount of ending reactive groups [108].

On top of that, others structures have been used as modifiers for epoxy resins. For example star polymers based on a core of polyester with polystyrene based arms have been

reported as DGEBA modifier. Nanoestructured materials with high T_g values were obtained, but mechanical properties were not evaluated [44].

Hydroxyl ended HBPs such as polyesters or poly(glycidol) are good starting cores to obtain multiarm-stars. It is known that cyclic esters, i.e. ε-caprolactone (ε-CL) or lactide, can be polymerized using tin catalysts, i.e. tin ethylhexanoate ($Sn(Oct)_2$), in combination with R-OH type initiators. Here, the polymerization starts once the hydroxylic group of the HBP and the catalyst form active species, such RO-Sn-Oct or RO-Sn-OR (Figure 1.18). Then, it is followed by the bonding to the monomer forming $–Sn-O-(CH_2)_5-CO-OR$ species, which by incorporating more monomers can propagate the polymerization.

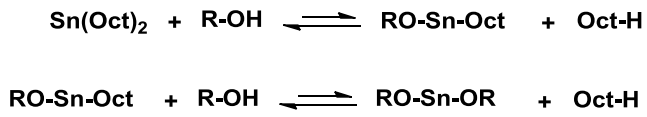

Figure 1.18. RO-Sn-Oct and RO-Sn-OR active species formation through reaction between $Sn(Oct)_2$ and OH groups. (Oct = $C_4H_9CH(C_2H_5)C(O)O^-$).

Then, the insertion of the monomer takes place, with the formation of a new active species which can propagate the polymerization reaction. Finally, by chain-transfer reactions between Oct-H acid and active chain, the catalyst can be regenerated (Figure 1.19).

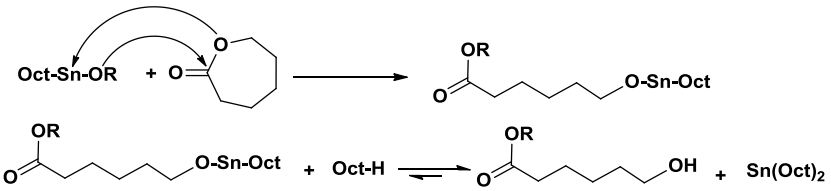

Figure 1.19. ε-CL ring opening polymerization catalyzed by $Sn(Oct)_2$

By means of this polymerization mechanism, some authors have described the preparation of star polymers by cationic ring opening polymerization of lactide or ε-caprolactone from a hyperbranched polymer core with hydroxyl or amine ending groups [109, 110] and their use as epoxy modifier [99-101]. In general, the addition of this kind of polymers to epoxy resins led to homogeneous materials with improvement on the impact strength, without compromising the processability and other properties such as glass transition temperature, Young modulus or hardness.

1.9. Objectives

The main objective of this Doctoral Thesis is to improve the mechanical properties of epoxy thermosets by the incorporation of different modifiers based on dendritic polymers, hyperbranched and multiarm stars. The epoxy formulations have been cured in thermal and photocuring conditions with several curing agents.

This general objective is achieved through a series of specific objectives:

- To study the use of isocyanates as curing agents of epoxy resins in the presence of a tertiary amine and the use of lanthanide triflates as new catalysts on the curing of epoxy-isocyanate based thermosets.

- To study the use of commercial hyperbranched polymer Boltorn H30, with different degree of modification with vinylic or epoxy terminated aliphatic moieties as chain ends, as toughness additives of diglycidyl ether resins cured with diisocyanates.

- To study the effect of the degree of 10-undecenoyl modification of a Boltorn H30 on the curing kinetics, thermal mechanical properties, toughness, and morphology of the thermosets obtained by curing with anhydride/amine.

- To synthesize new hyperbranched poly(glycidol)s with different degrees of modification with 10-undecenoyl groups as chain ends and use them as toughness modifiers of cycloaliphatic epoxy thermosets cured by ytterbium triflate.

- To prepare multiarm stars from Boltorn H20, H30 and H40 cores and poly(ε-caprolactone) arms and use them in the modification of thermal and photocured cycloaliphatic epoxy resins.

- To develop a new two-stage photoinitiated-thermal dual curing system based on thiol-ene and epoxy homopolymerization, using mixtures of an allyl terminated aromatic-aliphatic hyperbranched polyester, a cycloaliphatic epoxy resin and a trithiol compound and the characterization of the thermosets obtained.

1.10. References

[1] H. Lee and K. Neville, *Handbook of Epoxy Resins*, McGraw-Hill, New York, 1982.

[2] P. Castan, *US Pat.,* US2324483, 1943.

[3] H. Q. Pham and M. J. Marks, in *Ullmann's Encyclopedia of Industrial Chemistry*, Wiley-VCH Verlag GmbH & Co. KGaA, 2000.

[4] D. Ratna, *Handbook of Thermoset Resins*. Smithers Rapra Technology, London, 2009.

[5] E. M. Petrie, *Epoxy Adhesive Formulations*, McGraw-Hill, New York, 2006.

[6] S. Wu and M. D. Soucek, *Polymer*, 1998, **39**, 5747-5759.

[7] M. D. Soucek, O. L. Abu-Shanab, C. D. Anderson and S. Wu, *Macromolecular Chemistry and Physics*, 1998, **199**, 1035-1042.

[8] B. Ellis, *Chemistry and Technology of Epoxy Resins*, Blackie Academic & Professional, London, 1993.

[9] C. May, *Epoxy Resins: Chemistry and Technology*, Marcel Dekker, New York, 1988.

[10] J. J. Stevens, in *Epoxy Resin Technology*, ed. P. F. Bruins, Interscience Publishers, New York, 1968, ch. 2.

[11] H. Sautereau. J-P. Pascault, J. Verdu, R.J.Williams, *Thermosetting Polymers*, ed. Marcel Dekker, New York, 2002.

[12] M. Morell, X. Ramis, F. Ferrando, Y. Yu and A. Serra, *Polymer*, 2009, **50**, 5374-5383.

[13] D. Foix, Y. Yu, A. Serra, X. Ramis and J. M. Salla, *European Polymer Journal*, 2009, **45**, 1454-1466.

[14] X. Fernández-Francos, A. Rybak, R. Sekula, X. Ramis and A. Serra, *Polymer International*, 2012, **61**, 1710-1725.

[15] P. I. Kordomenos and J. E. Kresta, *Macromolecules*, 1981, **14**, 1434-1437.

[16] D. J. Brunelle, *Ring-Opening Polymerization: Mechanism, Catalysts, Structure and Utility*, Hanser Publishers, Munich, 1993.

[17] F. Ricciardi, W. A. Romanchick and M. M. Joullié, *Journal of Polymer Science: Polymer Chemistry Edition*, 1983, **21**, 1475-1490.

[18] I. E. Dell'Erba and R. J. J. Williams, *Polymer Engineering & Science*, 2006, **46**, 351-359.

[19] B. A. Rozenberg, in *Epoxy Resins and Composites II*, ed. K. Dušek, Springer, Berlin, 1986, vol. 75, ch. 4, pp. 113-165.

[20] M. Ghaemy and H. Khandani, *European Polymer Journal*, 1998, **34**, 477-486.

[21] M. Tackie and G. C. Martin, *Journal of Applied Polymer Science*, 1993, **48**, 793-808.

[22] P. Castell, M. Galià, A. Serra, J. M. Salla and X. Ramis, *Polymer*, 2000, **41**, 8465-8474.

[23] K. N. Delfrey, *Rare Earths: Research and Applications*, Nova Science Publishers, New York, 2008.

[24] C. Mas, A. Serra, A. Mantecón, J. M. Salla and X. Ramis, *Macromolecular Chemistry and Physics*, 2001, **202**, 2554-2564.

[25] P. Kubisa and S. Penczek, *Progress in Polymer Science*, 1999, **24**, 1409-1437.

[26] A. Endruweit, M. S. Johnson and A. C. Long, *Polymer Composites*, 2006, **27**, 119-128.

[27] A. Singh, *Nuclear Instruments and Methods in Physics Research Section B: Beam Interactions with Materials and Atoms*, 2001, **185**, 50-54.

[28] J. Raghavan and M. R. Baillie, *Polymer Composites*, 2000, **21**, 619-629.

[29] J. P. Fouassier and J. F. Rabek, *Radiation Curing in Polymer Science and Technology*, Elsevier, London, 1993.

[30] V. Narayanan and A. B. Scranton, *Trends in Polymer Science*, 1997, **5**, 415-419.

[31] C. Decker, *Pigment & Resin Technology*, 2001, **30**, 278-286.

[32] F. Boey, S. K. Rath, A. K. Ng and M. J. M. Abadie, *Journal of Applied Polymer Science*, 2002, **86**, 518-525.

[33] S. P. Pappas, *Radiation Curing Science and Technology*, Plenum Press, New York, 1992.

[34] J. V. Crivello, *Journal of Polymer Science Part A: Polymer Chemistry*, 1999, **37**, 4241-4254.

[35] R. Bagheri, B. T. Marouf and R. A. Pearson, *Polymer Reviews*, 2009, **49**, 201 - 225.

[36] D. Ratna, R. Varley and G. P. Simon, *Journal of Applied Polymer Science*, 2003, **89**, 2339-2345.

[37] L. Boogh, B. Pettersson and J.-A. E. Månson, *Polymer*, 1999, **40**, 2249-2261.

[38] J.-F. Fu, L.-Y. Shi, S. Yuan, Q.-D. Zhong, D.-S. Zhang, Y. Chen and J. Wu, *Polymers for Advanced Technologies*, 2008, **19**, 1597-1607.

[39] J. Karger-Kocsis, J. Fröhlich, O. Gryshchuk, H. Kautz, H. Frey and R. Mülhaupt, *Polymer*, 2004, **45**, 1185-1195.

[40] R. Mezzenga, C. J. G. Plummer, L. Boogh and J. A. E. Månson, *Polymer*, 2001, **42**, 305-317.

[41] R. Mezzenga and J. A. E. Manson, *Journal of Materials Science*, 2001, **36**, 4883-4891.

[42] L. Ruiz-Pérez, G. J. Royston, J. P. A. Fairclough and A. J. Ryan, *Polymer*, 2008, **49**, 4475-4488.

[43] L. Könczöl, W. Döll, U. Buchholz and R. Mülhaupt, *Journal of Applied Polymer Science*, 1994, **54**, 815-826.

[44] Y. Meng, X.-H. Zhang, B.-Y. Du, B.-X. Zhou, X. Zhou and G.-R. Qi, *Polymer*, 2011, **52**, 391-399.

[45] M. Morell, X. Ramis, F. Ferrando and À. Serra, *Polymer*, 2011, **52**, 4694-4702.

[46] H. Davies, *Proceedings of the IEE - Part B: Electronic and Communication Engineering*, 1962, **109**, 259-265.

[47] R. K. Sadhir and R. M. Luck, *Expanding Monomers: Synthesis, Characterization and Applications*, CRC Press, Boca Raton, 1992.

[48] R. F. Brady and F. E. Simon, *Journal of Polymer Science Part A: Polymer Chemistry*, 1987, **25**, 231-239.

[49] H. Nishida, F. Sanda, T. Endo, T. Nakahara, T. Ogata and K. Kusumoto, *Macromolecular Chemistry and Physics*, 1999, **200**, 745-750.

[50] T. Hino and T. Endo, *Macromolecules*, 2003, **36**, 5902-5904.

[51] C. Mas, X. Ramis, J. M. Salla, A. Mantecón and A. Serra, *Journal of Polymer Science Part A: Polymer Chemistry*, 2003, **41**, 2794-2808.

[52] R. Cervellera, X. Ramis, J. M. Salla, A. Mantecón and A. Serra, *Journal of Applied Polymer Science*, 2007, **103**, 2875-2884.

[53] X. Fernández-Francos, J. M. Salla, A. Cadenato, J. M. Morancho, A. Serra, A. Mantecón and X. Ramis, *Journal of Applied Polymer Science*, 2009, **111**, 2822-2929.

[54] C. Gao and D. Yan, *Progress in Polymer Science*, 2004, **29**, 183-275.

[55] G. K. Dalakoglou, K. Karatasos, S. V. Lyulin and A. V. Lyulin, *The Journal of Chemical Physics*, 2008, **129**, 034901-034912.

[56] D. Konkolewicz, R. G. Gilbert and A. Gray-Weale, *Physical Review Letters*, 2007, **98**, 238301.

[57] D. Konkolewicz, O. Thorn-Seshold and A. Gray-Weale, *The Journal of Chemical Physics*, 2008, **129**, 054901-054913.

[58] A. V. Lyulin, D. B. Adolf and G. R. Davies, *Macromolecules*, 2001, **34**, 3783-3789.

[59] P. F. Sheridan, D. B. Adolf, A. V. Lyulin, I. Neelov and G. R. Davies, *The Journal of Chemical Physics*, 2002, **117**, 7802-7812.

[60] D. Hölter, A. Burgath and H. Frey, *Acta Polymerica*, 1997, **48**, 30-35.

[61] R. H. Kienle and A. G. Hovey, *Journal of the American Chemical Society*, 1929, **51**, 509-519.

[62] R. H. Kienle, P. A. v. d. Meulen and F. E. Petke, *Journal of the American Chemical Society*, 1939, **61**, 2258-2268.

[63] R. H. Kienle, P. A. v. d. Meulen and F. E. Petke, *Journal of the American Chemical Society*, 1939, **61**, 2268-2271.

[64] G. G. Odian, *Principles of Polymerization*, Wiley-Interscience, Hoboken, 2004.

[65] P. J. Flory, *Journal of the American Chemical Society*, 1952, **74**, 2718-2723.

[66] E. Buhleier, W. Wehner and F. Vögtle, *Synthesis*, 1978, **1978**, 155-158.

[67] Y. H. Kim and O. W. Webster, *Journal of the American Chemical Society*, 1990, **112**, 4592-4593.

[68] Y. H. Kim and O. W. Webster, *Macromolecules*, 1992, **25**, 5561-5572.

[69] W. H. Stockmayer, *The Journal of Chemical Physics*, 1943, **11**, 45-55.

[70] W. H. Stockmayer, *The Journal of Chemical Physics*, 1944, **12**, 125-131.

[71] P. J. Flory, *Principles of Polymer Chemistry*, New York, 1953.

[72] C. R. Yates and W. Hayes, *European Polymer Journal*, 2004, **40**, 1257-1281.

[73] T. J. Prosa, B. J. Bauer, E. J. Amis, D. A. Tomalia and R. Scherrenberg, *Journal of Polymer Science Part B: Polymer Physics*, 1997, **35**, 2913-2924.

[74] D. J. Massa, K. A. Shriner, S. R. Turner and B. I. Voit, *Macromolecules*, 1995, **28**, 3214-3220.

[75] B. Voit, *Journal of Polymer Science Part A: Polymer Chemistry*, 2005, **43**, 2679-2699.

[76] R. M. Crooks, *ChemPhysChem*, 2001, **2**, 644-654.

[77] P. Ghosh and R. M. Crooks, *Journal of the American Chemical Society*, 1999, **121**, 8395-8396.

[78] P. Ghosh, M. L. Amirpour, W. M. Lackowski, M. V. Pishko and R. M. Crooks, *Angewandte Chemie International Edition*, 1999, **38**, 1592-1595.

[79] P. Ghosh, W. M. Lackowski and R. M. Crooks, *Macromolecules*, 2001, **34**, 1230-1236.

[80] D. Ratna and G. P. Simon, *Polymer*, 2001, **42**, 8833-8839.

[81] R. Mezzenga, L. Boogh and J.-A. E. Månson, *Composites Science and Technology*, 2001, **61**, 787-795.

[82] J. H. Oh, J. Jang and S.-H. Lee, *Polymer*, 2001, **42**, 8339-8347.

[83] M. Johansson, E. Malmström, A. Joansson and A. Hult, *Journal of Coatings Technology*, 2000, **72**, 49-54.

[84] S.-W. Zhu and W.-F. Shi, *Polymer Degradation and Stability*, 2002, **75**, 543-547.

[85] J. Lange, E. Stenroos, M. Johansson and E. Malmström, *Polymer*, 2001, **42**, 7403-7410.

[86] M. K. Mishra and S. Kobayashi, *Star and Hyperbranched Polymers*, Marcel Dekker, Inc., New York, 1999.

[87] M. Pitsikalis, S. Pispas, J. Mays and N. Hadjichristidis, in *Blockcopolymers - Polyelectrolytes - Biodegradation*, eds. V. Bellon-Maurel, A. Calmon-Decriaud, V. Chandrasekhar, N. Hadjichristidis, J. W. Mays, S. Pispas, M. Pitsikalis and F. Silvestre, Springer Berlin, 1998, vol. 135, ch. 1, pp. 1-137.

[88] R. P. Quirk, T. Yoo and B. Lee, *Journal of Macromolecular Science, Part A*, 1994, **31**, 911-926.

[89] H. A. M. Aert, M. H. P. Genderen and E. W. Meijer, *Polymer Bulletin*, 1996, **37**, 273-280.

[90] N. H. Aloorkar, A. S. Kulkarni, R. A. Patil and D. J. Ingale, *International Journal of Pharmaceutical Sciences and Nanotechnology*, 2012, **5**, 1675-1684.

[91] S. Maier, A. Sunder, H. Frey and R. Mülhaupt, *Macromolecular Rapid Communications*, 2000, **21**, 226-230.

[92] H. Gao and K. Matyjaszewski, *Progress in Polymer Science*, 2009, **34**, 317-350.

[93] W. Xia, G. Jiang and W. Chen, *Journal of Applied Polymer Science*, 2008, **109**, 2089-2094.

[94] C. Xia, X. Ding, Y. Sun, H. Liu and Y. Li, *Journal of Polymer Science Part A: Polymer Chemistry*, 2010, **48**, 4013-4019.

[95] X. Zhang, J. Cheng, Q. Wang, Z. Zhong and R. Zhuo, *Macromolecules*, 2010, **43**, 6671-6677.

[96] M. Adeli and R. Haag, *Journal of Polymer Science Part A: Polymer Chemistry*, 2006, **44**, 5740-5749.

[97] G. Lapienis, *Progress in Polymer Science*, 2009, **34**, 852-892.

[98] S. Zalipsky and J. M. Harris, in *Poly(ethylene glycol)*, American Chemical Society, San Francisco, 1997, vol. 680, ch. 1, pp. 1-13.

[99] J. Miao, G. Xu, L. Zhu, L. Tian, K. E. Uhrich, C. A. Avila-Orta, B. S. Hsiao and M. Utz, *Macromolecules*, 2005, **38**, 7074-7082.

[100] K. E. Steege, J. Wang, K. E. Uhrich and E. W. Castner, *Macromolecules*, 2007, **40**, 3739-3748.

[101] M. Morell, D. Foix, A. Lederer, X. Ramis, B. Voit and A. Serra, *Journal of Polymer Science Part A-Polymer Chemistry*, 2011, **49**, 4639-4649.

[102] M. Morell, A. Lederer, X. Ramis, B. Voit and A. Serra, *Journal of Polymer Science Part A: Polymer Chemistry*, 2011, **49**, 2395-2406.

[103] A. Hult, M. Johansson and E. Malmström, in *Branched Polymers II*, ed. J. Roovers, Springer Berlin Heidelberg, 1999, vol. 143, ch. 1, pp. 1-34.

[104] J. E. Klee, C. Schneider, D. Hölter, A. Burgath, H. Frey and R. Mülhaupt, *Polymers for Advanced Technologies*, 2001, **12**, 346-354.

[105] C. J. G. Plummer, L. Garamszegi, T. Q. Nguyen, M. Rodlert and J. A. E. Månson, *Journal of Materials Science*, 2002, **37**, 4819-4829.

[106] G. Jiang, L. Wang, H. Yu, C. Chen, X. Dong, T. Chen and Q. Yang, *Polymer*, 2006, **47**, 12-17.

[107] X. Fernández-Francos, D. Foix, À. Serra, J. M. Salla and X. Ramis, *Reactive and Functional Polymers*, 2010, 70, 798-806.

[108] D. Wilms, S.-E. Stiriba and H. Frey, *Accounts of Chemical Research*, 2009, 43, 129-141.

[109] M. Trollsås, C. J. Hawker, J. F. Remenar, J. L. Hedrick, M. Johansson, H. Ihre and A. Hult, *Journal of Polymer Science Part A: Polymer Chemistry*, 1998, 36, 2793-2798.

[110] P.-F. Cao, R. Xiang, X.-Y. Liu, C.-X. Zhang, F. Cheng and Y. Chen, *Journal of Polymer Science Part A: Polymer Chemistry,* 2009, 47, 5184-5193.

2.1. Differential scanning calorimetry (DSC)

Differential scanning calorimetry (DSC) is the most popular thermal analysis technique. It is a technique in which the heat flow rate difference into a substance and a reference is measured as a function of temperature, while the sample is subjected to a controlled temperature program. Among the applications of DSC must be mentioned the easy and fast determination of the glass transition temperature the heat capacity jump at the glass transition, melting and crystallization temperatures, heat of fusion, heat of reactions, very fast purity determination, fast heat capacity measurements, characterization of thermosets, and measurements of liquid crystal transitions [1].

For our propose a Mettler DSC821e, equipped with a robotic arm TSO801RO and able to go lower than room temperature by using liquid nitrogen cooling system, was used to perform DSC analyses and was calibrated using an indium standard (heat flow calibration) and an indium-lead-zinc standard (temperature calibration). Samples of 5 to 10 mg of weight were placed in covered aluminum pans. Figure 2.1 shows the calorimeters used.

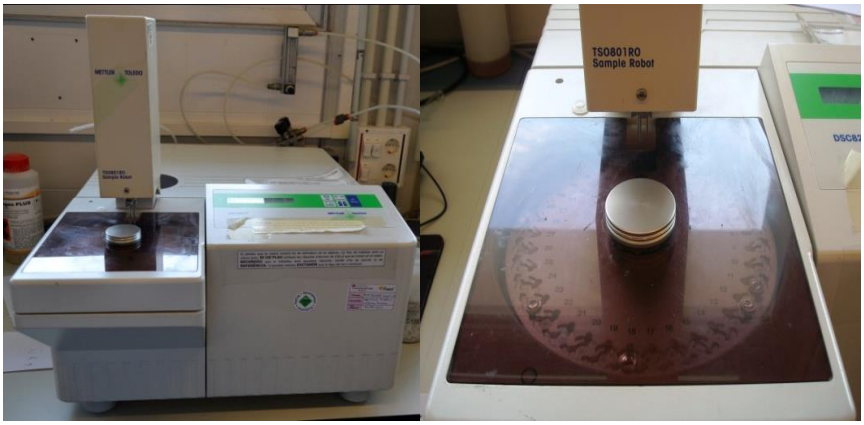

Figure 2.1. Pictures of the calorimeters and the robot used to study thermal curing systems.

2.1.1. Curing kinetics

Cure kinetics is the mathematical relationship between time, temperature, and conversion. In a kinetic study using DSC the heat released during the reaction is assumed to be proportional to the conversion degree [1]. Additionally, the curing rate (*dx/dt*) is directly related to this released heat (*dH/dt*). When the reaction is completed, the integral related to the signal obtained yields the total released heat ΔH_{total}. Reaction rate and conversion degree can be calculated with the following expression:

$$\frac{dx}{dt} = \frac{dH/dt}{\Delta H_{total}} = \frac{dh/dt}{\Delta h_{total}} \qquad (2.1)$$

$$x = \frac{\Delta H_t}{\Delta H_{total}} = \frac{\Delta h_t}{\Delta h_{total}} \qquad (2.2)$$

where *dh/dt* and Δh_{total} are the heat releasing rate and the total heat released normalized in respect to the sample size, ΔH_t is the heat released up to a time *t*, and Δh_t is the heat released normalized in respect to the sample size. It can be expressed in J/g or in kJ/ee. Finally *x* is the degree of curing, and can also be expressed as α.

The kinetics of a system can be studied in either isothermal or dynamic conditions. The dynamic experiments were preferred since they present some advantages when compared with isothermal experiments, being the most important fact using isothermal conditions the losing of information at the beginning of the curing process and, in another hand, the curing is not always completed [1].

2.1.2. Glass transition temperature (Tg)

The glass transition temperature is usually reported as the temperature at the half-height of the heat capacity increase ($\frac{1}{2}\Delta C_p$ see Figure. 2.2). *Tg* can also be taken as the inflexion point, which is slightly different and corresponds to the peak on the derivative of the heat flow or heat capacity against temperature.

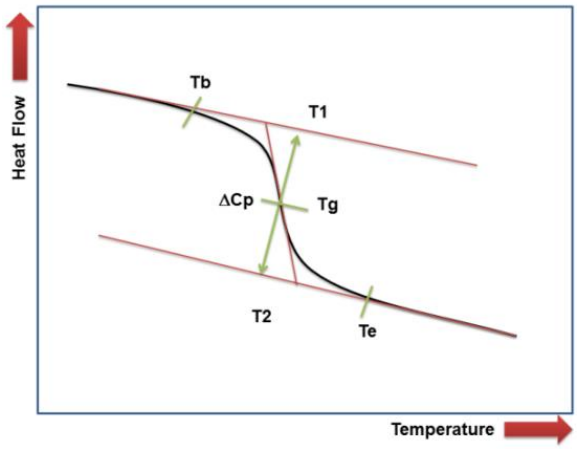

Figure 2.2. Determination of glass transition temperature in a heating experiment from an idealized DSC curve (endotherm down). Tb: beginning of deviation of DSC curve from linearity; T1: extrapolated onset temperature of *Tg*; *Tg*: glass transition temperature; T2: extrapolated end temperature of glass transition; Te: end temperature of *Tg* where *Cp*'s dependence becomes linear again.

In order to determine *Tg* values of cured materials as well as the synthetized HBPs, DSC at 10 ºC/min were performed.

2.2. Thermogravimetry (TGA)

Thermogravimetric analysis (TGA) is a technique where the mass of a polymer is measured as a function of temperature or time while the sample is subjected to a controlled temperature program in a controlled atmosphere [2]. The heart of the TGA is the thermobalance, which is capable of measuring the sample mass as a function of temperature and time while a purge gas flowing through the balance creates an atmosphere that can be inert, oxidizing or reducing. The moisture content of the purge gas can vary from dry to saturated [3].

For thermal degradation analysis of cured samples and synthesized hyperbranched polymers a thermobalance Mettler TGA/SDTA 851e (Figure 2.3) was used. Under dynamic conditions the degradation of samples at 10 ºC/min from 30 to 800 ºC under nitrogen or air flow was carried out. From TGA the initial degradation temperature or mass lost (normally between 2 and 5 %), which indicates the limit of material stability can be obtained. Also, the temperature of the maximum degradation rate and the char yield can be obtained.

Figure 2.3. Thermobalance used for the thermal stability evaluation.

2.3. Thermal mechanical analysis (TMA)

Thermomechanical analysis (TMA) measures changes in sample length or volume as a function of temperature or time under load at atmospheric pressure. The most important TMA measurements include determination of the coefficient of linear thermal expansion (CTE) and the glass transition temperature, T_g. However, several other measurements can be made by applying special modes and various attachments. These include stress relaxation, creep tensile properties of films and fibers, flexural properties and volume dilatometry [4].

Two thermomechanical analyzers, a Mettler TMA/SDTA840 and a Mettler TMA40 (figure 2.4), were used to evaluate the thermal expansion coefficient (CTE) of cured samples, conversion at the gel point and determination of the shrinkage percentage before and after gelation.

Figure 2.4. TMA apparatus used to perform thermomechanical analysis and magnification of the analyzing probe.

For the determination of CTEs, prismatic rectangular samples (ca. 5 x 5 x 2.5 mm^3) were sandwiched between two silica discs and heated at 10ºC/min from 30 up to 150ºC for a first scan, followed by a second scan at 5ºC/min up to 180ºC. Constant force of 0.02 N was applied on the samples. The coefficients of thermal expansion α_g and, α_r, below and above the T_g respectively (Figure 2.5), were obtained from the second scan at 5ºC/min and calculated as follows:

$$\alpha = \frac{1}{L_0}\cdot\frac{dL}{dT} = const \qquad (2.3)$$

where L and L_0 are the thickness at any temperature and at room temperature, respectively. The T_g was determined from the first derivative of the expansion curves L/L_0 as the half-way point in the increase of expansion coefficient step upon relaxation of the network.

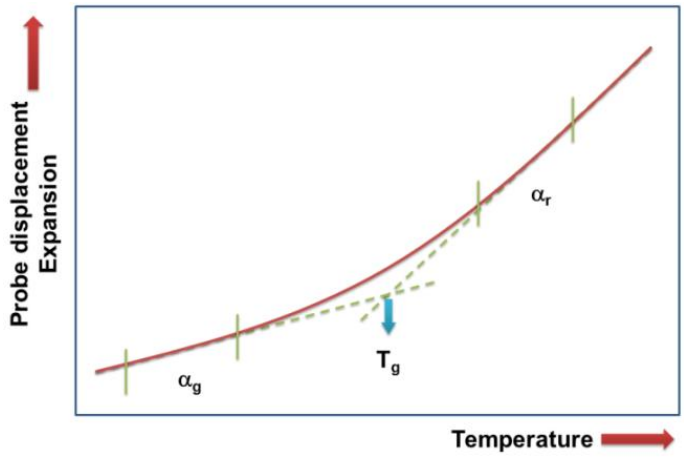

Figure 2.5. A typical TMA experiment of a cured epoxy thermoset (probe displacement is proportional to expansion) for determination of T_g; symbols α_g and α_r represent glassy and rubbery CTEs, respectively [5].

For conversion at the gel point determinations the samples were impregnated on a silanized glass fiber disk supported between two small circular ceramic plates. Non-isothermal experiments were performed in range and rate of temperature known applying a periodic force range. All experimental data and conditions are described in detail on each chapter. When the material reaches sufficient mechanical stability (gelation) the TMA measuring probe is not able to deform the sample and the amplitude of the oscillations is reduced. The gel point is taken in TMA as the temperature at which a sudden decrease in the amplitude of oscillations is observed. The gel conversion, α_{gel}, was determined as the DSC conversion at the gelation temperature determined by TMA [6]. (Figure 2.6).

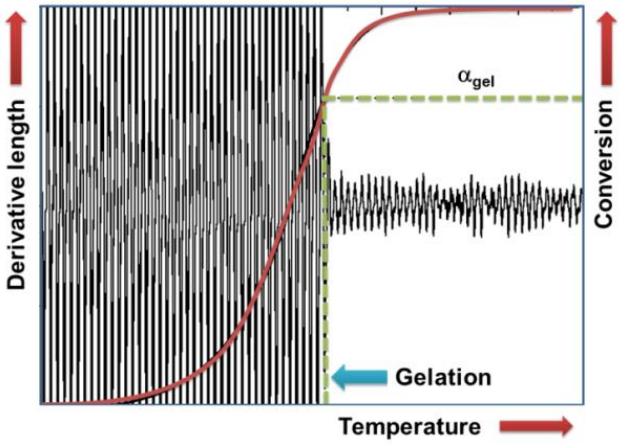

Figure 2.6. Example of the TMA curve for the determination of the gel point.

2.4. Dynamic mechanical thermal analysis (DMTA)

Dynamic mechanical thermal analysis involves imposing a small cyclic strain on a sample and measuring stress response, or equivalently, imposing a cyclic stress on a sample and measuring the resultant strain response. DMTA is used both to study molecules relaxation processes in polymers and to determine inherent mechanical or flow properties as a function of time and temperature [7]. In others words, DMTA studies the viscoelastic nature of a material by applying an oscillatory stress with a fixed frequency to the sample and monitoring its response at different temperatures. Likewise, the complex modulus (E^*) and the loss factor (tan δ) can be calculated. The modulus contains real and imaginary contributions ($E^*=E'+i\cdot E''$). In regard to real part, E', is the elastic response measure of the material, whilst imaginary part, E'', is the viscous response. The maximum obtained on tan δ curve is, in most cases accepted as, the T_g of a material although it changes with the frequency used in the experiment.

Young Modulus also can be calculated by DMTA. Using three point bending assembly the Young modulus in a non-destructive flexural test at room temperature can be obtained. The modulus of elasticity is calculated using the slope of the load deflection curve in accordance with Eq. (2.4).

$$E_f = \frac{L^3 m}{4bd^3} \qquad (2.4)$$

where, E_f is flexural modulus of elasticity (MPa); L is support span (mm); b is width of test beam (mm); d is depth of tested beam (mm); and m is the gradient (i.e., slope) of the initial straight-line portion of the load deflection curve (P/D) (N/mm).

For this thesis two different devices were used in order to perform the DMTA analyses (Figure 2.7). Firstly, a TA Instruments DMA Q800 at Universitat Politècnica de Catalunya (Barcelona) was used to carry out most of the analyses, either in three point bending mode or in single cantilever bending on prismatic rectangular samples previously cured isothermally in a

mould. Secondly, a Triton Technology DMA at Politecnico di Torino was used during the stay in Italy.

Figure 2.7. DMTA equipment (DMA Q800) (left) and Triton Technology DMA (right) used to study the viscoelastic properties of the prepared thermosets.

The samples were prepared by placing the corresponding formulation in a mould to obtain specimens with dimensions ca. 2 x 0.5 x 0.1 cm^3. The experimental conditions are described on the corresponding chapters. They were placed in steel templates and cured with the appropriate curing schedule, depending on each material, in order to obtain specimens from thermal curable formulations. For photocurable formulations, the samples were coated, by means of a wirewound applicator onto a glass substrate and photocured by exposing to UV radiation with a fusion lamp (H-bulb) in air.

2.5. Rheology

Rheology is the science of deformation and flow of materials [8]. Actually, all materials do flow, given sufficient time. In very short processing times, the polymer may behave as a solid, while in long processing times the material may behave as a fluid. This dual nature (fluid-solid) is referred to as viscoelastic behavior [9].

Viscosity is one of the most important flow properties to be measured by rheometry, and is the resistance to flow. Strictly speaking, it is the resistance to shearing and it can be defined as the ratio of the imposed shear stress and the shear rate [9].

In this way, rheological measurements are based on monitoring the tension generated in the sample as a response to the application of an oscillatory shear force. The viscoelasticity of a given polymer reflects in the difference in the applied and measured angle δ. Likewise, the complex viscosity (η*) is determined in multi-frequency experiments at a certain temperature and amplitude. This amplitude must be comprised within the range of linear viscoelasticity.

Rheological studies with an ARG2 rheometer (TA Instruments, UK, equipped with an electrically heated plates system in parallel mode, EHP, Figure 2.8) were carried out. Thus, the complex viscosity (η*) is determined in multi-frequency experiments at a certain temperature and amplitude. Moreover, this amplitude must be comprised within the range of linear viscoelasticity.

Figure 2.8 Rheometer ARG2 used, with a magnification of the geometry used.

2.6. Fourier-transformed infrared spectroscopy (FT-IR)

In infrared spectroscopy, IR radiation is passed through the sample, some is absorbed by the sample and some passes through, obtaining the absorption and transmission spectrum. IR spectroscopy has been the workhorse technique for materials analysis; an IR spectrum represents a fingerprint of a sample. The term Fourier transform is related from the fact that a mathematical process (Fourier transform) is required to convert the raw data into the FT-IR spectrum [10].

Since the absorbance obtained from the signals of FT-IR spectrum are related with the concentration of different functional groups through Lambert-Beer law, the curing process can be followed by the expression:

$$A = \varepsilon \times C \times L \qquad (2.5)$$

where A is absorbance of a specie at certain frequency, ε is the absorptivity coefficient, C is the concentration of the specie and L is the optical pathway.

Identifying the signals corresponding to reactive groups and monitoring them, it would be possible to follow the reaction, *i.e.* if a band of a functional group that reacts during the curing process is identified, and therefore disappears, it is possible to follow the curing process.

Due to the fact that absorbance is proportional to the optical pathway, L, it is necessary to normalize the target band in respect to a reference band that remains unaltered during the curing process. On that way the conversion x, determined by FT-IR measurements can be written as follows:

$$x = 1 - \frac{\overline{A^t}}{\overline{A^0}} \qquad (2.6)$$

where $\bar{A}^t$ is the normalized absorbance at a certain time and $\bar{A}^0$ is the initial absorbance that corresponds to the maximum.

In the case of UV cured samples, the formulations are coated onto a silicon wafer (about 50 μm thickness) with a wire-wound applicator. The sample can then be exposed simultaneously to the UV beam, which induces the polymerization, and to the IR beam, which analyses *in situ* the extent of the reaction.

Two different FT-IR devices were used. For thermal curing processes, cured and uncured samples were analyzed with a FTIR spectrometer Bruker Vertex 70 with an attenuated total reflection accessory with thermal control (able to be cooled down with liquid nitrogen) and a diamond crystal (Golden Gate Heated Single Reflection Diamond ATR, Specac-Teknokroma). Spectra were collected at different temperatures, resolutions and wavelength ranges described in detail on the corresponding chapters.

For UV curing processes a Thermo-Nicolet 5700 FTIR device equipped with a medium pressure mercury lamp Hamamatsu Lightningcure LC5 with an optical guide and a light intensity on the surface of the sample of about 5 $mW \cdot cm^{-2}$ was used. This device was cooled down with liquid nitrogen. Both devices can be observed in Figure 2.9.

Figure 2.9. FT-IR devices used for photoinitiated (left) and thermal (right) systems.

2.7. Density and shrinkage measurements

A gas pycnometer was used for measuring the density of materials by gas displacement and the volume:pressure relationship known as Boyle's Law [11]. The pressures observed upon filling the sample chamber and then discharging it into a second empty chamber allow the determination of the sample volume as follows:

$$V_s = V_C + \frac{V_r}{1 - \frac{P_1}{P_2}} \qquad (2.7)$$

where V_s is the volume of the sample, V_c is the volume of the empty sample chamber (known from calibration), V_r is the volume of reference (again obtained from calibration), P_1 is the

pressure of the sample chamber and P_2 the combined pressure after expanding the gas to the second chamber.

Afterwards, from the volume measured and knowing the weight, the density of a certain sample can be easily calculated since:

$$\rho = \frac{W}{V_s} \qquad (2.8)$$

where ρ is the calculated density of the sample, W is the known weight of the sample and V_s is the volume of the sample.

The evaluation of the shrinkage undergone during curing is obtained by comparison of the shrinkage of the curable formulation and the cured thermosets, using the following expression:

$$Shrinkage(\%) = \frac{\rho_{polym} - \rho_{mon}}{\rho_{polym}} \times 100 \qquad (2.9)$$

Density measurements of both uncured formulations and cured samples were determined using a Micromeritics AccuPyc 1330 Gas Pycnometer (Figure 2.10) thermostatized at 30 ºC.

Figure 2.10. Gas pycnometer employed for the density determination.

2.8. Scanning electron microscopy (SEM)

The scanning electron microscope (SEM) enables the investigation of specimens with a resolution down to the nanometer scale. Here an electron beam is generated by an electron cathode and the electromagnetic lenses of the column and finally swept across the surface of a sample. The main signals which are generated by the interaction of the primary electrons (PE) of the electron beam and the specimen´s bulk are secondary electrons (SE) and backscattered electrons (BSE) and furthermore X rays. The SE come from a small layer on the surface and yields the best resolution, which can be realized with a scanning electron microscope. The electrons interact with the atoms that make up the sample producing signals that contain information about the sample's surface topography, composition, and other properties such as

electrical conductivity [12]. Since the first SEM, several modifications have been done in order to improve their characteristics, one of those improvements have been the incorporation of a special type of electron gun that allows achieving higher spatial resolutions and minimizes the damaging of the sample, known as Field Emission Scanning Electron Microscopy (FE-SEM).

Two scanning electron microscopes were used: a Jeol JSM 6400 with 3.5 nm resolution and a ZEISS SUPRA™ 40 Field Emission Scanning Electron Microscope (FE-SEM) with a nominal resolution of 1.5 nm. (Figure 2.11). For standard SEM analysis, samples were coated with gold while for the FE-SEM analysis with carbon.

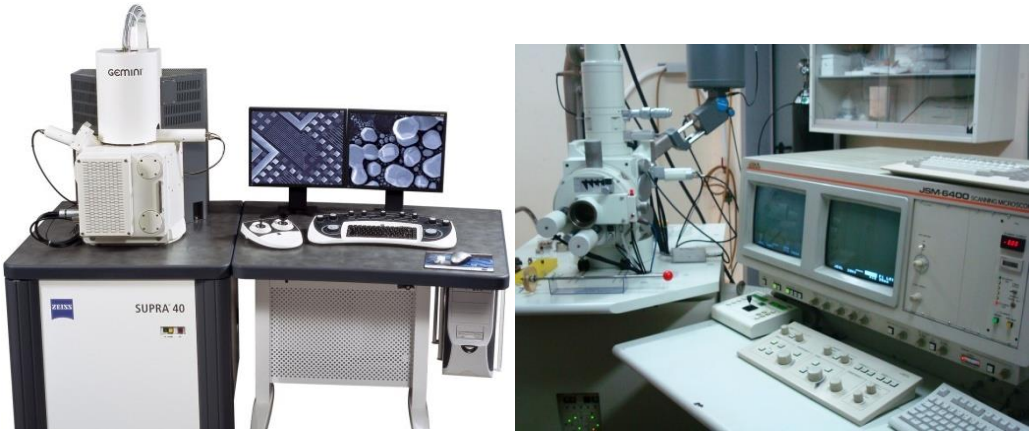

Figure 2.11. FE-SEM (left) and SEM (right) equipments used for obtaining surface images.

2.9. Transmission electron microscopy (TEM)

The transmission electron microscope (TEM) operates on the same basic principles as the light microscope but uses electrons instead of light. TEMs use electrons as "light source" and their much lower wavelength make it possible to get a resolution a thousand times better than with a light microscope. The source at the top of the microscope emits the electrons that travel through vacuum in the column of the microscope. Instead of glass lenses, the TEM uses electromagnetic lenses to focus the electrons into a very thin beam. The electron beam then travels through the specimen. At the bottom of the microscope the unscattered electrons hit a fluorescent screen, which gives rise to a "shadow image" of the specimen with its different parts displayed in varied darkness according to their density [13].

A Jeol 1011 microscope was used to perform TEM images. Samples were prepared either cutting thin films with an ultramicrotome at room temperature (cured thermosets) or by deposition of diluted solutions of the samples onto support grids (hyperbranched polymers).

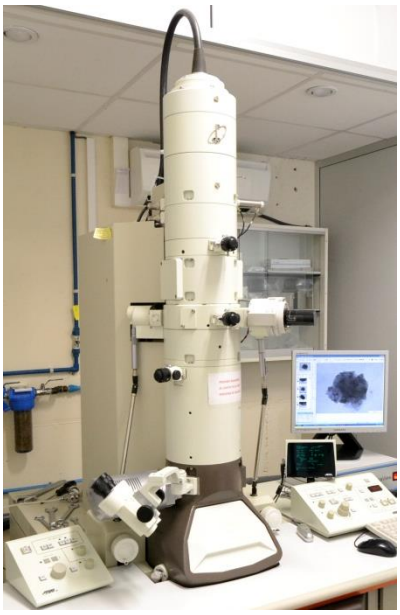

Figure 2.12. TEM equipment used to observe the morphology of the thermosets prepared.

2.10. Nuclear magnetic resonance (NMR)

Nuclear Magnetic Resonance (NMR) spectroscopy is an analytical chemistry technique used for determining the content and purity of a sample as well as its molecular structure. The principle behind NMR is that many nuclei have spin and all nuclei are electrically charged. If an external magnetic field is applied, an energy transfer is possible between the base energy to a higher energy level. The energy transfer takes place at a wavelength that corresponds to radio frequencies and when the spin returns to its base level, energy is emitted at the same frequency. The signal that matches this transfer is measured and processed in order to yield an NMR spectrum.

A Varian Mercury VX400 spectrometer and a Varian NMR System 400 spectrometer were used in order to elucidate and confirm the chemical structures of the synthesized polymers (Figure 2.13). Mainly two deuterated solvents were used, *i.e.* $CDCl_3$ and DMSO-d_6. In ^{1}H-NMR measurements at 400 MHz of magnetic field, 1 s of delay time (D1) and 14 accumulations as experimental conditions in order to obtain quantitative measurements were used. For ^{13}C-NMR measurements at 100.6 MHz magnetic field, a D1 of 0.5 s, 0.2 s acquisition time as experimental conditions were used.

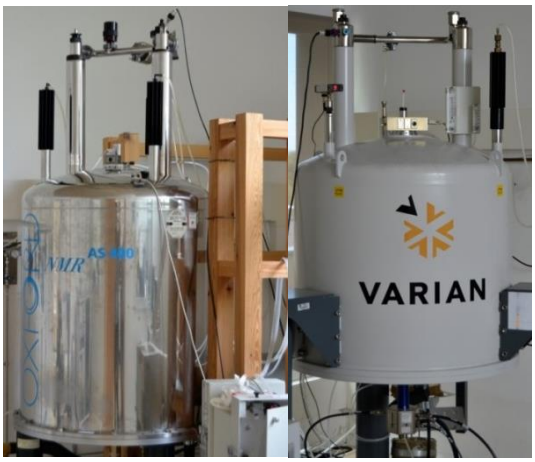

Figure 2.13. Picture of the NMR device used for the structural identification of the HBPs.

2.11. Impact test (Izod test)

Impact tests are designed to measure the resistance to failure of a material to a suddenly applied force such as collision, falling object or instantaneous blow. The test measures the impact energy, or the energy absorbed prior to fracture. The Izod test has become the standard testing procedure for comparing the impact resistances of plastics. The Izod test is most commonly used to evaluate the relative toughness or impact resistance of materials. The Izod test involves striking a test piece mounted at the end of a pendulum. The striker swings downwards impacting the test piece at the bottom of its swing [14].

A Zwick 5110 impact tester to perform impact test at room temperature was used (Figure 2.14). Impact test were carried out according to ASTM D4508-10 (2010) where prismatic rectangular specimens were used. Adjustable pendulum at different kinetic energy was used. Afterwards, in order to correlate the energy value obtained with the impact surface morphology, the broken samples were observed by means of SEM.

Figure 2.14. Impact testing machine used for the determination of the impact strength of the prepared thermosets.

The impact strength (IS) is calculated using the following equation:

$$IS = \frac{E}{A} \qquad (2.10)$$

where, "A" is the sample area (width (a) x thickness(b)), "E" are the energy of the pendulum after impact, respectively. "E" can be calculated as follow:

$$E = \frac{\%_{lost} \times E_P}{100} \qquad (2.11)$$

being "Ep" the energy of pendulum before impact, $\%_{lost}$ the difference between the measure (X) and the zero value related to the pendulum P_0 as the following equation shows:

$$\%_{lost} = X - P_0 \qquad (2.12)$$

Finally, bringing everything together the impact strenght can be calculated as follow:

$$IS = \frac{(X - P_0) \times E_P}{100 \times a \times b} \cdots \left[\frac{J}{mm^2} \right] \qquad (2.13)$$

2.12. Microhardness (Knoop microhardness)

A microhardness test is a mechanical hardness test used particularly for very brittle materials where only a small indentation may be made for testing purposes. Here, a pyramidal diamond point is pressed into the polished surface of the test material with a known force for a specified time. Thereby, the length of the long diagonal produced by the indentation of a rhomboidal tip can be related with the hardness of the material. Moreover, the length is directly related to the hardness of the material, so the shorter the diagonal the hardest the material [14].

Following the ASTM D1474-98(2002) standard procedure and using a Wilson Wolpert (MicroKnoop 401MAV) the microhardness measurements were carried out (Figure 2.15). For each material at least 10 measurements were made with a confidence level of 95%. The Knoop microhardness (HKN) was calculated following:

$$HKN = \frac{L}{A_p} = \frac{L}{l^2 \times C_p} \qquad (2.14)$$

where, L is the load applied to the indenter (0.025 Kg), A_p is the projected area of indentation in mm^2, l is the measured length of the long diagonal of indentation in mm, C_p is the indenter constant (7.028×10^{-2}) relating l^2 to A_p.

Figure 2.15. Microhardness tester used for the determination of the Knoop hardness of the prepared thermosets.

2.13. Nanoindentation

Nanoindentation is a variety of indentation hardness tests applied to small volumes [15]. The advantage of the technique is its ability to probe a surface and map its properties on a spatially resolved basis with a resolution of better than 1 μm. Thus, using sharp indenters the elastic modulus, hardness, and fracture toughness can be measured. These fundamental mechanical properties are related with three primary modes of deformation in solids, i.e. elasticity, plasticity, and fracture [16].

MTS Nanoindenter XP instrumented with a Berkovich tip calibrated against fused silica and with continuous stiffness measurement at 45 Hz and 2 nm amplitude was used. Indentations were done up to a maximum penetration depth of 3000 nm, corresponding to a maximum load of approximately 50mN, at a constant strain rate of 0.05 s^{-1}. Results were analyzed with the Oliver and Pharr method [17]. Nine indentations were done at each material.

2.14. References

[1] E. A. Turi, Thermal characterization of polymeric materials, Academic Press, San Diego, 1997.

[2] C. M. Earnest, in Compositional Analysis by Thermogravimetry, ed. ASTM, Philadelphia, 1988.

[3] R. B. Prime, H. E. Bair, S. Vyazovkin, P. K. Gallagher and A. Riga, in Thermal Analysis of Polymers, John Wiley & Sons, Inc., 2008, ch. 3, pp. 241-317.

[4] H. E. Bair, A. E. Akinay, J. D. Menczel, R. B. Prime and M. Jaffe, in Thermal Analysis of Polymers, John Wiley & Sons, Inc., 2008, ch. 4, pp. 319-385.

[5] E. A. Turi, Y. P. Khanna and T. J. Taylor, in A guide to Materials Characterization and Chemical Analysis, ed. J. B. Sibilia, VCH, New York, 1988, ch. 9.

[6] S. González, X. Fernández-Francos, J. Salla, A. Serra, A. Mantecón and X. Ramis, Journal of Applied Polymer Science, 2007, 104, 3406-3416.

[7] R. P. Chartoff, J. D. Menczel and S. H. Dillman, in Thermal Analysis of Polymers, John Wiley & Sons, Inc., 2008, ch. 5, pp. 387-495.

[8] J. Vlachopoulos and J. R. Wagner, The SPE Guide on Extrusion Technology and Troubleshooting., Society of Plastics Engineers, Brookfield CT, 2001.

[9] J. Vlachopoulos and D. Strutt, presented in part at the New Technologies for Extrusion, Milan, Italy, November 20 & 21, 2003.

[10] P. R. Griffiths and J. A. de Haseth, Fourier Transform Infrared Spectrometry, John Wiley & Sons, Inc., 2006.

[11] S. Tamari, Measurement Science and Technology, 2004, 15, 549.

[12] J. Goldstein, D. E. Newbury, D. C. Joy, C. E. Lyman, P. Echlin, E. Lifshin, L. Sawyer and J. R. Michael, Scanning Electron Microscopy and X-ray Microanalysis, Springer, New York, 2007.

[13] R. F. Egerton, Physical Principles of Electron Microscopy, Springer, Edmonton, Canada, 2011.

[14] R. Brown, Handbook of Polymer Testing - Short-Term Mechanical Tests, Rapra Technology, United Kingdom, 2002.

[15] A. C. Fischer-Cripps, Nanoindentation, Springer, New York, 2004.

[16] G. M. Pharr, Materials Science and Engineering A, 1998, 253, 151-159.

[17] W. C. Oliver and G. M. Pharr, J. Mater. Res., 1992, 7, 1564-1583.

Curing and Characterization of Oxazolidone-Isocyanurate-Ether Networks

Marjorie Flores,[1] Xavier Fernández-Francos,[2] Josep M. Morancho,[2] Àngels Serra,[1] Xavier Ramis[2]

[1] Departament de Química Analítica i Química Orgànica, Universitat Rovira i Virgili, Marcel·lí Domingo s/n, 43007 Tarragona, Spain
[2] Laboratori de Termodinàmica, ETSEIB, Universitat Politècnica de Catalunya, Diagonal 647, 08028 Barcelona, Spain.

Abstract

Oxazolidone-isocyanurate-ether networks were prepared by copolymerization of mixtures of DGEBA and toluene-2,4-diisocyanate (TDI) in presence of benzyldimethylamine (BDMA) as catalyst. Changes during curing and final properties of the cured materials were investigated by using DSC, FTIR/ATR, TMA, DMTA, TGA and densitometry. The influence of the molar ratio of isocyanate to epoxide groups on the properties and curing were studied. The kinetics of curing was analyzed by means of an integral isoconversional non-isothermal procedure. The fractions of oxazolidone, isocyanurate and ether groups present in the final network were evaluated and were found to be dependent on the initial isocyanate/epoxy ratio and curing conditions. By increasing the initial proportion of isocyanate the glass transition temperature, the thermal stability, the shrinkage and the amount of isocyanurate rings increase, whereas the fraction of ether linkages and oxazolidones decreases. It was observed that the gelation is controlled by the formation of isocyanurate rings at the beginning of the curing.

Key words: *Epoxy resins; isocyanurate; oxazolidone; curing of polymers; networks*

Introduction

Epoxy resins are a class of versatile thermosetting polymers widely used in structural adhesives, composites and coatings in electrics and electronics. An important drawback, which limits some industrial applications, is that the cured materials are inherently brittle [1]. The addition of a tough second phase can offset this drawback but can cause a significant drop in heat resistance and glass transition temperature [2,3,4].

Improving properties of epoxy resins at a lower cost is of a general great interest and can be used to make up for the decrease in certain properties when a second phase is added. A good strategy is to insert heterocyclic rings in the polymer structure, increasing the distance between crosslinks while increasing the rigidity of the structure. The reaction between diepoxides and diisocyanates can lead to thermosets containing isocyanurate and oxazolidone rings in their structure. Isocyanurates are crosslinking points, whereas oxazolidones are linear chain extenders that can improve the mechanical toughness of crosslinked isocyanurate containing networks. Both structures are well known for their high-thermal stability [5]. Although few studies report thermosets having these two kinds of heterocycles in the structure, it is accepted that these copolymers exhibit better properties than neat epoxy resins and other classical epoxy thermosets [6,7,8]. Consequently, the study of these systems has a remarkable interest.

A variety of catalysts has been claimed to be effective on the preparation of thermosets containing isocyanurate and oxazolidone rings. Among them, tertiary amines seem to be the most efficient and commonly used. The initiation mechanism catalyzed by tertiary amine has not been fully elucidated in bulk polymerization. Some authors proposed that two initiating species can be active in the anionic mechanism, a zwitterion formed by attack of the tertiary amine to the

epoxide or a zwitterion formed by attack of the tertiary amine to the isocyanate [9,10,11]. The understanding of reactive processes implied in the curing can lead to an optimization of the network structure.

According to certain authors [5,6,8,9,12] the main reactions that take place, in order of increasing temperature, in epoxy/isocyanate/tertiary amine formulations are the following: a) trimerization of isocyanate (isocyanurate formation), b) oxazolidone ring formation (epoxy-isocyanate reaction) and epoxy homopolymerization and c) isocyanurate decomposition to produce oxazolidone groups (isocyanurate-epoxy reaction). The fraction of oxazolidone, isocyanurate and ether groups present in the final network depends on the initial isocyanate/epoxy ratio and curing conditions (curing temperature, kind and amount of catalyst, etc.) In general, homopolymerization of epoxide groups is considered as a secondary reaction. Scheme 1 depicts the reaction pathway expected in the formation of oxazolidone and isocyanurate structures.

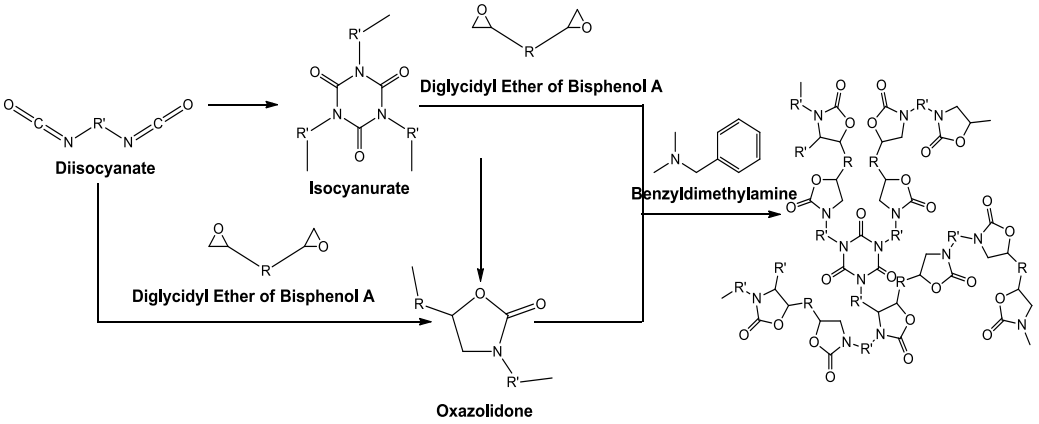

Scheme 1. Schematic reaction pathway for the formation of oxazolidone and isocyanurate structures

In the present study, a low molecular weight DGEBA resin was cured with TDI using BDMA as the catalyst. The aim of our work is to study the influence of the molar ratio of isocyanate to epoxide groups on the curing and on the characteristics of the materials obtained.

We tested as catalysts three different tertiary amines: benzyldimethylamine (BDMA), 1-methylimidazole (1-MI) and 4-(N,N-dimethylamino) pyridine (DMAP), but BDMA was selected, since it was not able to homopolymerize neat DGEBA. This study was made in order to establish that the zwitterion formed between tertiary amine and isocyanate is the active species of initiator, which in addition could initiate the homopolymerization of DGEBA.

The different reactions that take place during the curing process were followed by FTIR and the fraction of oxazolidone, isocyanurate and ether groups present in the final network were quantified by this technique. The properties of the materials were related with the final structure of the network, paying attention not only in the influence of the crosslinking density but also in the effect of the chain stiffness.

The kinetics of curing was studied by means of an isoconversional non-isothermal procedure that allowed us to determine the activation energy of the main reactive processes and reach some conclusions on the mechanism followed during curing.

Gelation was studied by means of non-isothermal TMA and DSC tests and the shrinkage during curing was determined by densitometric measurements. To the best of our knowledge, this is the first time that gelation and shrinkage have been determined for epoxy/isocyanate systems.

Thermal stability, glass transition temperatures and dynamomechanical properties were investigated by means of TGA, DSC and DMTA.

Experimental

Materials

Diglycidylether of Bisphenol A (DGEBA), Epitoke Resin 828 from Hexion Specialty Chemicals (epoxy equivalent = 187 g/eq) was used after drying under vacuum. Toluene-2,4-diisocyanate (TDI) from Aldrich was distilled. Benzyldimethylamine (BDMA), 1-methylimidazole (1MI) and 4-(N,N-dimethylamino)pirydine (DMAP) were purchased from Aldrich and used without further purification.

Preparation of the curing mixtures

Mixtures of TDI and DGEBA were carefully mixed with stirring and degassed under vacuum (at 80 ºC) during two hours to prevent the appearance of bubbles during curing. Samples were kept at -20 ºC before use to prevent polymerization. 1 phr of catalyst was added to the corresponding DGEBA/TDI mixtures at room temperature just before curing. Table I shows the notations and compositions of the different formulations studied. Thus, as an example, formulation notated as 2:1, contains 2 mol of DGEBA per 1 mol of TDI.

Table I. Notation and composition of the different formulations used in this work, in molar ratio (*n*:*n*) and equivalent ratio (eq/eq). Molar ratio is used as notation.

Formulation	n_{DGEBA}:n_{TDI}	eq_{BDMA}/eq_{TDI}	eq_{BDMA}/eq_{DGEBA}
DGEBA:TDI 2:1	2:1	0.03410	0.01705
DGEBA:TDI 1:1	1:1	0.02243	0.02243
DGEBA:TDI 1:2	1:2	0.01335	0.02671

Calorimetric measurements

Calorimetric analyses were carried out on a Mettler DSC-822e calorimeter with a TSO801RO robotic arm. Samples of approximately 10 mg in weight were cured in aluminium pans in a nitrogen atmosphere. Non-isothermal experiments were performed between 0 and 325 ºC at heating rates of 5, 7.5, 10, and 15 ºC/min in order to determine the reaction heat and the kinetics of curing. The degree of conversion, α, at a given temperature *T* was calculated as the

quotient between the heat released up to *T* and the total reaction heat associated with complete conversion of all reactive groups. The reaction rate, dα/d*t*, was expressed as the ratio of the instant heat released (calorimetric signal) to the total reaction heat.

The glass transition temperatures of the fully cured materials ($T_{g\infty}$),after isothermal or dynamic curing, were determined in a heating experiment at 10 ºC/min as the temperature of the half-way point of the jump in the heat capacity when the material changed from the glassy to the rubbery state. The T_g of the uncured materials was determined in a heating experiment 10 ºC/min starting at -100 ºC.

Kinetic analysis

Kinetic parameters were determined using integral isoconversional non-isothermal kinetic analysis named Kissinger-Akahira-Sunose (KAS). For each conversion degree, the linear representation of ln(β/T^2) versus 1/*T* makes it possible to determine *E* and ln[*AR*/g(α)*E*] from the slope and the intercept without knowing the kinetic model. β is the heating rate, *T* the temperature, *E* the activation energy, *A* the pre-exponential factor, *R* the gas constant, and g(α) the integral conversion function. Details of the kinetic methodology are given in a previous paper [13]. Although, the activation energy obtained by the integral procedure represents an average value up to a certain degree of conversion instead of the instantaneous and real value, it can be used for the discussion of the kinetics of curing [14].

Infrared spectroscopy (FTIR/ATR)

Cured and uncured samples were analyzed with a FTIR spectrometer Bruker Vertex 70 with an attenuated total reflection accessory with thermal control and a diamond crystal (Golden Gate Heated Single Reflection Diamond ATR, Specac-Teknokroma). Spectra were collected at 30 ºC in the absorbance mode at a resolution of 4 cm^{-1} in the wavelenghth range of 600 to 4000 cm^{-1}. 10 scans were averaged for each spectrum.

The disappearance of the absorbance peaks at 915 cm^{-1} (epoxy bending) and 2260 cm^{-1} (carbonyl of isocyanate) indicates that the epoxide and isocyanate groups had reacted. The increase in the absorbance peak at 1100 cm^{-1} (C-O-C stretching of aliphatic linear ether) is related to the homopolymerization of epoxide groups. The appearance of absorption peaks at 1750 cm^{-1} (carbonyl of oxazolidone) and 1710 cm^{-1} (carbonyl of isocyanurate) shows the formation of oxazolidone and isocyanurate groups. Alternatively, the peak at 1410 cm^{-1} can be used to evaluate the formation of isocyanurate groups. The peak at 830 cm^{-1} (*p*-phenylene) which should not change during the curing process was chosen as an internal standard.

Conversions of the different reactive groups, epoxide, isocyanate, isocyanurate and oxazolidone, were determined by the Lambert-Beer law from the normalized changes of absorbance at 915, 2260, 1710 and 1750 cm^{-1}, respectively. Maximum normalized absorbances of isocyanurate and oxazolidone were determined in formulations where isocyanate groups were completely transformed into isocyanurate or oxazolidone groups. Maximum normalized absorbance of isocyanate and epoxy groups were determined from the initial spectrum of mixtures without initiator. The final composition (%) of oxazolidone, isocyanurate and ether linkages was determined using FTIR conversion and the relative amounts of DGEBA and TDI present in the formulation. The homopolymerized DGEBA (ether linkages formed) was calculated

as the difference between all the reacted epoxy groups and the groups that reacted to form oxazolidone rings.

Thermomechanical analysis (TMA)

Thermal mechanical analysis was carried out in a nitrogen atmosphere using a Mettler TMA40 thermomechanical analyser. The samples were supported by two small circular ceramic plates and silanized glass fibres, which were impregnated with the sample. Non-isothermal experiments were performed between 30 and 325 ºC at heating rate of 5 ºC/min applying a periodic force that changed (cycle time=12 s) from 0.0025 N to 0.01 N. When the material reaches sufficient mechanical stability (gelation) the TMA measuring probe is not able to deform the sample and the amplitude of the oscillations is reduced. The gel point was taken in TMA as the temperature at which a sudden decrease in the amplitude of oscillations was observed. The gel conversion, α_{gel}, was determined as the DSC conversion at 5 ºC/min at the temperature of the material gelled in TMA in a non-isothermal experiment. Details of the employed methodology are described in a previous work [13].

Dynamomechanical analysis (DMTA)

DMTA was carried out with a TA Instruments DMA Q800. Single cantilever bending was performed on prismatic rectangular samples (ca. 0.5 x 12 x 25 mm^3). The apparatus was operated dynamically, at 3 ºC/min, from -125 to 325 ºC. The frequency of application of the force was 1 Hz and the amplitude of the deformation 30 μm. The samples used for the dynamomechanical analysis were cured isothermally by means of the following cure schedule: 1 h. at 80 ºC plus 15 h. at 200 ºC and finally subjected to a postcuring at 250 ºC for 1 h.

Thermogravimetric analysis (TGA)

Thermogravimetric analysis was carried out in a nitrogen atmosphere with a Mettler-Toledo TGA-50 thermobalance. Samples cured following the above curing schedule, with an approximate mass of 5 mg, were degraded between 40 and 600 ºC at a heating rate of 10 ºC min^{-1} in a nitrogen atmosphere.

Measurement of density

The overall shrinkage was calculated from the densities of the materials before and after curing, which were determined using a Micromeritics AccuPyc 1330 Gas Pycnometer thermostatized at 30 ºC. The shrinkage during curing was determined as:

$$\%shrinkage = 100\,\frac{\rho_\infty - \rho_0}{\rho_\infty}$$

where ρ_0 is the density of the uncured formulation and ρ_∞ is the density of the fully cured material obtained at the same conditions that DMTA samples.

Results and discussion

Initiation mechanism

First of all, we investigated the effect of three catalysts, the tertiary amines BDMA, DMAP and 1MI, on the initiation mechanism and on the final properties and structure of the thermoset. According to the literature [10], Scheme 2 show, as an example, the two active initiator species expected when BDMA is used as the catalyst in DGEBA:TDI formulations. We cured dynamically (between 0 and 325ºC at 10ºC/min) samples of DGEBA containing 1 phr of tertiary amine in the calorimeter. By non-isothermal DSC and FTIR of the samples cured in the DSC we proved that DMAP and 1MI can partially homopolymerize neat DGEBA whereas by using BDMA, no reaction was observed with DGEBA. However, Vazquez et al. [15] observed that this reaction took place using an appropriate amount of BDMA, at low temperature or employing low scanning rates in the DSC. When 5 phr of TDI was added to the formulations, neat DGEBA reacted completely with the three amines. These results suggest that DMAP and 1MI can form the two kinds of active species shown in Scheme 2. On the contrary, when BDMA is used, only the zwitterion formed between tertiary amine and isocyanate (Scheme 2 b) becomes the true initiating species, whereas the zwitterion formed between tertiary amine and epoxide (Scheme 2 a) is not active enough to homopolymerize DGEBA under the curing conditions used in this work. In order to go further in the formation of the active species of Scheme 2 a, we kept at 180ºC for 2 hours stoichiometric proportions of BDMA and phenylglycidylether (PGE) and then we registered the ^{1}H and ^{13}C NMR spectra. In this way we proved that BDMA is unable to form an active species with the epoxy and that it is only able to produce the zwitterion by reacting with isocyanate, which is the active species responsible for the curing.

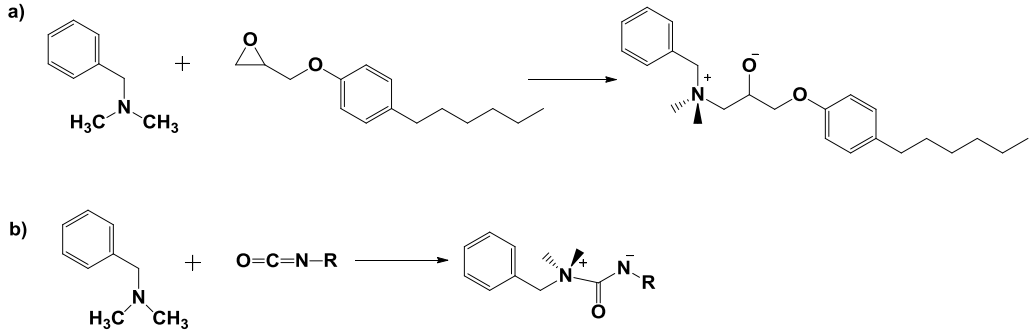

Scheme 2. Expected active initiating species formed (a) between BDMA and DGEBA and (b) between BDMA and TDI.

The DGEBA:TDI 1:1 stoichiometric formulations with 1 phr of BDMA, DMAP or 1MI were investigated by DSC. After non-isothermal curing, the FTIR spectra of the thermosets showed that isocyanate and epoxide groups had disappeared completely, indicating that the materials obtained were fully cured. Table II summarizes the results obtained. It can be seen that DMAP promotes the formation of oxazolidone, whereas BDMA favours the formation of isocyanurate rings. Moreover, the glass transition temperature increases when isocyanurate content increases, as it is expected. These results suggest that changing the catalyst it is possible to tune the final properties of the thermosets and to obtain tailor-made materials with the desired properties. In this work, we selected BDMA as initiator because of the higher glass transition temperature

achieved. In addition, BDMA is the only amine that cannot initiate the epoxide homopolymerization reaction.

Table II. Final composition and temperature of glass transition for the 1:1 DGEBA:TDI formulations cured dynamically with 1 phr of different amines.

Initiator	Oxazolidone [a] (%)	Isocyanurate [a] (%)	Ether [a] (%)	T_g (ºC)
BDMA	20 (33)	40 (67)	40 (67)	189
1MI	42 (59)	29 (41)	29 (41)	181
DMAP	84 (91)	8 (9)	8 (9)	164

[a] % of oxazolidone, isocyanurate and ether linkages in the final network. In brackets % of oxazolidone, isocyanurate and ether formed respect to the initial isocyanate or epoxy content.

Curing mechanism

Samples with different DGEBA:TDI ratio were dynamically cured at 10 ºC/min with 1 phr of BDMA in the DSC and then the composition was determined by FTIR. Figure 1 shows the thermograms of the formulations studied. Three main exothermic peaks, which vary with the formulation, appear in the thermogram, at approximately 45, 150 and 230 ºC. Moreover, the first peak has a shoulder close to 90 ºC. In order to determine the reactions involved, FTIR spectra of partially cured samples in the DSC up to several temperatures (i.e. 70º, 130º, 190 ºC and 325 ºC for 1:1 formulation) after each exothermic peak or shoulder were recorded. The resulting spectra are shown in Figure 2 for 1:1 formulation. The final compositions and the evolution during curing, for all formulations, are collected in Table III.

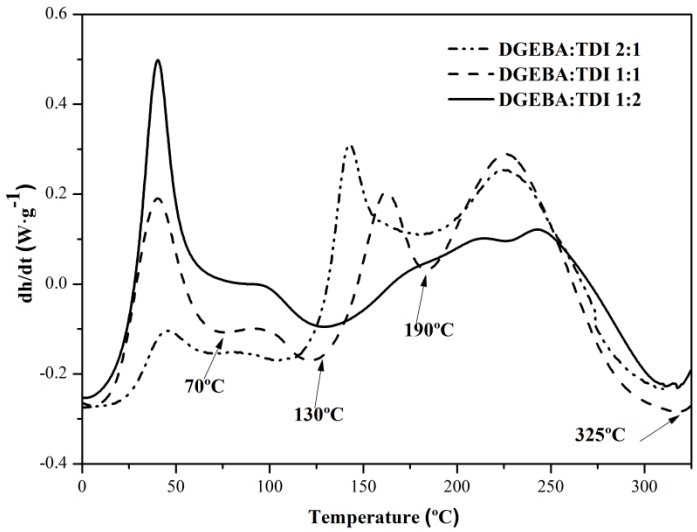

Figure 1. DSC thermograms of various DGEBA:TDI formulations cured with 1 phr of BDMA. Temperatures at FTIR spectra were recorded are indicated, as an example, for formulation DGEBA:TDI 1:1.

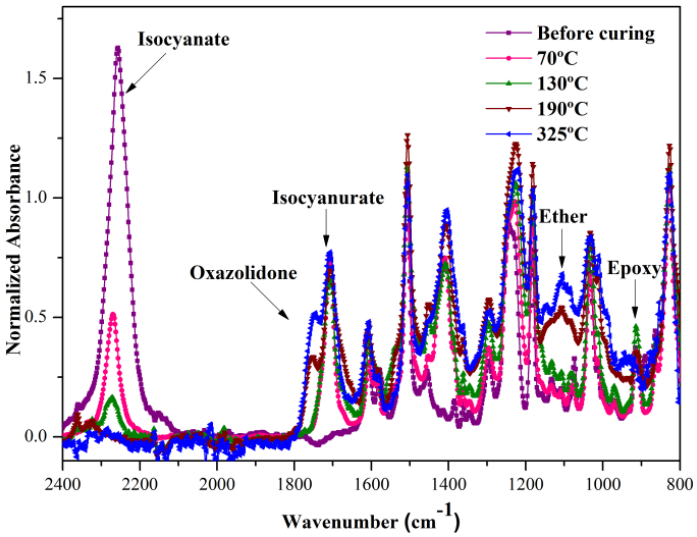

Figure 2. Evolution of the FTIR spectra of the DGEBA:TDI 1:1 formulations with 1 phr of BDMA during the DSC curing. FTIR spectrum before curing is included as reference.

Table III. Evolution of the content of different groups during non-isothermal curing up to different temperatures indicated in the table determined by FTIR spectroscopy.

Formulation	*T* (ºC)	Isocyanate[a] (%)	Epoxy[a] (%)	Oxazolidone[b] (%)	Isocyanurate[b] (%)	Ether[b] (%)
DGEBA:TDI 2:1	70	17	100	0	83	0
	110	7	100	0	*93*	0
	170	0	87	14	86	6
	310	0	0	88	12	56
DGEBA:TDI 1:1	70	20	100	0	80	0
	130	9	100	0	91	0
	190	0	44	12	88	44
	325	0	0	33	67	67
DGEBA:TDI 1:2	80	34	100	0	66	0
	130	24	100	0	76	0
	190	13	70	3	84	24
	325	0	0	18	82	64

1 phr of BDMA was used as catalyst in all formulations.
[a] % of unreacted isocyanate and epoxide.
[b] % of oxazolidone, isocyanurate and ether (epoxy homopolymerized) groups formed respect to the initial isocyanate or epoxy content.

The main reaction that takes place in the first exothermic peak (including the shoulder, until 110-130 ºC) is the formation of isocyanurate rings. This reaction proceeds close to completion except for formulation with excess of isocyanate, where the conversion of isocyanate

is about 75 %. The formation of oxazolidone and the reaction of epoxide groups do not take place in this range of temperatures. The presence of two DSC peaks for the formation of isocyanurate rings has been observed by several workers [6,10] and can be related with the different reactivity of the two isocyanate groups of TDI or with the existence of non-catalyzed isocyanate trimerization giving isocyanurate rings at higher temperatures (shoulder about 90 ºC).

The second exotherm (between 130 and 190 ºC) is related to the formation of oxazolidone rings by reaction between isocyanate and epoxy groups, since the amount of oxazolidones increases whereas the amount isocyanurates barely decreases or even increases. Moreover, it is interesting to note that epoxy homopolymerization is another important reaction that competes with oxazolidone formation in this range of temperatures.

The main process taking place in the last exothermic peak is the decomposition of isocyanurate rings by reacting with the epoxy excess to give oxazolidone rings. This reaction occurs in greater extension in DGEBA-rich formulation (i.e. DGEBA:TDI 2:1) leading to networks with a higher amount of oxazolidone rings. On the contrary, in the formulation with the lowest proportion of DGEBA (i.e. DGEBA:TDI 1:2) the decomposition of isocyanurate rings is a secondary reaction and the network formed contains higher proportions of isocyanurate rings. DGEBA thermal homopolymerization is also an important reaction in this range of temperatures.

Scheme 3 collects the reaction mechanisms leading to the formation of isocyanurates (a) and oxazolidone rings (b). It can be observed as the zwitterion formed between tertiary amine and isocyanate acts as the initiating species in isocyanate trimerization and in the formation of oxazolidone rings.

Although, observing the FTIR spectra, it is possible to assign one or two main reactions to each exothermic peak, this assignment is only approximated since these peaks are partially overlapped. The exact composition of the network formed, and consequently the reactions that take place during curing, should be quantified (as shown Table II and III). The initial composition of the formulation, the curing schedule and the catalyst used are the key parameters that control the composition of the resulting network.

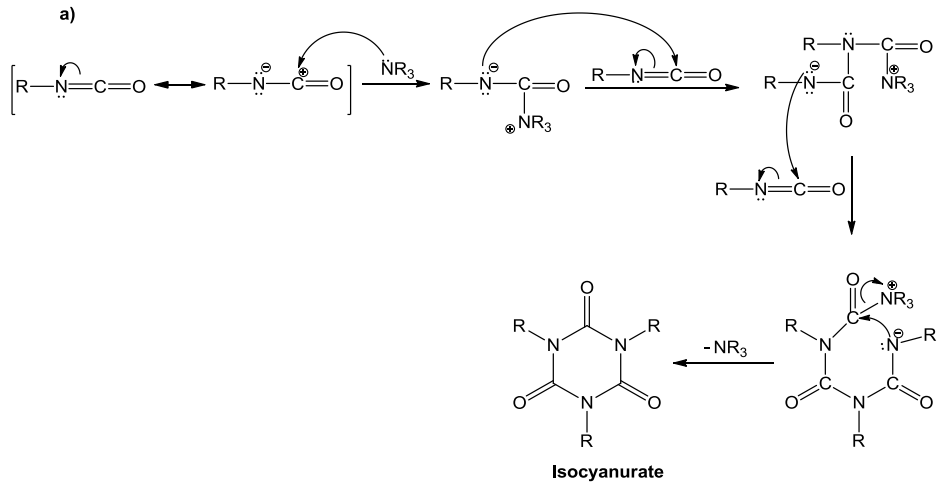

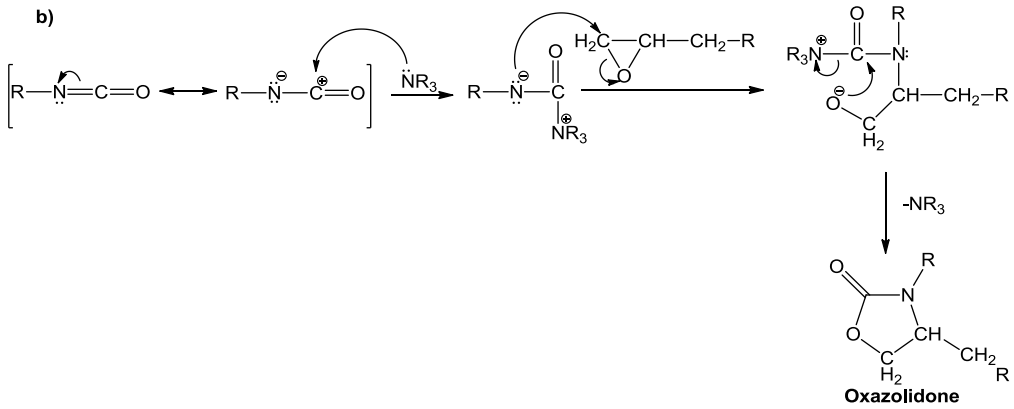

Scheme 3. Mechanisms of (a) isocyanate trimerization (isocyanurate formation) and (b) oxazolidone formation.

Kinetics of curing

The mixtures of DGEBA:TDI were cured at several heating rates in the DSC. Table IV shows the experimental and theoretical heats of curing. Experimental heat, Δh_{exp}, was calculated as the average heat of the experiments at different heating rates and used to evaluate the degree of conversion. By increasing the proportion of TDI, Δh_{exp} increases, due to the different reaction heats of the reactive processes and to the different compositions. Δh_{theo} was estimated using the final composition (Table III) and the reported heats for isocyanurate (207.9 kJ·mol^{-1}) and oxazolidone (179.5 kJ·mol^{-1}) formation and for epoxy homopolymerization (80 kJ·mol^{-1}) [16,17]. The similarity between the theoretical and experimental values indicates that both the isocyanate and epoxy groups reacted completely, as we confirmed by FTIR, and that DSC is capable of recording all the heat of polymerization. Consequently, the calculated conversions (absolute conversions) (Tables Va and Vb) are correct and can be used in the kinetic analysis.

Table IV. Curing enthalpies for the formulations studied with 1 phr of BDMA.

Formulation	Δh_{exp} (J·g^{-1})	Δh_{theo} (J·g^{-1})
DGEBA:TDI 2:1	450	405
DGEBA:TDI 1:1	590	580
DGEBA:TDI 1:2	620	640

Table Va. Kinetic parameters of the curing for DGEBA:TDI 2:1 and 1:1 formulations catalyzed with 1 phr BDMA.

α	DGEBA:TDI 2:1			DGEBA:TDI 1:1		
	E **(kJ·mol^{-1})**	**ln[*AR*/g(*α*)*E*] (s^{-1})**	***r***	***E*** **(kJ·mol^{-1})**	**ln[*AR*/g(*α*)*E*] (s^{-1})**	***r***
0.05	23.5	-0.76	0.9997	13.1	-4.68	0.9951
0.1	18.0	-3.35	0.9922	10.8	-5.69	0.9999
0.2	31.8	-0.02	0.9916	10.0	-6.35	0.9906
0.3	51.7	5.34	1.0000	21.3	-3.45	0.9920
0.4	45.0	2.99	0.9999	26.1	-2.53	0.9979
0.5	38.6	0.79	0.9999	27.7	-2.43	0.9997
0.6	37.9	0.20	0.9997	34.4	-1.04	0.9998
0.7	39.9	0.33	1.0000	37.4	-0.55	0.9988
0.8	39.1	-0.21	0.9993	38.8	-0.48	0.9974
0.9	35.9	-1.32	0.9985	41.2	-0.26	0.9966
0.95	34.3	-1.89	0.9993	44.9	0.33	0.9975

Table Vb. Kinetic parameters of the curing for DGEBA:TDI 1:2 formulation catalyzed with 1 phr BDMA.

α	DGEBA:TDI 1:2		
	E **(kJ·mol^{-1})**	**ln[*AR*/g(*α*)*E*] (s^{-1})**	***r***
0.05	38.8	6.14	0.9999
0.1	33.6	3.71	1.0000
0.2	22.3	-1.18	0.9996
0.3	19.2	-2.86	0.9957
0.4	18.8	-3.60	0.9944
0.5	35.0	0.32	0.9843
0.6	52.4	4.27	0.9970
0.7	61.5	5.85	0.9988
0.8	73.1	7.89	0.9992
0.9	98.5	12.79	0.9998
0.95	120.0	16.85	1.0000

Because of the complexity of the curing process the kinetics was studied by the non-isothermal integral isoconversional procedure, because it is possible to determine useful

information such as the apparent activation energy for every conversion without needing to know the kinetic model beforehand, which can change during the curing process. Tables Va and Vb summarize the results obtained for the different formulations studied. The high regression coefficients *r* obtained indicate that the methodology is suitable for describing the kinetics of curing of these complex systems. In general, the activation energy is lower during the first stages of the curing process and then increases slightly when the processes with greater activation energy initiate. Because of the compensation effect [18], it is not possible to compare the activation energy values of the different formulations, but their changes during curing can be related with the different reactive processes that take place during curing. The dependence of the activation energy and reaction rate on the degree of conversion is represented in Figure 3 for formulation DGEBA/TDI 1:1. Three regions of activation energy values (11.3, 23.7 and 37.4 $kJ \cdot mol^{-1}$) can be observed, in order of increasing degree of conversion or temperature, related to the three main DSC exotherms. The first region, where isocyanurate ring formation takes place, has an average activation energy of 11.3 $kJ \cdot mol^{-1}$. An average activation energy of 23.7 $kJ \cdot mol^{-1}$ should be associated with the formation of oxazolidones and the homopolymerization of epoxides (second region). In the third region, the decomposition of isocyanurate rings increases the average activation energy until a value of 37.4 $kJ \cdot mol^{-1}$. The values of activation energy obtained are consistent with the fact that isocyanurate formation takes place at low temperature, epoxy homopolymerization and oxazolidone formation at intermediate temperature and isocyanurate decomposition to lead oxazolidones at high temperatures.

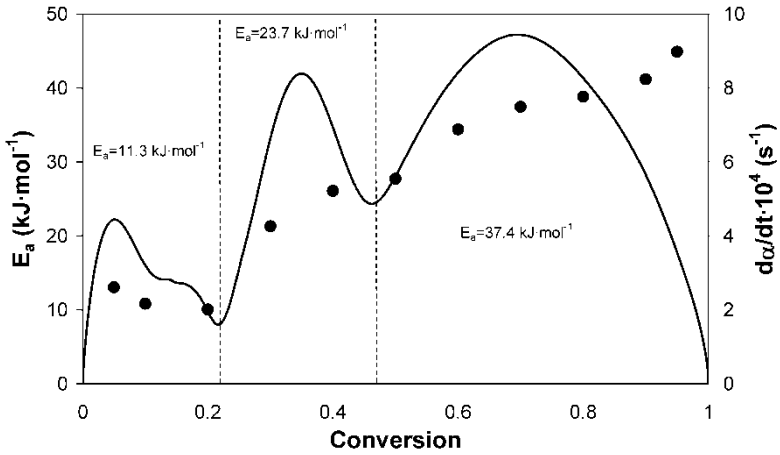

Figure 3. Dependence of activation energy (symbols) and reaction rate (line) on the degree of conversion for DGEBA:TDI 1:1 formulation catalyzed by 1 phr of BDMA.

The value of activation energy of 23.7 $kJ \cdot mol^{-1}$ is much lower than the obtained during the homopolymerization of neat DGEBA using tertiary amines different from BDMA, such as 1MI (60 $kJ \cdot mol^{-1}$) or DMAP (52 $kJ \cdot mol^{-1}$) [19]. This result confirms that the tertiary amine/TDI zwitterion is the true active species in the initiation of DGEBA:TDI formulations instead of the tertiary amine/DGEBA zwitterion that leads to higher activation energies.

General characterization

Taking into account all the previous results we decided to study the isothermal curing and the final properties of the three DGEBA:TDI formulations using 1 phr of BDMA as the catalyst.

In order to activate the different reactive processes, the polymerization was carried out in an oven in three stages: the first stage was achieved after one hour at 80 ºC, then the samples were put 15 hours at 200 ºC and finally a post-curing at 250 ºC during one hour was also applied.

By means of FTIR the final compositions of the materials after isothermal curing were calculated (Table VIa). It can be seen that an isocyanate excess favours isocyanurate formation, whereas an excess of epoxy favours the formation of oxazolidone, either directly by reaction between isocyanate and epoxy groups or by decomposition of isocyanurate rings at high temperatures. Homopolymerization of DGEBA is an important reaction even if an excess of isocyanate is used. This reaction should not be considered as secondary in any case, as some authors do [2,6,7], and should be quantified in order to know the composition and a better understanding of the properties of the network formed.

Table VIa shows that, by increasing the proportion of TDI the $T_{g\infty}$ strongly increases and the heat capacity step, $\Delta C_{p\infty}$, decreases. This result agrees with a higher crosslinking density *n* in formulations rich in isocyanurate rings (Table VIb). However, the type of crosslinks and the stiffness can also contribute to the $T_{g\infty}$ value. It must be taken into account that there are at least two different types of crosslinks in the network, the isocyanurate rings and the ones coming from the homopolymerized DGEBA. In addition, the stiffness of the chains linked to the crosslinks can also differ: trimerized TDI >> oxazolidone > DGEBA polyether (oxazolidone ring acts as a chain extender but is rigid and topologically bulky which hinders the network movement). A parameter *F* (network stiffness) has been calculated (see Table VIb) taking into account the crosslinking density and the chain stiffness, according to the methodology proposed in the literature [20]. It can be seen that the stiffness of the network strongly increases with the initial TDI content of the formulation in good agreement with the increasing $T_{g\infty}$. Therefore, the flexibility and mobility of the different structures formed, polyether, polyisocyanurate and polyoxazolidone have a strong contribution in the $T_{g\infty}$.

Table VIa Calorimetric and DMTA data and final composition of the network of the studied systems.

Formulation	T_{g0}[a] (ºC)	ΔC_{p0}[b] (J·g^{-1}·K^{-1})	$T_{g\infty}$[a] (ºC)	$\Delta C_{p\infty}$[b] (J·g^{-1}·K^{-1})	$T_{tan\delta}$[c] (ºC)	Ether[d] (%)	Oxazol.[d] (%)	Isocyanur.[d] (%)
DGEBA:TDI 2:1	-24	0.59	145	0.33	151	54 (55)	42 (88)	6 (12)
DGEBA:TDI 1:1	-29	0.56	191	0.19	191	39 (63)	22 (37)	39 (63)
DGEBA:TDI 1:2	-46	0.55	239	0.12	261	22 (66)	13 (17)	55 (83)

1 phr of BDMA was used as catalyst in all formulations
[a] Glass transition temperatures before and after isothermal curing obtained by DSC at 10ºC·min^{-1}.
[b] Difference in the heat capacity when the material changed from glassy to the rubbery state before and after isothermal curing obtained by DSC at 10ºC·min^{-1}.
[c] Temperature of the maximum of tan δ at 1 Hz
[d] % of oxazolidone, isocyanurate and ether linkages present in the final network. In brackets % of oxazolidone, isocyanurate and ether formed respect to the initial isocyanate or epoxy content.

Table VIb Characteristics of the network, conversion at the gelation, densities, shrinkage and TGA data of the studied systems.

Formulation	n^a (mol·kg^{-1})	F^a (g·mol^{-1})	α_{gel}	ρ_0 (g·cm^{-3})	ρ_∞ (g·cm^{-3})	Shrinkage (%)	$T_{5\%}{}^b$ (ºC)
DGEBA:TDI 2:1	2.5	24	12	1.179	1.275	7.5	360
DGEBA:TDI 1:1	2.7	30	18	1.185	1.338	11.4	347
DGEBA:TDI 1:2	2.6	40	24	1.193	1.352	11.8	331

[a] Average crosslinking density, *n*, calculated assuming that homopolymerized DGEBA leads to two trifunctional crosslinks and an isocyanurate ring (3 isocyanate groups) forms another trifunctional crosslink. The chain stiffness, *F*, has been calculated considering the contribution of the different crosslinks and different chains present in the network as explained by Pascault et al. [20].
[b] Temperature of a 5% of weight loss calculated by thermogravimetry.

Gelation and shrinkage

In TMA, gelation is seen as a reduction in the oscillation amplitude because the gelified material is less deformable. This reduction is better observed in the signal derivative, as it can be seen in Figure 4 for DGEBA:TDI 1:1 formulation. Figure 4 shows how the gelation takes place at the beginning of the curing during the formation of isocyanurate rings (first exothermal peak in non-isothermal curing). Other formulations present similar behavior. Table VIb shows that, by increasing the proportion of TDI and consequently the content of isocyanurate groups, the conversion at the gelation, α_{gel}, increases. Taking into account these results, it can be concluded that the gelation is controlled for isocyanate trimerization to form isocyanurate. As this process occurs at very low temperatures and in very short time, it is expected that this kind of materials have a very short pot-life and reduced processability.

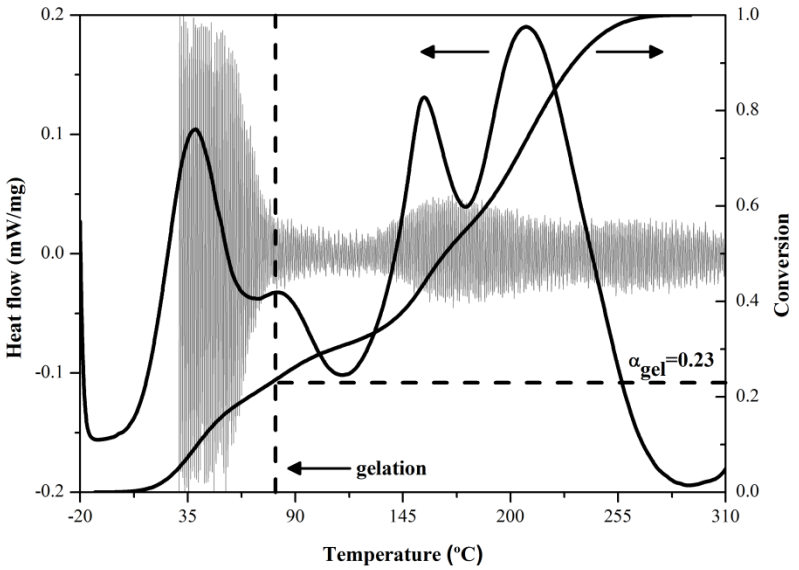

Figure 4. DSC thermograms and conversion for the DGEBA:TDI 1:1 formulation catalyzed with 1 phr of BDMA. TMA thermogram (derivative length in μm·s^{-1} versus temperature) in blue color and determination of gelation are also included.

It is also noticeable that in the region where the second and third exotherm appear the material becomes slightly more deformable, which can be related to the disappearance of isocyanurates and the corresponding formation of linear oxazolidone units.

Table VIb shows how an increase in the amount of TDI produces an unwanted increase in the global shrinkage. This increase can be related with the reaction processes taking place during curing. In general, all reactive processes lead to shrinkage because the van der Waals distances between monomers convert into covalent bonds in the final material. Taking into account this criterion, it is expected the following order in the shrinkage: isocyanurate formation > oxazolidone formation > etherification, due to the fact that in isocyanurate formation three molecules react forming three new linkages; in oxazolidone formation two molecules react forming two new bonds, whereas in epoxy homopolymerization a bond is broken simultaneously to the formation of another one. Consequently, the higher shrinkage observed in 1:2 formulation than in 2:1 formulation can be related with the higher content of isocyanurate groups in TDI-rich formulation.

The fact that most of the shrinkage (related with formation of isocyanurate) takes place before gelation is beneficial for the material because shrinkage only produces internal stresses if it is generated in the solid state (after gelation).

Thermal stability

Figure 5 shows the thermogravimetric curves in nitrogen atmosphere of the DGEBA:TDI samples and Table VIb includes the temperature of the onset decomposition on the TGA calculated at a 5% of weight loss. When the TDI proportion is increased the thermal stability of the material decreases although all formulations are very stable. It is accepted that thermosets containing heterocyclic rings, such as isocyanurate and oxazolidone, have a high thermal stability [5]. Taking into account the final composition of the materials (Table VIa), it seems that oxazolidone rings confer higher thermal stability than isocyanurate rings. Other factors, such as the degree of crosslinking and molecular interactions can also influence the thermal stability.

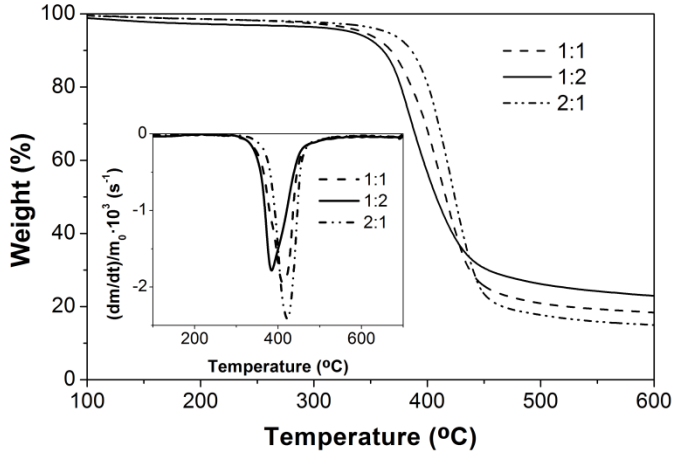

Figure 5. Thermogravimetric curves at 10 K·min^{-1} under nitrogen atmosphere for DGEBA:TDI formulations catalyzed by 1 phr of BDMA. The inset shows the rate of mass loss versus temperature.

Dynamomechanical properties

Figure 6 shows the mechanical reaction spectra at 1 Hz for the formulations studied. As the proportion of TDI increases, the modulus-temperature curves move towards higher temperatures and the value of the relaxed modulus slightly increases (it is not possible to determine this modulus for 1:2 formulation since it appears at very high temperature, where the material begins to degrade). The tan δ curves are displaced accordingly to higher temperatures. The peak temperatures of the tan δ relaxation curve $T_{tan\ \delta}$, which can be often used as a measure of $T_{g\infty}$, are somewhat higher than the calorimetric $T_{g\infty}$, as seen in Table VIa. The behaviour of the relaxation spectra is consistent with the higher value of $T_{g\infty}$ revealed by DSC. Again, these results can be interpreted in terms of the crosslinking density and stiffness (*n* and *F* in Table VIb). Homopolymerized DGEBA and isocyanurate rings lead to an increase in the crosslinking density, whereas oxazolidone rings are chain extenders but rigid and bulky groups that hinder mobility. The final temperature of glass transition and mechanical properties are a compromise between these two effects. Moreover, crosslinking density and chain stiffness also affect the damping behaviour, which is related to the area under the loss tan δ curve. These areas have not been numerically evaluated, but the evolution can be qualitatively appreciated in the figure.

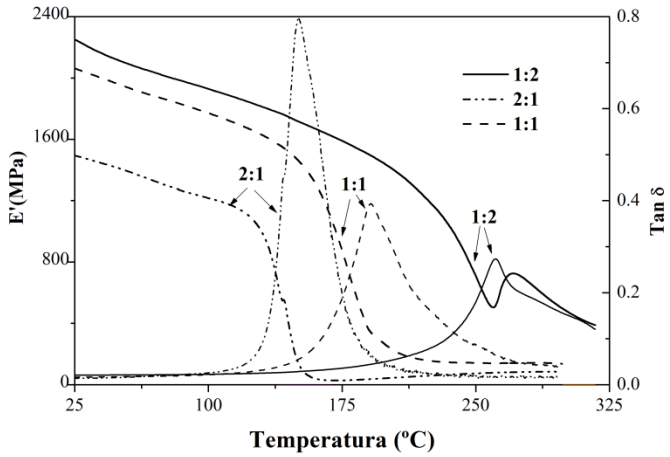

Figure 6. Temperature dependence of tan δ and storage modulus at 1 Hz for the DGEBA:TDI formulations catalyzed with 1 phr of BDMA.

Conclusions

The curing of DGEBA with TDI using a tertiary amine as catalyst leads to materials with oxazolidone, isocyanurate and ether groups in the chemical structure of the network. The initial composition of the formulation, the curing conditions and the catalyst used are the parameters that control the final structure of the network formed, the evolution of the curing and the final properties of the thermosets. The modification of these parameters allows obtaining tailor-made materials with the desired characteristics.

At low temperature (below 100 ºC) isocyanurate formation, that controls the gelation, is the only reaction taking place. At intermediate temperatures (between 110 and 190 ºC) two reactions compete, oxazolidone formation and epoxy homopolymerization and at high temperatures (above 190 ºC) isocyanurate decomposition to form oxazolidone rings is the main reaction taking place although thermal epoxy homopolymerization can also occur. When BDMA is

used as the catalyst in the curing of DGEBA:TDI formulations, the zwitterion formed between tertiary amine and isocyanate is the only active species.

Isocyanurate-rich formulations have higher glass transition temperature and shrinkage, whereas the formation of oxazolidone increases the thermal stability. The content in ether linkages, even in TDI-rich formulation, is another factor that tunes the properties and should be taken into account to establish the structure-properties relationship.

Acknowledgements

The authors would like to thank MICINN (Ministerio de Ciencia e Innovación) and FEDER (Fondo Europeo de Desarrollo Regional) (MAT2008-06284-C03-01 and MAT2008-06284-C03-02) and to the Comissionat per a Universitats i Recerca del DIUE de la Generalitat de Catalunya (2009-SGR-1512). M.F. acknowledges the grant FPI-2009 from the Spanish Government.

References

[1] In Epoxy Resin Chemistry and Technology, May. C.A.; Tanaka GY., Eds.; Marcel Dekker: New York, 1973.

[2] Bagheri, R.; Marouf, B.T.; Pearson, R.A. J Macromol Sci Part C Polym Rev 2009, 49, 201.

[3] Fernández-Francos. X.; Foix, D.; Serra, A.; Salla, J.M.; Ramis, X. React Funct Polym 2010, 70, 798.

[4] Foix, D.; Fernández-Francos, X.; Salla, J.M.; Serra, A,; Morancho, J.M.; Ramis, X. Polym Int 2010, 60, 389.

[5] Chian, K.S.; Yi, S. J Appl Polym Sci 2001, 82, 879.

[6] Caille, D.; Pascault, J.P.; Tighzert, L. Polym Bull 1990, 24, 23.

[7] Senger, J.S.; Yilgor, I.; McGrath, J.E. J Appl Polym Sci 1989, 38, 373.

[8] Kordomenos, P.I.; Frisch, K.C.; Kresta, J.E. Macromolecules 1987, 20, 2077.

[9] Caille, D.; Tighzert, L.; Pascault, J.P.; Grenier-Loustalot, M.F.; Grenier, P. Polym Networks Blends 1993, 3, 155.

[10] Galante, M.J.; Williams, R.J.J. J Appl Polym Sci 1995, 55, 89.

[11] Dabi, S.; Zilkha, A. Eur Polym J 1980, 17, 35.

[12] Lee, Y.S.K.; Hodd, K.; Wright, W.W.; Barton, J.M. British Polym J 1990, 22, 97.

[13] González, S.; Fernández-Francos, X.; Salla J.M.; Serra, A.; Mantecón, A.; Ramis, X. J Appl Polym Sci 2007, 104, 3406.

[14] Fernández-Francos, X.; Ramis, X.; Salla, J.M. Thermochim Acta 2005, 438, 144.

[15] Vazquez, A., Bentaleb, D., Williams, R.J.J. J Appl Polym Sci 1991, 43, 967.

[16] Okumoto, S.; Yamabe, S. J Com Chem 2001, 22, 316.

[17] Ivin, K.J. In Polymer Handbook, Brandrup, J.; Immergut, E.H., Eds.; Wiley: New York, 1987.

[18] Vyazovkin, S. Int Rev Phys Chem 1995, 14, 355.

[19] Fernández-Francos, X.; Salla, J.M.; Mantecón, A.; Serra, A.; Ramis, X. J Appl Polym Sci 2008, 109, 2304.

[20] Pascault, J.P.; Sautereau, H.; Verdu, J.; Williams, R.J.J. Thermosetting Polymers; Marcel Dekker: New York, 2002, pp 282-322.

Ytterbium triflate as a new catalyst on the curing of epoxy-isocyanate based thermosets

Marjorie Flores,[a] Xavier Fernández-Francos,[a] Josep M. Morancho,[b] Àngels Serra,[a] Xavier Ramis[b]

[a] Departament de Química Analítica i Química Orgànica, Universitat Rovira i Virgili, Marcel·lí Domingo s/n, 43007 Tarragona, Spain
[b] Laboratori de Termodinàmica, ETSEIB, Universitat Politècnica de Catalunya, Diagonal 647, 08028 Barcelona, Spain

Abstract

Networks containing oxazolidone, isocyanurate, urethane, allophanate and ether groups were prepared by copolymerization of mixtures of diglycidylether of bisphenol A and toluene-2,4-diisocyanate in presence of ytterbium triflate. It has been demonstrated that ytterbium triflate promotes six elemental reactions that coexist during curing and yield the aforementioned groups. Changes during curing, fraction of different groups present in the network and final properties of the cured materials were investigated by thermal analysis and infrared spectroscopy. The influence of the molar ratio of isocyanate to epoxide groups on the properties and curing has been studied. The curing kinetics were analyzed by means of an integral isoconversional non-isothermal procedure. The results obtained were compared with those obtained by using a common catalyst such as the benzyldimethylamine. The structure and the properties of the resulting thermosets are controlled by the initial composition of the formulation and the catalyst used.

Key words: *Epoxy resins, isocyanurate, oxazolidone, urethane, allophanate, ytterbium triflate*

Introduction

Epoxy resins have been used increasingly in structural adhesives, composites, surface coatings, and coatings in electronics. The final properties of these materials are very much dependent on the chemical structure and degree of crosslinking of the resins' networks. Despite its great versatility, epoxy systems, containing isocyanurate-oxazolidone resins, have not become very popular in industrial applications, due to their short gel time and pot-life during curing. The formation of isocyanurate rings on the first stages of the curing is the responsible of this behaviour that reduces significantly the processability of this family of epoxy thermosets [1]. The brittle characteristic of isocyanurate rings is another factor that has limited their applications [2].

Some authors had demonstrated that the curing of diepoxide with diisocyanate using a tertiary amine as catalyst leads to materials with oxazolidone, isocyanurate and ether groups in the chemical structure of the network [3,4]. In a previous work we studied the curing of mixtures of diglycidylether of bisphenol A (DGEBA) and 4-toluene-2,4-diisocyanate (TDI) in the presence of benzyldimethylamine (BDMA) as catalyst. The formation of isocyanurate rings by trimerization of isocyanates takes place well below room temperature up to 100 ºC. Between 110 and 190 ºC, the reaction between the remaining isocyanates and epoxy groups takes place leading to oxazolidone ring formation, along with the homopolymerization of epoxy groups. Above 190ºC, isocyanurate rings can react with the excess of epoxy to give rise to oxazolidone rings, and epoxy polyetherification also takes place. The DGEBA:TDI molar ratio of the formulation, the curing conditions and the catalyst used are the parameters that control the structure of the network formed, the curing evolution and the final properties. Isocyanurate-rich formulations have high

glass transition temperature and shrinkage, whereas the insertion of oxazolidone increases the thermal stability. The most important drawback of these systems is that gelation takes place at low conversions, between 0.1 and 0.2, with a short gel time [1].

Oxazolidone formation, from diepoxides and diisocyanates, has been studied extensively in the preparation of thermally stable polymer using both Lewis acids and bases as catalysts [5,6]. On the contrary, the trimerization of isocyanate to reach isocyanurate rings is only reported in basic conditions or at elevated temperatures [3,4,7].

Urethane linkages are produced by the well-known reaction of hydroxyl and isocyanate groups. By reaction of urethane with isocyanate, a trifunctional allophanate group is formed [8,9]. In epoxy resins containing hydroxyl groups both reactions are expected if the catalyst is active enough. However, some catalysts are not very active at room temperature but improve their reactivity with the temperature. Some authors described the cationic ring opening polymerization of oxazolidones to form poly(urethanes) in the presence of cationic initiators such as Lewis acids [10].

Lanthanide triflates are Lewis acids that can act as catalysts in the cationic curing of epoxy resins. These compounds are commercially available and maintain their catalytic activity even in humid environments. Lanthanide ions have low electronegativities and strong oxophilicities, which make it possible for the metal to coordinate to the oxygens in the substrate. In previous works we polymerized epoxy resins with five-membered lactones and carbonates. We observed that lanthanide triflates, besides being able to homopolymerize epoxy resins, were active enough to promote the formation of spiroorthoesters or spiroorthocarbonates and their copolymerization with epoxide or even their homopolymerization [11-14].

In the present study, a DGEBA resin was copolymerized with TDI in the presence of ytterbium triflate. The goals of the study are: to examine the effect of a Lewis acid, ytterbium triflate, on the curing and final properties of DGEBA:TDI systems and to compare these results with those obtained by using a basic catalyst, benzyldimethylamine, in order to overcome the limitations that the use of BDMA in these formulations have on the gelation time and the processability difficulties originated thereof. To the best of our knowledge, this is the first time that lanthanide triflates have been used as catalyst in epoxy/isocyanate systems. The investigation of the influence of the molar ratio of isocyanate to epoxide groups on the curing and on the characteristics of the materials obtained is another objective of this study.

Experimental

Materials

Diglycidylether of bisphenol A (DGEBA), Epitoke Resin 828 from Hexion Speciality Chemicals (epoxy equivalent = 187 g/eq), was used after drying under vacuum. 4-Toluene-2,4-diisocyanate (TDI) from Aldrich was distilled. Ytterbium triflate ($Yb(OTf)_3$) and benzyldimethylamine (BDMA) were purchased from Aldrich and used without further purification.

Preparation of the curing mixtures

Mixtures of freshly distilled TDI and DGEBA were carefully stirred and degassed under vacuum (at 80 ºC) during 2 h to prevent the appearance of bubbles during curing. 1 phr of

catalyst (ytterbium triflate or BDMA) was added to the corresponding mixtures DGEBA:TDI at room temperature. The formulations were kept at -20 ºC before use to prevent polymerization. Table 1 shows the notation and composition of the different formulations studied.

Table 1. Notation and composition of the different formulations used in this work, in molar ratio (n:n) and equivalent ratio (eq/eq). Molar ratio is used as notation.

Formulation	DGEBA:TDI 2:1	DGEBA:TDI 1:1	DGEBA:TDI 1:2
n_{epoxy}:n_{TDI}	2:1	1:1	1:2
eq_{OH}/eq_{TDI}	0.109	0.055	0.027
Catalyst: ytterbium triflate			
eq_{Yb}/eq_{TDI}	0.00846	0.00503	0.00331
eq_{Yb}/eq_{epoxy}	0.00423	0.00503	0.00662
Catalyst: benzyldimethylamine			
eq_{BDMA}/eq_{TDI}	0.03410	0.02243	0.01335
eq_{BDMA}/eq_{epoxy}	0.01705	0.02243	0.02671

DSC calorimetry

Calorimetric analyses were carried out on a Mettler DSC-822e calorimeter with a TSO801RO robotic arm. Samples of approximately 10 mg in weight were cured in aluminium pans in a nitrogen atmosphere. Non-isothermal experiments were performed between 0 and 325ºC at heating rates of 5, 7.5, 10, and 15 ºC/min in order to determine the reaction heat and the kinetic of curing. The degree of conversion, α, at a given temperature T was calculated as the quotient between the heat released up to T and the total reaction heat associated with complete conversion of all reactive groups.

The glass transition temperatures of the fully cured materials ($T_{g\infty}$) after non-isothermal curing were determined by heating samples at 10 ºC/min up to 300 ºC by the Richardson method as specified in the Mettler STARe^{TM} software. The T_{g0} of the uncured materials was determined in a similar way from the first scan.

Kinetic analysis

Kinetic parameters of non-isothermal curing were determined using an integral isoconversional procedure named Kissinger-Akahira-Sunose (KAS):

$$\ln\left(\frac{\beta}{T^2}\right) = \ln\left[\frac{AR}{g(\alpha)E}\right] - \frac{E}{RT} \qquad (1)$$

for each conversion degree, the linear plot of $\ln(\beta/T^2)$ versus $1/T$ makes it possible to determine E from the slope without knowing the kinetic model. β is the heating rate, T the temperature, E the activation energy, A the pre-exponential factor, R the gas constant, and $g(\alpha)$ the integral conversion function. The activation energy obtained by this integral procedure represents an

average value up to a certain degree of conversion instead of the instantaneous and real value. The latter can be obtained by differential analysis of experimental data and is more sensitive to changes in the curing mechanism in complex multi-step processes. However, the occurrence of thermal degradation at high temperatures did not allow us to establish a proper baseline and perform a reliable differential analysis. In such a case the utilization of a simple integral method such as KAS is accepted [15].

FTIR/ATR spectroscopy

Cured and uncured samples were analyzed with a FTIR spectrometer Bruker Vertex 70 with an attenuated total reflection accessory with thermal control and a diamond crystal (Golden Gate Heated Single Reflection Diamond ATR, Specac-Teknokroma). Spectra were collected at 30 ºC in the absorbance mode at a resolution of 4 cm^{-1}.

The disappearance of the absorbance peaks at 915 cm^{-1} (epoxy bending) and 2260 cm^{-1} (isocyanate carbonyl) indicates that the epoxy and isocyanate groups had polymerized. The growth of the peak at 1100 cm^{-1} (C-O-C stretching of aliphatic linear ester) is related to the homopolymerization of epoxy groups. The appearance of absorption peaks at 1750 cm^{-1} (oxazolidone carbonyl), 1730 cm^{-1} (urethane-allophanate carbonyl) and 1710 cm^{-1} (isocyanurate carbonyl) show the formation of oxazolidone, urethane-allophanate and isocyanurate groups. The peaks at the carbonyl region were deconvoluted using Gaussian-Lorentzian functions using the OPUS^{TM} software. The increase in the peak at 1410 cm^{-1} also indicates the formation of isocyanurate groups. It was assumed that all hydroxyl groups coming from DGEBA first react with isocyanates to form urethanes and, later on, part of these urethane groups can react with a second isocyanate to form an allophanate group. The peak at 830 cm^{-1} (*p*-phenylene), which should not change during the curing process, was chosen as an internal standard.

Conversions (formation or disappearance) of the different reactive groups, epoxide, isocyanate, isocyanurate urethane-allophanate and oxazolidone, were determined by the Lambert-Beer law from the normalized changes of absorbance at 915, 2260, 1710, 1730 and 1750 cm^{-1}, respectively. Maximum normalized absorbance of isocyanurate, oxazolidone and urethane-allophanate were determined in formulations where isocyanate groups were completely transformed in isocyanurate, oxazolidone or urethane-allophanate groups. Maximum normalized absorbance of isocyanate and epoxy groups were determined from the initial spectrum of mixtures without initiator.

Thermomechanical analysis (TMA)

Thermal mechanical analysis was carried out in a nitrogen atmosphere using a Mettler TMA40 thermomechanical analyzer. The samples were supported by two small circular ceramic plates and silanized glass fibres, which were impregnated with the sample. Non-isothermal experiments were performed between 30 and 325 ºC at heating rate of 5 ºC/min applying a periodic force that changed (cycle time=12 s) from 0.0025 N to 0.01 N. When the material reaches sufficient mechanical stability (gelation) the TMA measuring probe is not able to deform the sample and the amplitude of the oscillations is reduced. The gel point was taken in TMA as the temperature at which a sudden decrease in the amplitude of oscillations was observed. This temperature, T_{gel}, is proportional to the gel time and has been used to establish which formulation reacts more quickly. The gel conversion, α_{gel}, was determined as the DSC conversion at 5 ºC/min at the temperature of T_{gel} [16]. Gelation and kinetic analysis were not performed in isothermal

conditions since at high temperatures the formulations can gel during stabilisation of the apparatus and at low temperatures the heat is released slowly and it can fall below the DSC's sensitivity range. Moreover non-isothermal conditions permit the observation of the progressive activation of the different reactive processes.

Thermogravimetric analysis (TGA)

Thermogravimetric analysis was carried out in a nitrogen atmosphere with a Mettler-Toledo TGA-50 thermobalance. Non-isothermally cured samples with an approximate mass of 5 mg were degraded between 40 and 600 ºC at a heating rate of 10 ºC/min in a nitrogen atmosphere. A blank curve with an empty crucible was run prior to the measurement with the sample in the same crucible. The blank curve was then substracted from the sample curve. For the determination of temperatures at 5% of mass loss two samples were analyzed and the results were averaged.

Results and discussion

Curing mechanism

According to certain authors and our previous results [1-9], Scheme 1 depicts the reactions expected in the curing process of DGEBA:TDI formulations in the presence of ytterbium triflate: a) trimerization of isocyanate to give rise to isocyanurate rings, b) epoxy-isocyanate reaction leading to oxazolidone rings, c) hydroxyl-isocyanate reaction forming urethane groups, d) ring-opening polymerization of oxazolidone rings to polyurethanes, e) allophanate formation from urethane and isocyanate groups, f) epoxy homopolymerization and g) isocyanurate decomposition and reaction with epoxy groups producing oxazolidone rings.

The formation of polyurethanes by polymerization of oxazolidone rings (reaction d) has only been described in special conditions [10] and it will not be considered in this work. As the reaction c) leads to the same linkages than reaction d), the discussion in the manuscript would still be true in case reaction d) takes place.

Samples with different DGEBA:TDI ratios were non-isothermally cured at different heating rates with 1 phr of $Yb(OTf)_3$ in the DSC. Figure 1 shows the thermogram at 10 ºC/min for the 2:1 formulation and includes the thermogram of the same formulation but catalyzed by BDMA for comparison purposes. The thermogram of the formulation with $Yb(OTf)_3$ exhibits four well-defined but overlapping exothermic peaks, centered at 75 (broad), 110, 168 and 275 ºC. The evolution of functional groups and, indirectly, the development of the network structure, can be followed by observing the changes in their FTIR absorption spectra during the non-isothermal cure. Typical spectra are shown in Figure 2 for 2:1 formulation reacted in the DSC up to temperatures of 90, 130, 200, 280 and 315 ºC. These temperatures were selected since they correspond to the final of each exothermic peak or close to the maximum of the main exotherm in the case of 280 ºC. The evolution of the different functional groups during curing for the 2:1 formulation is collected in Table 2.

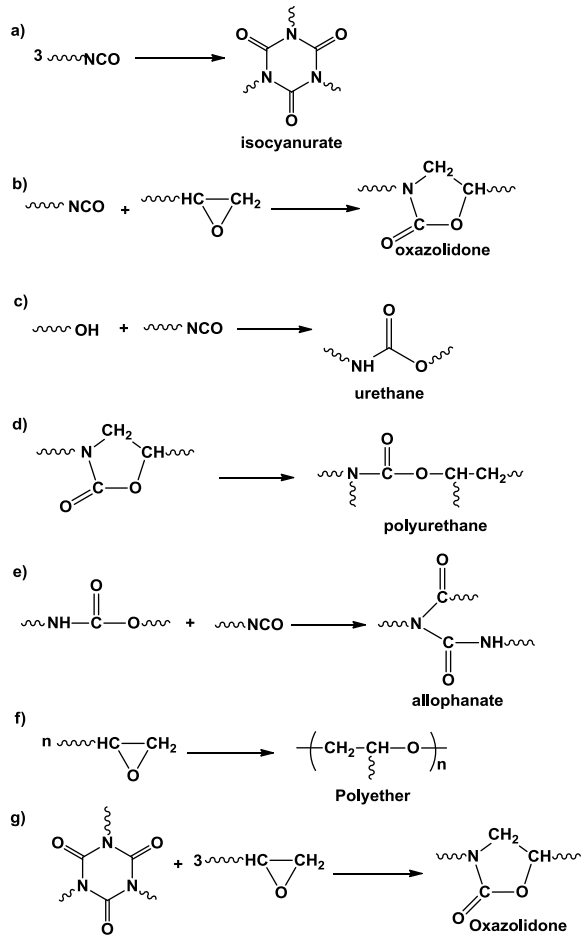

Scheme 1. Reactions expected in the curing process of DGEBA:TDI formulations in the presence of ytterbium triflate.

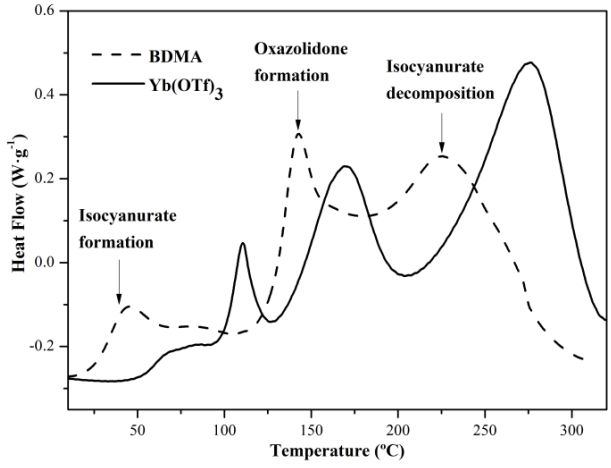

Figure 1. DSC thermograms of the DGEBA:TDI 2:1 formulation cured with 1 phr of $Yb(OTf)_3$ or BDMA. With BDMA the main reactions taking place are also indicated.

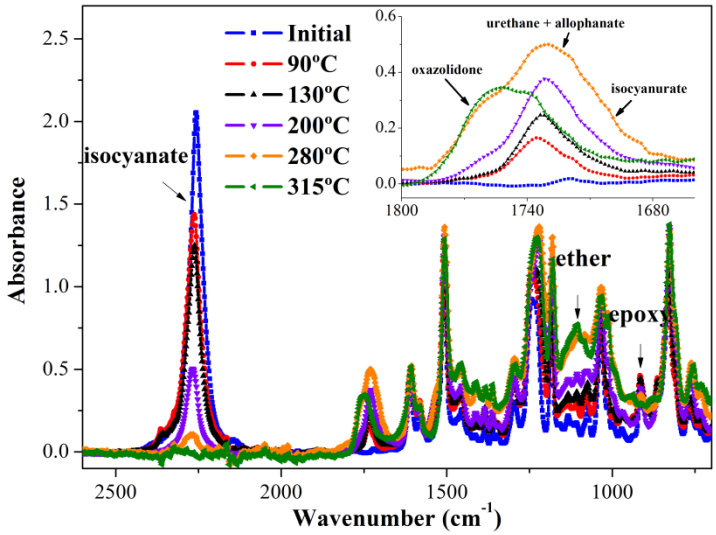

Figure 2. FTIR spectra of some selected samples of the DGEBA:TDI 2:1 formulations with 1 phr of $Yb(OTf)_3$ taken during the dynamical curing in the DSC. Initial FTIR spectrum before curing is included as the reference. The inset shows a magnification of carbonyl region.

The first exotherm (up to 90 ºC) is related with urethane formation by reaction between hydroxyl groups of DGEBA and isocyanates and with the formation of allophanate groups by reaction between urethanes previously formed and isocyanates. During the second exothermic peak (between 90 and 130 ºC), the formation of more allophanate groups takes place. The appearance of a stretching vibration of the N-H group at 3375 cm^{-1} confirms the presence of urethane linkages (figure not shown). The same absorption appears for allophanate structures and therefore it is no possible differentiate them from urethanes, since both have also a carbonyl absorption at 1730 cm^{-1}. Thus, we have supposed that, hydroxyl groups react first with isocyanates to form urethanes and when hydroxyl groups are exhausted, urethanes previously formed react with isocyanates to form allophanates. This hypothesis is consistent with the accepted idea that allophanates can be obtained by heating urethanes in presence of isocyanates [17]. Taking into account the initial composition (Table 1), a 10.9% (hydroxyl content) of the initial isocyanate is the maximum amount of urethane that can be formed in 2:1 formulation. The formation of oxazolidone and isocyanurate rings does not take place during the first and the second peak (up to 130 ºC), because $Yb(OTf)_3$ is not enough active in this range of temperature to promote these reactions. On the contrary, epoxy homopolymerization can occur in this range. This fact is coherent with the known ability of lanthanide triflates, even in very little proportions, to crosslink epoxide resins at moderate temperature [13].

The main reaction taking place in the third exothermic peak (up to 200 ºC) is the formation of isocyanurate rings, although a small number of oxazolidone, allophanate and ether groups are also formed.

The last exothermic peak is the result of a complex reactivity, probably due to the existence of thermally activated, non-catalyzed reactions at high temperatures. Initially the formation of oxazolidone rings by reaction between isocyanate and epoxy groups is the most favoured reaction, but isocyanurate formation also takes place to a lesser extent. At very high

temperatures (above 280 ºC) the decomposition of isocyanurate rings to produce oxazolidones and the epoxy homopolymerization are the most important processes. Probably, these latter reactions are thermally activated instead of being activated by $Yb(OTf)_3$.

Table 2. Evolution of the content of different groups for the 2:1 DGEBA:TDI formulation during non-isothermal curing up to different temperatures as determined by FTIR spectroscopy.

T (ºC)	Isocyanate[a] (%)	Epoxy[a] (%)	Urethane[b] (%)	Allophanate[b] (%)	Oxazolidone[b] (%)	Isocyanurate[b] (%)	Ether[c] (%)
Initial	100	100	0.0	0.0	0	0	0
90	81	73	10.9	8.1	0	0	27
130	69	63	10.9	20.1	0	0	37
200	39	55	10.9	22.1	6	22	42
280	0	44	10.9	27.1	28	34	42
315	0	0	10.9	29.1	52	9	74

[a] % of unreacted isocyanate and epoxide.
[b] % of urethane, allophanate, oxazolidone, isocyanurate linkages formed with respect to the initial isocyanate.
[c] % of ether (epoxy homopolymerized) linkages formed with respect to the initial epoxy content.

Despite the fact that it is difficult to establish the order in which the many different competitive reactions occur, it can be tentatively established that the main reactions that take place, in order of increasing temperature are the following: the formation of urethane, allophanate, isocyanurate and oxazolidone moieties and the decomposition of isocyanurate groups. Epoxy homopolymerization can occur at relatively low temperatures ($Yb(OTf)_3$-catalyzed reaction) or at higher temperatures (un-catalyzed reaction).

In Figure 1 the main reactions that take place in each exothermic peak of the curing of DGEBA:TDI 2:1 formulation catalyzed by 1 phr of BDMA (identified by FTIR) are also shown [1]. Although DSC traces of formulations catalyzed by $Yb(OTf)_3$ and BDMA are quite similar, the reactions that take place and their reaction temperature ranges are very different. By using BDMA as catalyst, isocyanurate formation begins at room temperature and urethane and allophanate formation are not observed. At intermediate temperatures oxazolidone formation occurs and at high temperatures the isocyanurate decomposition is observed. In a 2:1 formulation all isocyanate groups have reacted and transformed into oxazolidone (88%) and isocyanurate rings (12%) [1]. This result is very different from that obtained by using $Yb(OTf)_3$ catalyst (Table 2). Therefore, it is expected that both materials show significantly different properties.

Curing kinetics

DGEBA:TDI mixtures of different composition were cured with 1 phr of $Yb(OTf)_3$ at several heating rates in the DSC in order to characterize the curing kinetics. By means of calorimetric tests and by FTIR of samples dynamically cured by DSC, it was proved that both the epoxy and isocyanate groups had reacted completely, since no residual heat was observed by DSC and FTIR showed that the characteristic bands associated with epoxy and isocyanate groups had disappeared completely. Due to the complexity of the curing process, as it was explained in the experimental section, the kinetics of non-isothermal curing was studied by

Kissinger-Akahira-Sunose procedure. Figure 3 shows the calorimetric and conversion curves of DGEBA:TDI 1:1 formulation at different heating rates. As expected, on increasing the heating rate the curves shifted to higher temperatures. As it was discussed in Figure 1 the shape of the curves is complex due to the concurrence between different reactive processes. DSC traces of other formulations show similar patterns to the ones shown in Figure 3.

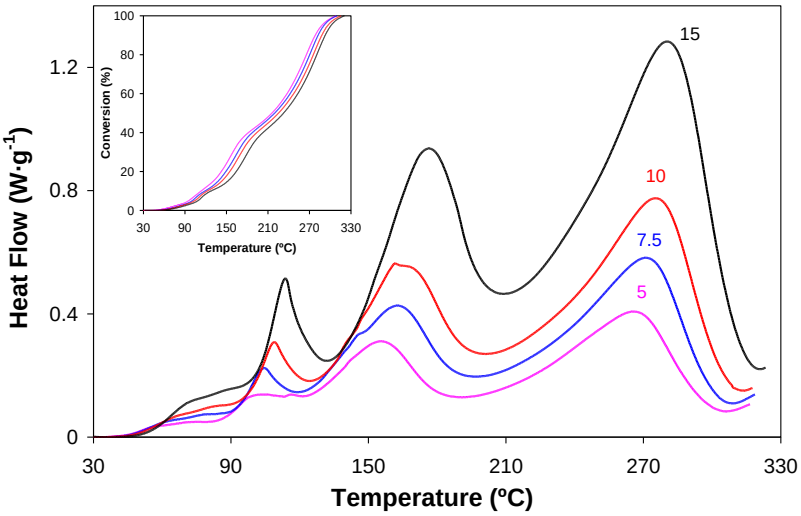

Figure 3. DSC scans at different heating rate of the non-isothermal curing for the DGEBA:TDI 1:1 formulation catalyzed by 1 phr of $Yb(OTf)_3$ (indicated in the figure in ºC·min^{-1}). The inset shows the conversion versus temperature curves at the same heating rates.

Figure 4 shows, as an example, the dependence of activation energy and reaction rate on the degree of conversion for DGEBA:TDI 1:1 formulation catalyzed by 1 phr of $Yb(OTf)_3$. The DSC trace can be divided into three regions, each one with a corresponding level of activation energy. The first region, at low conversions/temperatures, has an average activation energy of 87.8 kJ·mol^{-1} that can be associated fundamentally with the formation of urethane and allophanate linkages. Epoxy homopolymerization catalyzed by $Yb(OTf)_3$, which can also take place in this region, has an activation energy close to 70 kJ·mol^{-1} [12,13,16] and does not contribute significantly to the global value of 87.8 kJ·mol^{-1}. In the second region the activation energy is practically constant (average activation energy of 56.8 kJ·mol^{-1}) and can be related with isocyanurate formation, which is the main process taking place. In the third region, activation energy is relatively constant at the beginning but increases strongly as conversion increases. Along with the formation of oxazolidone, which is the main reaction that occurs initially in this peak, thermal activated reactions such as isocyanurate rings decomposition and the epoxy homopolymerization take place at higher conversions, increasing the activation energy from 85 to 109 kJ·mol^{-1}. Although we are aware that it is not possible to assign a constant activation energy in this region, tentatively and for the purpose of comparison, we have attributed an average activation energy of 66.3 kJ·mol^{-1} for the oxazolidone formation process (0.5-0.7 conversion range).

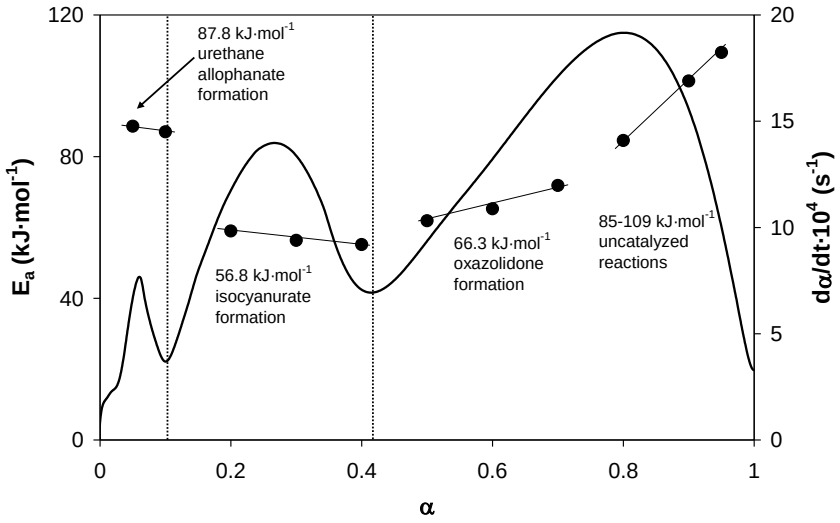

Figure 4. Dependence of activation energy (symbols) and reaction rate (line) on the degree of conversion for the DGEBA:TDI 1:1 formulation initiated by 1 phr of $Yb(OTf)_3$.

In general, the activation energies obtained for other formulations (2:1 and 1:2) are similar and the discussion of their evolution during curing is equivalent than for 1:1 formulation.

In a previous work [1], using BDMA as catalyst of DGEBA:TDI systems, we had determined activation energy values of 11.3, 23.7 and 37.4 $kJ \cdot mol^{-1}$ respectively for isocyanurate and oxazolidone formation and isocyanurate decomposition (see Figure 1). These low values contrast with the higher values obtained by using $Yb(OTf)_3$ and represent a significant difference between BDMA and $Yb(OTf)_3$ in terms of curing kinetics and network development, as seen in the previous section.

Effect of the stoichiometry

In order to study the influence of the stoichiometry on the curing and on the final properties, samples with different DGEBA:TDI ratios were dynamically cured at 10 $^{o}C \cdot min^{-1}$ in the presence of 1 phr of $Yb(OTf)_3$ and the composition of the cured networks was determined by FTIR. Figure 5 shows the FTIR spectra of the different thermosets obtained and Table 3 collects the compositions determined from them. It can be observed that an excess of isocyanate favours isocyanurate and oxazolidone formation, whereas an excess of epoxy favours the polyetherification (epoxy homopolymerization) and the formation of urethane-allophanate groups. Urethane and allophanate formation are conditioned by the hydroxyl content and consequently by the amount of epoxy resin. Given the limited amount of hydroxyl groups initially present in the mixture, we hypothesize that the relatively high amount of allophanate groups can be explained by the subsequent reaction of the N-H of the allophanate with another isocyanate giving rise to a poly(allophanate) structure (not shown in Scheme 1). However, when the temperature is increased $Yb(OTf)_3$ is more active as a catalyst for isocyanurate formation or even for oxazolidone formation than for allophanate propagation.

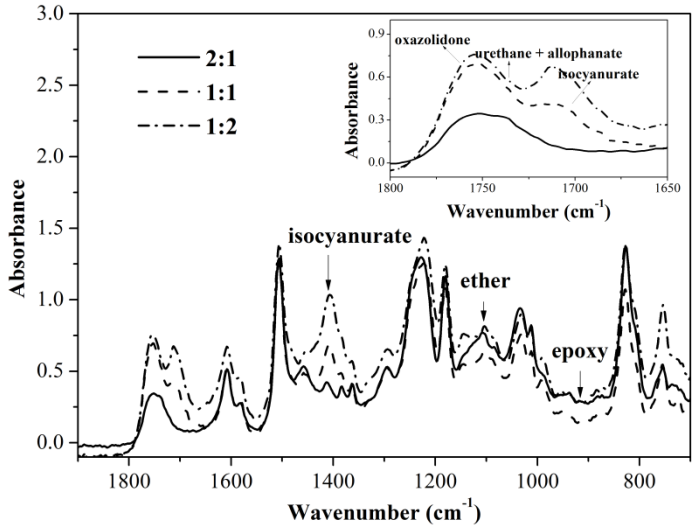

Figure 5. FTIR spectra of the thermosets obtained from the different DGEBA:TDI formulations with 1 phr of $Yb(OTf)_3$ after a dynamic curing in DSC. The inset shows a magnification of the carbonyl region.

All these results contrast with those obtained previously using BDMA as catalyst [1]. In that case an isocyanate excess led to isocyanurate-rich structures and oxazolidone formation could hardly occur. On the contrary, an excess of epoxy favoured the formation of oxazolidone. With BDMA, epoxy homopolymerization could also take place but only at high temperatures, and urethane and allophanate groups formation did not occur because isocyanate trimerization, catalyzed by the tertiary amine, was by far the most favourable reaction even at low temperatures.

Therefore, it seems that the initial composition of the formulation and the type of catalyst used are the parameters that control the final structural composition of the network. These significant changes in network composition and structure undoubtedly have an effect on the final properties of the thermosets.

Table 3 Composition (%) in the final network after non-isothermal curing determined by FTIR for the formulations cured with 1 phr of $Yb(OTf)_3$.

Formulation	Oxazolidone (%)	Isocyanurate (%)	Urethane (%)	Allophanate (%)	Ether (%)
DGEBA:TDI 2:1	20.5	3.6	4.1	12.0	59.8
DGEBA:TDI 1:1	26.8	22.1	3.2	11.4	36.5
DGEBA:TDI 1:2	36.7	42.7	2.3	9.5	9.1

Tables 4a and 4b show thermal properties, crosslinking density, *n*, and stiffness, *F*, for the DGEBA:TDI formulations cured using 1 phr of $Yb(OTf)_3$. In order to calculate the crosslinking density *n* we have considered that three isocyanate groups that react to produce an isocyanurate group constitute a single crosslink. In addition, homopolymerized epoxy, allophanate and urethane groups contribute each one with a single crosslink. In contrast, oxazolidone rings

produce linear structures which do not contribute to the crosslinking density. The stiffness *F* of the crosslinking points in the network structure was calculated according to the procedure described by Pascault *et al*. [18], considering all the possible strands emanating from each crosslinking point. By increasing the proportion of TDI, the $T_{g\infty}$ strongly increases initially, but then slightly decreases, whereas the $\Delta C_{p\infty}$ shows the opposite trend. These results cannot be understood only in terms of the degree of crosslinking. Despite the increase in the proportion of isocyanurate rings when the TDI content is increased, the decrease in the amount of homopolymerized epoxy groups is dramatic and the proportion of linear oxazolidone moieties also increases (see Table 3), leading to a significant overall reduction in the crosslinking density. In addition to the degree and the type of crosslinks, the rigidity of the chains between the different crosslinking points in the final network should be considered [1,18]. The increase in the amount of TDI increases the stiffness of strands between crosslinking points because of 1) the formation of rigid isocyanurate and allophanate structures with short and rigid strands between crosslinks, 2) the increase in the amount of rigid linear oxazolidone chains and 3) the decrease in the amount of flexible polyether chains resulting from epoxy homopolymerization. The stiffness of the crosslinks increases in the following order: polyether, urethane, allophanate and isocyanurate. The contributions of both allophanate and isocyanurate are the most relevant in terms of stiffness as the TDI content increases, especially the latter, according to Table 4b. The final properties of the materials are a compromise between the effects of the crosslinking density and the chain stiffness, which can contribute to increase or decrease the glass transition temperature of the materials. In this work the DGEBA:TDI 1:1 formulation shows the highest glass transition temperature but medium *n* and *F* values. On the contrary, the 2:1 formulation, which has the lowest TDI amount, has the highest crosslinking density but the lowest $T_{g\infty}$ because of the stronger effect of its lower overall stiffness.

Table 4a. Calorimetric data for the formulations cured with 1 phr of $Yb(OTf)_3$

Formulation	T_{g0} [a] (ºC)	ΔC_{p0} [b] ($J \cdot g^{-1} \cdot K^{-1}$)	$T_{g\infty}$ [a] (ºC)	$\Delta C_{p\infty}$ [b] ($J \cdot g^{-1} \cdot K^{-1}$)
DGEBA:TDI 2:1	-24	0.59	125	0.31
DGEBA:TDI 1:1	-29	0.56	217	0.15
DGEBA:TDI 1:2	-46	0.55	205	0.22

[a] Glass transition temperatures before and after isothermal curing obtained by DSC at 10 ºC·min^{-1}.
[b] Difference in the heat capacity when the material changed from glassy to the rubbery state before and after isothermal curing obtained by DSC at 10 ºC·min^{-1}.

Table 4b. Crosslinking density, chain stiffness and contribution of the different groups to the total stiffness for the formulations cured with 1 phr of $Yb(OTf)_3$.

Formulation	n [a] ($mol \cdot kg^{-1}$)	F [b] ($g \cdot mol^{-1}$)	$F_{isocyanur}$ [c] ($g \cdot mol^{-1}$)	$F_{allophanr}$ [c] ($g \cdot mol^{-1}$)	$F_{urethane}$ [c] ($g \cdot mol^{-1}$)	F_{epoxy} [c] ($g \cdot mol^{-1}$)
DGEBA:TDI 2:1	4.2	26.6	1.0	6.1	1.7	17.8
DGEBA:TDI 1:1	3.4	33.5	8.9	8.0	1.9	14.7
DGEBA:TDI 1:2	2.1	50.1	29.8	11.5	2.4	6.4

[a] Average crosslinking density, *n*, calculated assuming that homopolymerized DGEBA leads to two trifunctional crosslinks and each isocyanurate ring (3 isocyanate groups), urethane linkage and allophanate group forms another trifunctional crosslink.
[b] The total chain stiffness, *F*, has been calculated considering the composition and the contribution of the different crosslinks and different chains present in the network as explained by Pascault *et al.* [18].
[c] Chain stiffness contribution of the different groups to the total chain stiffness *F*.

In a previous work using BDMA as the catalyst of DGEBA:TDI systems [1], we could see that on increasing the TDI content the $T_{g\infty}$ increased accordingly, reaching higher $T_{g\infty}$ values than in the present study. In that case, it was observed that both the crosslinking density and the chain stiffness increased with the TDI content, especially by the increasing contribution of isocyanurate rings caused by the early trimerization of isocyanate into isocyanurate rings at the very beginning of the process. These differences illustrate the importance of the choice of the initiator in the composition and properties of the resulting networks.

Gelation

In order to assess the processability of the DGEBA:TDI formulations we determined the gelation by means of TMA and DSC. As an example in Figure 6 the gelation calculation method for the 2:1 formulation catalyzed by 1 phr $Yb(OTf)_3$ is represented. The materials were cured at 5 $^{o}C \cdot min^{-1}$ in TMA and DSC and the TMA derivative signal and DSC traces overlapped. Gelation is seen as a sudden reduction in the oscillation amplitude of the TMA derivative signal. It can be seen how the gelation takes place at the first part of the third exothermal peak. According to Table 2 data, we can state that urethane and allophanate formation and DGEBA homopolymerization are mainly the reactions that control the gelation. This behaviour is similar for all the formulations studied. When BDMA was used as the catalyst, the gelation was controlled for the isocyanate trimerization that took place at the beginning of the curing process [1].

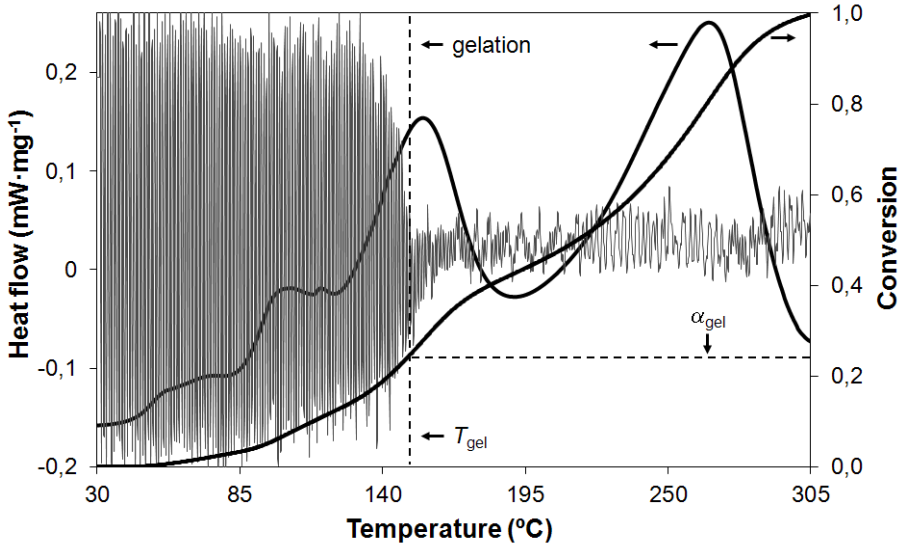

Figure 6. DSC thermograms and conversion curves for the DGEBA:TDI 2:1 formulation initiated with 1 phr of $Yb(OTf)_3$. TMA thermogram (derivative length in $\mu m \cdot s^{-1}$ versus temperature) in blue color and determination of gelation are also included.

Table 5 shows the temperature of gelation of the material calculated by TMA, T_{gel}, for formulations catalyzed by $Yb(OTf)_3$ or BDMA. It can be observed as gelation takes place at much higher temperature in formulations catalyzed by $Yb(OTf)_3$. The different reactivity induced for both catalysts, especially in the initial step of the curing, is the responsible of this behaviour. As a

conclusion of these results, it can be stated that $Yb(OTf)_3$ catalyzed formulations have longer pot-life and easier processability than those catalyzed by BDMA.

Table 5. Thermogravimetric and gelation data of the studied systems.

Formulation	$Yb(OTf)_3$		BDMA	
	T_{gel} (ºC)	$T_{5\%}$ (ºC)	T_{gel} (ºC)	$T_{5\%}$ (ºC)
DGEBA:TDI 2:1	148	263	70	373
DGEBA:TDI 1:1	135	334	67	356
DGEBA:TDI 1:2	150	342	69	344

Gel conversions, α_{gel}, were determined according to the procedure described in the experimental part. Formulations with $Yb(OTf)_3$ showed, depending on the formulation, α_{gel} from 0.2 to 0.24 without any regular trend. α_{gel} varied from 0.12 to 0.24 in BDMA catalyzed formulations. It is difficult to relate these data to the chemistry of the curing because of the multiple reactive processes, which take place before gelation.

Thermal stability

In order to study the thermal stability of DGEBA:TDI mixtures, non-isothermal cured samples of the different materials were thermally degraded in nitrogen atmosphere. Figure 7 collects the TGA curves of the formulations 2:1, 1:1, and 1:2 catalyzed by ytterbium triflate. As the proportion of TDI increases, the thermal stability increases. Formulation 2:1 shows a clearly lower stability.

It is known that urethane and allophanate groups are thermolabiles. The reported upper stability temperature of urethane groups varies from 120 to 250 ºC depending on the type of urethane linkages [19]. Allophanates can dissociate, ending in the reformation of urethane and isocyanate through the reverse of reaction c) (Scheme 1). The thermal stability of allophanates depends on the type of structure and on the temperature. Some authors had reported the allophanate dissociation in a considerable extension at 130-150 ºC [20]. Other authors reported that allophanate dissociation is measurable above 100 ºC [8].

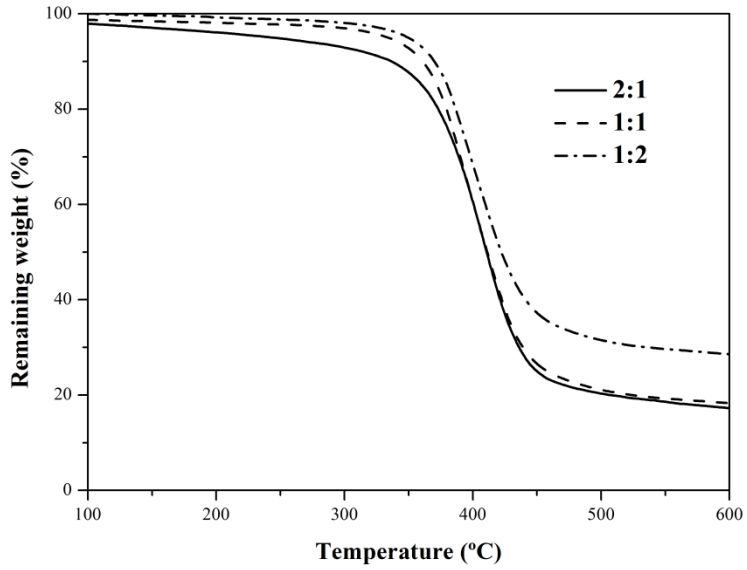

Figure 7. Thermogravimetric curves at 10 K/min under nitrogen atmosphere for the DGEBA:TDI formulations initiated by 1 phr of $Yb(OTf)_3$.

Although isocyanurate and oxazolidone rings are well known for their thermal stabilities [2], authors do not agree in which of both rings is the most thermal stable. According to Kodormenos *et al.* [21] the thermostability of the groups increases in the following order: urethane < oxazolidone < isocyanurate. Chian et al. [2] claimed the highest thermal stability of oxazolidones in front of isocyanurates. Indeed, we reported that oxazolidone-rich formulations had higher thermal stability than isocyanurate-rich formulations [1]. These results suggest that the thermal stability of both groups, oxazolidone and isocyanurate, is strongly influenced by the neighbouring substituents and by the structure.

According to our data, the high content of urethane-allophanate linkages in the DGEBA:TDI 2:1 formulation, coupled with the low proportion of stable isocyanurate and oxazolidone groups, is probably responsible for their low thermal stability. On the contrary, in TDI-rich formulations the higher stability can be due to the high content of oxazolidone and isocyanurate structures.

Table 5 summarizes the temperature of the onset decomposition at 5% of weight loss for DGEBA:TDI mixtures cured by using $Yb(OTf)_3$ or BDMA as catalyst. It can be seen that the materials obtained with $Yb(OTf)_3$ are thermally more degradable. This behaviour could be attributed to two different effects: the existence of urethane-allophanate groups in the network and a greater catalytic activity of ytterbium triflate that facilities the rupture of the more labile linkages, due their coordination ability to oxygen atoms [22,23]. In a previous manuscript we reported that the thermal stability of formulations with BDMA decreases when TDI content increases, which was related with the lower content of oxazolidone rings in TDI-rich formulations [1]. In the present case, on increasing the TDI content the presence of oxazolidone moieties increases as well, thus increasing the thermal stability. Despite the inverse trends with respect to the TDI content, the effect is very similar in both cases because the increase in thermal stability can be explained by the higher presence of stable oxazolidone and isocyanurate moieties.

Conclusion

Networks containing oxazolidone, isocyanurate, urethane, allophanate and ether groups can be obtained by using ytterbium triflate as catalyst of diglycidylether of bisphenol A and toluene-2,4-diisocyanate mixtures.

Ytterbium triflate promotes, in order of increasing temperature, the following reactions: urethane and allophanate formation, isocyanate trimerization and oxazolidone formation. Epoxy homopolymerization is activated by ytterbium triflate at moderate temperatures. At very high curing temperatures, both epoxy homopolymerization and isocyanurate decomposition can be thermally activated. The activation energy of the different processes was determined by using an integral isoconversional procedure.

The initial composition of the diepoxide:diisocyanate formulation and the catalyst used are the parameters that control the network development, the final structure and the final characteristics of the thermosets obtained.

The most relevant differences between ytterbium triflate and benzyldimethylamine catalyzed curing processes are the longer pot-life, the lower thermal stability and the formation of urethane and allophanate groups with the acidic catalyst.

The composition of the final network, the crosslinking density, and the chain stiffness between crosslinking points are the responsible of the glass transition temperatures of the fully cured materials. By using ytterbium triflate as catalyst the maximum glass transition temperature was reached for DGEBA:TDI 1:1 formulation.

Acknowledgements

The authors would like to thank CICYT and FEDER for their financial support (grants MAT2011-27039-C03-01, MAT2011-27039-C03-02 and to the Generalitat de Catalunya (2009-SGR-1512). M.F. acknowledges the grant FPI-2009 from the Spanish Government.

References

[1] M. Flores, X. Fernández-Francos, J.M. Morancho, A. Serra, X. Ramis, Curing and characterization of oxazolidone-isocyanurate-ether networks, J. Appl. Polym. Sci. 125 (2012) 2779.

[2] K.S. Chian, S.S. Yi, Synthesis and characterization of an isocyanurate–oxazolidone polymer: effect of stoichiometry, J. Appl. Polym. Sci. 82 (2001) 879.

[3] M.J. Galante, R.J.J. Williams, Polymer networks based on the diepoxide–diisocyanate reaction catalyzed by tertiary amines, J. Appl. Polym. Sci. 55 (1995) 89.

[4] D. Caille, J.P. Pascault, L. Tighzert, Reaction of a diepoxide with a diisocyanate in bulk. I. Use of a tertiary amine catalyst, Polym. Bull. 24 (1990) 23.

[5] Javni, A. Guo, Z.S. Petrovic, The Study of Oxazolidone Formation from 9,10-Epoxyoctadecane and Phenylisocyanate, J. Am. Oil Chem. Soc. 80 (2003) 595.

[6] K. Harada, A. Deguchi, J. Furukawa, Copolymerization of various isocyanates with ethylene oxide, Die Makromol. Chem. 132 (1970) 281.

[7] Y.S.-K. Lee, K. Hodd, W.W. Wright, J.M. Barton, A study in the formation and characterisation of oxazolidone-isocyanurate polymers using differential scanning calorimetry and infrared spectroscopy, British Polym. J. 22 (1990), 97.

[8] A. Lapprand, F. Boisson, F. Delolme, F. Méchin, J.-P. Pascault, Reactivity of isocyanates with urethanes: conditions for allophanate formation, Polym. Degrad. Stab. 90 (2005) 363.

[9] K. Dusek, M. Spirková, I. Havlicek, Network formation of polyurethanes due to side reactions**,** Macromolecules 23 (1990) 1774.

[10] M. Miyamoto, K. Aoi, M. Morimoto, Y. Chujo, T. Saegusa, Ring-opening isomerization polymerization of cyclic iminocarbonates, Macromolecules 25 (1992) 5878.

[11] C. Mas, A. Mantecón, A. Serra, X. Ramis, J.M. Salla, Influence of lanthanide triflate compounds on formation of networks from DGEBA and γ-butyrolactone, J. Polym. Sci. Part A: Polym. Chem. 42 (2004) 3782.

[12] R. Giménez, X. Fernández-Francos, J.M. Salla, A. Serra, A. Mantecón, X. Ramis, New degradable thermosets obtained by cationic copolymerization of DGEBA with an s(γ-butyrolactone), Polymer 46 (2005) 10637.

[13] P. Castell, M. Galià, A. Serra, J.M. Salla, X. Ramis, Study of lanthanide triflates as new curing initiators for DGEBA, Polymer 41 (2000) 8465.

[14] X. Fernández-Francos, X. Ramis, J.M. Salla, Cationic copolymerization of cycloaliphatic epoxy resin with an spirobislactone with lanthanum triflate as initiator: kinetics of the curing process, Thermochim. Acta 144 (2005) 438.

[15] S. Vyazovkin, A.K. Burnham, J.M. Criado, L.A. Pérez-Maqueda, C. Popescu, N. Sbirrazzuoli, ICTAC Kinetics Committee recommendations for performing kinetic computations on thermal analysis data, Thermochim. Acta 520 (2011) 1.

[16] S. González, X. Fernández-Francos, J.M. Salla, A. Serra, A. Mantecón, X. Ramis, New thermosets obtained by cationic copolymerization of DGEBA with γ-caprolactone with improvement in the shrinkage. II. Time–Temperature–Transformation (TTT) cure diagram, J Appl Polym Sci 104 (2007) 3406.

[17] L.I. Kopusov, V.V. Zharkov, Spectral studies on the structure of polyurethane elastomers, J. Appl. Spectrosc. 5 (1966) 95.

[18] J.P. Pascault, H. Sautereau, J. Verdu, J, R.J.J. Williams, Thermosetting Polymers, Marcel Dekker, New York, 2002, pp 282-322.

[19] O. Bayer, Das Diisocyanate-Polyadditions-Verfahren, Carl Hanser Verlag, Müchen, 1963.

[20] I.C. Kogon, Chemistry of aryl isocyanates: rate of decomposition of some arylalkyl biurets and ethyl α,γ-diphenylallophanate, J. Org. Chem. 23 (1958) 1594.

[21] P.I. Kordomenos, J.E. Kresta, K.C. Frisch, Thermal stability of isocyanate-based polymers. 2. Kinetics of the thermal dissociation of model urethane, oxazolidone, and isocyanurate block copolymers, Macromolecules 20 (1987) 2077.

[22] H.C. Aspinall, J.L.M. Dwyer, N. Greeves, E.G. McIver, J.C. Wooley, Solubilized lanthanide triflates: Lewis acid catalysis by polyether and poly(ethylene glycol) complexes of $Ln(OTf)_3$, Organometallics 17 (1998) 1884.

[23] L. González, X. Ramis, J.M. Salla, A. Mantecón, A. Serra, The degradation of new thermally degradable thermosets obtained by cationic curing of mixtures of DGEBA and 6,6-dimethyl(4,8-dioxaspiro[2.5]octane-5,7-dione), Polym. Degrad. Stab. 92 (2007) 596.

New Epoxy Thermosets Obtained from Diglycidylether of Bisphenol A and Modified Hyperbranched Polyesters with Long Aliphatic Chains Cured by Diisocyanates

Marjorie Flores,[1] Xavier Fernández-Francos,[2] Emilio Jiménez-Piqué,[3] David Foix,[1] Àngels Serra,[1] Xavier Ramis[2]

[1] Departament de Química Analítica i Química Orgànica, Universitat Rovira i Virgili, Marcel·lí Domingo s/n, 43007 Tarragona, Spain.
[2] Laboratori de Termodinàmica, ETSEIB, Universitat Politècnica de Catalunya, Diagonal 647, 08028 Barcelona, Spain.
[3] Departament de Ciència dels Materials i Enginyeria Metal·lúrgica, Universitat Politècnica de Catalunya, Diagonal 647, 08028 Barcelona, Spain.

Abstract

Hyperbranched polyesters modified with long aliphatic chains with vinyl or epoxy groups as chain ends were synthesized and added as modifiers to diglycidyl ether of bisphenol A:toluene-2,4-diisocyanate mixtures in the presence of benzyldimethylamine as catalyst. The influence of the addition of these modifiers on the curing was investigated by thermal analysis and infrared spectroscopy. The materials obtained were investigated by electron microscopy and some mechanical characteristics were determined by nanoindentation tests. Epoxy terminated hyperbranched led to homogeneous materials with high crosslinking densities, whereas vinyl terminated hyperbranched produced phase separated morphologies. The materials showing phase separation presented a tough fracture, whereas the homogeneous materials obtained with epoxidated hyperbranched showed increased brittleness on increasing the proportion of modifier. On increasing the proportion of vinyl terminated hyperbranched in the thermosets, Young's modulus and hardness decreased but the addition of epoxy terminated hyperbranched did not influence these parameters. The addition of vinylic hyperbranched to the formulations produced a decrease in the curing shrinkage, whereas the epoxidic hyperbranched did not.

Key words: *Epoxy resins; curing of polymers; networks*

Introduction

Over a period of many years now, considerable effort has been directed towards the improvement in the toughness of epoxy thermosets [1]. While rigidity and strength are desired for many applications, brittleness limits their applicability [2]. Toughness implies energy absorption and it is achieved through various deformation mechanisms. One of the most successful routes towards toughness improvement is to incorporate a second soft phase to the matrix. Soft organic particles include elastomers [3-5] thermoplastics [6], or core-shell particles [7,8] as modifiers in the epoxy matrix to form fine morphological structures.

The toughness mechanism consists in the activation of yielding processes due to the reduction of the local yield stress. In this case, a substantial amount of energy is dissipated within the plastic zone near the crack tip. Rubber toughening, however, is at the expense of matrix' modulus and it is usually accompanied by a reduction in the processability by increasing the viscosity of the formulation. If the size of rubber particles is reduced to nanometric level the high-specific surface area can lead to the formation of a large interface particle/matrix in the material and the materials acquire transparent optical characteristics [9]. It has been proved that the

inclusion of only a small proportion of nanoparticles can increase the toughness while Young's modulus and strength at break remain unaffected [10].

Nowadays, the strategies to form nanostructures in thermosets can be divided into two classes. The first is based on the addition at low loadings of block copolymers, which consist of two or more chemically different substructures, covalently linked, most of them with an amphiphilic character. This mechanism was first reported by Bates et al. [11] and the formation of the nanostructure is based on the self-assembly of block copolymers when the precursors of the thermosets act as the selective solvents of a sub-chain of the block copolymer. The subsequent curing process only serves to fix the formed nanophase in the matrix. This method fails when all the sub-chains of block copolymers are miscible with the precursor [12].

The second strategy involves reaction-induced microphase separation (RIMPS) [13,14]. In this mechanism the curing starts from a completely homogeneous mixture and the phase separation takes place during the curing reaction. According to the thermodynamics of mixing, the driving force for RIMPS is the unfavourable entropic contribution to the mixing free energy resulting from the great increase in molecular weight of the epoxy network due to the epoxide polymerization. The phase behavior of thermosetting blends is also dependent on the kinetics of the curing and gelation [15]. The domain size decreases with increasing the curing temperature, because gelation occurs quicker due to the faster reaction [16]. According to this scenario, the kinetics of the curing is crucial for obtaining well distributed nanoparticles in the matrix by RIMPS, and therefore the curing agent and the conditions should be properly selected.

Hyperbranched polymers (HBPs) have been used to improve toughness in epoxy thermosets. They can create core-shell particles [17] can lead to separated morphologies by RIMPS [18,19] or can act as homogeneous reinforcement [20,21].

Hydroxyl terminated Boltorn type polyesters have been extensively used as toughness enhancers of epoxy thermosets cured with amines [18,22] or anhydrides [23]. In a previous paper [24] we reported the formation of microstrucured thermosets with dispersed HBP particles of ca 1-2 μm when Boltorn H30 esterified with long aliphatic chains was added as modifiers of diglycidylether of bisphenol A (DGEBA) cured by $Yb(OTf)_3$ as cationic initiator. When these modified hyperbranched polyesters had epoxy groups in the chain ends homogeneous materials were obtained.

As the kinetics of the curing process and gelation have a notable influence in the particle size in reaction induced microphase separated thermosets, in the present work we have studied the effect of changing the curing mechanism of DGEBA/esterified Boltorn H30 formulations.

The reaction between diepoxides and diisocyanates leads to thermosets containing isocyanurate and oxazolidone rings in their structure [25]. Isocyanurates are crosslinking points, whereas oxazolidones are linear chain extenders that can improve the mechanical toughness. Both structures are well known for their high-thermal stability [26]. We have recently studied the mechanism and kinetics of DGEBA:toluenediisocyanate formulations catalyzed by tertiary amines and determined that gelation occurred at low conversions (about 20%) depending on the composition of the formulation [27]. This fact encouraged us to apply this curing system to DGEBA/esterified Boltorn H30 formulations in order to obtain phase-separated thermosets when using vinylic Boltorn H30 hyperbranched as modifier. The possibility of transforming the unreactive vinylic groups into reactive epoxides opens new possibilities to the study on the

reinforcement of homogeneous thermosets and the morphologies originated when the epoxidation is only partial. The effect of the length of the aliphatic chain in the HBP structure on the phase separation process has been also investigated. The structures of the materials used are collected in Scheme 1.

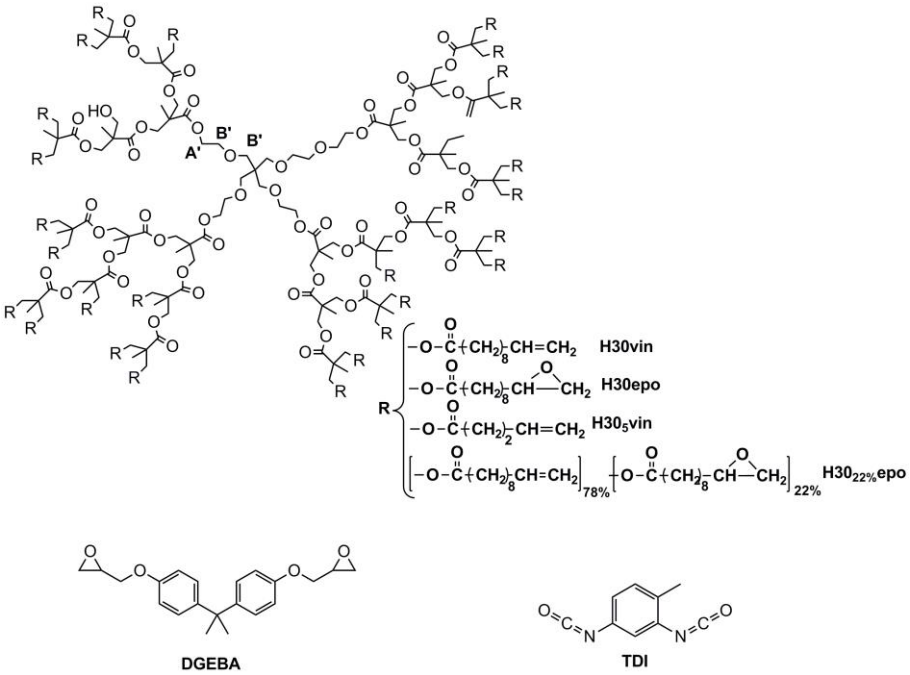

Scheme 1. Structure of the hyperbranched polymers, resin and curing agent used.

Experimental

Materials

Diglycidylether of Bisphenol A (DGEBA), Epitoke Resin 828 from Hexion Specialty Chemicals (epoxy equivalent = 187 g/eq) was used after drying under vacuum during 4h at 80 ºC. 4-toluene-2,4-diisocyanate (TDI), 10-undecenoyl chloride and 4-pentenoyl chloride from Aldrich were distilled before using. Benzyldimethylamine (BDMA), triethylamine (TEA), m-chloroperbenzoic acid (MCPBA) and 5-tert-butyl-4-hydroxy-2-methylphenyl sulphide (SANTONOX) were purchased from Aldrich and used without further purification. Boltorn H30 (M_w = 3500 g/mol, hydroxyl number = 480–510 g KOH/g polymer and an average number of hydroxyl groups of 32 per molecule, according to its datasheet) was kindly provided by Perstorp and was used as received. All solvents were dried and purified by conventional procedures.

H30vin preparation

Boltorn H30 was esterified with undecenoyl units (H30vin) by reacting it with 10-undecenoyl chloride in the presence of TEA as described in a previous publication [24]. The characterization by NMR spectroscopy confirmed that the modification degree achieved was practically quantitative.

H30$_5$vin preparation

Boltorn H30 was modified by reacting with 4-pentenoyl chloride in the presence of TEA similarly to the preparation of Boltorn H30vin.

^{1}H-NMR (400MHz, $CDCl_3$) δ (ppm): 1–1,4 (m, 139 H, -CH_2- and CH_3); 2,29 (m, 64 H, C=C-CH_2-); 2,86 (t, 64 H CH_2-CO-O-); 3,30–3,70 (m, 21 H, -CH_2-O- and -CH_2-OH); 4,20 (m, 90 H, -CH_2-O-CO-); 5,02-5,07 (m, 64 H, C=CH_2); 5,70-5,80 (m, 32 H, -CH=C).

H30epo preparation

H30epo was obtained following a previously described procedure [24]. The characterization of this polymer by NMR spectroscopy confirmed the complete epoxidation. Epoxy equivalent: 291.4 g/eq.

H30$_{22\%}$epo preparation

The partially modified epoxy H30$_{22\%}$epo was synthesized following the previous procedure, but a lower proportion of MCPBA was used. To 16 g of H30vin (0.06 mol of vinyl groups), 2.6 g (0.015 mol) of MCPBA were added in one batch. The degree of epoxidation (22%) was calculated by ^{1}H NMR analysis (400 MHz, $CDCl_3$), (ppm): 1.05–1.65 (m, -CH_2- and -CH_3); 2.0 (m, C=C-CH_2-); 2.25 (t, -CH_2-CO-O); 2.40 (m, -CH_2- of epoxide group); 2.68 (m, -CH- of epoxide group); 2.85 (m, -CH_2- of epoxide group); 3.30–3.70 (m, -CH_2-O- and -CH_2-OH); 4.20 (m, -CH_2-O-CO-); 4.95 (m, H_2C=C-); 5.70-5.80 (m, -CH=C).

Preparation of the curing mixtures

Mixtures containing a molar ratio 1:1 of epoxy and isocyanate groups and the selected proportion of the modified hyperbranched polymer were carefully stirred by mechanical beating until homogeneous appearance and degassed under vacuum (at 80 ºC) during two hours to prevent the appearance of bubbles during curing. Samples were kept at -20 ºC before use to prevent polymerization. 1 phr (1 part per hundred parts of mixture) of the liquid catalyst was added to the corresponding mixture at room temperature and homogenized, and then the sample was cured. Table 1 show the notation and composition of the different formulations studied. H30epo mixtures were prepared taking into account the epoxy content of this additive.

Calorimetric measurements (DSC)

Calorimetric analyses were carried out on a Mettler DSC-822e calorimeter with a TSO801RO robotic arm. Samples of approximately 10 mg were cured in aluminium pans under nitrogen atmosphere at a heating rate of 5 ºC/min. A second dynamic scan at 10 ºC/min was performed to determine the glass transition temperatures of the fully cured materials ($T_{g\infty}$) as the temperature of the half-way point of the jump in the heat capacity when the material changed from the glassy to the rubbery state. The T_g of the uncured materials was determined in a similar way from the first scan.

FT-IR/ATR spectroscopic analysis

Cured and uncured samples were analyzed with a FTIR spectrometer Bruker Vertex 70 with an attenuated total reflection accessory with thermal control and a diamond crystal (Golden Gate Heated Single Reflection Diamond ATR, Specac-Teknokroma). Spectra were collected at 30 ºC in the absorbance mode at a resolution of 4 cm^{-1}.

Table 1. Notation and composition in weight percentage and equivalent ratio of the different mixtures of DGEBA, TDI and H30vin and H30 epo initiated by 1 phr of BDMA.

Formulation	DGEBA (%)	TDI (%)	$eq_{cat}:eq_{TDI}$	$eq_{cat}:eq_{epoxi}$
Neat	68.3	31.7	0.0203	0.0203
H30vin				
2%	66.9	31.1	0.0207	0.0207
5%	65.0	30.0	0.0215	0.0215
10%	61.4	28.6	0.0227	0.0227
15%	58.0	27.0	0.0238	0.0238
H30epo				
2%	66.4	31.6	0.0204	0.0204
5%	63.7	31.3	0.0206	0.0206
10%	59.0	31.0	0.0210	0.0210
15%	54.6	30.4	0.0214	0.0214

Thermomechanical analysis (TMA)

Thermal mechanical analysis was carried out in a nitrogen atmosphere using a Mettler TMA40 thermomechanical analyser. The samples were supported in two small circular ceramic plates and silanized glass fibre, which were impregnated with the sample. Non-isothermal experiments were performed between 30 and 325 ºC at a heating rate of 5ºC/min applying a periodic force that changed (cycle time=12 s) from 0.0025 N to 0.01 N. When the material reaches sufficient mechanical stability (gelation) the TMA measuring probe is not able to deform the sample and the amplitude of the oscillations is reduced. The gel point was taken in TMA as the temperature at which a sudden decrease in the amplitude of oscillations was observed. The gel conversion, α_{gel}, was determined from the DSC conversion curve at 5 ºC/min at the temperature at which the material gelled in the TMA. Details of the employed methodology are described in a previous work [28].

Dynamomechanical analysis (DMTA)

DMTA was carried out with a TA Instruments DMA Q800. Single cantilever bending was performed on prismatic rectangular samples (ca. 0.5 x 12 x 25 mm^3). The apparatus was operated dynamically, at 3 ºC/min, from -125 to 325 ºC. The frequency of application of the force

was 1 Hz and the amplitude of the deformation 30 μm. Samples were cured isothermally in a Teflon mould following this cure schedule: 1 h at 80 ºC plus 15 h at 200 ºC and finally subjected to a post-curing at 250 ºC for 1 h.

Thermogravimetric analysis (TGA)

Thermogravimetric analysis was carried out using a Mettler-Toledo TGA-50 thermobalance. Cured samples with an approximate mass of 5 mg were heated from 40 to 600 ºC at 10 ºC/min in a nitrogen atmosphere.

Measurement of density and shrinkage

The overall shrinkage was calculated from the densities of the materials before and after curing, which were determined using a Micromeritics AccuPyc 1330 Gas Pycnometer thermostatized at 30 ºC. The error in the determination of the densities is ±0.1%. The shrinkage during curing was determined as:

$$\%shrinkage = 100\,\frac{\rho_\infty - \rho_0}{\rho_\infty} \qquad (1)$$

where ρ_0 is the density of the uncured formulation and ρ_∞ is the density of the fully cured material obtained at the same conditions of DMTA samples.

Electron microscopy analysis (SEM and TEM)

The fracture area of samples was metalized with gold and observed with a scanning electron microscope (SEM) Jeol JSM 6400. The transmission electron microscopy (TEM) images were performed with a Jeol 1011 microscope on samples prepared using an ultramicrotome at room temperature and stained with RuO_4.

Nanoindentation tests

The nanoindentation tests were performed in a MTS Nanoindenter XP instrumented with continuous stiffness measurement at 45 Hz and 2 nm amplitude. The tests were done with a Berkovich tip calibrated against fused silica. Indentations were done up to a maximum penetration depth of 3000 nm, corresponding to a maximum load of approximately 50 mN, at a constant strain rate of 0.05 s^{-1}. Results were analyzed with the Oliver and Pharr method [29]. Nine indentations were done at each material.

Results and discussion

Synthesis and characterization of the modified Boltorn polymers

The chemical modification of Boltorn H30 with vinylic structures of different length was performed by esterification reaction as reported previously [24]. Their structures are represented in Scheme 1. In the same paper the quantification of the degree of modification by NMR spectroscopy was explained. Boltorn H30vin and $H30_5$vin were obtained with an almost

quantitative degree of modification. H30vin was completely or partially epoxidized to obtain H30epo and $H30_{22\%}$epo, respectively. The evaluation of the degree of epoxidation was calculated by ^{1}H-NMR spectroscopy. Figure 1 shows the spectrum for the partially epoxidized polymer. As we can see, the vinylic signals between 4.7 and 6 ppm appear in the spectrum in addition to the epoxy signals between 2.3 and 3 ppm. The degree of esterification was determined from the intensities of the signals A + A' and B + B'. The signals A and B correspond to the methylene protons directly linked to ester and hydroxyl groups respectively, whereas A' and B' correspond to methylene protons of the core of Boltorn H30, as it is detailed in Scheme 1. The degree of epoxidation was calculated from the intensities of the vinylic protons (signal 9') and epoxidic protons (signal 10b). The spectrum of H30epo did not show any absorbance in the vinylic region [24].

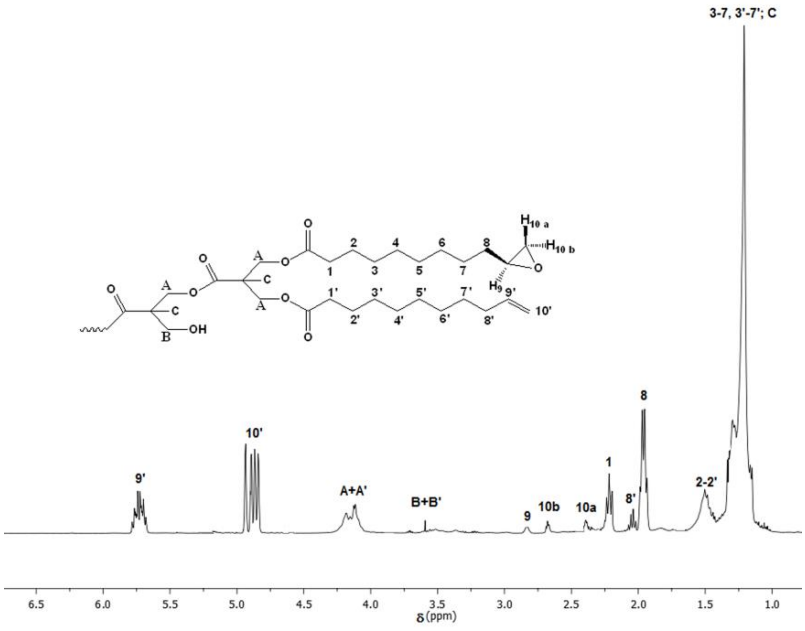

Figure 1. ^{1}H NMR spectrum in $CDCl_3$ of Boltorn H30 epoxidized in 22% ($H30_{22\%}$epo) with the signal assignments.

Study of the curing process

The curing mechanism of DGEBA:diisocyanate mixtures catalyzed by BDMA has been previously studied [25-27]. Several reactions occur during the curing process: a) trimerization of diisocyanate to give rise to isocyanurate rings, b) formation of oxazolidone rings and c) polyetherification (Scheme 2). As investigated previously [27] by non-isothermal DSC and FTIR of DGEBA:TDI:BDMA formulations, the formation of isocyanurate rings by trimerization of isocyanates takes place well below room temperature up to 110-130 ºC. Between 130 and 190 ºC, reaction between remaining isocyanate groups and epoxy groups takes place leading to oxazolidone ring formation, along with the homopolymerization of epoxy groups. Above 190 ºC, isocyanurate rings can react with the excess epoxy to give rise to oxazolidone rings, and epoxy polyetherification takes also place.

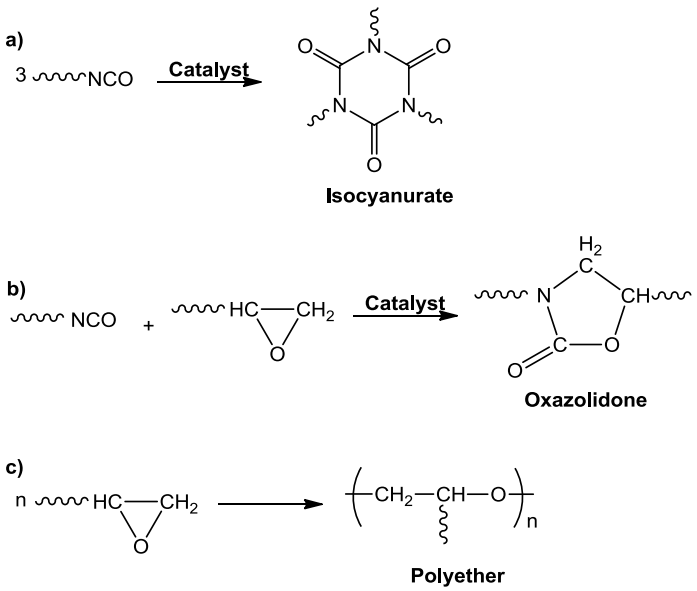

Scheme 2. Reactions taking place in the curing process

The DGEBA:TDI molar ratio is another factor that affects the structure and final composition of the network. Higher proportions of DGEBA favour the formation of oxazolidone structures, whereas higher proportions of TDI favour the isocyanurate formation. The higher the proportion of DGEBA the more polyetherification is observed. We selected DGEBA:TDI 1:1 (mol/mol) formulations with 1 phr of BDMA as the neat sample to be investigated by DSC, which is a compromise between these three different processes, leading to thermosets with 22% oxazolidone, 39% isocyanurate and 39% of polyether in the network structure [27]. To this formulation, different proportions of H30vin or H30epo were added in order to know the effect of these modifiers in the curing process.

The effect of the addition of both hyperbranched polymers in the curing process was assessed with DSC. Figure 2 plots the non-isothermal DSC scans of the formulations studied. It can be observed that the addition of H30vin to the reactive mixture mainly produces a delay in the first exotherm, which corresponds to the isocyanurate formation, and which is proportional to the amount of modifier. As a consequence of this delay, the temperature is increased and thus the initial curing rate is higher as well. The higher viscosity of the reactive mixture on adding H30vin and the decrease in the concentration of the reactive groups could account for such an initial curing delay. The second and third exothermic peaks are practically not affected by the addition of the HBP.

In Figure 2b it can be seen that the formation of isocyanurate ring is slightly affected on adding H30epo, especially in the curing rate but without a regular trend. Thus, whereas the addition of a 2% of H30epo increases the curing rate a notable decrease is observed when a proportion of a 15% of this modifier is in the formulation. The other processes are also influenced, but without apparent trend, which may be caused by the participation of the epoxy groups of the HBP in both oxazolidone formation and polyetherification. In experiments carried out by DSC and FTIR we could prove that the epoxy groups of H30epo reacted quantitatively in stoichiometric

formulations with TDI. It should be pointed out that the viscosities of the formulations containing H30epo are much lower than those of the H30vin and the delay in the curing process of H30vin may be attributed to this fact.

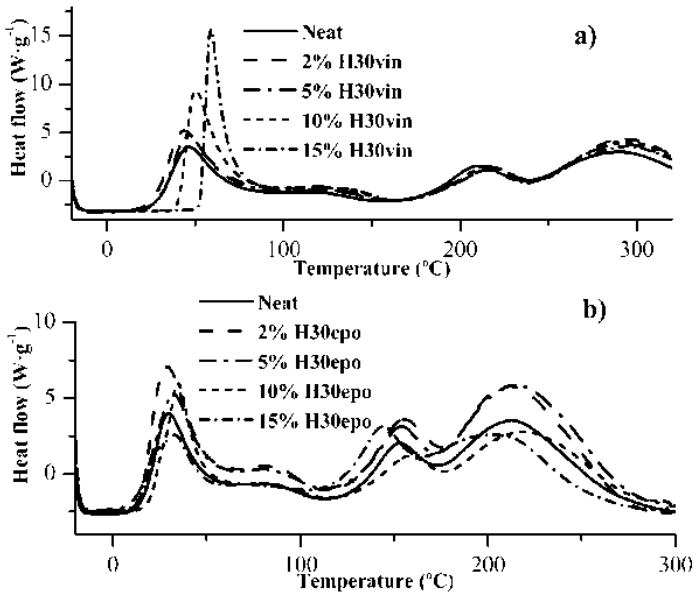

Figure 2. DSC thermograms for formulations DGEBA:TDI 1:1 with different proportions of a) H30vin and b) H30epo catalyzed with 1 phr of BDMA.

In order to quantify the amount of isocyanurate, oxazolidone and ether structures and linkages in the final network we registered FTIR spectra of all the materials obtained from the formulations cured for 1 h at 80 ºC, 15 h at 200 ºC and post-cured 1 h at 250 ºC.

The disappearance of the absorbance peaks at 915 cm^{-1} (epoxy bending) and 2260 cm^{-1} (carbonyl of isocyanate) indicates that the epoxide and isocyanate groups reacted. The increase in the absorbance peak at 1100 cm^{-1} (C-O-C stretching of aliphatic linear ester) is related to the homopolymerization of epoxide groups. The appearance of absorption peaks at 1750 cm^{-1} (carbonyl of oxazolidone) and 1710 cm^{-1} (carbonyl of isocyanurate) shows the formation of oxazolidone and isocyanurate groups. Alternatively, the peak at 1410 cm^{-1} can be used to evaluate the formation of isocyanurate groups. In order to properly evaluate the oxazolidone and isocyanurate bands, the absorbance of the carbonyl ester band of H30vin and H30epo before curing, which is observed at 1740 cm^{-1} and should not change during curing, was subtracted from the spectra of the cured materials. The peak at 830 cm^{-1} (*p*-phenylene), which should not change during the curing process, was chosen as an internal standard. Conversions of the different reactive groups, epoxide, isocyanate, isocyanurate and oxazolidone, were determined by the Lambert-Beer law from the normalized changes of absorbance at 915, 2260, 1710 and 1750 cm^{-1}, respectively. Maximum normalized absorbances of isocyanurate and oxazolidone were determined in formulations where isocyanate groups were completely transformed into isocyanurate or oxazolidone groups. Maximum normalized absorbance of isocyanate and epoxy groups were determined from the initial spectrum of mixtures without initiator.

Figure 3 shows the FTIR spectra before and after curing of the formulations containing a 15% of H30vin and H30epo. As stated above, a small amount of ester groups from H30vin and H30epo are present in the initial spectrum. In the final spectrum isocyanate and epoxy groups have disappeared completely, indicating complete cure of the formulation. The percentage of isocyanurates, oxazolidones and polyetherification is collected in Table 2. The differences observed on adding both HBPs in reference to the neat formulation are not significant, which implies that the epoxy groups of H30epo react similarly to the ones of DGEBA and the high viscosity and the dilution effect of the H30vin in the formulations does not influence the reactive processes in the curing schedule applied.

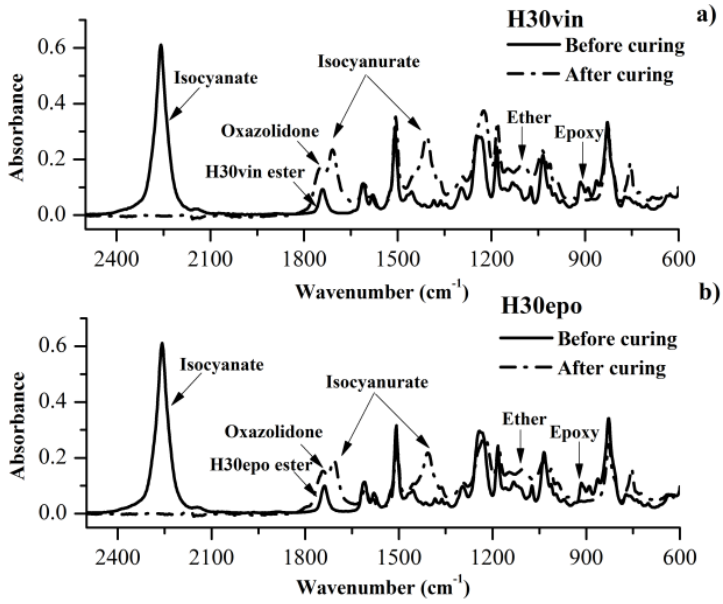

Figure 3. FTIR spectra before and after curing of the DGEBA:TDI 1:1 formulation with (a) 15% of H30vin and (b) 15% of H30epo with 1 phr of BDMA.

Table 2. Final compositions for DGEBA:TDI 1:1 formulations with different proportions of H30vin and H30epo cured dynamically in the DSC with 1 phr of BDMA.

Formulation	Oxazolidone (%)	Isocyanurate (%)	Ether (%)
Neat	22	39	39
H30vin			
2%	24	38	38
5%	20	40	40
10%	40	30	30
15%	18	41	41
H30epo			
2%	22	39	39
5%	20	40	40
10%	28	36	36
15%	24	38	38

In previous studies we observed that the addition of HBPs to the epoxy formulation notably affected the conversion at gelation [21, 30]. We used TMA and DSC to calculate this parameter for the different formulations. In TMA, the gelation process can be observed as a reduction in the oscillation amplitude because the gelified material is less deformable but this reduction can be better observed in the derivative of the curve. Figure 4 shows the plot obtained by TMA overlapped with the calorimetric curve obtained by DSC for the formulation DGEBA:TDI:15% H30epo catalyzed by 1 phr of BDMA. In the figure we can observe that gelation occurs at a low degree of conversion, during the trimerization reaction of diisocyanates, because the resulting isocyanurate groups are crosslinking points. Some isocyanurate groups will react with epoxides to form oxazolidone rings during the curing process, resulting in a reduction of the crosslinking density that can be observed as a small increase in the amplitude of the oscillations in Figure 4, which coincides with the second and third exotherms in the DSC plot. All the formulations studied showed a similar behavior. The conversions at gelation are collected in Table 3. It can be seen that by increasing the proportion of H30vin or H30epo no significant changes are observed in this parameter in reference to the neat formulation, since the conversion at the gelation is only controlled by the formation of isocyanurate groups.

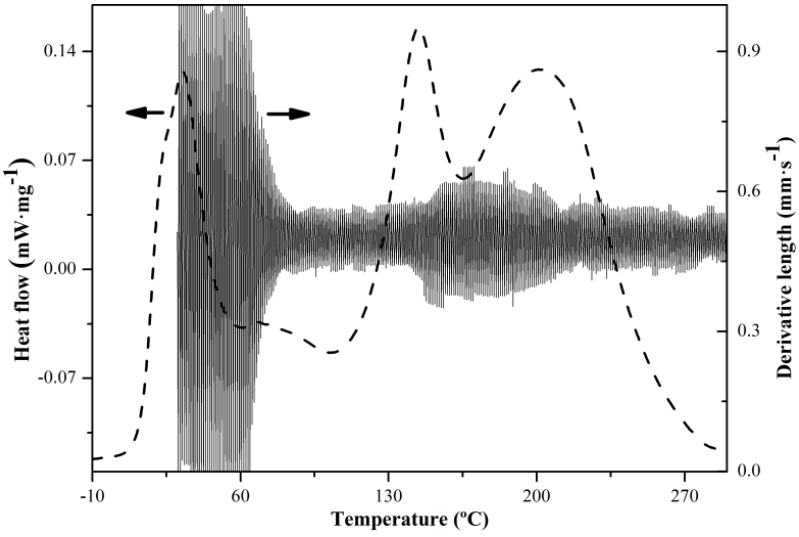

Figure 4. DSC thermogram and derivative length obtained by TMA versus temperature for DGEBA:TDI 1:1 formulation containing a 15% of H30epo catalyzed by 1 phr of BDMA.

Shrinkage during curing affects negatively the performance of the epoxy thermosets and especially the shrinkage generated after gelation because in this range the material loses its mobility and stresses and defects are originated. The shrinkage is usually originated because Van der Waals distances between monomers are converted into covalent bonds in the network during the curing process. Table 3 shows the densities of the different formulations before and after curing and the global shrinkage calculated from them. The addition of H30vin to the formulations reduces the global shrinkage, which can be explained by the reduction of the amount of covalent bonding on increasing its proportion in the formulation. In addition to that, the phase separation (which will be confirmed afterwards with the help of electronic microscopy) should also influence the shrinkage because H30vin separated phases have a higher free volume and as a consequence the global shrinkage should be smaller. On the other hand, the addition of

H30epo does not influence much the global shrinkage because of the reaction of the epoxide groups of the HBP. Shrinkage should be higher at the beginning of curing, during isocyanurate formation, because three isocyanate molecules are needed to form this structure. The fact that most of the shrinkage takes place before gelation is beneficial for the performance of the material because shrinkage only produces internal stresses if it is generated in the solid state.

Table 3. Conversion at the gel point α_{gel}, densities before and after curing and shrinkage calculated for the different formulations.

Formulation	α_{gel} (%)	ρ_0 ($g \cdot cm^{-3}$)	ρ_∞ ($g \cdot cm^{-3}$)	Shrinkage (%)
Neat	18	1.185	1.338	11.4
H30vin				
2%	20	1.178	1.294	9.0
5%	18	1.180	1.295	8.9
10%	20	1.193	1.296	8.0
15%	19	1.214	1.297	6.4
H30epo				
2%	17	1.186	1.324	10.4
5%	18	1.185	1.332	11.0
10%	17	1.184	1.332	11.1
15%	15	1.184	1.331	11.1

Network formation and thermomechanical properties

The glass transition temperatures before and after curing were determined for all the formulations by DSC. The values obtained are collected in Table 4. It should be pointed out that the T_gs of H30vin and H30epo were -65 and -52 ºC respectively [24]. Thus, the addition of these modifiers to the formulation should affect proportionally the T_{g0} of the formulations before curing if the solubility in the DGEBA was complete. Although from the data of the table the influence of the H30vin in this parameter seems to indicate a great compatibility with DGEBA, the appearance of the mixtures at room temperature was milky and it became clear on heating at 60-70 ºC. On the contrary H30epo mixtures were completely homogeneous from the very beginning.

In Table 4 we can also see how on increasing the proportion of both HBPs the T_g of the cured materials decreases, but the materials containing H30epo present higher values than those containing H30vin. This is caused by the participation of H30epo epoxide groups in the curing process, thus contributing to the crosslinking, while the solubilized H30vin may act only as a plasticiser because no reaction can occur.

Table 4. Glass transition temperatures before and after curing for the formulation studied.

Formulation	T_{g0}[a] (ºC)	$T_{g,DSC}$[b] (ºC)	$T_{g,DSC,Fox}$[c] (ºC)	$T_{g,Tan\ \delta}$[d] (ºC)
Neat	-56	195	195	191
H30vin				
2%	-57	183	184	184
5%	-58	180	167	179
10%	-60	168	143	162
15%	-61	162	126	158
H30epo				
2%	-53	193	189	187
5%	-54	183	180	174
10%	-55	184	166	172
15%	-56	180	152	178

[a] Glass transition temperature of uncured samples at a rate of 10 K·min^{-1}.
[b] Glass transition temperature of samples cured at a rate of 10 K·min^{-1}.
[c] Glass transition temperature calculated using the DSC data and FOX equation assuming an homogeneous mixture of DGEBA and H30epo.
[d] Tan δ values determined by DMTA experiments of cured samples.

Mezzenga et al. [31] used the Fox equation to predict the T_g of the homogeneous cured materials modified with HBPs. The following equations were used in our case to calculate the final T_g*S*:

$$\frac{1}{T_g} = \frac{w}{T_{g,H30vin}} + \frac{1-w}{T_{g,DGEBA:TDI}} \qquad (2)$$

$$\frac{1}{T_g} = \frac{w}{T_{g,H30epo:TDI}} + \frac{1-w}{T_{g,DGEBA:TDI}} \qquad (3)$$

where w is the weight fraction, $T_{g,\text{H30vin}}$ is the glass transition temperature of pure H30vin, $T_{g,\text{DGEBA:TDI}}$ is the T_g of a cured material obtained from a DGEBA:TDI 1:1 formulation and $T_{g,H30epo:TDI}$ is the T_g of the material obtained from an stoichiometric mixture H30epo:TDI 1:1 completely crosslinked. The values of $T_{g,\text{H30epo:TDI}}$, $T_{g,\text{H30vin}}$, $T_{g,\text{DGEBA:TDI}}$ determined by DSC at 10 ºC/min are 40, -65 y 195 ºC, respectively.

If we compare in Table 4 the T_g values determined experimentally with those calculated by the Fox equation we can observe that the former are higher than the latter. In the case of H30epo, in which the materials obtained should be homogeneous, the differences may be caused by the different reactivity of DGEBA and H30epo epoxy groups in the formulation, in comparison with the individual DGEBA and H30epo formulations. Therefore, a network structure with different properties from those of a homogeneous mixture of networks is obtained, in this case with a higher degree of crosslinking than expected. On the other hand, the use of the vinylic

modifier can lead to inhomogeneous materials. The addition of 2% of H30vin to the formulation leads to unappreciable differences in the predicted and determined values but when this proportion increases the differences become greater. These differences can be explained if we consider the low compatibility of H30vin with DGEBA that can lead to a partial plasticization of the epoxy network and to the appearance of a phase separated morphology, when the proportion of this modifier is higher than 2%.

The materials obtained after an isothermal curing were also investigated by DMTA. The values for the maximum of tan δ peaks have been included in Table 4. These values are in good agreement with those obtained by DSC experiments. Figure 5 shows the plot of tan δ against temperature from -120 to 30 ºC for the neat material and the material containing a 15% of H30vin. As we can see, the spectrum of the modified material shows a shoulder in the relaxation peak, at about -40 ºC, that can be attributed to the T_g of pure H30vin which is -65 ºC (determined by DSC), which would indicate the existence of phase-separated H30vin. DMTA spectra of modified materials containing H30epo do not show evidences of a H30epo relaxation peak. The values of the storage modulus in the rubbery region were measured but no significant trend was observed because this parameter is affected not only by the structure of the HBP and its proportion but also by the proportion of isocyanurates, oxazolidones and polyether groups in the network.

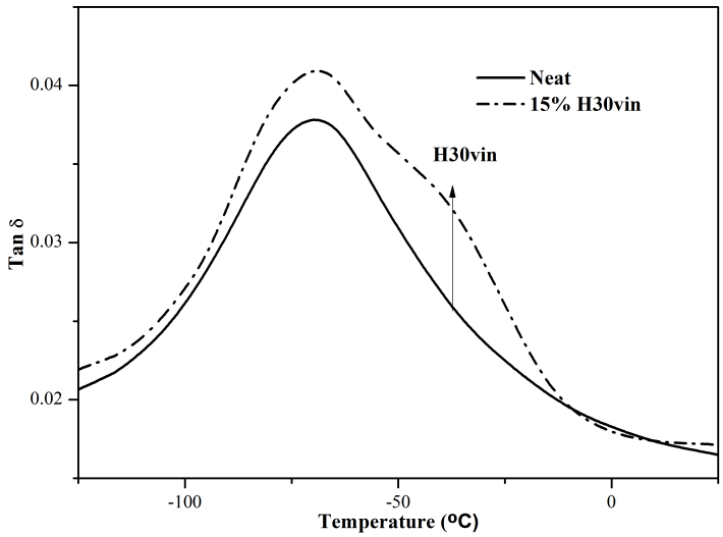

Figure 5. Tan δ plot against temperature in the range between -120 to 25ºC for neat DGEBA:TDI 1:1 formulation and modified material containing a 15% of H30vin with 1 phr of BDMA.

The thermal stability of the thermosets was studied by TGA. Table 5 collects the temperature of the initial decomposition calculated at a 5% of weight loss and the temperature of the maximum degradation rate. The shape of the derivative curves for all the materials were unimodal, indicating that there were no regions or structures in the material with significant differences in thermal stability. As we can see from the values of the table there is not a clear tendency on the initial decomposition temperature. All the thermosets show a high thermal stability due to the presence of isocyanurate and oxazolidone rings in the structure. [26] The low influence of the HBPs added on the initial decomposition temperature is an unexpected result because the presence of ester groups, which can suffer degradation by a β-elimination process,

usually leads to a notable reduction of this parameter. In previous works carried out in our group, thermally reworkable epoxy thermosets were obtained by adding hyperbranched polyesters [21, 30]. The use of H30vin and H30epo as modifiers in the curing of DGEBA:$Yb(OTf)_3$ systems [24] led to materials with a slightly lower thermal stability than the ones obtained in the present study. The presence of isocyanurate and oxazolidone groups in the network should be the responsible in the maintenance of the thermal stability.

Table 5. Thermogravimetric data at 10 $K \cdot min^{-1}$ for the thermosets obtained from formulations DGEBA:TDI 1:1 with different proportions of H30vin and H30epo catalyzed by 1 phr of BDMA.

Formulation	$T_{5\%}$ [a] (ºC)	$T_{máx}$ [b] (ºC)
Neat	347	426
H30vin		
2%	359	422
5%	350	426
10%	347	429
15%	364	431
H30epo		
2.5%	334	427
5%	353	433
10%	342	432
15%	348	439

[a]Temperature of a 5% of weight loss calculated by thermogravimetry.
[b] Temperature of maximum weight loss rate.

Morphologies of the thermosets and fracture characteristics

The morphology of the cured materials was studied by TEM in order to determine the existence of segregated domains of the HBPs in the epoxy matrix. Figure 6 shows the micrographs for the materials containing a 10 wt % of H30vin and H30epo. As we can see, the addition of H30epo leads to a completely homogeneous material, whereas the addition of the vinylic modifier leads to a phase-separated morphology with particle sizes between 50 and 500 nm. It was previously described that phase separated morphologies were formed in epoxy thermosets modified with HBPs when the final groups were not reactive in the curing system selected [17-19]. The reason behind this is a reaction induced microphase separation (RIMPS), caused by the decrease in the entropy of mixing and changes in the solubility parameter during curing and network formation. It was previously reported that the addition of H30vin to DGEBA:$Yb(OTf)_3$ systems also led to phase separated morphologies, but in that case the size of the domains was 1-2 μm [24]. These differences in particle size could be attributed to the different gelation times. When diisocyanates are used as curing agents, gelation time is much shorter, leading to the blocking of nanometer sized particles.

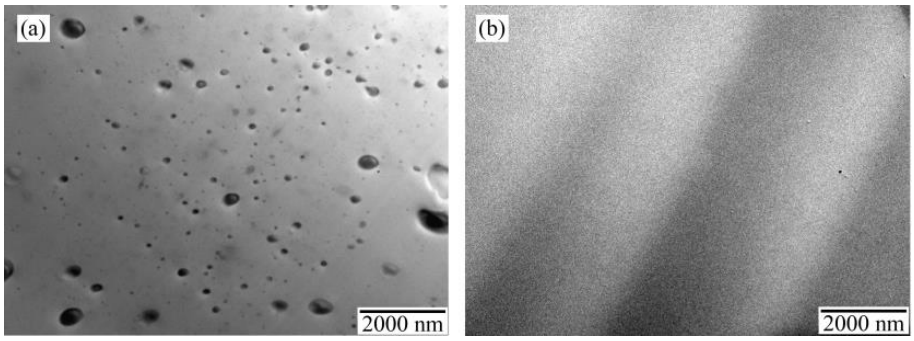

Figure 6. TEM micrographs for materials obtained from DGEBA:TDI 1:1 formulations containing (a) 10% H30vin and (b) 10% H30epo catalyzed by 1 phr of BDMA.

Figure 7 presents the SEM micrographs of the cryofracture surfaces of the neat DGEBA:TDI material (a) and the one containing 10 wt % H30vin (b and c). It can be seen that the neat material presents a smooth and fragile fracture with some cracks but very little evidence of deformation, which accounts for its poor impact resistance. In the micrographs of the H30vin modified material a great amount of tortuous cracks appear in the fracture surface, resulting from the formation of shear bands near the plastic HBP particles. The uniformly dispersed particles create stress concentration and act as sites for initiating shear bands. Some cracks deviate from their original plane leading to a significant increased surface area. These facts, in addition to the more flexible matrix reflected by the lower T_g in the 10% H30vin modified thermoset, contribute to an increased toughness for the materials containing H30vin. Figure 7 (c) shows that the particles observed by SEM are bigger than the ones observed by TEM (100-1000 nm in comparison to 50-500 nm). The explanation to this difference is due to the cavitation and void growth mechanism that contributes to the increase in toughness, although it cannot be discarded that the fraction of H30vin solubilized in the epoxy matrix acts as plasticizer and enhances the yielding of the matrix. Figure 8 shows the influence of the H30vin content in the morphology of the material. On increasing the percentage of this modifier the particle size increase notably and the number of particles is reduced. This can be related to the initial curing rate differences observed in Figure 2 for H30vin formulations. The higher the proportion of H30vin, the lower reactivity in the formation of isocyanurate structures thus favouring particle growth.

When H30epo was used as modifier the fracture surfaces are homogenous with few shear bands of plastic deformations, indicating a fragile fracture (Figure 9). On increasing the percentage of H30epo in the material the number of shear bands decreases indicating a higher fragility. This fact is consistent with the reactivity of epoxy final groups in the HBP structure, which leads to a higher degree of crosslinking than expected, resulting in somewhat more fragile structures.

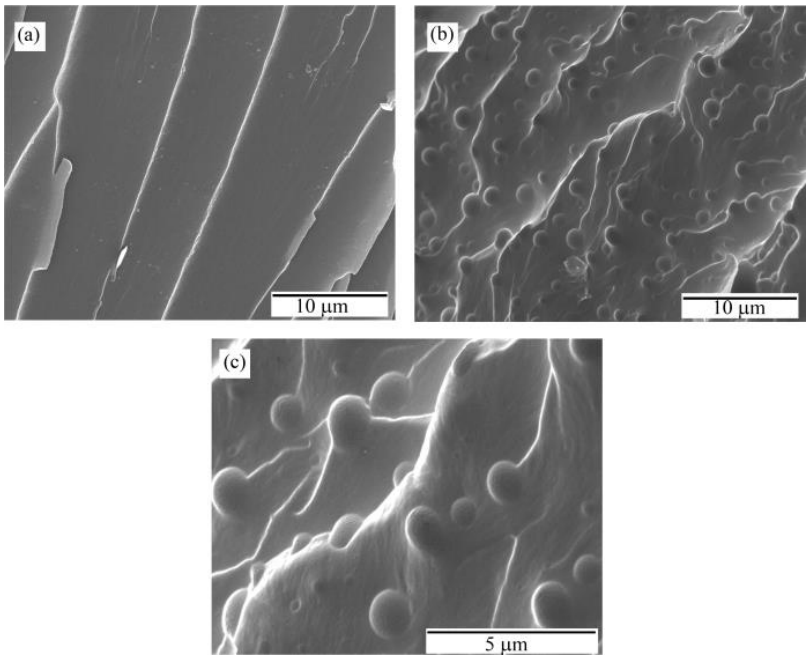

Figure 7. SEM micrographs of the cryofracture surface for materials obtained from (a) neat DGEBA:TDI 1:1 formulation catalyzed by 1 phr of BDMA and (b) and (c) material containing a 10% H30vin at different magnifications.

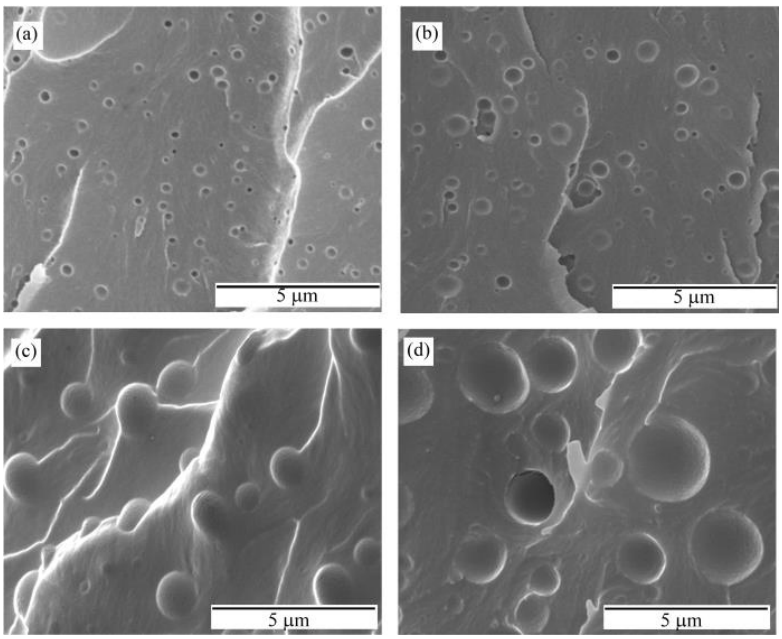

Figure 8. SEM micrographs of the cryofracture surface for materials obtained from DGEBA:TDI 1:1 formulation catalyzed by 1 phr of BDMA containing different weight percentages of H30vin, (a) 2% (b) 5% (c) 10% and (d) 15%.

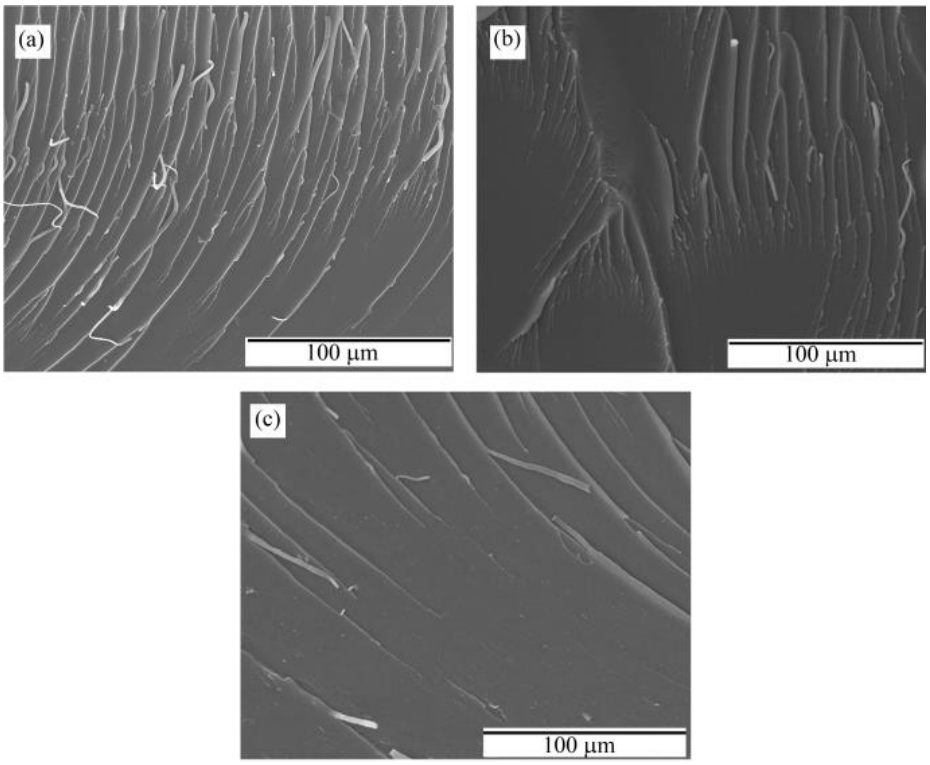

Figure 9. SEM micrographs of the cryofracture surface for materials obtained from (a) neat DGEBA:TDI 1:1 formulation catalyzed by 1 phr of BDMA, (b) material containing a 5% of H30epo and (c) formulation containing a 10% H30epo.

The results obtained put into evidence the great importance of the reactivity of the final groups of the hyperbranched structure on the morphology and toughness. In order to further study this effect we added as modifier a 10% of the HBP $H30_{22\%}$epo to the formulation, which has a 22% of epoxy and a 78% of vinylic final groups. The micrographs of the cryofracture surfaces are shown in Figure 10. As we can see, particles are appreciated within the matrix and the fracture pattern is that of a tough material, similar to the one obtained in H30vin materials. However, the particle size is bigger, between 500 and 1500 nm, and seems to be better compatibilized with the matrix, due to the reactivity of the epoxy groups present in the HBP structure. The vinylic groups are the responsible for the phase separation observed, and the epoxy groups lead to a best interface bonding to the matrix compared to H30vin modified materials, which present delamination or pulling out of H30vin particles. This fact can explain the tougher fracture observed for $H30_{22\%}$epo thermoset.

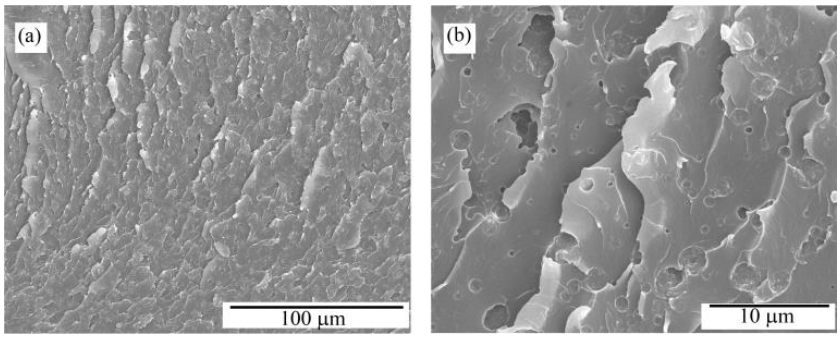

Figure 10. SEM micrographs of the cryofracture surface for materials obtained from DGEBA:TDI 1:1 formulation catalyzed by 1 phr of BDMA containing a 10% of $H30_{22\%}$epo at, (a) 100 μm and (b) 10 μm.

Figure 11 shows the cryofracture surface of a thermoset containing a 10% of $H30_5$vin. In this case, the fracture surface is completely homogeneous but some shear deformation appears. However, the toughness of the material seems to be lower than those of the H30vin containing materials (Figure 7). Although in this case the final groups are not reactive the length of the aliphatic chains of the vinylic units introduced is not enough to generate a phase separation. According to that, not only the characteristics of the final groups but also the polarity of the modifier structure affect the morphology and toughness characteristics of the thermosets obtained.

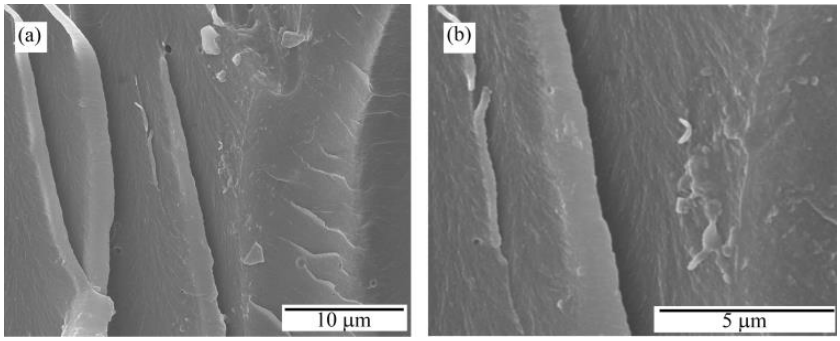

Figure 11. SEM micrographs of the cryofracture surface for materials obtained from DGEBA:TDI 1:1 formulation catalyzed by 1 phr of BDMA containing a 10% of $H30_5$vin at (a) 10 μm and (b) 5 μm.

Mechanical characteristics of the thermosets by nanoindentation tests

The results of the nanoindentation tests are collected in Table 6 for all the materials prepared. As we can see, on increasing the proportion of H30vin in the thermosets, Young's modulus and hardness decrease, due to the flexibility introduced by the H30vin. In contrast, the addition of H30epo does not influence these parameters, possibly due to the higher crosslinking density achieved by the reaction of epoxy final groups of the HBP. This effect can compensate the flexibility introduced by the long aliphatic chains. On comparing the materials containing H30vin and H30epo we can state that the studied mechanical characteristics are slightly higher for the latter. The differences should be attributed to the reactivity of epoxy terminal groups in H30epo, since the structure of both HBPs is similar. The presence of long aliphatic chains in the

HBP structure leads to a reduction of the Young's modulus and hardness. This is put into evidence on comparing the material obtained with a 10% of $H30_5$vin, with a shorter aliphatic chain, with the one containing a 10% of H30vin. The former has better mechanical characteristics as expected. For the material containing a 10% of $H30_{22\%}$epo the characteristics studied yielded intermediate values between those measured for H30vin and H30epo modified thermosets, although closer to the latter. These results confirm the great effect that the reactivity of the HBP modifier has in the characteristics of the thermoset. In general, the existence of reactive terminal groups, although in a reduced proportion, allows the chemical incorporation of the HBP to the epoxy matrix and obtaining materials with a higher crosslinking density. The presence of long aliphatic structures in the HBP improves flexibility.

Table 6. Mechanical characteristics obtained by nanoindentation tests.

HBP	Formulation	Young's modulus (GPa)	Hardness (GPa)
	Neat	4.10 (± 0.20)	0.36 (± 0.02)
H30vin			
	2%	3.97 (± 0.09)	0.31 (± 0. 01)
	5%	3.63 (± 0.24)	0.27 (± 0.02)
	10%	3.53 (± 0.19)	0.27 (± 0.02)
	15%	3.46 (± 0.14)	0.26 (± 0.01)
$H30_5$vin	10%	3.96 (± 0.17)	0.30 (± 0.02)
H30epo			
	2%	4.18 (± 0.08)	0.32 (± 0.01)
	5%	3.88 (± 0.16)	0.31 (± 0.02)
	10%	4.03 (± 0.13)	0.33 (± 0.02)
	15%	3.98 (± 0.09)	0.30 (± 0.01)
$H30_{22\%}$epo	10%	4.02 (± 0.14)	0.31 (± 0.02)

Conclusions

The addition of hyperbranched polyesters modified with long aliphatic chains with vinyl or epoxy groups at their ends to DGEBA:TDI mixtures did not change significantly the proportions of oxazolidone, isocyanurate and ether groups in the chemical structure of the network.

The addition of H30vin produced a delay in the isocyanurate formation, while H30epo did not have a significant effect on the curing kinetics, which may be explained by the different viscosities of both formulations. Conversion at gelation was not affected by the presence of either HBP because it is controlled only by the formation of isocyanurate groups.

On increasing the proportion of both HBPs in the formulation the T_g of the cured materials decreases, but the materials containing H30epo present higher values than those

containing H30vin, due to the reaction of epoxide groups at the chain ends with isocyanates, which increased the crosslinking density.

The curing of formulations containing H30vin took place with a lower shrinkage that in the neat formulation. However, H30epo did not affect significantly the shrinkage on curing.

The use of H30vin led to phase-separated materials by reaction-induced microphase separation, with particle sizes on the nanometric or the micrometric scale depending on the amount of H30vin in the formulation which enhanced toughness. On the contrary, H30epo produced homogeneous and more fragile materials due to the increased crosslinking density. By reducing the chain length of the vinyl-terminated HBPs the polarity of the HBP was changed and the compatibility between the HBP and the matrix was enhanced, leading to homogeneous materials.

On increasing the proportion of H30vin in the thermosets, Young's modulus and hardness decreased, due to the flexibility introduced by the H30vin. In contrast, the addition of H30epo did not influence these parameters, due to the higher crosslinking density achieved by the reaction of epoxy final groups of the HBP. The mechanical characteristics of the material containing a 10% of $H30_{22\%}$epo were intermediate between those measured for H30vin and H30epo modified thermosets but more similar to the latter, although it presented a phase separated morphology and a tough fracture.

Acknowledgements

The authors would like to thank MICINN (Ministerio de Ciencia e Innovación) and FEDER (Fondo Europeo de Desarrollo Regional) (MAT2011-27039-C03-01 and MAT2011-27039-C03-02) and to the Comissionat per a Universitats i Recerca del DIUE de la Generalitat de Catalunya (2009-SGR-1512). Marjorie Flores acknowledges the grant FPI-2009 from the Spanish Government. David Foix acknowledges FPU-2007 grant from the Spanish government. Perstorp Specialities is also acknowledged.

Chapter 5

Novel epoxy-anhydride thermosets modified with a hyperbranched polyester as toughness enhancer. I. Kinetics study

Marjorie Flores,[a] Xavier Fernández-Francos,[a,*] Xavier Ramis,[b] Angels Serra[a]

[a] Department of Analytical and Organic Chemistry, Universitat Rovira i Virgili, C/ Marcel·lí Domingo s/n, 43007, Tarragona, Spain.
[b] Thermodynamics Laboratory, ETSEIB, Universitat Politècnica de Catalunya, Av. Diagonal 647, 08028, Barcelona, Spain.

Abstract

A hyperbranched polyester (Boltorn™ H30) has been modified in order to partially replace the terminal hydroxyl groups with aliphatic vinyl chains. This novel hyperbranched polymer (HBP) has been used as a modifier of epoxy-anhydride thermosets with the purpose of enhancing the fracture toughness. The curing kinetics of the neat and the modified formulations have been studied in detail with DSC and FTIR. Model-free and model-fitting kinetic methods have been applied to DSC data to determine the kinetic parameters. The curing mechanism has been elucidated with FTIR. Incorporation of the HBP into the thermoset matrix is assured by the reaction of remaining hydroxyl groups.

Keywords: epoxy, anhydride, hyperbranched, FTIR, DSC, kinetics

Introduction

Epoxy resins are one of the most important classes of thermosetting polymers, widely used world-wide in coatings, adhesives, moulding compounds and polymer composites, because of their good thermomechanical properties and ease of processability. However, the use of epoxy resins is often restricted by their fragility, which places strong constraints on design parameters. Fragility and toughness are issues of great importance in terms of impact resistance, fatigue behaviour and damage tolerance [1, 2], which are properties which greatly influence the durability of the components that use epoxy resins as one of their relevant constituents.

Many efforts have been made until now in order to improve the toughness of epoxy thermosets. Toughness implies energy absorption and it is achieved through various deformation mechanisms before failure occurs [3, 4]. One of the most effective mechanisms to increase toughness is the addition of a second phase that induces the formation of particles [5-9]. The effect produced depends on the particles characteristics, *e.g.* size, interparticle distance, particle/matrix interaction, among others. The use of hyperbranched polymers (HBPs) has been proposed [1, 10-13] in order to overcome the limitations of traditional modifiers such as linear thermoplastics or rubber particles. Hyperbranched polymers (HBPs) are a type of dendronised polymers that can be used as modifiers of thermosetting materials because of 1) their high degree of branching, which makes them less viscous than their linear counterparts with the same equivalent molecular weight and 2) the high concentration of surface groups which can be modified in order to fine-tune their physical compatibility with the matrix or make possible their covalent linkage to the matrix. The properties of the final material can thus be tailored as a function of the core structure, the degree of branching and the type of functional end-groups [14]. In order to obtain an effective toughening, good compatibility between the matrix and the modifier is required. For instance, Mezzenga et al. [10] successfully modified an epoxy-amine formulation with different reactive epoxy-terminated HBPs and found that the best toughness enhancement

was achieved using partially modified HBPs which were rather compatible but could phase-separate. Boogh et al. [1] hypothesized that there was a concentration gradient within the separated particles as a consequence of the good compatibility with the matrix, and which ensured a good transmission of stress between the matrix and the particle. A certain degree of physical compatibility rather than chemical grafting could also help to increase the toughness of HBP-modified epoxy-amine thermosets, as reported by Ratna and Simon [11]. A significant *in-situ* reinforcement could also be achieved in homogeneous HBP-modified epoxy-anhydride formulations [15] or photocured epoxy formulations [16].

The effect of HBPs on the curing kinetics of epoxy thermosets depend largely on the structure and molecular weight of the HBPs, its solubility in the resin and the curing mechanism [17-23]. We recently found that the curing of epoxy-anhydride formulations was accelerated with the use of hydroxyl-terminated HBPs [24, 25]. In a more detailed study we elucidated the curing mechanism in homogeneous epoxy-anhydride thermosets modified with a hyperbranched poly(ester-amide) [26]. Incorporation of the HBP into the network structure could be assured by the early esterification of hydroxyl groups with anhydride and subsequent esterification of epoxy groups with the resulting carboxylic acid. Frohlich et al. studied the effect of various synthesized HBPs as phase-separating toughnening agents in epoxy-anhydride formulations but did not analyse the curing kinetics in detail [27]. Understanding the effect of such modifiers not only on the final properties but also on the cure kinetics is of key importance to optimize their use in an industrial application.

In this work we have modified H30 replacing terminal hydroxyl groups with long aliphatic chains ended in vinyl groups with different degrees of modification and used these modified HBPs in epoxy-anhydride formulations. In previous works, we used similar a totally modified HBPs as modifiers in cationic epoxy [28] and epoxy-isocyanate formulations [29]. The objective of this work is to determine the effect of the degree of modification and the amount of HBP on the curing kinetics. The curing has been monitored by DSC and FTIR. The kinetics has been analyzed following both model-free and model-fitting approaches, and the curing mechanism has been elucidated. The viscosity of the different polymeric modifiers has been studied by rheology. The thermal and mechanical properties of the cured materials will be dealt with in a forthcoming paper.

Theoretical

Epoxy-anhydride curing mechanism

The curing mechanism of epoxy-anhydride formulations, summarized in Scheme 1, is quite complex [15, 24, 26, 30]. To begin with, the presence of tertiary amine promotes the anionic alternating copolymerization of epoxy and anhydride groups (Scheme 1.a), but the presence of hydroxyl groups favours the uncatalyzed hydroxyl-anhydride copolymerization (Scheme 1.b) leading to the formation of carboxylic acid. Subsequent esterification of epoxy groups with carboxylic acid can take place with the aid of a tertiary amine [31]. It must also be pointed out that while the anionic copolymerization (Scheme 1.a) is a ring-opening polyaddition process, the other esterification reactions follow condensation reaction kinetics. The presence of reactive HBPs with end hydroxyl groups can accelerate the reaction of both anhydride and epoxy groups because hydroxyl groups can react with anhydride groups (as seen in Scheme 1.b) but also promote the initiation of the copolymerization with the tertiary amine [26]. Regeneration of the tertiary amine, as reported in other studies [26, 32, 33], can also take place. Homopolymerization of epoxy

groups was observed to occur to a very limited extent [26]. Incorporation of HBPs is assured by the reaction of the end hydroxyl groups with anhydride and subsequent reaction with epoxy groups, as shown in Scheme 1.b. The occurrence of chain-transfer reactions would also make possible its incorporation into the network structure. The presence of the HBP may alter the network structure, but the overall thermal-mechanical properties may not be sacrificed to a significant extent due to the activation of internal branching points of the HBP, and enhanced intra-molecular interactions within the network structure [34].

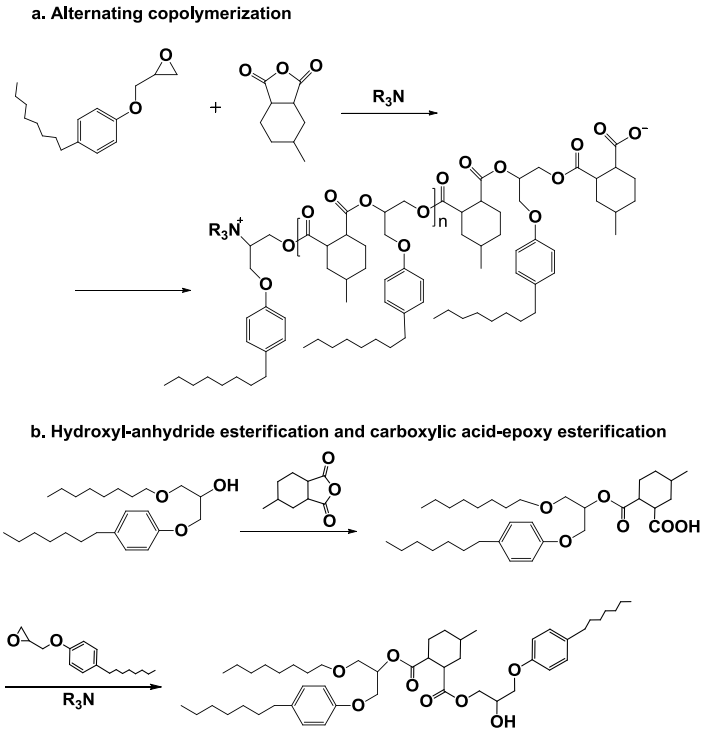

Scheme 1. Summary of the most significant reaction pathways in the curing of DGEBA/MHHPA thermosets.

Curing kinetics

The curing kinetics were analyzed using the isoconversional methodology [35]. It is assumed that the curing kinetics can be represented by the following equation

$$\frac{dx}{dt} = k \cdot f(x) \qquad (1)$$

where $k=A \cdot exp(-E/R \cdot T)$ is the rate constant, E is the activation energy, A the preexponential factor and $f(x)$ is a function of conversion representing the curing mechanism. Integration of eq (1) in constant heating rate experiments leads to the following expression

$$g(x) = \int_0^x \frac{dx}{f(X)} = \frac{A}{\beta} \int_{T_0}^{T} \exp\left(-\frac{E}{R \cdot T}\right) \cdot dT \qquad (2)$$

where β is the heating rate and *g(x)* is the integral form of the kinetic model that governs the curing process. Because there is no analytical solution of the so-called temperature integral [35, 36], different approximations can be used. One of the most popular is the Coats-Redfern approximation which, assuming that $2 \cdot R \cdot T/E << 1$ and after some rearrangement, leads to

$$\ln\left(\frac{\beta}{T^2}\right) = \ln\left(\frac{A \cdot R}{g(x) \cdot E}\right) - \frac{E}{R \cdot T} \qquad (3)$$

which is the basis for the isoconversional procedure of Kissinger-Akahira and Sunose (KAS). The apparent activation energy at a certain degree of conversion is given by the slope of the linear regression of $\ln(\beta/T^2)$ against $-1/R \cdot T$ for the different heating rates [37]. For comparison purposes, we also used the built-in model-free kinetics option in the STARe software provided by Mettler, which is based on an advanced isoconversional procedure [35, 38].

Assuming that the approximation given by expression (3) is valid, we can determine the kinetic model that best describes the curing process by rearranging expression (3) as

$$\ln\left(\frac{g(x) \cdot \beta}{T^2}\right) = \ln\left(\frac{A \cdot R}{E}\right) - \frac{E}{R \cdot T} \qquad (4)$$

which is the basis for the composite integral method for the determination of the kinetic model [39-41]. The plot of $\ln(g(x) \cdot \beta/T^2)$ against $-1/R \cdot T$ for all the heating rates should yield a perfectly straight line, with a slope *E* equivalent to the isoconversional activation energy if the kinetic model *g(x)* is right. Deviations from linearity such as the appearance of multiple lines corresponding to the different heating rates clearly indicate that a model is not suitable [39]. Some other deviations may occur in complex multi-step processes with significant changes in isoconversional activation energy throughout the curing, which limits its use to constant activation energy conversion ranges [41]. Given that the curing of epoxy-anhydride has been satisfactory modelled using autocatalytic-like models [24, 26, 42, 43] with an overall reaction order around 2, we have fitted the experimental data to autocatalytic kinetic models with $n+m=2$, $n \neq 1$ (it must be noted that the restriction $n+m=2$ is necessary in order to derive an integral expression *g(x)* for the autocatalytic model). We have also fitted the experimental data to n-th order and Avrami reaction models. All these models are commonly used in the kinetic analysis of isothermal and nonisothermal data [37, 44]. The differential and integral functions of these models, *f(x)* and *g(x)* respectively, are presented in Table 1. We have limited the fitting to the conversion ranges where the apparent activation energy could be considered constant, and used *n* as a fitting parameter so that the slope of the linear regression produced an activation energy similar to the isoconversional values and the correlation coefficient r^2 was close to 1.

Table 1. Kinetic models used for the fitting of the experimental data.

Model	*f*(*x*)	*g*(*x*)
Autocatalytic *n*+*m*=2	$x^{2-n}(1-x)^{n}$	$\frac{1}{n-1}\left(\frac{1-x}{x}\right)^{1-n}$ ($n\neq1$)
n-th order	$(1-x)^{n}$	$\frac{1-(1-x)^{1-n}}{1-n}$ ($n\neq1$) $-\ln(1-x)$ ($n=1$)
Avrami	$n(1-x)(-\ln(1-x))^{1-\frac{1}{n}}$	$(-\ln(1-x))^{\frac{1}{n}}$

Experimental

Reactants

Diglycidyl Ether of Bisphenol A (DGEBA, Araldite GY 240, Huntsman) (182 g/mol) was dried under vacuum at 80 ºC for 6 hours before use. Methylhexahydrophtalic anhydride (MHHPA, Aldrich) (168 g/mol) was redistilled under vacuum before use. 10-Undecenoyl chloride, benzyldimethylamine (BDMA), triethylamine (TEA), were purchased from Aldrich and used without further purification. Hyperbranched polymer Boltorn H30 (Mw = 3500 g/mol, hydroxyl number = 480 – 510 g KOH/g polymer, according to its datasheet) were donated by Perstorp and were used as received. All solvents were dried and purified by conventional procedures. Scheme 2 shows the structure of DGEBA, MHHPA and BDMA.

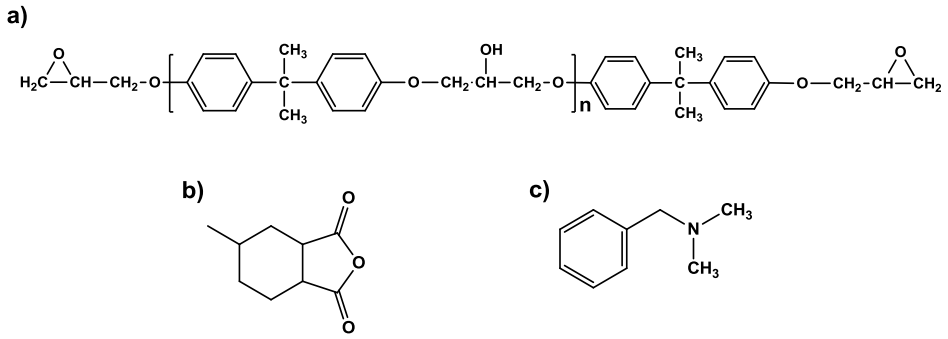

Scheme 2. Structures of a) DGEBA (182 g/eq, *n*=0.084), b) MHHPA and c) BDMA

H30$_{xxx}$vin with different degrees of modification (*xxx* stands for the percentage of modification) was prepared starting from Boltorn H30 and different stoichiometric ratios of 10-undecenoyl chloride, following a conventional acylation procedure using THF as solvent and triethylamine as hydrochloric acid acceptor [28]. The degree of modification was determined by NMR spectroscopy as previously described [28]. The following polymers were prepared: H30$_{25\%}$vin (25% modification), H30$_{60\%}$vin (60% modification), H30$_{76\%}$vin (76% modification), and H30$_{93\%}$vin (93% modification). The modification is shown in Scheme 3, along with the idealized structure of H30$_{xxx}$vin. The polymers were obtained as yellowish liquids. Table 2, summarizes

relevant characteristics of the modified HBPs. The molecular weight of the HBPs increases with the degree of modification, but the hydroxyl equivalent weight increases more dramatically due to the reduction in the remaining amount of hydroxyl groups. All HBPs have a T_g around -60 ºC.

Table 2. Number molecular weight M_n, hydroxyl equivalent weight and glass transition temperature T_g of the modified HBPs.

HBPs	M_n[a] (g/mol)	OH equiv.wt[a] (g/equiv.$_{OH}$)	T_g[b] (ºC)
H30$_{25\%}$vin	4828	201	-65
H30$_{60\%}$vin	6654	512	-58
H30$_{76\%}$vin	7484	940	-65
H30$_{93\%}$vin	8480	4240	-57

[a] Determined by NMR
[b] Determined by DSC at 10 ºC/min

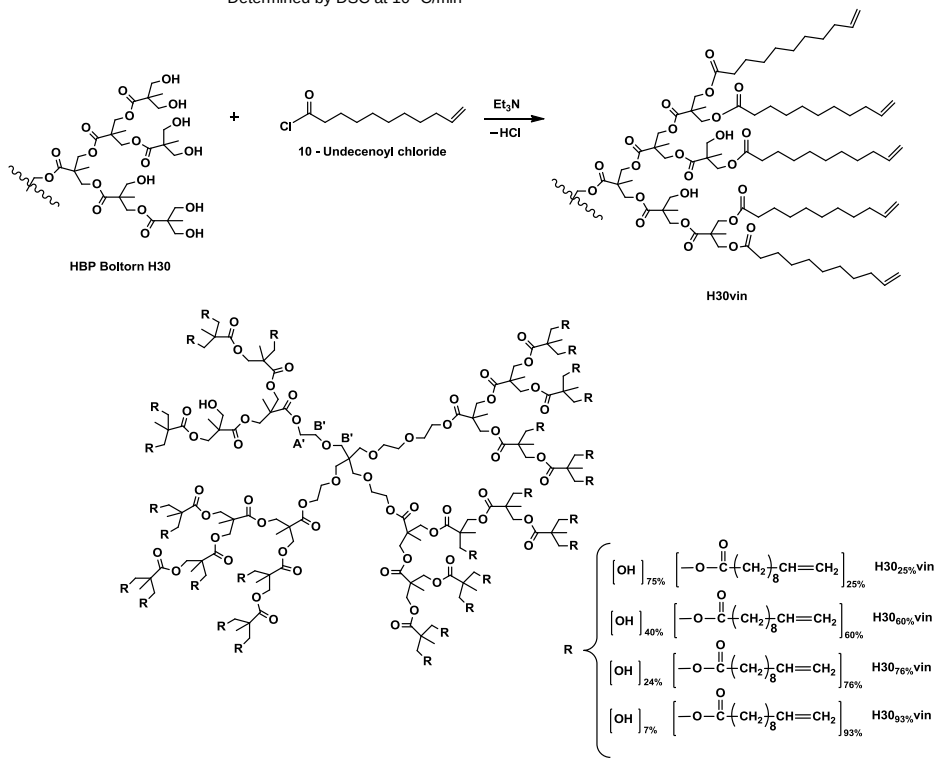

Scheme 3. Modification of OH-ended H30 and idealized structure of H30$_{xx}$vin with the different degrees of chemical modification obtained.

Preparation of formulations

Table 3 shows the composition of the DGEBA:MHHPA neat formulation and the DGEBA:MHHPA formulations with 5 and 10 wt.% of H30vin with different degrees of modification. DGEBA and MHHPA were used in stoichiometric proportions in the neat formulation. An excess

of anhydride groups was used in the H30vin formulations to compensate for the extra hydroxyl groups according to previous results [15, 24], so that they are anhydride over-stoichiometric with respect to the epoxy. For all formulations, the amount of initiator was 1 phr (parts per hundred) with respect to the anhydride. The different components were added to a vial and mixed by mechanical stirring. The formulations were degassed under vacuum before use.

Table 3. Composition of the formulation with different weight percentage of $H30_{25\%}$vin, $H30_{60\%}$vin, $H30_{76\%}$vin, $H30_{93\%}$vin. In percentage by total weight (%wt) of the mixture and equivalent ratio, ($X_{equiv.}$).

Formulation	DGEBA		MHHPA		BDMA		OH from HBP	
	$X_{equiv.}$	wt.%	$X_{equiv.}$	wt.%	$X_{equiv.}$	wt.%	$X_{equiv.}$	wt.%
DGEBA/MHHPA	1.00	51.8	1.00	47.8	0.0062	0.5	0.00	0.0
5% $H30_{25\%}$vin	0.96	48.1	1.05	46.5	0.0064	0.5	0.09	5.0
10% $H30_{25\%}$vin	0.91	44.4	1.10	45.2	0.0065	0.5	0.18	10.0
5% $H30_{60\%}$vin	0.98	48.7	1.02	45.8	0.0063	0.5	0.04	5.0
10% $H30_{60\%}$vin	0.96	45.7	1.04	43.9	0.0063	0.4	0.07	10.0
5% $H30_{76\%}$vin	0.99	48.9	1.01	45.6	0.0062	0.5	0.02	5.0
10% $H30_{76\%}$vin	0.98	46.1	1.02	43.5	0.0063	0.4	0.04	10.0
5% $H30_{93\%}$vin	1.00	49.1	1.00	45.4	0.0062	0.5	0.00	5.0
10% $H30_{93\%}$vin	1.00	46.5	1.00	43.1	0.0062	0.4	0.01	10.0

NMR Characterization

^{1}H NMR 400 MHz and ^{13}C NMR 100.6 MHz NMR spectra were obtained using a Varian Gemini 400 spectrometer with Fourier Transformed. ^{1}H spectra were acquired in 1 min and 16 scans with a 1.0 s relaxation delay (D1). ^{13}C NMR spectra were obtained using a D1 of 0.5 s and an acquisition time of 0.2 s. 500 accumulations were recorded. $CDCl_3$ was used as solvent and TMS as internal standard.

Differential scanning calorimetry (DSC)

A Mettler DSC822e calorimeter equipped with a robotic arm was used for the curing of ca 10 mg samples at the heating rates of 2, 5, 10 and 15 ºC/min up to 300 ºC in nitrogen atmosphere. A heating at 10 ºC/min up to 200 ºC was performed after the nonisothermal curing to verify the degree of cure and determine the T_g, which was calculated by the Richardson method as specified in the Mettler STARe^{TM} software. The degree of conversion *x* and the reaction rate *dx/dt* were calculated as follows

$$x = \frac{\Delta h_t}{\Delta h_{total}} \qquad \frac{dx}{dt} = \frac{dh/dt}{\Delta h_{total}} \qquad (5)$$

where Δh_t is the reaction heat evolved up to a time *t*, Δh_{total} is the total reaction heat evolved (i.e. in isothermal experiments it would be the sum of the isothermal heat and residual heat if detected) and *dh*/*dt* is the heat flow evolved during the curing process.

Infrared spectroscopy (FTIR)

A Bruker Vertex 70 FTIR spectrometer equipped with an ATR device with temperature control (Golden Gate heated single-reflection diamond ATR, Specac-Teknokroma) was used to determine the FTIR spectra of the cured materials and to monitor the evolution of functional groups during isothermal curing of the formulations at 100, 120 and 140 ºC.

The FTIR was used at a resolution of 4 cm^{-1} and 20 scans were averaged for each spectrum. In order to correct the penetration depth of the radiation in the samples, the spectra were multiplied by *W/1000*, where *W* is the wavenumber. A background was run before every series of measurements.

The conversion of reactive groups was determined using the Lambert-Beer law

$$A = \varepsilon \cdot c \cdot l \qquad (6)$$

where *A* is the absorbance of a species at a specific wavelength, ε is the absorbance coefficient at the wavelength, *c* is the concentration of the species and *l* is the optical length of the sample.

The conversion of a disappearing species was calculated as

$$x = 1 - \frac{A'_{spec,t}}{A'_{spec,0}} \qquad (7)$$

and the conversion of a species that is being formed or, equivalently, its normalized concentration, was calculated as

$$x = \frac{A'_{spec,t} - A'_{spec,0}}{A'_{spec,\infty} - A'_{spec,0}} \qquad (8)$$

where $A'_{spec} = A_{spec} / A_{ref}$ is the normalized absorbance of a species, the subindexes *spec* and *ref* relate to the wavenumber of the monitored species and a reference species, used for the normalization. The subindexes *0*, *t* and ∞ refer to the beginning of the curing, an instant t, and the maximum achievable value, respectively.

The disappearance of the two peaks at 1860 and 1785 cm^{-1} was used to monitor the conversion of anhydride groups. The growth of the peak at 1732 cm^{-1} was used to monitor the formation of ester groups. A shoulder in the carbonyl ester band at 1705 cm^{-1} was associated with the presence of carboxylic acid. The peaks at the carbonyl region were be deconvoluted using Gaussian-Lorentzian functions using the OPUS™ software. The disappearance of epoxy groups could not be monitored because of the overlapping of epoxy band at 915 cm^{-1} with two strong absorption bands of the anhydride at 895 and 915 cm^{-1}. The peak at 1508 cm^{-1},

associated with the DGEBA aromatic rings, was used for the normalization of the absorbances. The conversion of the functional groups in the carbonyl region were calculated as follows

$$x_{anh} = 1 - \frac{A'_{1860+1785,t}}{A'_{1860+1785,0}} \qquad (9)$$

$$x_{ester} = \frac{A'_{1732,t} - A'_{1732,0}}{A'_{1732+1705,\infty} - A'_{1732,0}} \qquad (10)$$

$$x_{acid} = \frac{A'_{1705,t} - A'_{1705,0}}{A'_{1732+1705,\infty} - A'_{1702,0}} \qquad (11)$$

where x_{anh}, x_{ester} and x_{acid} correspond to anhydride, ester and acid groups, respectively. Note that, for the maximum absorbance of ester and acid groups, we have used the same value $A'_{1732+1705,\infty}$ for both. Taking this into account and the fact the hydroxyl-anhydride esterification (see Scheme 1.b) leads to acid and ester formation, x_{acid} defined this way can reach a maximum value of 0.5. The number of acid groups formed with respect to the initial amount of epoxy groups can be calculated as

$$n_{acid} = 2 \cdot R \cdot x_{anh} \qquad (12)$$

where R is the stoichiometric ratio between anhydride and epoxy groups. In order to estimate the relative contribution of the non-catalyzed hydroxyl-anhydride esterification to the curing process, a ratio between acid formation and anhydride reaction, r_{acid}, was calculated as

$$r_{acid} = \frac{A'_{1705,t}}{\left(A'_{1732,t} - A'_{1705,0}\right)/2 + A'_{1705,t}} \qquad (13)$$

where $(A'_{1732,t} - A'_{1705,t})/2$ means half the ester groups formed by copolymerization, that is, the amount of anhydride groups that have copolymerized and formed two ester groups, either by the anionic copolymerization mechanism, Scheme 1.a, or following the pathway shown in Scheme 1.b, with intermediate carboxylic acid, while $A'_{1705,t}$ gives the amount of anhydride groups that have reacted only with a hydroxyl group to form an acid and an ester.

The conversion of epoxy groups x_{epoxy} was estimated indirectly from the absorbance of the combined epoxy and anhydride band at 895 and 915 cm^{-1} as follows

$$A'_{epoxy,t} = A'_{915+895,t} - \left(1 - x_{anh}\right) \cdot A'_{915+895,0} \cdot F \qquad (14)$$

$$x_{epoxy} = 1 - \frac{A'_{epoxy,t}}{A'_{epoxy,0}} \qquad (15)$$

where F is the contribution of the anhydride to the combined band.

Rheological measurements

TA Instruments AR G2 was used to determine the complex viscosity of the modified HBPs, by means of a frequency sweep from 0.1 to 100 rad/s and a 10% strain at different temperatures. Assuming that the Cox-Merz rule is valid, the values of the complex viscosity are comparable to those obtained in steady state viscosity measurements with shear rates equivalent to the oscillation frequency.

Results

DSC curing kinetics

Figure 1 plots the dynamic curing at 10 ºC/min of the neat DGEBA-MHHPA formulation and the modified formulations with 10 wt.% of the different HBPs. We can see in Table 4 that the average reaction heat in kJ/ee is similar for all formulations and within the reported literature values for analogue epoxy-anhydride systems [15, 24, 26, 42, 43], which indicates that all the formulations are able to cure completely. In Figure 1 it can be observed that all the formulations cure within the same temperature range. It has been reported that the use of hydroxyl-terminated HBPs can accelerate the curing of epoxy-anhydride formulations [15, 24, 26] but no clear effect is observed. Moreover, it is also reported that the curing can be slowed down due to a decrease in the mobility of the reaction medium [28, 45] but, again, no significant differences between any of the formulations is observed. From the peak temperatures reported in Table 4 it is not possible to determine any significant difference in reactivity either.

Table 4. Calorimetric data of DGEBA/MHHPA/BDMA mixture with different percentages of $H30_{25\%}$vin, $H30_{60\%}$vin, $H30_{76\%}$vin, $H30_{93\%}$vin.

Formulation	Δh^{a} (J/g)	$\Delta h^{a,b}$ kJ/ee)	$T_{max}{}^{c}$ (ºC)	$T_{g,DSC}{}^{d}$ (ºC)
DGEBA/MHHPA	314	110	159	149
5% $H30_{25\%}$vin	296	112	160	125
10% $H30_{25\%}$vin	286	117	161	115
5% $H30_{60\%}$vin	327	122	163	135
10% $H30_{60\%}$vin	329	130	161	128
5% $H30_{76\%}$vin	276	103	157	142
10% $H30_{76\%}$vin	275	108	159	139
5% $H30_{93\%}$vin	300	111	163	144
10% $H30_{93\%}$vin	265	104	159	141

[a] Average data from calorimetric experiments at 2,5,10 and 15 ºC/min
[b] Enthalpies per equivalent of epoxy group.
[c] Temperature of the maximum of the curing exotherm at 10 ºC/min
[d] Glass transition temperature. Second scan after dynamic curing at 10 ºC/min.

The use of the HBP decreases the value of T_g but, as the degree of modification of the HBP increases, it rises up to values close to the unmodified DGEBA/MHHPA formulation. This can be rationalized in terms of the solubility of the HBP in the epoxy-anhydride matrix. When the

degree of modification is low, the solubility of the HBP is higher, thus acting as an internal plasticizer and reducing the T_g. When the HBP is further modified, above 60%, the compatibility decreases and can phase-separate during the curing process, leading to a material with a T_g corresponding to an epoxy-anhydride matrix, comparable to that of the unmodified formulation. This is, however, out of the scope of this work and is going to be discussed in a forthcoming paper.

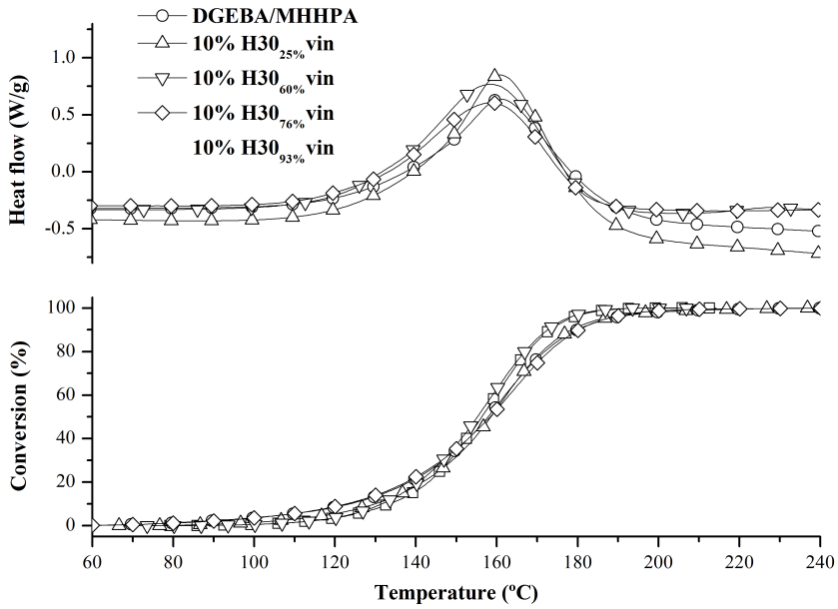

Figure 1. Non-isothermal DSC curing at 10 ºC/min of DGEBA-MHHPA formulations with 10 wt.% of the different HBPs.

In order to determine whether there is any effect of the amount and degree of modification of the HBP on the curing kinetics we analyzed the curing kinetics according to the procedures described in theoretical section.

Figure 2 shows the result of the isoconversional analysis of the curing of the neat formulation and the formulations with 5 wt.% of the modifier using the KAS method. We compared the results provided by the STARe software and the KAS method and obtained almost identical isoconversional activation energy throughout the analyzed conversion range. This must be attributed to the fact that, within the experimental temperature and conversion range, the accuracy of the Coats-Redfern solution of the temperature integral is sufficient. Therefore we can safely assume that the values provided by the KAS method are valid and reliable kinetic parameters can be obtained based on this approximation.

The activation energy for all the formulations is around 70-90 kJ/mol, with no clearly defined trend. Apparently, H30$_{25\%}$vin and H30$_{60\%}$vin decrease the activation energy but further modification makes it increase. For the most modified polymer, however, the activation energy reaches lower values than the rest of them. A similar trend was obtained for the formulations with 10 wt.% of the modifier, except for the one with 10 wt.% of H30$_{93\%}$vin, which gave very high activation energy values and was excluded for further calculations. In spite of the complexity of

the curing process, the activation energy is fairly constant throughout the whole conversion range. Similar results were obtained in the curing of DGEBA-THPA with unmodified H30 [24]. Deviations at the beginning and at the end of the curing process were assumed to arise as a consequence of uncertainty in the determination of the baseline. This allows us to consider the overall curing as a single-step process and determine, with some degre of ascertainment, an overall kinetic model using the model-fitting methods described in the theoretical section.

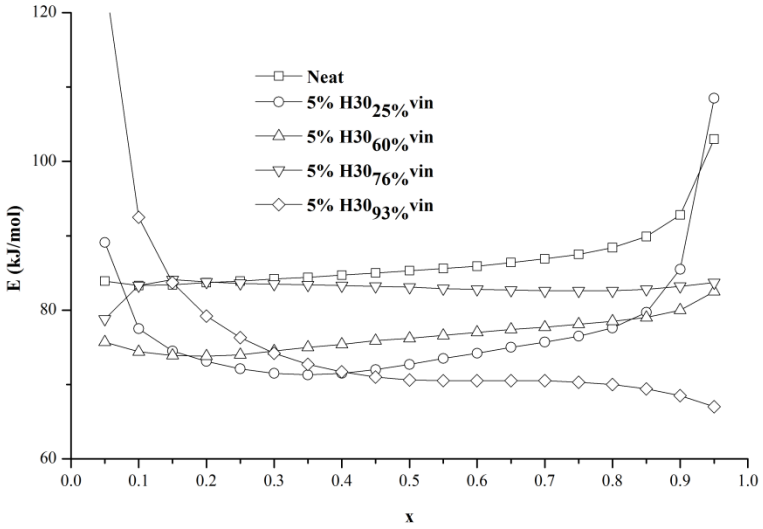

Figure 2. Dependence of the apparent activation energy *E* on the degree of conversion *x* for the neat formulation and the formulations with 5 wt.% of the different modifiers.

Table 5. Kinetic parameters corresponding to the best fitting of the different models used in this work for the unmodified DGEBA/MHHPA formulation.

Model	*n*	E (kJ/mol)	ln A (min^{-1})	r^2
Autocatalytic	1.68	84.87	23.84	0.9900
n-th order	0.67	87.68	23.71	0.9971
Avrami	1.13	85.50	23.24	0.9985

Table 5 shows the result of the application of the composite integral method to the curing of the unmodified DGEBA/MHHPA formulation in the conversion range from 0.05 to 0.85. It can be seen that all models provide a fairly good fitting with similar activation energy, but the best adjustment was obtained with the Avrami model, *n*=1.13. Moreover, it also yielded the activation energy closest to the average isoconversional energy, 85.42 kJ/mol. One must bear in mind that the adjustment of these parameters is somewhat arbitrary, it is only valid as a phenomenological description of the curing process and cannot be directly associated with the true underlying curing mechanism. It is useful, however, for the prediction of the reaction rate and degree of cure for different temperature programs other that the constant heating rate. We performed this same analysis for the different formulations and found that the Avrami model was

the most suitable, but with slightly different *n* parameter. The results of the fitting for the different formulations using this model are summarized in Table 6. The adjustment is excellent in all cases (note that the 10% $H30_{93\%}$vin formulation was excluded from the calculations as it was not possible to determine a constant average activation energy).

Table 6. Kinetic parameters corresponding to the best fitting of the Avrami model to the different formulations. E_{iso} is the average isoconversional activation energy in the conversion range.

Formulation	x	E_{iso} (kJ/mol)	*n*	E (kJ/mol)	ln A (min^{-1})	r^2	$R_{x=0.5,100ºC}$
DGEBA/MHHPA	0.05-0.85	85.42	1.13	85.50	23.24	0.9985	1
5% $H30_{25\%}$vin	0.1-0.9	74.92	1.17	74.73	19.79	0.9957	1.03
10% $H30_{25\%}$vin	0.15-0.95	76.20	1.16	72.20	19.08	0.9964	1.17
5% $H30_{60\%}$vin	0.05-0.95	76.61	1.26	76.63	20.57	0.9961	1.26
10% $H30_{60\%}$vin	0.1-0.95	71.75	1.31	71.55	18.91	0.9979	1.22
5% $H30_{76\%}$vin	0.1-0.95	83.19	1.18	83.45	22.58	0.9959	1.05
10% $H30_{76\%}$vin	0.15-0.9	77.63	1.35	77.62	20.83	0.9992	1.13
5% $H30_{93\%}$vin	0.2-0.9	71.73	1.32	71.58	18.85	0.9986	1.09

In order to analyze the effect of the different modifiers in the curing kinetics, we have defined a relative reaction rate between the modified formulations and the DGEBA/MHHPA formulation, R_x, as follows

$$R_x = \frac{dx/dt}{dx/dt_{neat}} \qquad (17)$$

where the subindex x is a specific degree of conversion and the subindex neat refers to the DGEBA/MHHPA formulation. The calculated R_x at 100 ºC and a degree of conversion 0.5 are shown in Table 6. It is seen how the presence of the modifier somewhat accelerates the curing at this temperature, but the trend is complex.

It was previously reported [15, 24, 26] that the use of unmodified hydroxyl-ended HBPs in epoxy-anhydride formulations produced an increase in the reaction rate because of their positive effect on the initiation by the tertiary amine [26]. This effect was more important taking into account the decrease in mobility produced by the increased viscosity of the formulations and the participation of the HBP in the curing process. Concerning the effect of the degree of modification of the HBP and the amount of HBP in the formulations, one should take into account 1) the positive effect of hydroxyl groups on the curing and 2) the increase in viscosity and the reduced mobility caused by the presence and participationof the HBP in the process. We have measured the complex viscosity of the HBPs in the rheometer in the oscillatory mode at 40 ºC and found a newtonian behaviour between 0.1 and 30 rad/s. We obtained the following values with increasing degree of vinyl group modification: 3.09, 1.96, 0.93 and 2.03 (corresponding to $H30_{25\%}$vin, $H30_{60\%}$vin, $H30_{76\%}$vin and $H30_{93\%}$vin, respectively). On decreasing the amount of hydroxyl groups we reduce the amount of inter-molecular hydrogen-bond interactions, which

tends to decrease the viscosity. However, the molecular weight of the modifier increases which, eventually, produces an increase in the viscosity, hence the lower viscosity of $H30_{76\%}$vin with respect to $H30_{93\%}$vin. The effect of hydroxyl groups in the curing is counterbalanced by the decrease in the mobility of the species during curing due to the increased viscosity of the formulation.

FTIR curing monitoring

The curing of the DGEBA/MHHPA formulation has been monitored with FTIR at different temperatures in order to identify the main reactions taking place during curing. Figure 3 plots the FTIR spectra recorded during curing of this formulation at 120 ºC in the FTIR. The general features of the epoxy-anhydride curing reaction can be observed: the decrease of the combined epoxy-anhydride band (895 and 915 cm^{-1}) and anhydride (1784 and 1860 cm^{-1}) groups, which react giving rise to ester groups (1732 cm^{-1}). As stated in the experimental section, epoxy groups could not be monitored individually with FTIR but their evolution was nevertheless estimated. It must be noted the appearance and growth of a shoulder (1705 cm^{-1}) that can be assigned to the formation of carboxylic acid overlapping the carbonyl ester band. After reaching a maximum, once the anhydride is almost exhausted, the shoulder at 1705 cm^{-1} decreases and almost disappears. This can be explained by the formation of carboxylic acid groups by esterification of anhydride with hydroxyl groups present in the mixture, e.g. coming from DGEBA, and later on, once the anhydride groups are almost exhausted, by the epoxy-carboxylic acid esterification giving rise to terminal hydroxyl groups, following the reaction steps shown in Scheme 1.b. Indeed, in the lower graph of Figure 3 it is observed that, at the end of the process, when the anhydride is almost exhausted, there is only epoxy remaining (the peak at 915 cm^{-1}), which then reacts by the esterification with the carboxylic acid. This is an indication that the conversion of epoxy groups is delayed with respect to the anhydride, as observed in our previous kinetic study on analogous formulations [26] and in contrast with other studies on the curing of epoxy-anhydride formulations, where it is assumed that the epoxy and anhydride can be grouped as a single reacting pair [33].

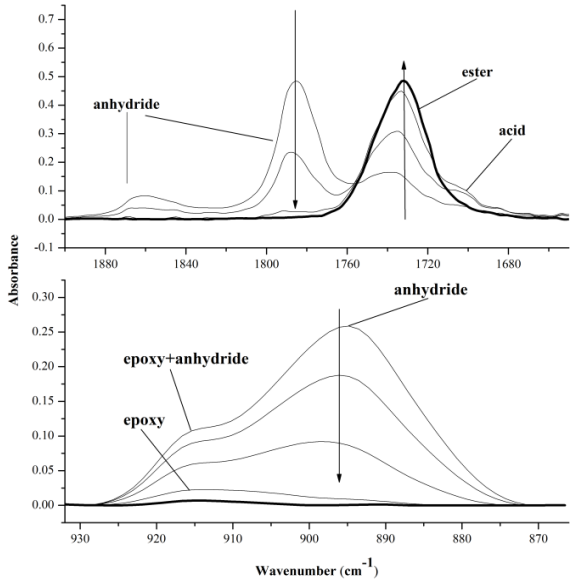

Figure 3. FTIR spectra recorded during curing of DGEBA/MHHPA formulation at 120 ºC. The last spectrum is highlighted in a thicker line. The spectra were acquired at 0, 300, 780, 2880 and 4800s.

Figure 4 plots the conversion of anhydride, ester, acid and epoxy groups (x_{anh}, x_{ester}, x_{acid} and x_{epoxy} respectively) with respect to time (upper graph), and the conversion of ester, acid and epoxy groups with respect to the conversion of anhydride groups (lower graph). The curing has been divided into different stages:

1) Up to $x_{anh} \cong 0.4$, there is a steady increase of x_{acid} and r_{acid} indicating that, at the beginning of the process, the esterification of hydroxyl and anhydride groups is being favoured with respect to the anionic copolymerization, resulting in a lower x_{ester} with respect to x_{anh}. This may be explained by tertiary amine regeneration, leading to an increase in the amount of available hydroxyl groups which can react with anhydrides [26]. The gap between x_{epoxy} and x_{anh} is even higher, indicating that, at the beginning of the curing, the anhydride-hydroxyl esterification prevails over the alternating copolymerization in Scheme 1.a.

2) From $x_{anh} \cong 0.4$ up to $x_{anh} \cong 0.95$ r_{acid} levels off at ca 0.3 and slowly decreases, while x_{acid} increases up to ca 0.14, indicating that esterification of hydroxyl groups with anhydrides is still taking place throughout the curing process. x_{epoxy} increases due to the occurrence of the alternating copolymerization, but the gap between x_{anh} and x_{epoxy} still increases. The number of carboxylic acids with respect to the initial amount of anhydride at the end of this stage is twice the maximum x_{acid}, 0.28, and given that this is a stoichiometric formulation, it would be the same with respect to the initial amount of epoxy gorups. According to the initial amount of hydroxyl groups in the mixture (0.042 hydroxyl groups per epoxy group for a 182 g/eq DGEBA), we can expect a maximum of ca 0.04. This significant deviation from the expected value can be explained by regeneration of tertiary amine as the curing progresses.

3) Above $x_{anh} \cong 0.9$ both x_{acid} and r_{acid} start to decrease dramatically, followed by an increase in x_{ester} and x_{epoxy} due to the carboxylic acid-epoxy esterification depicted in Scheme 1.b. Only when the anhydride groups are exhausted, carboxylic acids can react with epoxy groups to a measurable extent leading to formation of ester groups and more hydroxyl groups, but no more carboxylic acid groups can be formed in the absence of anhydride.

These results show that both reaction pathways depicted in Scheme 1 occur. The relative contribution of the non-catalyzed hydroxyl-anhydride esterification, given by the value of r_{acid} in Figure 4, is rather high and constant throughout the during, which can be ascribed to the regeneration of tertiary amines. The carboxylic acid-epoxy esterification takes place only to a significant extent at the end of the process, once the anhydride is almost exhausted, because of its high activation energy [31], above 100-130 kJ/mol. In Figure 4 it can be noticed an excess of carboxylic acid groups at the end of the process, $x_{acid} \cong 0.05$ which corresponds to an amount of acid of 0.1 with respect to the epoxy groups. Given the uncertainty in the estimation of the epoxy conversion and the fact that the curing temperature is below T_g (see Table 4), it is difficult to determine whether all remaining acid groups can react with epoxy or some epoxy polyetherification can take place to a certain extent [26].

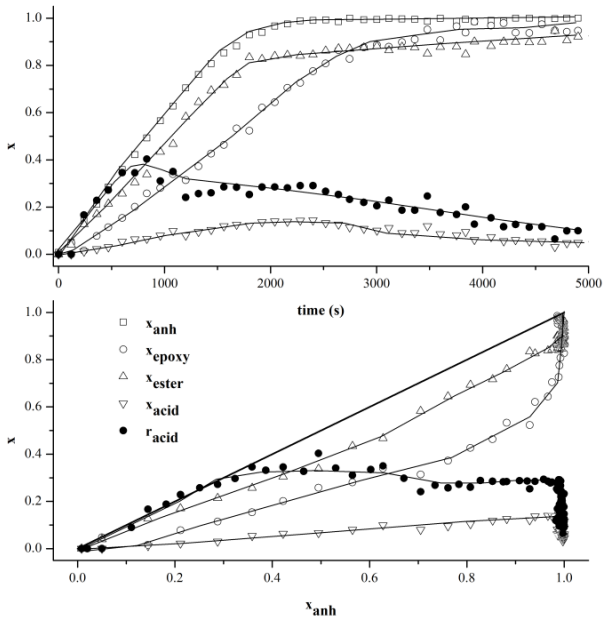

Figure 4. Conversion of anhydride, epoxy, ester and acid groups of the DGEBA/MHHPA formulation at 120 ºC with respect to time (upper graph) and with respect to the anhydride conversion (lower graph, the thick straight line represents the anhydride conversion). The lines have been drawn to guide the eye.

We studied the curing kinetics of the modified formulations with 10% $H30_{25\%}$vin and 10% $H30_{76\%}$vin in order to determine the effect on the curing kinetics of the presence of the modifier and the degree of modification. These two formulations have been selected as representative examples of a highly soluble modifier and a phase-separating modifier respectively, which will be studied in more detail in a forthcoming work. Similar features were observed in the curing of both formulations, so they are not going to be discussed individually but in comparison with the DGEBA/MHHPA formulation.

Figure 5 compares the conversion-time curves of the formulation with 10% $H30_{76\%}$vin at 120 ºC. It is observed how the anhydride conversion is faster with 10% of $H30_{25\%}$vin than with 10% $H30_{76\%}$vin, which in turn is faster than that of the unmodified formulation. This can be explained by the higher amount of hydroxyl groups coming from the HBP, which promotes the hydroxyl-anhydride esterification and is a first step for the incorporation or the compatibilization of the HBP with the thermoset matrix. The conversion of epoxy groups with either modifier is faster than that of the unmodified formulation, with the same trend as in the case of the anhydride group, taking into account the uncertainty of this estimation. The higher initial amount of hydroxyl groups in the 10% of $H30_{25\%}$vin formulation promotes the initiation and the anionic epoxy-anhydride copolymerization and faster epoxy conversion than 10% of $H30_{76\%}$vin but eventually conversion of epoxy groups with both modifiers proceeds at a similar rate in the middle of the process, in agreement with the data reported in Table 6.

When the evolution of acid groups is analyzed, it is observed that the amount of acid throughout the curing is higher for the formulation with more added hydroxyl groups. This is consistent with the faster anhydride reaction which obviously leads to a higher amount of acid groups. In the case of $H30_{25\%}$vin, x_{acid} reaches a maximum of 0.21, which is equivalent to 0.42

acid groups per initial amount of anhydride groups. This value is twice as much as the expected taking into account the initial composition of the formulation in Table 3, which can only be explained by tertiary amine regeneration. This is even more evident in the case of H30$_{76\%}$vin, because the amount of added hydroxyl groups is lower. Given that an extra amount of anhydride is added in the modified formulations, there should be a certain amount of remaining acid groups is the cured material. The remaining acid is apparently higher than expected in all cases, which indicates that epoxy polyetherification may take place to some extent, but given the uncertainty in the determination of ester, acid and epoxy groups conversion, this cannot be calculated with precision. The fact that acid is formed by the reaction of hydroxyl groups from the HBP and subsequently reacts with epoxy groups ensures incorporation of the HBP into the network structure or good compatibility between the matrix and the phase-separated HBP, in any case.

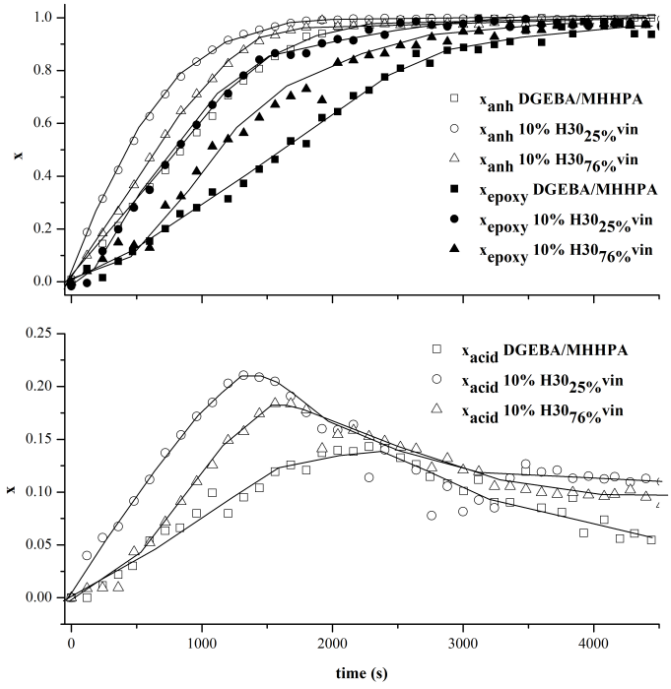

Figure 5. Conversion of anhydride, epoxy (upper graph) and acid groups (lower graph) of the DGEBA/MHHPA, 10% H30$_{25\%}$vin and 10% H30$_{76\%}$vin formulations at 120 ºC. The lines have been drawn to guide the eye.

Conclusions

Novel HBPs with different ratio of hydroxyl and undecenoyl end groups were synthesized starting from Boltorn H30, of which the terminal hydroxyl groups were partially replaced with undecenoyl chains. These novel HBPs have been used as polymeric modifiers for DGEBA/MHHPA formulations.

In the present work, the curing kinetics of neat and modified DGEBA/MHHPA formulations has been studied with DSC and FTIR. While DSC gives limited insight into the curing mechanism, a more detailed picture of the process can be obtained using FTIR. The

curing mechanism is complex and involves a series of competing reactions, as determined with FTIR. The effect of the HBPs on the curing kinetics is complex and depends on the amount of reactive hydroxyl groups and the changes in viscosity and mobility that arise from the different degree of modification. The participation of hydroxyl groups from the HBP in the curing may enhance the reaction rate but the lower mobility of the HBP may slow down the process. Incorporation of the HBP into the matrix is assured by the formation of carboxylic acid and subsequent esterification with epoxy groups.

Acknowledgements

The authors would like to thank MICINN, FEDER and Generalitat de Catalunya (MAT2011-27039-C03-01, MAT2011-27039-C03-02, 2009-SGR-1512, JCI-2010-06187 and BES-2009-025226) for giving financial support. Perstorp and Huntsman are acknowledged for kindly providing Boltorn™ H30 and Araldite GY 240, respectively.

References

[1] L. Boogh, B. Pettersson, J.-A.E. Manson, Dendritic hyperbranched polymers as toughening for epoxy resins, Polymer, 40 (1999) 2249-2261.

[2] G. Qipeng, A. Habrard, Y. Park, P.J. Halley, G.P. Simon, Phase separation, porous structure, and cure kinetics in aliphatic epoxy resin containing hyperbranched polyester, Journal of Polymer Science, Part B Polymer Physics, 44 (2006) 889-899.

[3] C.B. Arends, Polymer Toughening, in: C.B. Arends (Ed.), Marcel Dekker, New York, 1996.

[4] R.A. Pearson, A.F. Yee, Toughening mechanisms in thermoplastic-modified epoxies: 1. Modification using poly(phenylene oxide), Polymer, 34 (1993) 3658-3670.

[5] Q. Guo, R. Thomann, W. Gronski, T. Thurn-Albrecht, Phase behavior, crystallization, and hierarchical nanostructures in self-organized thermoset blends of epoxy resin and amphiphilic poly(ethylene oxide)-block-poly(propylene oxide)-block-poly(ethylene oxide) triblock copolymers, Macromolecules, 35 (2002) 3133-3144.

[6] P.M. Lipic, F.S. Bates, M.A. Hillmyer, Nanostructured thermosets from self-assembled amphiphilic block copolymer/epoxy resin mixtures, Journal of the American Chemical Society, 120 (1998) 8963-8970.

[7] J.M. Dean, R.B. Grubbs, W. Saad, R.F. Cook, F.S. Bates, Mechanical properties of block copolymer vesicle and micelle modified epoxies, Journal of Polymer Science, Part B: Polymer Physics, 41 (2003) 2444-2456.

[8] N. Schroder, L. Konczol, W. Doll, R. Mulhaupt, Mechanical properties of epoxy-based hybrid composites containing glass beads and α,ω-oligo(butylmethacrylate)diol, Journal of Applied Polymer Science, 88 (2003) 1040-1048.

[9] E. Serrano, A. Tercjak, C. Ocando, M. Larranaga, M.D. Parellada, S. Corona-Galvan, D. Mecerreyes, N.E. Zafeiropoulos, M. Stamm, I. Mondragon, Curing behavior and final properties of nanostructured thermosetting systems modified with epoxidized styrene-butadiene linear diblock copolymers, Macromolecular Chemistry and Physics, 208 (2007) 2281-2292.

[10] R. Mezzenga, J.A.E. Manson, Thermo-mechanical properties of hyperbranched polymer modified epoxies, Journal of Materials Science, 36 (2001) 4883-4891.

[11] D. Ratna, G.P. Simon, Thermomechanical properties and morphology of blends of a hydroxy-functionalized hyperbranched polymer and epoxy resin, Polymer, 42 (2001) 8833-8839.

[12] D. Ratna, R. Varley, G.P. Simon, Toughening of trifunctional epoxy using an epoxy-functionalized hyperbranched polymer, Journal of Applied Polymer Science, 89 (2003) 2339-2345.

[13] J. Xu, H. Wu, O.P. Mills, P.A. Heiden, Morphological investigation of thermosets toughened with novel thermoplastics. I. Bismaleimide modified with hyperbranched polyester, Journal of Applied Polymer Science, 72 (1999) 1065-1076.

[14] B. Voit, New developments in hyperbranched polymers, Journal of Polymer Science, Part A: Polymer Chemistry, 38 (2000) 2505-2525.

[15] M. Morell, X. Ramis, F. Ferrando, Y. Yu, A. Serra, New improved thermosets obtained from DGEBA and a hyperbranched poly(ester-amide), Polymer, 50 (2009) 5374-5383.

[16] M. Sangermano, G. Malucelli, R. Bongiovanni, A. Priola, A. Harden, Investigation on the effect of the presence of hyperbranched polymers on thermal and mechanical properties of an epoxy UV-cured system, Polymer International, 54 (2005) 917-921.

[17] R. Mezzenga, L. Boogh, J.-A.E. Manson, B. Pettersson, Effects of the Branching Architecture on the Reactivity of Epoxy a Amine Groups, Macromolecules, 33 (2000) 4373-4379.

[18] D. Ratna, G.P. Simon, Thermal and mechanical properties of a hydroxyl-functional dendritic hyperbranched polymer and trifunctional epoxy resin blends, Polymer Engineering and Science, 41 (2001) 1815-1822.

[19] D. Santiago, X. Fernàndez-Francos, X. Ramis, J.M. Salla, M. Sangermano, Comparative curing kinetics and thermal-mechanical properties of DGEBA thermosets cured with a hyperbranched poly(ethyleneimine) and an aliphatic triamine, Thermochimica Acta, 526 (2011) 9-21.

[20] X. Fernández-Francos, J.M. Salla, A. Cadenato, J.M. Morancho, A. Serra, A. Mantecón, X. Ramis, A new strategy for controlling shrinkage of DGEBA resins cured by cationic copolymerization with hydroxyl-terminated hyperbranched polymers and ytterbium triflate as an initiator, Journal of Applied Polymer Science, 111 (2009) 2822-2929.

[21] D. Foix, M. Erber, B. Voit, A. Lederer, X. Ramis, A. Mantecon, A. Serra, New hyperbranched polyester modified DGEBA thermosets with improved chemical reworkability, Polymer Degradation and Stability, 95 (2010) 445-452.

[22] D. Santiago, M. Morell, X. Fernandez-Francos, À. Serra, J.M. Salla, X. Ramis, Influence of the end groups of hyperbranched poly(glycidol) on the cationic curing and morphology of diglycidylether of bisfenol A thermosets, Reactive and Functional Polymers, 71 (2011) 380-389.

[23] M. Sangermano, A. Priola, G. Malucelli, R. Bongiovanni, A. Quaglia, B. Voit, A. Ziemer, Phenolic hyperbranched polymers as additives in cationic photopolymerization of epoxy systems, Macromolecular Materials and Engineering, 289 (2004) 442-446.

[24] D. Foix, Y. Yu, A. Serra, X. Ramis, J.M. Salla, Study on the chemical modification of epoxy/anhydride thermosets using a hydroxyl terminated hyperbranched polymer, European Polymer Journal, 45 (2009) 1454-1466.

[25] M. Morell, M. Erber, X. Ramis, F. Ferrando, B. Voit, A. Serra, New epoxy thermosets modified with hyperbranched poly(ester-amide) of different molecular weight, European Polymer Journal, 46 (2010) 1498-1509.

[26] X. Fernández-Francos, A. Rybak, R. Sekula, X. Ramis, À. Serra, Modification of epoxy-anhydride thermosets using a hyperbranched poly(ester-amide). I. Kinetics study, Polymer International, 61 (2012) 1710-1725.

[27] J. Fröhlich, H. Kautz, R. Thomann, H. Frey, R. Mülhaupt, Reactive core/shell type hyperbranched blockcopolyethers as new liquid rubbers for epoxy toughening, Polymer, 45 (2004) 2155-2164.

[28] X. Fernández-Francos, D. Foix, À. Serra, J.M. Salla, X. Ramis, Novel thermosets based on DGEBA and hyperbranched polymers modified with vinyl and epoxy end groups, Reactive and Functional Polymers, 70 (2010) 798-806.

[29] Flores M, Fernández-Francos X, Jiménez-Piqué E, Foix D, Serra A, Ramis X. Polym Eng Sci 52 (2012) 2597-2610.

[30] J.P. Pascault, H. Sautereau, J. Verdu, R.J.J. Williams, Thermosetting Polymers, Marcel Dekker, New York, 2002.

[31] A. Cherdoud-Chihani, M. Mouzali, M.J.M. Abadie, Etude par DSC de la reticulation de systemes DGEBA/polyacides, European Polymer Journal, 33 (1997) 969-975.

[32] K. Dusek, S. Lunak, L. Matejka, Gelation in the Curing of Epoxy Resins with Anhydrides, Polymer Bulletin (Berlin), 7 (1982) 145-152.

[33] A.N. Mauri, N. Galego, C.C. Riccardi, R.J.J. Williams, Kinetic model for gelation in the diepoxide-cyclic anhydride copolymerization initiated by tertiary amines, Macromolecules, 30 (1997) 1616-1620.

[34] X. Fernandez-Francos, A. Rybak, R. Sekula, X. Ramis, F. Ferrando, L. Okrasa, A. Serra, Modification of epoxy-anhydride thermosets using a hyperbranched poly(ester-amide). II. Thermal reworkability and material properties, Polymer International, 128 (2012) 4001-4013.

[35] S. Vyazovkin, N. Sbirrazzuoli, Isoconversional kinetic analysis of thermally stimulated processes in polymers, Macromolecular Rapid Communications, 27 (2006) 1515-1532.

[36] M.J. Starink, The determination of activation energy from linear heating rate experiments: a comparison of the accuracy of isoconversion methods, Thermochimica Acta, 404 (2003) 163-176.

[37] X. Ramis, J. Salla, A. Cadenato, J. Morancho, Simulation of isothermal cure of a powder coating, Journal of Thermal Analysis and Calorimetry, 72 (2003) 707-718.

[38] S. Vyazovkin, Evaluation of activation energy of thermally stimulated solid-state reactions under arbitrary variation of temperature, Journal of Computational Chemistry, 18 (1997) 393-402.

[39] A. Cadenato, J. Morancho, X. Fernández-Francos, J. Salla, X. Ramis, Comparative kinetic study of the non-isothermal thermal curing of bis-GMA/TEGDMA systems, Journal of Thermal Analysis and Calorimetry, 89 (2007) 233-244.

[40] E.-H.M. Diefallah, Kinetic analysis of thermal decomposition reactions : Part VI. Thermal decomposition of manganese(II) acetate tetrahydrate, Thermochimica Acta, 202 (1992) 1-16.

[41] P. Budrugeac, E. Segal, On the use of Diefallah's composite integral method for the non-isothermal kinetic analysis of heterogeneous solid-gas reactions, Journal of Thermal Analysis and Calorimetry, 82 (2005) 677-680.

[42] S. Montserrat, G. Andreu, P. Cortes, Y. Calventus, P. Colomer, J.M. Hutchinson, J. Malek, Addition of a reactive diluent to a catalyzed epoxy-anhydride system. I. Influence on the cure kinetics, Journal of Applied Polymer Science, 61 (1996) 1663-1674.

[43] J. Xu, M. Holst, M. Wenzel, I. Alig, Calorimetric studies on an anhydride-cured epoxy resin from diglycidyl ether of bisphenol-A and diglycidyl ether of poly(propylene glycol). I. onset of diffusion control during isothermal polymerization, Journal of Polymer Science, Part B: Polymer Physics, 46 (2008) 2155-2165.

[44] S. Vyazovkin, C.A. Wight, Model-free and model-fitting approaches to kinetic analysis of isothermal and nonisothermal data, Thermochimica Acta, 340-341 (1999) 53-68.

[45] D. Foix, X. Fernández-Francos, J.M. Salla, A. Serra, J.M. Morancho, X. Ramis, New thermosets obtained from DGEBA and hydroxyl ended hyperbranched polymers partially blocked with benzoyl and trimethyl silyl groups, Polymer International, 60 (2011) 389-397.

Efficient impact resistance improvement of epoxy/anhydride thermosets by adding hyperbranched polyesters partially modified with undecenoyl chains

Marjorie Flores,[a] Xavier Fernández-Francos,[a] Francesc Ferrando,[b] Xavier Ramis,[c] Àngels Serra[a*]

[a] Department of Analytical and Organic Chemistry, Universitat Rovira i Virgili, C/ Marcel·lí Domingo s/n, 43007, Tarragona, Spain.
[b] Department of Mechanical Engineering, Universitat Rovira i Virgili, C/ Països Catalans, 26, 43007, Tarragona, Spain.
[c] Thermodynamics Laboratory, ETSEIB Universitat Politècnica de Catalunya, Av. Diagonal 647, 08028, Barcelona, Spain.

Abstract

Boltorn H30 hyperbranched polyester has been modified by acylation with 10-undecenoyl chloride to obtain HBPs with different degree of modification. These HBPs have been used as reactive modifiers, in a proportion of 5 and 10%, of DGEBA/MHHPA/BDMA formulations. The materials obtained have been characterized and their mechanical properties evaluated. Depending on the degree of modification of the HBP, homogeneous or phase separated materials were obtained, which influence the properties. When the degree of modification of the HBP was a 76%, a 4-fold increase in impact resistance was achieved without sacrificing thermomechanical characteristics, thermal stability or processability. This has been attributed to the regular microphase separation achieved and to the good interfacial interaction of the microparticles with the epoxy matrix by formation of covalent bonds between the remaining hydroxyl groups at the shell of the HBP and the anhydride as the curing agent.

Keywords: *Hyperbranched polymers, epoxy resins, toughness.*

Introduction

Epoxy resins are commonly used as thermosetting materials due to their excellent thermomechanical properties and chemical and environmental stability. They present also good processability before curing. These materials are one of the most important classes of thermosetting polymers, used world-wide since their industrial introduction in 1946 in the field of coatings, adhesives, moulding compounds and polymer composites [1]. Their broad range of applications can be explained due to the fact that they are probably one of the most versatile thermosets because not only the type of resin and the chemistry of the curing can be varied, but also a huge number of organic and inorganic modifiers and fillers can be added to improve their properties [2].

Although rigidity and strength are desired properties in engineering applications, toughness is one of the restrictions in the use of epoxy resins. The low toughness, coming from the high crosslinking density, affects the durability of coatings and places strong constraints on design parameters [3].

The first attempts to improve toughness were based on the addition of liquid rubbers or thermoplastics, but usually these additives compromise the modulus and thermomechanical characteristics of the thermosets and the processability of the formulation [4]. Toughness implies energy absorption and it is achieved through various deformation mechanisms before failure

occurs. One of the most effective methods of preventing the crack to freely develop after impact is the addition of a second phase that induces the formation of particles that absorb the impact energy and deflect the crack. It has been recognized that a combination of cavitation around the rubber particles with shear yielding in the matrix produces a cooperative effect in the energy dissipation [5]. The effect reached depends on the particle characteristics, *e.g.* size, interparticle distance, distribution, particle/matrix interaction, among other [6,7]. Generally, the particles are generated by reaction-induced phase separation (RIPS) from a homogeneous solution composed of the resin, curing agent and modifiers. The phase separated morphology in the blends depends on the kinetics of curing and on the dynamics of the phase separation process. From the thermodynamic point of view, the driving force for the reaction-induced phase separation is the unfavourable entropic contribution to the mixing free energy resulting from the extremely high increase in molecular weight of epoxy structure during curing [4].

To overcome the limitations of rubbers or linear thermoplastics used as tougheners that leads to a reduction of the thermomechanical characteristics and to an increased viscosity before curing, the use of hyperbranched polymers (HBPs) has been proposed by several authors [8-12]. The dendritic structure of HBPs makes these modifiers very promising in terms of processability because of the low entanglement that leads to low viscosities in comparison to linear polymers [13]. By partial or complete modification of their numerous terminal groups, it is possible to tune their interaction with the matrix or facilitate its covalent linkage to the epoxy matrix, which can lead to phase separated or homogeneous morphologies [14]. Since the best toughness characteristics are attributed to a larger plastic zone size, which is observed in systems clearly showing particles partially linked to the matrix, the presence of non-modified hydroxyl groups in the HBP shell can improve the interaction in the interface between the separated particles and the matrix.

Taking this into account, in the present work we propose the use of a series of partially modified Boltorn type polyesters with undecenoyl moieties as modifier for DGEBA thermosets cured with anhydrides in the presence of a tertiary amine as a catalyst. In a previous publication [15], we have reported the kinetic of the curing process of these systems, using differential scanning calorimetry and FTIR as experimental techniques. FTIR gave a more detailed picture of the process, which is complex from the reaction point of view, because there is a competition among the reaction of epoxide and anhydride and the esterification of hydroxyl groups of the HBP. Our interest is to investigate the influence of the degree of modification on the pre-polymer viscosity, on the possible phase-separation during curing and on the mechanical and thermal characteristics of the prepared material, emphasizing toughness improvement. The possibility of tailoring the hyperbranched polyester shell chemistry enables synthesizing HBPs with different degrees of compatibility with the resin that opens a new way to reach, by this easy procedure, a series of epoxy thermosets with different final characteristics.

Experimental section

Materials

Diglycidylether of Bisphenol-A (DGEBA), GY 240 was provided by Huntsman Advanced Materials (epoxy equivalent = 182 g/eq), and was used after drying under vacuum. Methylhexahydrophthalic anhydride (MHHPA) (Aldrich) was distilled before use. 10-Undecenoyl chloride, benzyldimethylamine (BDMA) and triethylamine (TEA), were purchased from Aldrich and used without further purification. Hyperbranched polymer Boltorn H30 (Mw = 3500 g/mol,

hydroxyl number = 480 – 510 g KOH/g polymer, according to its datasheet) was donated by Perstorp and was used as received. All solvents were dried and purified by conventional procedures.

Chemical modification of Boltorn H30 with undecenoyl chloride

Partially modified Boltorn H30 was synthesized following a previously reported procedure using a conventional acylation procedure [16]. The partial modification was achieved by reaction of the HBP with different ratios of 10-undecenoyl chloride in the presence of TEA. The different modification degrees reached were calculated by means of NMR spectroscopy. Table 1 shows the main characteristics of the modified HBPs synthesized. The calculation of molecular weight and hydroxyl equivalent was done taking into account the degree of modification achieved and the values that appear in the data sheet of Boltorn H30.

Table 1. Characteristics of the modified HBPs synthesized.

HBPs	Mn[a] (g/mol)	OH eq. wt.[b] (g/eq_{OH})	T_g[c] (ºC)	ΔC_p[c] (J/g·ºC)	T_m[c] (ºC)	Δh_m[c] (J/g)	$T_{5\%}$[d] (ºC)	T_{max}[e] (ºC)
$H30_{25\%}$vin	4828	201	-61	0.319	-22	1.62	223	432
$H30_{60\%}$vin	6654	512	-56	0.273	-14	5.09	341	423
$H30_{76\%}$vin	7484	940	-57	0.223	-12	8.66	344	423
$H30_{93\%}$vin	8480	4240	-60	0.189	-12	10.46	355	429

[a] Calculated average molecular weight in number
[b] Calculated hydroxyl equivalent weight
[c] Determined by DSC at 10 ºC/min
[d] Temperature of a 5% of weight loss determined by TGA.
[e] Temperature of maximum degradation rate by TGA.

Table 2. Composition of the neat and modified formulations with different weight percentage of $H30_{25\%}$vin, $H30_{60\%}$vin, $H30_{76\%}$vin, $H30_{93\%}$vin, in equivalent ratio, (X_{eq}) and weight percentage (%wt).

Formulation	DGEBA		MHHPA		BDMA		OH from HBP	
	X_{eq}	wt%	X_{eq}	wt%	X_{eq}	wt%	X_{eq}	wt%
Neat	1.00	51.8	1.00	47.8	0.0062	0.5	0.00	0.0
5% $H30_{25\%}$vin	0.96	48.1	1.05	46.5	0.0064	0.5	0.09	5.0
10% $H30_{25\%}$vin	0.91	44.4	1.10	45.2	0.0065	0.5	0.18	10.0
5% $H30_{60\%}$vin	0.98	48.7	1.02	45.8	0.0063	0.5	0.04	5.0
10% $H30_{60\%}$vin	0.96	45.7	1.04	43.9	0.0063	0.4	0.07	10.0
5% $H30_{76\%}$vin	0.99	48.9	1.01	45.6	0.0062	0.5	0.02	5.0
10% $H30_{76\%}$vin	0.98	46.1	1.02	43.5	0.0063	0.4	0.04	10.0
5% $H30_{93\%}$vin	1.00	49.1	1.00	45.4	0.0062	0.5	0.00	5.0
10%$H30_{93\%}$vin	1.00	46.5	1.00	43.1	0.0062	0.4	0.01	10.0

Preparation of the curing mixtures

Mixtures containing DGEBA, MHHPA and the selected proportion of the modified hyperbranched polymer were carefully stirred and degassed under vacuum (at 80 ºC) during fifteen minutes to prevent the appearance of bubbles during curing. Samples were kept at -20 ºC before use to prevent polymerization. 1 phr (1 part of catalyst per hundred parts of mixture) of catalyst (BDMA) was added to the corresponding mixture at room temperature. Table 2 shows the notation and composition of the different formulations studied. It should be pointed out that the molar composition is calculated taking into account that 1 mol of anhydride reacts with 1 mol of epoxide or with 2 mol of hydroxyl groups.

Characterization

NMR Characterization

^{1}H NMR 400 MHz and ^{13}C NMR 100.6 MHz NMR spectra were obtained using a Varian Gemini 400 spectrometer with Fourier Transformed. ^{1}H-NMR spectra were acquired in 1 min and 16 scans with a 1.0 s relaxation delay (D1). ^{13}C-NMR spectra were obtained using a D1 of 0.5 s and an acquisition time of 0.2 s. 500 accumulations were recorded. DMSO-d_6 and $CDCl_3$ was used as solvent for Boltorn H30 and the modified undecenoyl derivatives respectively, and TMS as internal standard.

Infrared spectroscopy (FTIR)

A Bruker Vertex 70 FTIR spectrometer equipped with an ATR device with temperature control (Golden Gate heated single-reflection diamond ATR, Specac-Teknokroma) was used to determine the FTIR spectra of the materials before and after curing.

Calorimetric measurements (DSC)

Calorimetric analyses were carried out on a Mettler DSC-822e calorimeter with a TSO801RO robotic arm. The glass transition temperatures of the hyperbranched polymers prepared and the fully cured materials (T_g^{∞}) were determined after a dynamic heating scan at 10 ºC/min, as the temperature of the half-way point of the jump in the heat capacity when the material changed from the glassy to the rubbery state.

Thermogravimetric analysis (TGA)

Thermogravimetric analysis was carried out in a nitrogen atmosphere with a Mettler-Toledo TGA/SDTA 851e thermobalance. Cured samples with an approximate mass of 5 mg were degraded between 30 and 800 ºC at a heating rate of 10 ºC/min in a nitrogen atmosphere.

Rheometric measurements

Rheometric measurements were carried out in the parallel plates (geometry of 25 mm) mode with an ARG2 rheometer (TA Instruments, UK, equipped with an electrically heated plates system, EHP). Complex viscosity (η^*) of the pre-cured mixtures was recorded as function of angular frequency (0.1 – 100 rad/s) stating a constant deformation of 50% at 30 ºC.

Dynamomechanical analysis (DMTA)

Thermal–dynamic–mechanical analyses (DMTAs) were carried out with a TA Instruments DMA Q800. Single cantilever bending was performed on prismatic rectangular samples (10 x 10 x 1.5 mm^3) previously cured isothermally in a mould in two steps: first, 2h at 150 ºC and then, 2h at 180 ºC. The apparatus was operated dynamically, at 2 ºC/min, from 40 to 200 ºC. The frequency of application of the force was 1 Hz and the amplitude of the deformation 10 μm.

A three point bending assembly was used to obtain the Young modulus in a non-destructive flexural test at room temperature. The support span of the assembly was 10 mm and a load rate of 3 N/min was used. The modulus of elasticity is calculated using the slope of the load deflection curve in accordance with Eq. (1).

$$E_f = \frac{L^3 m}{4bd^3} \qquad (1)$$

where:

- E_f = flexural modulus of elasticity (MPa)
- L = support span (mm)
- b = width of test beam (mm)
- d = depth of tested beam (mm)
- m = the gradient (i.e., slope) of the initial straight-line portion of the load deflection curve (P/D) (N/mm)

Thermomechanical analysis (TMA)

A Mettler TMA 40 thermomechanical analyzer was used to determine the thermal expansion coefficients of the samples cured following the above curing schedule below and above their T_g. Samples of 5 mm diameter and 1-1.5 mm thick were sandwiched between two silica discs and heated at 10 ºC/min from 30 up to 150 ºC in a first scan and at 5 ºC/min up to 180 ºC in a second scan, which was used for the calculations. A blank curve determined using only the silica discs was substracted. The expansion curves of three samples were averaged. The coefficients of thermal expansion α_g and, α_r, below and above the T_g, respectively were calculated as follows:

$$\alpha = \frac{1}{L_0} \cdot \frac{dL}{dT} = const. \qquad (2)$$

where L and L_0 are the thickness at any temperature and at room temperature, respectively. The T_g was determined from the expansion curves as the crossover of the two tangents above and below the change of slope**.**

Measurement of density and shrinkage

The overall shrinkage was calculated from the densities of the materials before and after curing, which were determined using a Micromeritics AccuPyc 1330 Gas Pycnometer thermostatized at 30 ºC. The shrinkage during curing was determined as:

$$\%shrinkage = \frac{\rho_\infty - \rho_0}{\rho_\infty} \qquad (3)$$

where ρ_0 is the density of the uncured formulation and ρ_∞ is the density of the fully cured material obtained at the same conditions than DMTA samples.

Microhardness

Microhardness was measured with a Wilson Wolpert (Micro- Knoop 401MAV) device following the ASTM D1474-98 (2008) standard procedure. The Knoop microhardness (HKN) was calculated from the following equation:

$$HKN = \frac{L}{A_p} = \frac{L}{l^2 C_p} \qquad (4)$$

where, L is the load applied to the indenter (0.025 kg), A_p is the projected area of indentation in mm^2, l is the measured length of long diagonal of indentation in mm, C_p is the indenter constant (7.028×10^{-2}) relating l^2 to A_p. The values were obtained from 10 determinations with the calculated precision (95% of confidence level).

Impact resistance

The impact test was performed at room temperature by means of a Zwick 5110 impact tester, according to ASTM D4508-10 using rectangular samples (25 x 15 x 2 mm^3). The pendulum employed had a kinetic energy of 1 J.

Electron microscopy analysis (SEM)

The fracture area of samples were metalized with gold and observed with a scanning electron microscopy (SEM) Jeol JSM 6400. The samples were fractured by impact at room temperature or cryofractured in liquid nitrogen.

Results and discussion

Synthesis and characterization of the modified hyperbranched polymers

In a previous paper [16] we reported the generation of separated particles of 1-2 μm when Boltorn H30 esterified with long aliphatic chains was added as modifier of DGEBA cured by $Yb(OTf)_3$ as thermal cationic initiator. The thermomechanical characteristics of these materials were studied but no mechanical studies were performed.

Since Boltorn H30 possesses high number of hydroxyls as end groups, which can be modified in different extent, partial modifications with undecenoyl moieties of this polymer were performed. The structure and notation of the HBPs obtained are represented in Scheme 1. The aim of this strategy is that the modified HBPs can phase separate from the epoxy matrix whereas increasing the interface interaction, by the remaining hydroxyl groups that can form covalent linkages with the matrix.

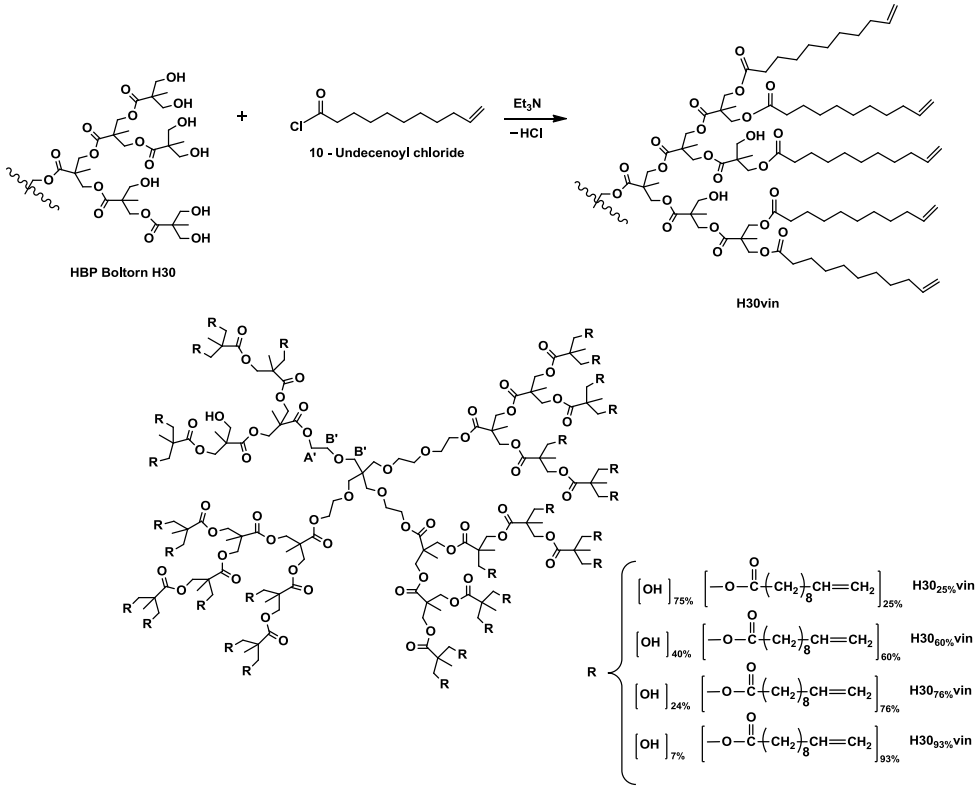

Scheme 1. Synthetic procedure and chemical structures and notations of H30vin Boltorn H30 modified polymers

The synthetic process consists in a simple acylation with undecenoyl chloride in the presence of triethylamine as HCl acceptor. On changing the proportion of acyl chloride to OH groups, different modification percentages can be achieved. The degree of modification was calculated by ^{1}H NMR spectroscopy. Figure 1 shows the ^{1}H NMR spectra of the vinyl modified HBP with the proton assignments.

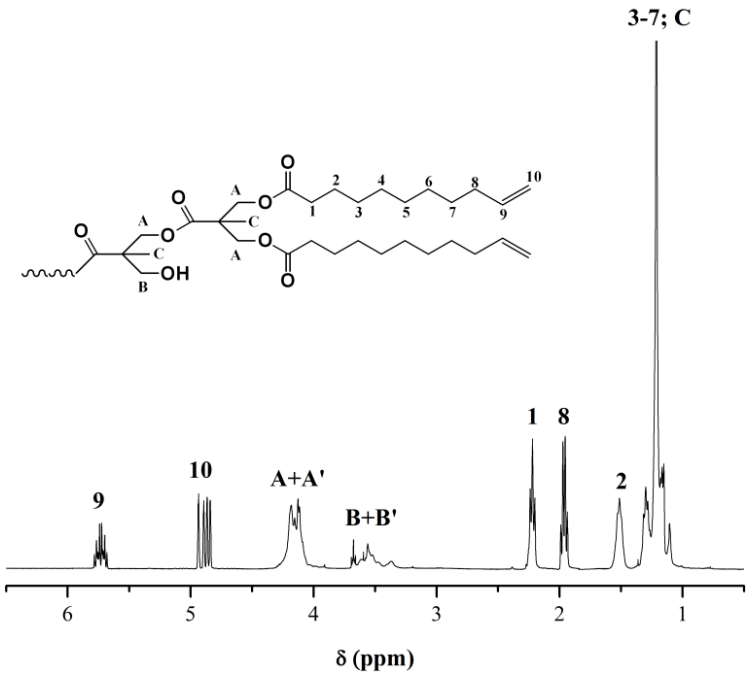

Figure 1. ^{1}H NMR spectra of vinyl modified Boltorn H30 ($H30_{60\%}$vin) with the proton assignments.

Signals A, B and C corresponds to the shell of Boltorn H30 and A' and B' to the core (ethoxylated pentaerythritol as represented in Scheme 1). From the intensities of the signals C and A+A', it is possible to calculate the intensity of signal B, by using the following equations:

$$I_{core} = I_{A+A'} + I_{B+B'} - \frac{4}{3}(I_c)$$

$$I_{B'} = \frac{10}{14} I_{core}$$

$$I_B = I_{B+B'} - I_{B'}$$

In the modification, B is transformed into A but B' remains unaltered. If the modification reaction were complete no B signals would be left and therefore, the ratio of the methylene ester signals at 4.2 ppm and the signal of methylene linked to ether groups (B'), which appear between 3.3 and 3.7 ppm, could be calculated as follows:

$$R_{100\%} = \frac{I_{A+A'} + I_B}{I_{B'}}$$

To calculate the degree of esterification achieved the intensity of the signals A + A' can be divided by the intensity of B + B' in the spectrum of the modified HBP (R_{H30vin}) and then compared this value with the complete modified, $R_{100\%}$. This procedure led to the degree of modification achieved.

$$Modification(\%) = \frac{R_{H30vin}}{R_{100\%}} \cdot 100$$

As can be observed in Table 1, the presence of the long aliphatic chains at the ends leads to a decrease of the T_g of the unmodified Boltorn H30, which is 16 ºC, and the HBPs obtained are viscous liquids at room temperature. As it is detailed in the table there is not systematic variation of T_g with the degree of acylation. This is an unexpected result but it can be rationalized by the presence of a little proportion of crystalline phase. This crystalline phase was observed as a broad endotherm in the calorimetric curves. The peak temperatures (T_m) are collected in the same table, together with the measured fusion enthalpy (Δh_m). As it is observed, on increasing the degree of modification the fusion enthalpy increases and the heat capacity step (ΔC_p), corresponding to the glass transition of the amorphous phase, decreases. Long undecenoyl chains are known to crystallize below room temperature as reported in the literature [17]. Thus, the T_g of the amorphous phase does not change regularly as expected, because of the partial separation of undecenoyl chains in the crystalline phase. Luciani et al. [18] reported that the modification of the final OH groups of Boltorn with long aliphatic chains resulted in a gradual decrease of the T_g because of the decrease in the hydrogen bonding and the increase in free volume of the aliphatic structure. However, they only achieved a degree of modification of 60% and the determination of this parameter was done by cooling on a rheometer. The differences in both techniques and the observation in our case of the crystalline phase accounts for the differences observed. Some effects can also be originated by the presence of the vinylic group at the end of the aliphatic chains in our HBPs.

The presence of esters in the Boltorn H30 structure makes it thermally degradable at low temperature, but the higher the modification achieved the higher the initial degradation temperature. However, the degree of modification has no significant effect on the temperature of the maximum degradation rate.

The evolution of the complex viscosity (η^*) as a function of angular frequency at 30 ºC of the modified HBPs is shown in Figure 2. To compare, the complex viscosity of the DGEBA resin has also been included. As we can see, the complex viscosity of the HBP with a degree of modification of 76% is the lowest, and quite similar to the one of DGEBA. The highest viscosity is obtained in case of the HBP having the lowest degree of modification. The HBPs with a degree of modification of a 93% and a 60% have a similar viscosity. To explain this unexpected behavior two factors should be taken into account: a) the lower the degree of modification, the higher the interaction among HBP molecules by hydrogen bonding of OH groups on their surface shell and b) the higher the degree of modification, the higher the molecular weight and the more feasible the entanglement of the polymeric chains, both factors leading to an increased viscosity. According to that, there is a compromise between both factors that lead to a less viscous polymer in case of $H30_{76\%}$vin, which seems to be the best candidate to be used as modifier without much affecting the processability of the formulation. These results are in partial agreement with those reported by Luciani et al. [18], who observed that the viscosity decreases on increasing the degree of modification. However, they only reached a maximum degree of modification of 60%. In our case, we observed a decreasing trend of the viscosity up to a degree of modification of 76%, and a subsequent increase when the polymer was almost completely modified.

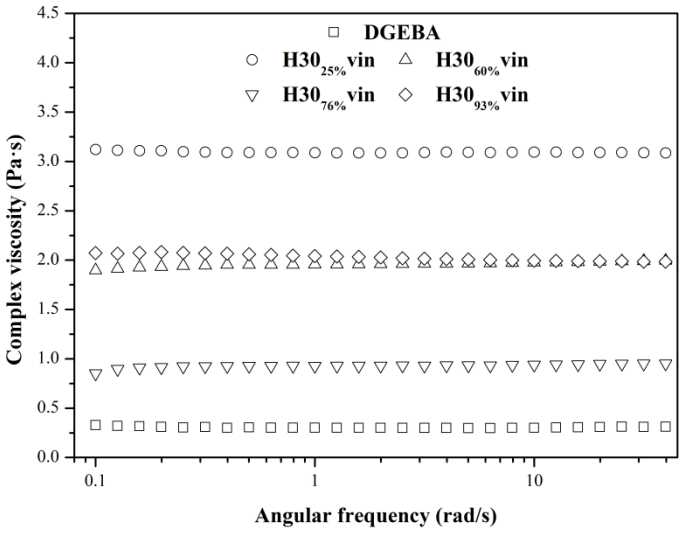

Figure 2. Complex viscosity (η*) versus angular frequency at 30 ºC of the modified HBPs.

Curing mechanism and chemical structure of the thermosets

As the aim of this study was to generate soft particles by addition of an HBP to DGEBA maintaining a certain interface interaction between the particles and the epoxy matrix after curing, we selected anhydride as curing agent. The use of anhydrides as curing agents has been extensively reported [19,20], and there are even some papers in the use of hydroxyl ended modified HBPs in epoxy formulations [21,22,23].

Anhydrides can react with both epoxide and hydroxyl groups by a complex reaction mechanism, but it can be summarized as shown in Scheme 2. The reaction of epoxides and anhydrides (Scheme 2.a) follows an alternate ring-opening copolymerization mechanism that leads to polyester networks. Remaining hydroxyl groups on the shell of the HBP react with anhydrides by a polycondensation mechanism, giving rise to ester units and acids that in turn react with epoxide forming new ester and hydroxylic groups (Scheme 2.b). This last mechanism allows the covalent incorporation of the HBP through the remaining OH groups to the epoxy matrix. Both mechanisms are competitive and are catalyzed by a tertiary amine.

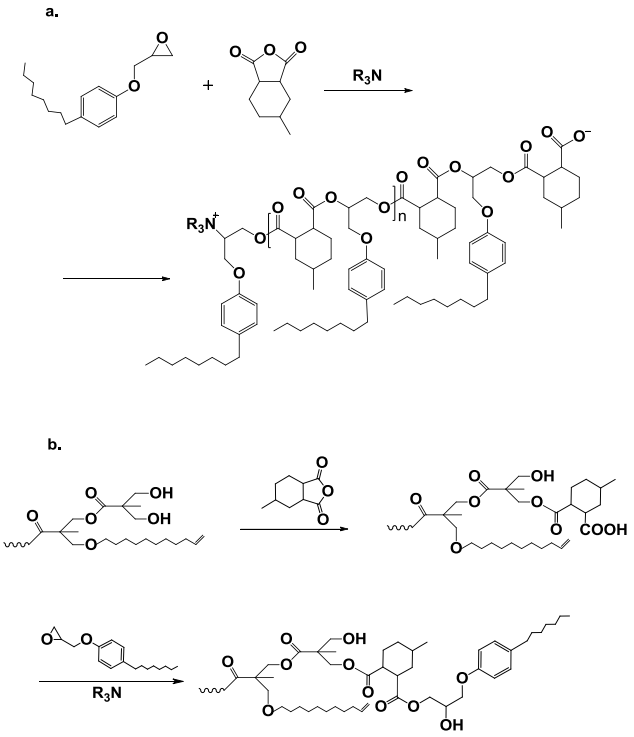

Scheme 2. Reaction mechanisms in the curing of epoxy resins/hydroxyl ended HBPs mixtures with anhydride in the presence of a tertiary amine

In some previous studies [15,24], we demonstrated by FTIR that modified HBPs were incorporated into the matrix by formation of carboxylic groups and subsequent esterification with epoxides. The incorporation of OH groups takes place in the first stages of the reaction and their presence in the formulation produces an accelerative effect in the curing process. In the last stages of curing, carboxylic groups react with epoxides producing polyester moieties. In Figure 3 the spectra of the formulation with a 10% $H30_{76\%}$vin at 120 ºC during curing are collected.

The disappearance of the two peaks at 1860 and 1780 cm^{-1} indicates the complete conversion of anhydride groups. The peak at 1735 cm^{-1} corresponds to the ester groups of the Boltorn HBP and to the ones formed during the curing. The band of epoxy group at 916 cm^{-1} appears overlapped with the absorption band of the anhydride (895 cm^{-1}), but both have disappeared at the end of the curing. In the inset of the figure it can be appreciated that hydroxyl groups appear during curing [15,24].

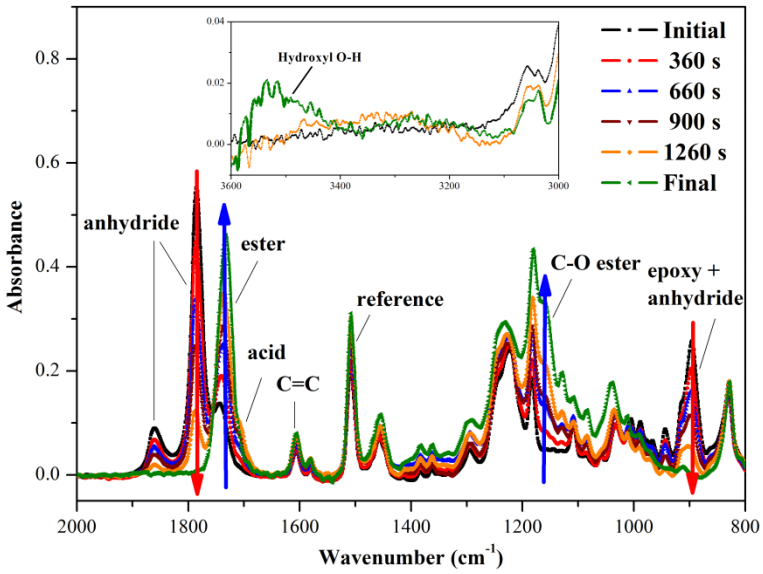

Figure 3. FTIR-ATR spectra before and after curing of the mixture with 10% $H30_{76\%}vin$ at 120 ºC.

Thermal and thermomechanical properties of the thermosets obtained

Table 3 summarizes the results of the thermomechanical characterization of the materials by DMA and DSC. The tan δ plot against temperature for all the thermosets with a 10% of the modified HBPs are represented in Figure 4.

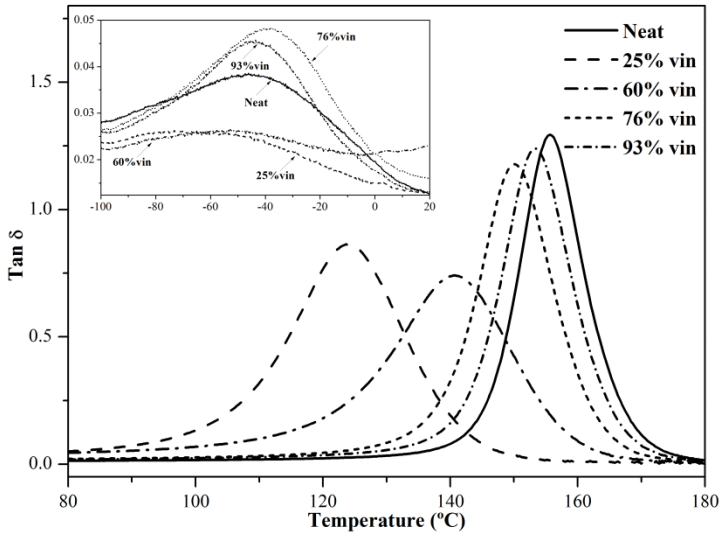

Figure 4. Tan δ against temperature for the materials obtained of the curing of DGEBA/MHHPA and DGEBA/MHHPA mixture containing 10% wt. of H30vin with different modification degrees.

Table 3. Thermal and thermomechanical data of DGEBA/MHHPA/BDMA formulations with different percentages of $H30_{25\%}$vin, $H30_{60\%}$vin, $H30_{76\%}$vin, $H30_{93\%}$vin.

Formulation	$T_{g,DSC}$ [a] (ºC)	$T_{tan\delta,DMA}$ [b] (ºC)	$T_{5\%}$ [c] (ºC)	T_{max} [d] (ºC)
Neat	149	156	362	412
5% $H30_{25\%}$vin	125	146	360	415
10% $H30_{25\%}$vin	115	131	313	417
5% $H30_{60\%}$vin	135	144	347	417
10% $H30_{60\%}$vin	128	141	317	415
5% $H30_{76\%}$vin	142	152	357	412
10% $H30_{76\%}$vin	139	149	352	410
5% $H30_{93\%}$vin	144	153	355	412
10% $H30_{93\%}$vin	141	155	358	410

[a] Glass transition temperature determined by DSC in a second scan after dynamic curing.
[b] Temperature of the maximum of the tan δ of isothermally cured samples.
[c] Temperature of a 5% of weight loss determined by thermogravimetry.
[d] Temperature of maximum degradation rate determined by thermogravimetry.

When the degree of modification of the HBP is low, a significant decrease in T_g is observed by DSC and DMA, which is more important as the proportion of modifier increases from 5% to 10%. Such a significant decrease was not at all expected because the reaction of OH groups of the HBP and the presence of internal branching points in its structure should contribute to the crosslinking of the material. When the degree of modification increases, the reduction in T_g is less significant. It is noticeable that when the HBP added has a degree of modification of 76 % or higher this value is not much affected, in spite of the larger proportion of long aliphatic chains that could plasticize the materials. These results suggest that a phase separation occurs when the degree of modification of the HBP is high enough, leading to a thermosetting matrix with a T_g close to that of the unmodified material and a softer phase rich in the HBP. This is confirmed by DMA, by the presence of a β transition which becomes more evident when the degree of modification of the HBP increases (see inset in Figure 4). It should also be mentioned, that the materials containing $H30_{25\%}$vin and $H30_{60\%}$vin show a broader α relaxation, indicating a heterogeneity of the material by the chemical incorporation of the HBP to the epoxy matrix. In these materials a higher ductility can be expected, which should increase the matrix shear yielding, thus achieving a certain improvement in toughness [25].

Logical discrepancies appear between the DMA and DSC values, as a consequence of (1) the different heating rate used for the determination, (2) the effect of the frequency on the mechanical relaxation measured with DMA and (3) the fact that the isothermal curing schedule of the samples analyzed with DMA and the non-isothermal curing of the samples analyzed with DSC may lead to slight differences in the network structure and glass transition. However, the above discussion on the effect of the different HBPs is not affected by these differences.

The Young modulus at room temperature was evaluated using DMA for all the thermosets prepared and the values are collected in Figure 5. As we can see, there is only a

slight reduction of this parameter by adding the modifier, in reference to the neat material and the maximum reduction in the modulus is observed when 10% of 93%vin was in the formulation.

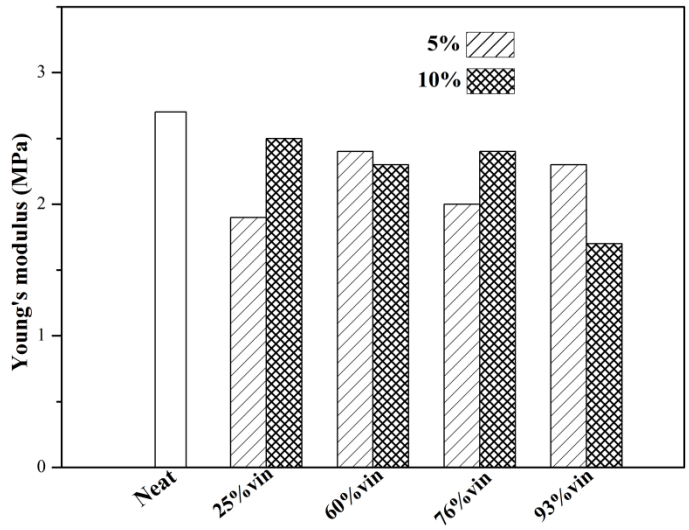

Figure 5. Young's modulus of DGEBA/MHHPA thermosets containing 5 and 10% wt. of HBPs with different modification degrees

Table 3 summarizes also the results of the thermogravimetric analysis of these materials. Figure 6 shows the thermogravimetric and the derivative curves for the thermosets containing a 10% of the modified HBPs.

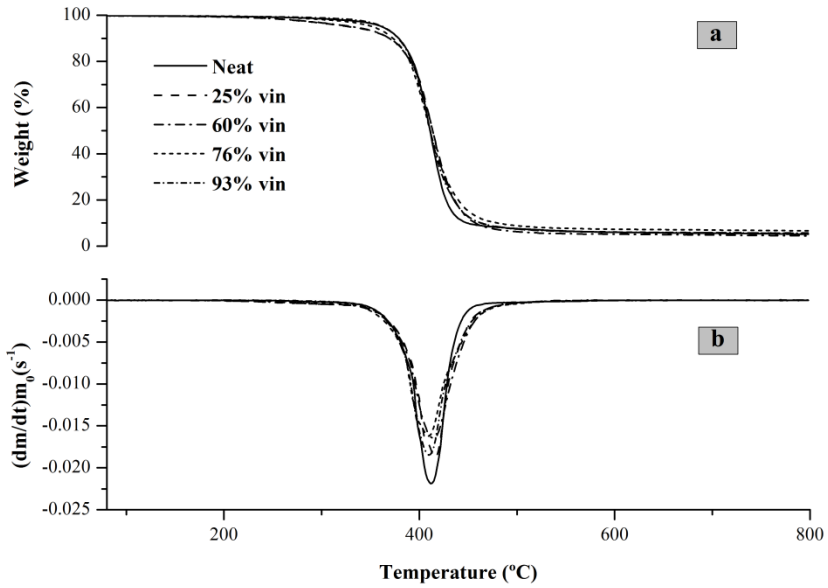

Figure 6. a) TGA and b) DTG curves at 10 ºC/min in N_2 atmosphere of thermosetting materials obtained from neat DGEBA/MHHPA and the formulations containing 10% wt. of H30vin with different modification degrees.

The shape of the derivative curves is unimodal indicating that breakage of bonds in the network structure occurs simultaneously. The peak observed in DTG plot corresponds to the degradation of the crosslinked network and it remains similar for all materials. The only differences in the thermal stability can be observed in the initial degradation temperature ($T_{5\%}$). In Table 3, we can see that the thermosets containing a 10% of the $H30_{25\%}$vin or $H30_{60\%}$vin show a lower value indicating their lower thermal stability. This is due to the presence of a higher proportion of ester groups, which are more degradable. In contrast, the materials obtained with the HBPs with a higher degree of modification show values similar to the one measured for the neat material. This fact can be attributed to a lower proportion of ester groups and to the phase separated character of these thermosets. The HBP particles are surrounded by the epoxy matrix, which may prevent the elimination of volatile fragments.

One of the causes of internal stress in coatings is the mismatch between the thermal expansion coefficients (CTEs) of the epoxy coating and the metal substrate. Thus, the reduction of CTEs is one of the desired goals to be achieved in the field of coating for metal substrates. In some previous studies, the addition of HBPs to epoxy formulations allowed us to decrease these coefficients in both the glassy and the rubbery state [23,26]. By TMA we have evaluated the CTEs on both states of the thermosets containing a 10% of HBP and the values obtained are collected in Table 4.

Table 4. Thermal expansion coefficients, α_g and α_r, below and above glass transition respectively, determined by TMA

Formulation	T_g[a] (ºC)	α_g x 10^6 ($ºC^{-1}$)	α_r x 10^6 ($ºC^{-1}$)
Neat	144	69.89 ± 1.46	185.73 ± 1.90
10 % $H30_{25\%}$vin	110	85.36 ± 0.76	187.96 ± 1.28
10 % $H30_{60\%}$vin	121	94.57 ± 3.51	186.64 ± 1.59
10 % $H30_{76\%}$vin	131	84.01 ± 0.67	188.96 ± 1.78
10 % $H30_{93\%}$vin	140	71.49 ± 0.07	187.06 ± 1.69

a. Glass transition temperature of isothermally cured thermosets determined by TMA

In contrast to the previously reported diminution of CTEs on adding this type of modifiers, in the present study an increase is observed in the glassy state and similar values are measured in the rubbery state. This difference could be attributed to the more flexible structure of H30vin that expand much more easily on heating by their conformational freedom than the previously studied poly(ester-amide) HBPs with unmodified OH groups, completely reacted with the epoxy matrix. It is worth noting that the values of CTEs in the glassy state increase with the degree of modification until reaching a maximum for the thermoset containing a 10% of $H30_{60\%}$vin. At higher modification degrees this parameter begins again to decrease and the α_g for the thermoset containing a 10% of $H30_{93\%}$vin is similar to the one measured for the neat material. This non-linear behaviour can be attributed to the fact that the materials with highly modified HBP lead to phase separated morphologies. When the HBP modifier is insoluble in the epoxy matrix its effect is reduced and the CTE becomes defined by the rigid epoxy phase.

Shrinkage

In thermosetting coatings, the reduction of the shrinkage is one of the milestones, since the contraction tends to originate deformation and cracks and originate internal stress that reduces toughness and protection capability. The reduction of the shrinkage on curing by the addition of HBPs has been reported previously [23,27,28]. Table 5 collects the densities before and after curing and the shrinkage calculated from them for all the formulations studied.

Table 5. Densities and global shrinkage on curing of the formulations studied

Formulation	ρ_0 ($g \cdot cm^{-3}$)	ρ_∞ ($g \cdot cm^{-3}$)	Shrinkage (%)
Neat	1.149	1.175	2.25
5% $H30_{25}$%vin	1.147	1.176	2.45
10% $H30_{25}$%vin	1.143	1.175	2.76
5% $H30_{60}$%vin	1.144	1.173	2.48
10% $H30_{60}$%vin	1.142	1.172	2.51
5% $H30_{76}$%vin	1.139	1.170	2.65
10% $H30_{76}$%vin	1.138	1.165	2.31
5% $H30_{93}$%vin	1.139	1.164	2.16
10% $H30_{93}$%vin	1.134	1.155	1.84

As we can see, the formulations containing $H30_{25\%}$vin and $H30_{60\%}$vin behaves in a different manner than those containing $H30_{76\%}$vin and $H30_{93\%}$vin. Whereas the formers leads to an increased shrinkage on increasing the proportion of modifier, the latter leads to less shrinkage on increasing the proportion of HBP, and even a reduction of the global shrinkage is obtained when the degree of modification of the HBP is the highest. Again, the phase separation seems to play a role in this parameter.

In a previous work of our research team on the modification of an epoxy resin with commercial Boltorn H30 cured by tetrahydrophtalic anhydride, we observed that on increasing the proportion of Boltorn H30 in the formulation, the shrinkage increased. This was attributed to the higher extension of the polycondensation reaction between hydroxyl groups and anhydrides, which takes place with a higher contraction [29]. Accordingly, in the present case the HBPs which do not phase separate and react in a higher extent with the anhydride lead to a higher shrinkage.

It should be noted that in the previous study on the kinetics and mechanism of these formulations, it was confirmed that the reaction of OH groups with anhydride takes place in the first stages of the reaction [15]. A similar result was observed by us in the curing of an epoxy resin with hydroxyl terminated HBPs and anhydride as curing agent [23]. In that case the shrinkage before and after gelation was evaluated by TMA. It could be concluded that the shrinkage before gelation increased, but it was reduced after this point. A similar trend is expected in the present case. This is important from the point of view of the generation of internal stresses, since the contraction produced in the liquid state, before gelation, does not produce any

type of tension because of the free flow of the resin. If the contraction after gelation is less, the defects and stresses generated should be accordingly diminished.

Mechanical characterization and morphology

For coating applications hardness is a desired property. The microhardness measurements are very useful in rating coatings on rigid substrates to know on the resistance that one body offers against penetration to another under static loads. Microhardness measurements were carried out with a Knoop microindenter and the results are shown in Figure 7.

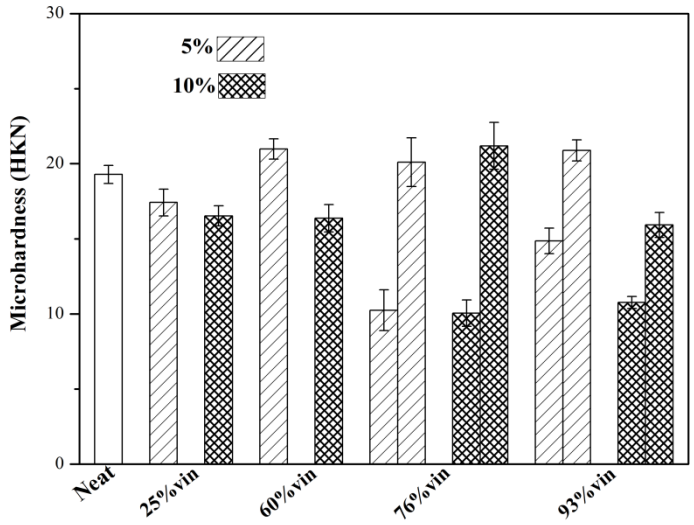

Figure 7. Microhardness values of the modified thermosets prepared.

In general, the values are not much affected on adding the modifier and even in some cases this parameter slightly increases. For thermosets containing $H30_{76\%}$vin or $H30_{93\%}$vin, two sets of values were obtained. This confirms that there are two different regions, one with a low hardness, related to presence of the HBP microparticles, and another with a higher microhardness value corresponding to the epoxy matrix. Again, the modification of the materials with a 10% of $H30_{93\%}$vin seems to be detrimental to this characteristic.

It has been reported that HBPs could act as effective toughness additives for epoxy resins [8,9,23,30], especially when phase separated morphologies are formed [31,32]. However, an increase higher than two-fold by adding HBPs have not been reported up to our knowledge [9,12,33]. When we measured the impact strength by an Izod test a great increase of more than 400% was observed when a 10% of 76%vin was added to the formulation as it is represented in Figure 7. In general, on increasing the degree of modification and the proportion of hyperbranched from 5 to 10% this property was enhanced, but it reached a maximum and the addition of a highly modified hyperbranched ($H30_{93\%}$vin), especially in a proportion of 10%, worsened toughness characteristics. The good results obtained in the present case can be attributed to a good phase separation of particles with HBP, acting as soft particles but having a good interface interaction with the matrix.

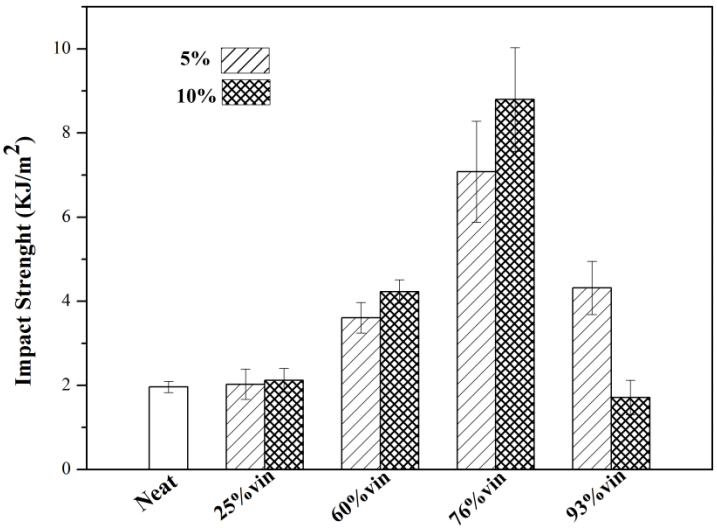

Figure 8. Impact strength of DGEBA/MHHPA thermosets containing 5% and 10% wt. of HBPs with different modification degrees.

It is known that, in order to improve the impact resistance of a material, it is important to introduce mechanisms which can contribute to energy dissipation, impeding crack propagation. Soft particles concentrate applied stresses in the matrix at their equators when a toughened material is loaded. Upon loading, stresses in the matrix can be transferred to the rubber particles if strong interfacial interactions exist. The size of the particles is also of a great importance, since only particles larger than 100 nm can store sufficient elastic energy and produce an adequate stress concentration effect [34]. On the other hand, particles with diameters larger than 10 μm have been found to be relative inefficient [35]. Because of the stress concentration and the stress transfer to the rubber particles, the following energy absorption mechanisms may be activated upon load: (1) shear yielding, which involves plastic deformation within the matrix and in close vicinity of the particles, and (2) cavitation of the particles. Pearson and Yee observed that, on increasing the matrix ductility, the plastic strain to failure increases as well [36]. These authors also described that while the fracture toughness of the neat resin is almost independent on the crosslinking density, the crack growth resistance is highly dependent on the resin structure.

The increasing degree of modification of the HBP with end vinyl chains promotes phase separation upon curing, but at the same time a good compatibility between the particles and the matrix is retained and a certain plasticization of the matrix is produced because of the presence of reactive hydroxyl groups in the HBP. Therefore, the toughness mechanisms described above may be operative depending on the presence and degree of modification of the HBP. Boogh et al. [8] reported that HBPs have a particular ability to reach a gradient property within the phase separated particles. In our case, it could be a variation in the degrees of reaction of OH groups with anhydrides and the epoxy groups produced during the curing by the phase-separation process. This leads to a broader range of interactions with the matrix and to an increased ability to transfer stress to the particles [9]. Moreover, the flexible groups of the Boltorn H30 derivatives can also dissipate the impact energy when they are partially or totally compatibilized with the epoxy matrix, which is made more ductile and can contribute to a higher extent to the shear deformation [3]. Both factors may explain the significant toughness enhancement obtained with

10% of 76%vin. On the contrary, an excessive degree of modification results in an excessive extent of phase separation with poor compatibility and low matrix ductility, with a combined adverse effect on toughness.

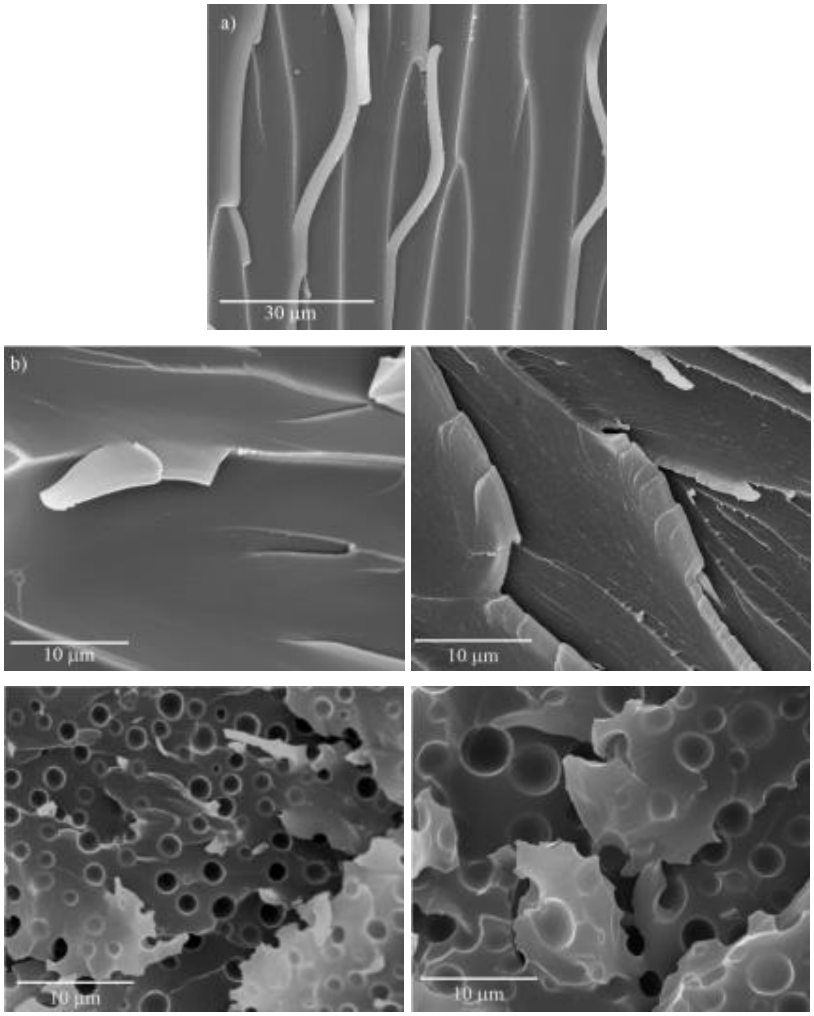

Figure 9. SEM micrographs of the fracture surface of the materials obtained from DGEBA/MHHPA formulations: a) Neat (x 1000) and modified (x 3500) with b) 10% $H30_{25\%}$vin; c) 10% $H30_{60\%}$vin; d) 10% $H30_{76\%}$vin; e) 10% $H30_{93\%}$vin.

Figure 9 presents the SEM micrographs of impact fractured surfaces of the thermosets prepared. First of all, it can be observed that the fracture surfaces of the neat material and the formulations containing HBPs with a low degree of modification ($H30_{25\%}$vin and $H30_{60\%}$vin) are homogeneous, without traces of phase separation. With low degrees of HBP modification, its incorporation into the matrix, through hydroxyl-anhydride reactions, is complete. A higher degree of modification, which implies a lower hydroxyl content and the presence of nonpolar aliphatic chains, leads to the formation of phase-separated morphologies ($H30_{76\%}$vin and $H30_{93\%}$vin), in agreement with the previous observations.

The material containing H30$_{76\%}$vin shows well distributed microparticles. The measurement of these particles leads to values of 1.71 (± 0.40) μm, but the size of the particles observed in cryofractured materials are a little smaller 1.58 (± 0.35) μm. This difference can be attributed to the cavitation, which is more important in the impact test than in the cryofracture. The presence of the microparticles affects notably the crack propagation with the formation of shear bands near them, leading to an increased fracture resistance. The fact that the separated particles interact covalently with the epoxy matrix by the OH groups of the HBP, which react with the curing agent, promotes cavitation and favors the enhancement in toughness observed. In the case of the material modified with a 10% of H30$_{93\%}$vin, the low compatibility between the matrix and the HBP promotes the formation of larger particles of 2.74 (± 0.91) μm, with a broader distribution of the sizes in comparison to the previous and not as homogeneously distributed, eventually resulting in a lower impact resistance for the reasons explained above. The inspection of the sample with H30$_{60\%}$vin, which is not phase separated but still presents a significant improvement in toughness allows us to see cracks with riverline structures, which in this case can be attributed to an *in situ* reinforcing mechanism and a plasticization of the matrix.

Conclusions

The shell structure of the Boltorn H30 has been successfully modified to different extents by a simple acylation procedure with undecenoyl chloride and the degree of modification achieved has been determined by ^{1}H-NMR spectroscopy. This series of modified hyperbranched polymers has been used as modifiers of DGEBA/anhydride thermosets.

It has been possible to enhance 4-fold the impact resistance of the thermosets by adding a 10% of H30$_{76\%}$vin to the formulation without affecting thermal stability, thermomechanical characteristics or processability.

By selection of the adequate degree of modification of the HBP used as modifier a regular microphase separation can be obtained with a good interfacial interaction with the epoxy matrix, which can explain the great enhancement on the impact resistance achieved. The tailoring of the chemical structures of the HBP to produce phase separated particles with a partial covalent interaction with the matrix seems therefore to be a promising way for that purpose.

Acknowledgements

The authors would like to thank MINECO (MAT2011-27039-C03-01, MAT2011-27039-C03-02) and Generalitat de Catalunya (2009-SGR-1512) for giving financial support. X.F. acknowledges the contract JCI-2010-06187 and M.F. the grant BES-2009-025226. Perstorp and Huntsman are acknowledged for kindly providing Boltorn H30 and Araldite GY 240, respectively.

References

[1] May CA, Tanaka GY. In: C.A. May, editor. Epoxy Resins. Chemistry and Technology. New York: Marcel Dekker, 1988, Chapter 1.

[2] Petrie EM. Epoxy Adhesive Formulations. New York: McGraw-Hill, 2006.

[3] Bagheri R, Marouf BT, Pearson RA. J Macromol Sci Part C: Polym Rev 2009; 49:201-225.

[4] Zheng S. In: J.P. Pascault, R.J.J. Williams, editors. Epoxy Polymers. New Materials and Innovations. Weinheim: Wiley-VCH, 2010, Chapter 5.

[5] Brooker RD, Kinloch AJ, Taylor AC. J Adhes 2010; 86:726-741.

[6] Ruiz-Pérez L, Royston GJ, Fairclough JPA, Ryan AJ. Polymer 2008; 49:4475-4488.

[7] Qian JY, Pearson RA, Dimonie VL, Shaffer OL, El-Aasser MS. Polymer 1997; 38:21-30.

[8] Boogh L, Pettersson B, Månson J-A E. Polymer 1999; 40:2249-2261.

[9] Varley RJ, Tian W. Polym Int 2004; 53: 69-77.

[10] Xu G, Shi W, Gong M, Yu F, Feng J. Polym Adv Technol 2004; 15:639-644.

[11] Sangermano M, Malucelli G, Bongiovanni R, Priola A, Harden A. Polym Int 2005; 54:917-921.

[12] Zhang D, Jia D. J Appl Polym Sci 2006; 101:2504-2511.

[13] Voit B, Lederer A, Chem Rev 2009; 109 :5924-5973.

[14] Flores M, Fernández-Francos X, Jiménez-Piqué E, Foix D, Serra A, Ramis X. Polym Eng Sci 2012; 52:2597-2610.

[15] Flores M, Fernández-Francos X, Ramis X, Serra A. Thermochim Acta 2012; 544: 17-26.

[16] Fernández-Francos X, Foix D, Serra A, Salla JM, Ramis X. React Funct Polym 2010; 70:798-806.

[17] Reina A, Cádiz V, Mantecón A, Serra A. Angew Makromol Chem 1993; 209:95-109.

[18] Luciani A, Plummer CJG, Nguyen T, Garamszegi L, Månson J-A E. J Polym Sci Part B: Polym Phys 2004; 42:1218-1225.

[19] Fisch W, Hofman W, Koskikallio J. J Appl Chem 1956; 6:429-41.

[20] Montserrat S, Flaqué C, Calafell M, Andreu G, Malek J. Thermochim Acta 1995; 269:213-29.

[21] Yang JP, Chen ZK, Yang G, Fu AY, Ye L. Polymer 2008; 49:3168-75.

[22] Foix D, Yu Y, Serra A, Ramis X, Salla JM. Eur Polym J 2009; 45:1454-1466.

[23] Morell M, Erber M, Ramis X, Ferrando F, Voit B, Serra A. Eur Polym J 2010; 46:1498-1509.

[24] Fernández-Francos X, Rybak A, Sekula R, Ramis X, Serra A. Polym Int 2012; 61:1710-1725.

[25] Chen TK, Jan YH, Polym Eng Sci 1995; 35: 778-785.

[26] Morell M, Ramis X, Ferrando F, Yu Y, Serra A. Polymer 2009; 50: 5374-5383.

[27] Eom Y, Boogh L, Michaud V, Månson J-A E. Polym Compos 2002; 23:1044-1056.

[28] Foix D, Khalyavina A, Morell M, Voit B, Lederer A, Ramis X, Serra A. Macromol Mater Eng 2012; 297:85-94.

[29] Foix D, Rodríguez MT, Ferrando F, Ramis X, Serra A. Prog Org Coat 2012; 75:364-372.

[30] Cicala G, Recca G., Polym Eng Sci 2008; 48: 2382-2388.

[31] Fröhlich J, Kautz H, Thomann R, Frey H, Mülhaupt R. Polymer 2004; 45:2155-2164.

[32] Mezzenga R, Månson J-A E. J Mater Sci 2001;36:4883-4891.

[33] Zhang J, Guo Q, Fox B. J Polym Sci Part B: Polym Phys 2010; 48:417-424.

[34] Lazzeri A, Bucknall CB. J Mat Sci 1993; 28: 6799-6808.

[35] Pearson RA, Yee AF. J Mat Sci 1991; 26:3828-3844.

[36] Pearson RA, Yee AF, J Mat Sci 1989; 24: 2571-2580.

Enhancement of the impact strength of cationically cured cycloaliphatic diepoxide by adding hyperbranched poly(glycidol) partially modified with 10-undecenoyl chains

Marjorie Flores,[1] Mireia Morell,[1] Xavier Fernández-Francos,[1*] Francesc Ferrando,[2] Xavier Ramis,[3] Àngels Serra[1]

[1] Department of Analytical and Organic Chemistry, Universitat Rovira i Virgili, C/ Marcel·lí Domingo s/n, 43007, Tarragona, Spain.
[2] Department of Mechanical Engineering, Universitat Rovira i Virgili, C/ Països Catalans, 26, 43007, Tarragona, Spain.
[3] Thermodynamics Laboratory, ETSEIB Universitat Politècnica de Catalunya, Av. Diagonal 647, 08028, Barcelona, Spain.

Abstract

A hyperbranched poly(glycidol) has been synthesized and modified by acylation with 10-undecenoyl chloride to obtain hyperbranched polymers (HBPs) with different degree of modification. These HBPs have been used as reactive modifiers in a proportion of 3, 5 and 10% with respect to a biscicloaliphatic diepoxide cured using ytterbium triflate as thermal cationic initiator. The materials obtained have been characterized and their mechanical properties evaluated. Phase separated materials have been obtained, with a 2-fold increase in impact resistance without sacrificing thermomechanical properties, thermal stability or processability. This good combination of properties can be explained by the achievement of a regular microphase separation with a good interfacial interaction between the microparticles and the epoxy matrix. The compatibility between the HBP and the matrix can be tuned by changing the degree of modification, which leads to a variable amount of available hydroxyl groups of the HBP that can react with the epoxy groups. This chemical bonding occurs through the activated monomer mechanism (AM) which is typical of the cationic homopolymerization of epoxides.

Keywords: *cycloaliphatic epoxy, thermoset, hyperbranched polymer, impact strength.*

Introduction

Epoxy resins are commonly used as thermosetting materials due to their excellent thermomechanical properties and chemical and environmental stability. They present also good processability before curing. These materials are one of the most important classes of thermosetting polymers, used world-wide since their industrial introduction in 1946 in the field of coatings, adhesives, moulding compounds and polymer composites [1]. Their broad range of applications can be explained due to the fact that they are probably one of the most versatile thermosets because not only the type of resin and the chemistry of the curing can be varied, but also a huge number of organic and inorganic modifiers and fillers can be added to improve their properties [2]. Although rigidity and strength are desired properties in engineering applications, toughness is one of the restrictions in the use of epoxy resins. The low toughness, coming from the high crosslinking density, affects the durability of coatings and places strong constraints on design parameters [3].

The first attempts to improve toughness were based on the addition of liquid rubbers or thermoplastics, but usually these additives compromise the modulus and thermomechanical characteristics of the thermosets and the processability of the formulation [4]. Toughness implies

energy absorption and it is achieved through various deformation mechanisms before failure occurs. One of the most effective methods of preventing the crack to freely develop after impact is the addition of a second phase that induces the formation of particles that absorb the impact energy and deflect the crack. A combination of cavitation around the rubber particles with shear yielding in the matrix produces a cooperative effect in the energy dissipation [5]. The effect reached depends on the particle characteristics, *e.g.* size, interparticle distance, distribution, particle/matrix interaction, among others [6, 7]. Generally, the particles are generated by reaction-induced phase separation (RIPS) from a homogeneous solution composed of the resin, curing agent and modifiers. From the thermodynamic point of view, the driving force for the reaction-induced phase separation is the unfavourable entropic contribution to the mixing free energy resulting from the extremely high increase in molecular weight of epoxy structure during curing [5]. The phase separated morphology in the blends depends on the kinetics of curing and on the dynamics of the phase separation process.

To overcome the limitations of rubbers or linear thermoplastics used as tougheners, which leads to a reduction of the thermomechanical characteristics and to an increased viscosity before curing, the use of hyperbranched polymers (HBPs) has been proposed by several authors [8-12]. The dendritic structure of HBPs makes these modifiers very promising in terms of processability because of the low entanglement that leads to low viscosities in comparison to linear polymers [13]. By partial or complete modification of their numerous hydroxyl terminal groups, it is possible to tune their interaction with the matrix or facilitate their covalent linkage to the epoxy matrix, which can lead to phase separated or homogeneous morphologies. The presence of non-modified reactive groups in the HBP shell can improve the interaction in the interphase between the separated particles and the matrix.

While there is abundant literature on the toughening on epoxy thermosets based on diglycidyl ether of bisphenol A (DGEBA), the reports on the toughening of cycloaliphatic epoxides are scarce and the field is still open for research. For example, some authors have reported the modification of biscycloaliphatic epoxy formulations using high viscosity CTBN rubbers [14, 15], poly(ethylenephtalate) [16], inorganic fillers such as nanosize silicon dioxide [17] or carbon nanotubes [18], oligofluorosiloxanes [19] or reactive copolymers [20]. Reactive hyperbranched polymers have also been used as reactive modifiers in the UV-curing of cycloaliphatic epoxides, producing in most of the cases a toughness increase at the expense of reducing the glass transition temperature T_g and the elastic modulus [11, 21, 22].

Very recently we reported the use of partially modified Boltorn type polyesters with undecenoyl moieties in DGEBA thermosets cured with anhydrides, resulting in a significant increase in impact strength up to 400% with respect to the neat formulation without sacrificing thermal and mechanical properties [23]. Efficient toughening was obtained because of reaction-induced phase separation leading to well dispersed hyperbranched particles covalently attached to the thermosetting matrix by the unmodified hydroxyl groups of the HBP. Sunder et al. reported the synthesis and thermal properties of a hyperbranched poly(glycidol) (PGOH) of different molecular weight and the partial or total esterification of their end hydroxyl groups with acyl chlorides of different chain length [24]. Other star-like PGOH derivatives have been successfully used as toughening agents in different thermosetting formulations [25, 26]. Following a similar approach to that of these previous works [23, 24], we have synthesized a PGOH and modified partially the final hydroxyl groups by acylation with 10-undecenoyl chains. The modified HBPs have been incorporated into a biscycloaliphatic epoxy formulation with the purpose of enhancing the impact strength. The reason for the change of the hyperbranched core is the high solubility of

hyperbranched aliphatic polyesters in biscycloaliphatic epoxy resins, which might not produce a suitable phase-separated morphology with enhanced toughness. The synthesized HBPs have been characterized by NMR and DSC. The curing of these formulations has been monitored by DSC. The thermal and dynamomechanical properties have been measured using DSC, TGA, TMA and DMA. Mechanical tests have been performed to determine the impact strength of the resulting thermosets.

Experimental

Materials

The biscycloaliphatic epoxy resin 3,4-epoxycyclohexylmethyl 3',4'-epoxycyclohexyl carboxylate (BCDE, epoxy equivalent = 126 g/eq), Araldite CY 179, was provided by Vantico and used after drying under vacuum. Ytterbium triflate ($Yb(OTf)_3$, 99%) (Aldrich) was used as received. Glycidol (96%) (Aldrich) was distilled under reduced pressure and stored over molecular sieves at 2 – 5 ºC. Dioxane was dried over calcium hydride and subsequently distilled and pyridine was dried over molecular sieves (4 Å) and distilled under reduced pressure. Both solvents were purchased from Scharlab together with potassium carbonate (99%). 10-Undecenoyl chloride (97%) was distilled and trimethylolpropane (TMP, 97%) and potassium methylate solution (25% v/v in methanol) were used without further purification. All these products were acquired from Sigma-Aldrich. Dialysis tubes based on regenerated cellulose membrane (MWCO 2,000 g/mol) were acquired from Roth.

Synthesis of the hyperbranched poly(glycidol) (PGOH)

Hyperbranched poly(glycidol), PGOH, $\overline{M_n}$ (by ^{1}H NMR) 7,000 g/mol with an average of 94 hydroxyl groups per molecule was prepared according to already published procedures and dried under vacuum for 2 days at 50 ºC [27, 28]. PGOH was obtained as a highly viscous, clear and transparent oil with a glass transition temperature with T_g of -30 ºC (see Table 1).

^{1}H NMR (400 MHz, DMSO-d_6, ppm): 4.9-4.3 (O**H**), 4.0-3.2 (C**H**O/C**H**OH/C**H$_2$**O/C**H$_2$**OH, poly(glycidol) backbone), 1.27 (C**H$_2$**, TMP in the PGOH) and 0.81 (C**H$_3$**, TMP in the PGOH); ^{13}C NMR (100.6 MHz, DMSO-d_6, ppm): 80.9-80.1 (**C**H linear unit), 78.8-78.0 (**C**H dendritic unit), 73.8-72.7 (**C**H$_2$ linear unit), 72.7-70.3 (**C**H$_2$/**C**H terminal and dendritic unit), 69.1-68.3 (**C**H linear unit), 63.4-62.8 (**C**H$_2$ terminal unit) and 61.3-60.7 (**C**H$_2$ linear unit).

The signal assignment and the degree of branching (*DB*) of PGOH, according to the Frey's definition, were determined according to a previously published article [27]. *DB* was 0.41, calculated from ^{13}C NMR signal intensities obtained under quantitative conditions.

Table 1. Characterization of the synthesized HBPs.

Polymer	Mn (g/mol)[a]	OH (eq/g)[a]	% vinyl[a]	T_g (ºC)[b]	T_m (ºC)[b]	Δh_m (J/g)[b]
PGOH	7000	0.0134	-	-30	-	-
$PG_{45\%}$vin	13972	0.0037	44.7	-47	-21	9.64
$PG_{80\%}$vin	19450	0.0010	79.8	-56	-34	12.50

[a]Determined by ^{1}H NMR
[b]Determined by DSC on a heating scan at 10ºC/min from -100 to 50ºC in nitrogen atmosphere.

Chemical modification of PGOH with 10-undecenoyl chloride

The synthesis is exemplified for $PG_{45\%}$vin. In a 250 mL three-necked round bottomed flask 6.2 g (0.89 mmol) of PGOH (83.3 mmol hydroxyl groups) were placed and dissolved under argon atmosphere in 120 mL of anhydrous pyridine at room temperature. 9.25 mL (43.1 mmol, 0.50 eq) of 10-undecenoyl chloride were slowly added dropwise over 30 min under vigorous stirring using an ice bath to prevent the temperature to rise severely. The initial yellow color of the pyridinium salt disappeared immediately. After about half the amount was added, pyridinium chloride precipitated. Once the addition was completed, the system was kept at room temperature and 11.5 g (83.2 mmol) of K_2CO_3 were added while maintaining the vigorous stirring for additional 12 hours. The precipitate was filtered off and pyridine was removed by azeotropic distillation with dry and degassed toluene. The product was purified by dialysis against chloroform during 3 days to completely remove low molecular weight impurities. After removal of the solvent under reduced pressure, 10.5 g (85%) of a pale yellow viscous product was obtained. Degree of modification achieved (calculated by ^{1}H NMR): 45%, which represents an average number of 42 10-undecenoyl groups and 52 unreacted hydroxyl groups per molecule. The ^{1}H NMR spectrum of $PG_{45\%}$vin and the proton assignments are shown in Figure 1.

^{1}H NMR (400 MHz, $CDCl_3$, ppm): 1.05–1.45 (m, C**H$_2$**, **3**-**7**); 1.58 (m, C**H$_2$**, **2**); 2.00 (m, C**H$_2$**, **8**); 2.28 (m, C**H$_2$**, **1**); 3.31-3.78 (m, -C**H$_2$**-/C**H**, PG core); 4.00-4.47 (m, C**H$_2$**-OOC, ***); 4.86-5.03 (m, **H$_2$**C=CH, **10**/**11**); 5.05-5.30 (m, C**H**-OOC, ****); and 5.69-5.91 (m, H_2C=C**H**, **9**).

^{13}C NMR (100.6 MHz, $CDCl_3$, ppm): 24.1 (**C**H_2, **2**); 27.8-29.0 (**C**H_2, **3**-**7**); 32.8-33.7 (**C**H_2, **1**/**8**); 61.3-78.6 (**C**H_2/**C**H PG core and **C**H_2-OOC */**C**H-OOC **); 113.4 (H_2**C**=CH); 138.3 (H_2C=**C**H); and 172.6 (**C**=O).

The degree of modification, the molecular weight and the thermal characterization data of the synthesized polymers are shown in Table 1. $PG_{45\%}$vin was obtained as a yellow viscous liquid with a T_g of -47 ºC. $PG_{80\%}$vin was obtained as a brown viscous liquid with a T_g of -56 ºC.

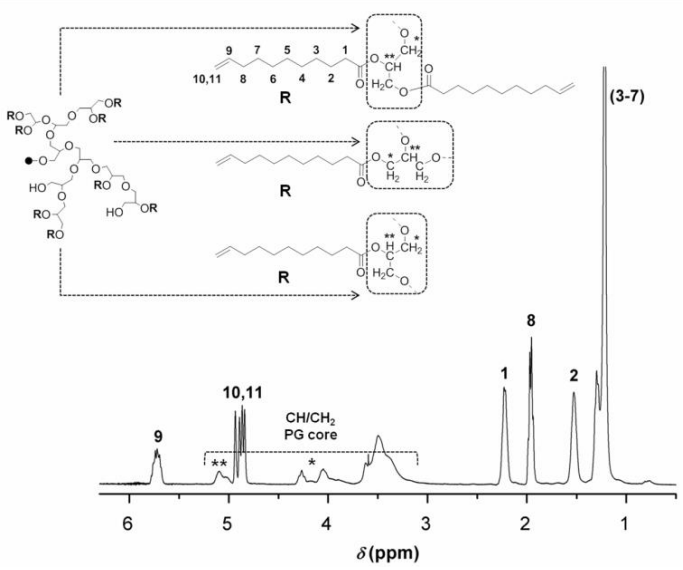

Figure 1. ^{1}H NMR spectrum of $PG_{80\%}$vin in $CDCl_3$.

Preparation of the curing mixtures

Mixtures containing BCDE and the selected proportion of the modified HBP were heated gently until the modifier was dissolved and the solution became clear. The initiator was used at a concentration of 1 phr (part per hundred of BCDE or BCDE/HBP mixture). The samples were carefully stirred and kept at -18 ºC before use to prevent polymerization. Table 2 shows the notation and composition of the different formulations studied.

Table 2. Neat and modified formulations with different amount of $PG_{80\%}$vin or $PG_{45\%}$vin in equivalent ratio (Xeq) and weight percentage (%Wt.). In the case of the HBP, Xeq corresponds to the equivalent amount of hydroxyl groups coming from the HBP in the formulation.

Formulation	BCDE		Yb		HBP	
	X_{eq}	% Wt.	X_{eq}	% Wt.	X_{eq}	% Wt.
BCDE/Yb	0.0793	99.01	0.0003	0.99	0.0000	0.00
BCDE/Yb + 3% $PG_{80\%}$vin	0.0769	96.04	0.0003	0.99	0.0006	2.97
BCDE/Yb + 5% $PG_{80\%}$vin	0.0753	94.06	0.0003	0.99	0.0009	4.95
BCDE/Yb + 10% $PG_{80\%}$vin	0.0713	89.11	0.0003	0.99	0.0019	9.90
BCDE/Yb + 10% $PG_{45\%}$vin	0.0713	89.11	0.0003	0.99	0.0075	9.90

Characterization

NMR characterization

^{1}H NMR 400 MHz and ^{13}C NMR 100.6 MHz NMR spectra were obtained using a Varian Gemini 400 spectrometer with Fourier Transformed. ^{1}H spectra were acquired in 1 min and 16 scans with a 1.0 s relaxation delay (D1). Quantitative ^{13}C NMR experiments were obtained using a D1 of 8 s and inverse gated proton decoupling. $CDCl_3$ was used as solvent. For internal calibration the solvent signal was used: δ (^{13}C) = 77.16 ppm and δ (^{1}H) = 7.26 ppm.

Calorimetric measurements (DSC)

Calorimetric analyses were carried out on a Mettler (DSC)-822e thermal analyzer. Samples of ~ 5 mg in weight were placed in aluminum pans under nitrogen atmosphere. The calorimeter was calibrated using an indium standard (heat flow calibration) and an indium-lead-zinc standard (temperature calibration).

Non-isothermal curing experiments were performed from 50 to 200 ºC at a heating rate of 10 ºC/min to determine the reaction heat. In a non-isothermal curing process, the degree of conversion by DSC was calculated as follows

$$Conversion = \frac{\Delta H_T}{\Delta H_{dyn}} \qquad (1)$$

where ΔH_T is the heat released up to a temperature T, obtained by integration of the calorimetric signal up to this temperature, and ΔH_{dyn} is the total reaction heat associated with the complete conversion of all reactive groups.

The synthesized polymers were analyzed by a heating scan at 10 ºC/min from -100 to 50 ºC. The glass transition temperature (T_g) was determined as the halfway point in the heat capacity step (ΔC_p) during the glass transition. The fusion peak temperature (T_m) and the fusion enthalpy (Δh_m) were determined using a straight baseline for the integration.

The STARe software by Mettler was used for the analysis of the calorimetric curves.

Thermogravimetric analysis (TGA)

Thermogravimetric analysis was carried out in a nitrogen atmosphere with a Mettler TGA/SDTA 851e/LF/1100 thermobalance. Samples with an approximate mass of 8 mg were degraded between 30 and 800 ºC at a heating rate of 10 ºC/min in a nitrogen atmosphere (100 cm^3/min measured in normal conditions).

Dynamomechanical analysis (DMTA)

Dynamic mechanical analyses were carried out with a TA Instruments DMA Q800. The samples were cured isothermally in a mould at 120 ºC for 1.5 h and then post-cured for 1 h at 150 ºC. Single cantilever bending at 1 Hz and amplitude of deformation of 10 μm was performed at 2 ºC/min, from -125 ºC to 200 ºC on prismatic rectangular samples (10 x 9 x 1.5 mm^3).

Thermomechanical analysis (TMA)

A Mettler TMA/SDTA840 thermomechanical analyzer was used. Prismatic rectangular samples (ca. 5 x 5 x 2.5 mm^3) were sandwiched between two silica discs and heated at 10 ºC/min from 30 up to 150 ºC in a first scan and at 5 ºC/min up to 180 ºC in a second scan. A constant force of 0.02 N was applied on the samples. The coefficients of thermal expansion α_g and, α_r, below and above the T_g respectively, were obtained from the second scan at 5 ºC/min and calculated as follows

$$\alpha = \frac{1}{L_0} \cdot \frac{dL}{dT} = const. \qquad (2)$$

where L and L_0 are the thickness at any temperature and at room temperature, respectively. The T_g was determined from the first derivative of the expansion curves L/L_0 as the half-way point in the increase of expansion coefficient step upon relaxation of the network. Two samples were analyzed for each formulation and the results were averaged.

Impact resistance

The impact test was performed at room temperature by means of an Izod 5110 impact tester, according to ASTM D 4508-05 (2008) using rectangular samples (25.4 x 12.7 x 2 mm^3). The pendulum employed had a kinetic energy of 1 J. For each material, 9 determinations were

made. The impact strength (*IS*) was calculated from the energy absorbed by the sample upon fracture as

$$IS = \frac{E - E_0}{S} \qquad (3)$$

where E and E_0 are the energy loss of the pendulum with and without sample respectively, and S is the cross-section of the samples.

Electron microscopy analysis (SEM)

The fracture area of samples were metalized with gold and observed with a scanning electron microscopy (SEM) Jeol JSM 6400. The samples were fractured by impact at room temperature.

Results and discussion

Synthesis and characterization of the modified hyperbranched polymers

In this work, hyperbranched poly(glycidol) (PGOH) was prepared according to previously published procedures by anionic polymerization of glycidol using as initiator the potassium salt of trimethylolpropane (TMP) as it is depicted in Scheme 1 [29]. The number of hydroxyl groups per molecule of PGOH was determined by first determining the molecular weight ($\overline{M_n}$ by ^{1}H NMR = 7,000 g/mol) by ^{1}H NMR and then assuming one hydroxyl group per repeating unit. Thus, it resulted to be on average of 94. Subsequently, the hydroxyl groups of PGOH were partially modified in order to generate two modified PG derivatives with different number of 10-undecenoyl chains (Scheme 1).

One of the most employed methods used to modify hydroxyl terminated hyperbranched polymers (HBPs) consists in the acylation by means of the use of acyl chlorides due to the higher reactivity towards their acid derivatives [30-33]. Following this methodology, the chemical modification of hyperbranched poly(glycidol) (PGOH) has been done by reacting it with 10-undecenoyl chloride, using pyridine as hydrochloric acid acceptor. To evaluate the extent to which the acylation took place, ^{1}H NMR spectroscopy has been employed.

Figure 1 shows the ^{1}H NMR spectrum of the vinyl modified PGOH with a 80% of modification ($PG_{80\%}$vin) with the proton assignments. After the esterification reaction new signals appear in the region from 4.0 to 5.3 ppm, due to the shift on the methine and methylene protons produced by the modification of primary and secondary hydroxyl groups. Signals from **1**-**8** correspond to the methylene protons of the 10-undecenyl chains and signals **9**-**11** to the protons associated to the terminal double bond. The achieved degree of modification was calculated by integration of the signals of PGOH core in the region from 3.3-4.5 ppm (non-esterified methine and methylene protons and esterified methylene units of the PGOH core) and from 5.1-5.3 ppm (esterified methine units of the PGOH core), and the signals corresponding to the methylene protons of 10-undecenyl groups of the esterified units (**1**-**8**), as shown in the following expression.

$$Modification\ (\%) = \frac{\frac{I_{1-8}}{16}}{\frac{I_{PGOHcore}}{5}} \cdot 100 \qquad (4)$$

The results of the characterization of the different synthesized polymers are shown in Table 1. One noticeable characteristic of the modified polymers is the gradual decrease in their T_g as the degree of modification increases. This is a feature that is commonly observed in analogous modified HBPs [23, 24, 34], caused by both the decrease in the intensity of inter- and intra-molecular H-bonding interactions and the increase in free volume associated with the presence of the 10-undecenoyl chains. Sunder et al. [24] reported the appearance of a complex crystalline phase in PGOH esterified with long alkyl chains, with a melting point above room temperature. PGOH esterified with dodecanoyl chloride showed a melting point below room temperature but for undecanoyl and shorter alkyl substituents no crystalline phase was detected [24]. In contrast, in PGOH modified with 10-undecenoyl chains it is observed the appearance of a small melting endotherm below room temperature (see Table 1) that can be explained by the association and crystallization of 10-undecenoyl pendant chains, in agreement with the results of Reina et al. [35] for modified poly(epichlorohydrin) and, more recently, the results of Flores et al. [23] for modified Boltorn™ hyperbranched polyesters. In the present case we can also observe a decrease in the melting temperature and an increase in the melting enthalpy with increasing degree of modification. This somewhat complex behaviour may be explained by the formation of different crystalline domains involving not only 10-undecenoyl chains but also unmodified moieties of the PGOH backbone, depending on the degree of modification.

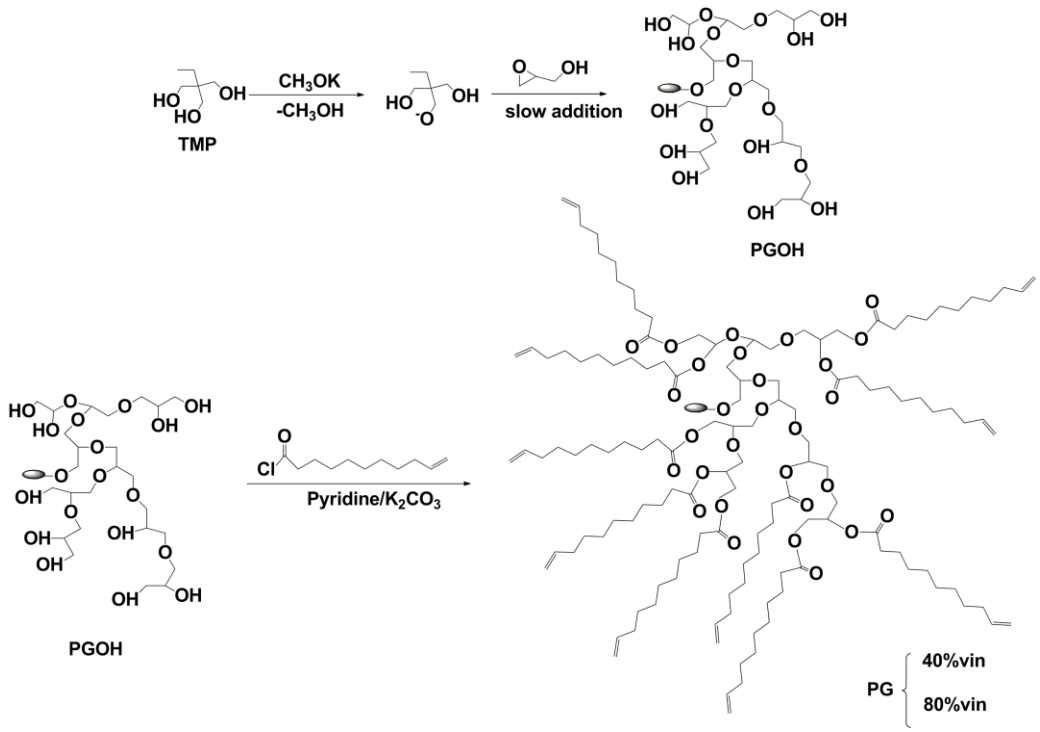

Scheme 1. Synthetic procedure and chemical structures of PGOH, $PG_{80\%}$vin and $PG_{45\%}$vin.

Effect of the modified HBPs on the curing kinetics

Figure 2 compares the curing thermograms of the neat formulations and the formulations with 10% of $PG_{80\%}$vin and $PG_{45\%}$vin. Table 3 summarizes relevant data from the curing of the formulations. It is observed that the reaction heat of all formulations is around 70 kJ/ee, which is in agreement with previously reported data of BCDE cured with rare earth triflates [36, 37]. From the data in the figure and the table, it can be deduced that the progressive addition of $PG_{80\%}$vin produces a delay in the curing process but the effect is even more important when $PG_{45\%}$vin is the modifier.

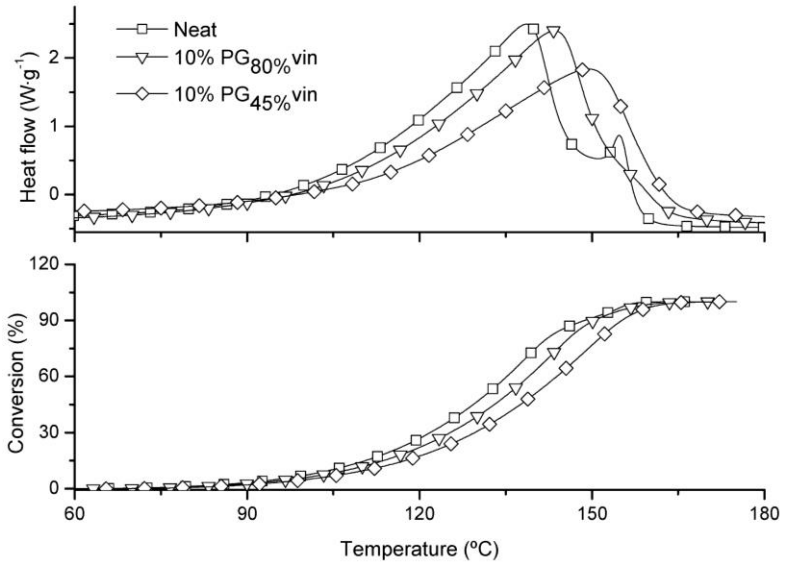

Figure 2. DSC scanning curves (top) and degree of conversion (bottom) against temperature of the curing of the neat and the modified formulations with 10% of the PG80%vin and PG45%vin at a heating rate of 10 ºC/min.

Table 3. Thermal and thermomechanical data of neat and modified formulations with different amount of $PG_{80\%}$vin and 10% of $PG_{45\%}$vin.

Formulation	ΔH (J/g)	ΔH[a] (KJ/ee)	T_{max}[b] (ºC)	$T_{tan\delta,DMA}$[c] (ºC)	$T_{5\%}$[d] (ºC)	$T_{máx}$[e] (ºC)
BCDE/Yb	569	73	139	146	242	267
BCDE/Yb + 3% $PG_{80\%}$vin	575	76	140	146	254	282
BCDE/Yb + 5% $PG_{80\%}$vin	510	68	139	131	257	279
BCDE/Yb + 10% $PG_{80\%}$vin	505	71	144	142	266	304
BCDE/Yb + 10% $PG_{45\%}$vin	495	70	150	139	252	286

[a] Enthalpies per equivalent of epoxy group.
[b] Temperature of the maximum of the curing exotherm.
[c] Temperature of the maximum of the tan δ curve.
[d] Temperature of a 5% of weight loss calculated by thermogravimetry.
[e] Temperature of the maximum degradation rate determined by TGA.

As reported previously by Kubisa and Penczek [38], hydroxylic compounds are known to participate in the cationic curing of epoxides following the so-called activated monomer (AM) mechanism, by which a hydroxylic group attacks a tertiary oxonium ion leading to a chain-transfer of an active proton to an unreacted epoxy group. The secondary oxonium ion formed can then propagate the polymerization by the active chain-end mechanism (ACE), leading to the formation of another hydroxyl chain end and another tertiary oxonium ion. Hydroxyl-terminated HBPs are known to accelerate the cationic curing of BCDE because of their participation in the curing process by the AM mechanism [11, 22]. However, their effect is complex and may also depend on the amount of HBP incorporated into the reactive mixture [32]. In a previous work, we found that the curing of DGEBA/Yb formulations was slowed down by the addition of PGOH or partially end-capped PGOH [39], which is in agreement with the present results. In that case we pointed out that this delay was caused by the participation of hydroxyl groups in the curing processes and the formation of less active complexes [40] by the interaction of the oxonium cations and the ether groups of the PGOH structure. The formation of inactive, dormant tertiary oxonium cations had also been described by Matejka et al. as a termination reaction occurring during the cationic curing of DGEBA [41]. This has also been observed by Foix et al. in the photocuring of BCDE with a pegylated HBP [42]. Thus, the positive contribution of the participation of the hydroxyl groups of the HBP is offset by the formation of less active cations, which is highly favoured due to the abundance of ether linkages in the HBP structure, thus reducing the amount of active species and slowing down the curing process. In order to explain the different effect of $PG_{80\%}$vin and $PG_{45\%}$vin we must take into account that: 1) the amount of available hydroxyl groups in $PG_{45\%}$vin is significantly higher (see Table 1), which would have a positive effect on the curing but 2) the relative amount of ether groups is also higher in $PG_{45\%}$vin due to its lower degree of modification, which has the opposite effect.

Thermal and thermomechanical properties of the thermosets obtained

Table 3 and Table 4 summarize relevant thermal-mechanical properties of the different cured formulations, determined using DSC, DMA and TMA. First, it can be observed that the addition of either modifier produces only a slight decrease in the T_g of the cured materials. In the literature [10,23,32] this is commonly attributed to the occurrence of phase separation during curing, resulting in a hardly modified matrix and softer particles distributed throughout. While T_g alone is only an indication of this phenomenon, further ascertainment can be obtained using DMA. Figure 3 and Figure 4 plot the *tan* δ and storage modulus *E'* obtained during the temperature sweeps at 1 Hz of the different materials. Note that the spectra were stopped at 200 ºC because of thermal degradation. It is clearly observed that the main relaxation temperature of the materials (given by the *tan* δ peak temperature), which is related to their glass transition, is hardly affected by the use of either HBP. However, important changes are observed in terms of the shape of the relaxation. Moreover, at lower temperatures it is noticeable the appearance of a secondary relaxation which can be related to the presence of a second phase in the material [23, 32], a feature commonly related with an improvement in toughness [23] (this is not shown for the formulation containing $PG_{45\%}$vin). This is consistent with the evolution of *E'* shown in Figure 4, where it is observed a more significant drop at lower temperatures in the modified formulations with respect to the unmodified formulation.

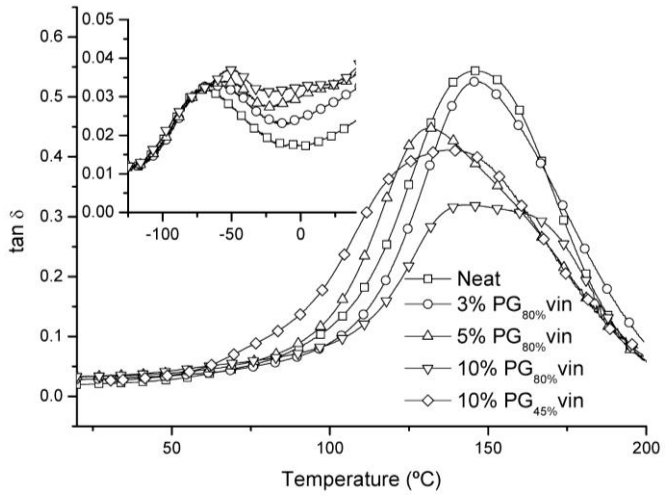

Figure 3. Plot of tan δ against temperature of the cured formulations.

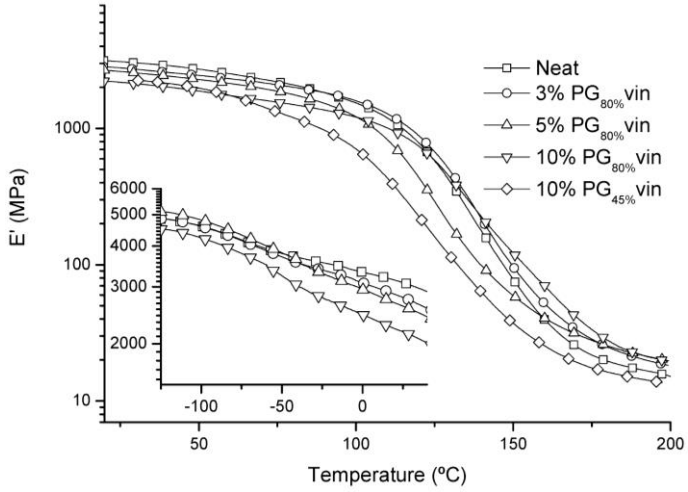

Figure 4. Plot of the storage modulus E' against temperature of the cured materials.

There is an important difference between the formulations with 10% of $PG_{45\%}$vin and 10% of $PG_{80\%}$vin. In the first case there is a significant broadening of the relaxation, which can be associated with a higher miscibility [8] of $PG_{45\%}$vin in comparison with $PG_{80\%}$vin, which might ultimately result in a looser network structure and different morphological features and material properties. Another significant feature of the formulations containing $PG_{80\%}$vin is the gradual and significant decrease in the *tan* δ peak area with respect to the unmodified formulation. This results from restrictions in the network mobility leading to a decrease in the segmental motion of the polymeric chains in the network structure. Similar effects are commonly reported for reinforced epoxy thermosets [21, 43-45], and more recently in HBP-modified homogeneous epoxy thermosets [46]. We hypothesize that, in the present case, the presence of phase-separated particles with a significant interfacial interaction with the matrix, along with further restrictions occasioned by the densely branched structure of the PG core, are the responsible for

this network mobility restriction. An effective particle-matrix interaction is guaranteed by the reaction of some of the available hydroxyl groups in $PG_{80\%}$vin with the epoxy groups of the matrix by the AM mechanism and extensive H-bonding. However, this was not observed previously [23] where good compatibility between the matrix and the particles was also observed. Such differences may also be a consequence of the different matrix and/or the HBP core used which, in the present case, has a larger amount of reactive hydroxyl groups and a more densely branched structure.

It was also found previously [23] that excessive compatibility between the matrix and the modifier might not result in a significant improvement in toughness, but it was also noticed that a too low compatibility might be detrimental to the toughness of the resulting material due to ineffective stress transfer from the matrix to the particle and poor shear yielding of the unmodified matrix. In order to elucidate which is the dominant effect in the present case, impact tests and morphology analysis were performed as well and will be discussed afterwards.

Table 4 shows the results of the TMA analysis of the cured formulations. It can be shown that, within experimental error, the use of these modifiers does not produce any significant change in the T_g of the cured materials, in agreement with DMA data. The values are different from those obtained with DMA (see Table 3 and Figure 3), which can be explained by the different experimental conditions and the definition of T_g in each case. It is observed how, on increasing the amount of $PG_{80\%}$vin in the formulation, the thermal expansion coefficient below T_g, α_g, increases accordingly, while the expansion coefficient above T_g, α_g, remains constant. One may attribute this to the presence of a softer second phase in the material, which would contribute positively to the expansion coefficient below T_g. However, these results are somewhat different from those obtained using an epoxy-anhydride matrix modified with hyperbranched polyester with 10-undecenoyl chains [23]. One must take into account that the thermosetting matrix and modifier used in each case are different, and that the matrix-particle interactions may be different as well. In the present case, the number of available hydroxyl groups is much higher, which surely affects the compatibility between the matrix and the phase-separated particles. One negative consequence of the increase in α_g is the increase in the internal stresses generated in the cooling stage after curing [47].

Table 4. Thermal expansion coefficients, α_g and α_r, below and above glass transition respectively, determined by TMA.

Formulation	T_g[a] (ºC)	α_g (μm/m)	α_r (μm/m)
BCDE/Yb	124	80.00 ± 2.31	166.09 ± 2.03
BCDE/Yb + 3% $PG_{80\%}$vin	129	85.08 ± 9.34	166.74 ± 2.15
BCDE/Yb + 5% $PG_{80\%}$vin	128	89.23 ± 2.38	167.59 ± 0.81
BCDE/Yb + 10% $PG_{80\%}$vin	122	95.39 ± 3.11	167.35 ± 0.37
BCDE/Yb + 10% $PG_{45\%}$vin	113	91.69 ± 5.54	177.18 ± 2.35

[a] Glass transition temperature of isothermally cured thermosets determined by TMA as the half-way point in the thermal expansion coefficient step observed upon relaxation of the material.

The results of the thermogravimetric analysis are shown in Table 3 and Figure 5. It can be seen how the addition of $PG_{80\%}$vin increases the thermal stability of the cured materials, which is advantageous taking into account that rare earth triflates are also known to catalyze the

thermal degradation of epoxy thermosets [48]. In our case, the higher thermal stability of the ether groups of the modified $PG_{80\%}$vin in comparison with the ester groups of BCDE, coupled with the covalent bonding between the phase-separated $PG_{80\%}$vin particles and the matrix, may account for the observed increase in thermal stability. Noteworthy, it is seen how the use of a $PG_{45\%}$vin instead of $PG_{80\%}$vin results in a lower increase in thermal stability. This difference might be caused by the higher miscibility of $PG_{45\%}$vin, which results in a loosening of the network structure of the modified material, and the presence of a higher amount of OH groups in the formulation containing $PG_{45\%}$vin, which can also contribute to its lower thermal stability in comparison with the one containing $PG_{80\%}$vin. In a previous work using PGOH and benzoyl end-capped PGOH as modifiers in DGEBA formulations, a slight decrease in thermal stability was observed [39], which my be explained by the higher thermal stability of the DGEBA network in comparison with that of BCDE.

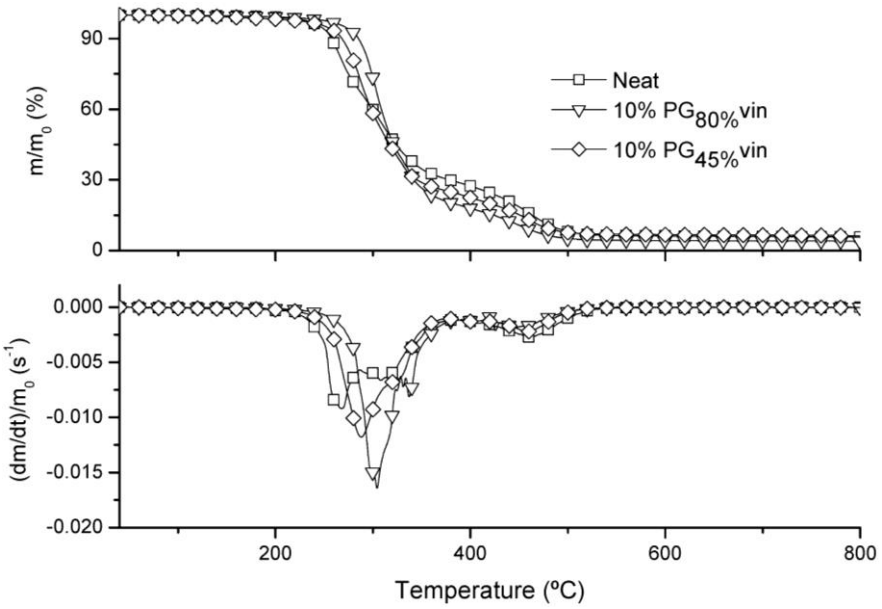

Figure 5. TGA (top) and DTG (bottom) curves at 10ºC/min in N_2 atmosphere of the materials obtained from the neat formulation and formulations with 10% $PG_{80\%}$vin and 10% $PG_{45\%}$vin (m is the mass of the sample at any temperature, m_0 is the initial mass, dm/dt is the rate of mass loss).

Mechanical characterization and morphology

In a recent paper we reported a significant increase in impact strength of an epoxy-anhydride formulation by addition of a hyperbranched polyester of the Boltorn™ family of which part of the hydroxyl groups were replaced by acylation with 10-undecenoyl chains [23]. We observed that the toughening effect was determined not only by the amount of polymeric modifier but also, and more importantly, by the degree of modification of the hyperbranched polyester. In the present work we have obtained similar results. In Figure 6 it is shown that upon the addition of only 3% of $PG_{80\%}$vin the impact strength doubles. Further addition of up to 5% of $PG_{80\%}$vin produces a further increase in impact strength but an increase of $PG_{80\%}$vin up to 10% only results in a marginal increase in impact strength. In contrast, it is observed how the modification with 10% of $PG_{45\%}$vin produces only a poor increase in this property. These results are in agreement with those reported previously [23], which evidenced that a too low degree of modification,

resulting in an excessive compatibility between the matrix and the HBP, did not result in a significant increase in impact strength in comparison with the optimum.

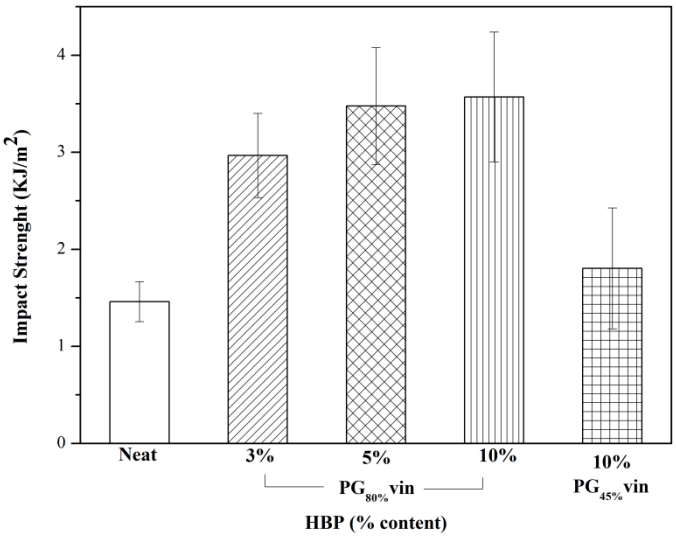

Figure 6. Impact strength of BCDE/Yb thermosets containing different percentages of $PG_{80\%}$vin and 10% of $PG_{45\%}$vin.

The morphology of the fractured surfaces was observed by SEM. Figure 7 shows how, upon addition of $PG_{80\%}$vin, regular and well-distributed particles are visible, increasing in number as the amount of $PG_{80\%}$vin increases. This is in agreement with the DMA data in Figure 3, where it was noticed the appearance of a relaxation below room temperature which was then ascribed to the presence of a second phase. The presence of such particles, which have also a good compatibility with the matrix because of the reaction of some of the remaining hydroxyl groups by the AM mechanism taking place in the cationic curing of epoxides, must be responsible for the efficient toughening effect of $PG_{80\%}$vin. Boogh et al. [8] proposed that HBPs have a particular ability to reach a gradient property within the phase separated particles. In our case, it could be a variation in the degrees of reaction of OH groups produced during the curing by the phase-separation process. Soft rubber particles concentrate applied stresses in the matrix at their equators when a toughened material is loaded. Upon loading, stresses in the matrix can be transferred to the rubber particles if strong interfacial interactions exist, as it is the case, given that the OH groups of the HBP can participate in the curing. In consequence, the following energy absorption mechanisms may be activated: (1) shear yielding, which involves plastic deformation within the matrix and in close vicinity of the particles, and (2) cavitation of the particles. The size of the particles is also of a great importance, since only particles larger than 100 nm can store sufficient elastic energy and produce an adequate stress concentration effect [49]. It has been described that particles with diameters larger than 10 μm can be relatively inefficient [50]. As seen in Figure 7, particles ranging from 2 up to 5 micrometers have been obtained, which are within the optimum range.

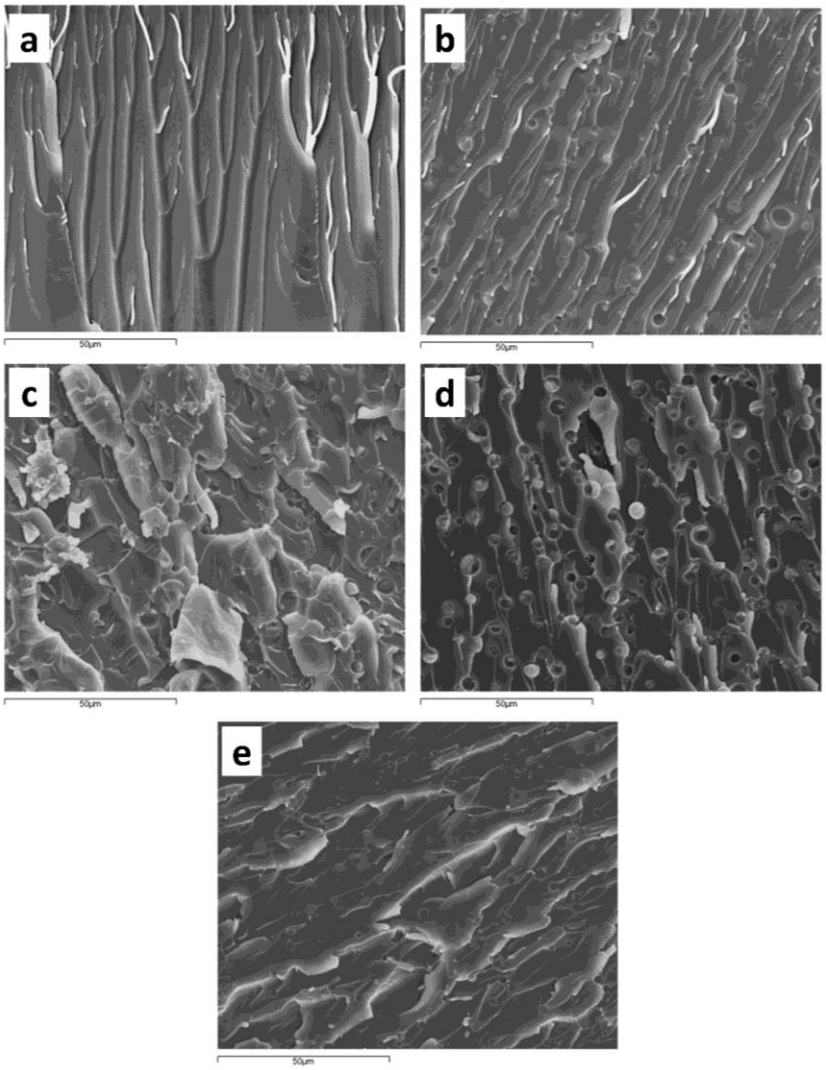

Figure 7. SEM micrographs of fracture surface for materials obtained from neat and modified formulations: a) neat, b) 3% $PG_{80\%}$vin, c) 5% $PG_{80\%}$vin, d) 10% $PG_{80\%}$vin, e) 10% $PG_{40\%}$vin.

In contrast, the fracture surface of the formulation with 10% $PG_{45\%}$vin reveals only traces of less-defined particles present in the material, and in a lower number than in the corresponding formulation with $PG_{80\%}$vin. This must be related to its lower degree of modification, which allows the HBP to be more compatible with the epoxy matrix by participation of its hydroxyl groups in the AM mechanism and by the smaller proportion of 10-undecenoyl chain ends. Because of that, the driving force for the formation of a segregated phase is weaker, thus leading to looser network structure with a more homogeneous morphology and without a significant effect on impact strength.

The improvement achieved in this work is not as outstanding as the one we obtained previously for an epoxy-anhydride formulation [23]. However, the results are remarkable, all the

more taking into account that brittle, highly crosslinked networks are difficult to toughen [3]. As stated above in the introduction section, modification of BCDE with hyperbranched polymers has led only to either little improvement [22] or to a significant improvement but at the expense of other thermomechanical properties [11]. In our case, we obtain a significant improvement without sacrificing either T_g or the rigid modulus. A further advantage is the much lower viscosity of the hyperbranched modifier compared with other polymeric modifiers such as CTBN rubbers employed for the toughening of cycloaliphatic epoxy resins [14, 15], and the use of a much smaller amount to obtain a significant enhancement. Indeed, it was previously reported that the modification with long alkyl chains greatly reduced the viscosity due to the decrease in inter-molecular H-bond interactions [23, 34]. The same phenomenon was qualitatively observed in the present case. The use of low viscosity modifiers represents a great advantage, from the processability point of view, thus making making these novel modified HBPs highly attractive as toughness enhancers.

Conclusions

A hyperbranched poly(glycidol) (PGOH) has been synthesized and the final hydroxyl groups have been partially modified by acylation with 10-undecenoyl chloride. Different degrees of modification of 45% ($PG_{45\%}$vin) and 80% ($PG_{80\%}$vin) have been achieved and determined by ^{1}H-NMR spectroscopy. The modified HBPs have been used as modifiers in bis-cycloaliphatic epoxy formulations cured with ytterbium triflate as cationic initiator.

A significant increase in impact strength greater than 200% with respect to the unmodified material has been achieved using an optimum concentration of only 5% of $PG_{80\%}$vin. This enhancement is the consequence of the formation of a well defined morphology consisting of soft $PG_{80\%}$vin microparticles homogeneously distributed within the thermosetting matrix, with a good compatibility among phases due to the covalent linkage of the remaining OH groups of the HBP with the epoxy network by their participation in the curing following the AM mechanism. On the contrary, the use of $PG_{45\%}$vin has not produced an efficient toughness enhancement due to its excessive compatibility with the matrix, leading to a less defined microstructure.

The enhancement in impact strength has been achieved without sacrificing thermal-mechanical properties such as the glass transition temperature, T_g. The thermal stability of the resulting materials has been improved, which is beneficial taking into account the catalytic effect of ytterbium triflate on the degradation of epoxy thermosets. Further advantages derived from the use of such modifiers are 1) the relatively small amount needed to produce a significant enhancement and 2) the low viscosity of the modifiers, which does not compromise the processability of the formulations.

The possibility of tailoring the shell chemistry enables synthesizing HBPs with different degrees of compatibility with the resin that opens a new way to reach, by this easy procedure, a series of epoxy thermosets with different final characteristics.

Acknowledgements

The authors would like to thank MINECO (MAT2011-27039-C03-01, MAT2011-27039-C03-02) and Generalitat de Catalunya (2009-SGR-1512) for giving financial support. X.F-F. acknowledges the contract JCI-2010-06187 and M.F. the grant BES-2009-025226.

References

[1] May CA. Epoxy Resins: Chemistry and Technology. In: May CA, Tanaka Y, editors. New York: Marcel Dekker; 1973.

[2] Petrie EM. Epoxy Adhesive Formulations. New York, McGraw-Hill; 2006.

[3] Bagheri R, Marouf BT, Pearson RA. Rubber-toughened Epoxies: A Critical Review. Polymer Reviews. 2009; 49(3): 201-225.

[4] Zheng S. Epoxy polymers: New materials and Innovations. In: Pascault J-P, Williams RJJ, editors. Epoxy polymers: New materials and Innovations. Weinheim: Wiley-VCH; 2010.

[5] Brooker RD, Kinloch AJ, Taylor AC. The morphology and fracture properties of thermoplastic-toughened epoxy polymers. Journal of Adhesion. 2010;86(7):726-741.

[6] Qian JY, Pearson RA, Dimonie VL, Shaffer OL, El-Aasser MS. The role of dispersed phase morphology on toughening of epoxies. Polymer. 1997;38(1):21-30.

[7] Ruiz-Pérez L, Royston GJ, Fairclough JPA, Ryan AJ. Toughening by nanostructure. Polymer. 2008;49(21):4475-4488.

[8] Boogh L, Pettersson B, Mänson J-AE. Dendritic hyperbranched polymers as toughеners for epoxy resins. Polymer. 1999;40(9):2249-2261.

[9] Ratna D, Simon GP. Thermomechanical properties and morphology of blends of a hydroxy-functionalized hyperbranched polymer and epoxy resin. Polymer. 2001;42(21):8833-8839.

[10] Ratna D, Varley R, Simon GP. Toughening of trifunctional epoxy using an epoxy-functionalized hyperbranched polymer. Journal of Applied Polymer Science. 2003;89(9):2339-2345.

[11] Sangermano M, Malucelli G, Bongiovanni R, Priola A, Harden A. Investigation on the effect of the presence of hyperbranched polymers on thermal and mechanical properties of an epoxy UV-cured system. Polymer International. 2005;54(6):917-921.

[12] Zhang D, Jia D. Toughness and strength improvement of diglycidyl ether of bisphenol-A by low viscosity liquid hyperbranched epoxy resin. Journal of Applied Polymer Science. 2006;101(4):2504-2511.

[13] Voit B, Lederer A. Hyperbranched and highly branched polymer architectures-synthetic strategies and major characterization aspects. Chemical Reviews. 2009;109(11):5924-5973.

[14] Tripathi G, Srivastava D. Effect of carboxyl-terminated butadiene acrylonitrile copolymer concentration on mechanical and morphological features of binary blends of nonglycidyl-type epoxy resins. Advances in Polymer Technology. 2007;26(4):258-271.

[15] Tripathi G, Srivastava D. Toughened Cycloaliphatic Epoxy Resin for Demanding Thermal Applications and Surface Coatings. Journal of Applied Polymer Science. 2009;114(5):2769-2776.

[16] Lijima T, Fujimoto KI, Tomoi M. Toughening of cycloaliphatic epoxy resins by poly(ethylene phthalate) and related copolyesters. Journal of Applied Polymer Science. 2002;84(2):388-399.

[17] Zhang X, Xu W, Xia X, Zhang Z, Yu R. Toughening of cycloaliphatic epoxy resin by nanosize silicon dioxide. Materials Letters. 2006;60(28):3319-3323.

[18] Zhang X-H, Zhang Z-H, Xu W-J, Chen F-C, Deng J-R, Deng X. Toughening of cycloaliphatic epoxy resin by multiwalled carbon nanotubes. Journal of Applied Polymer Science. 2008;110(3):1351-1357.

[19] Gao N, Liu W, Ma S, Tang C, Yan Z. Cycloaliphatic epoxy resin modified by two kinds of oligo-fluorosiloxanes for potential application in light-emitting diode (LED) encapsulation. Journal of Polymer Research.19(8):9923-9923.

[20] Ochi M, Ichikawa N, Harada M, Hara M, Uchida H. Toughening of cycloaliphatic epoxy resin improved by reactive copolymers with flexible alkyl side chains. Journal of Applied Polymer Science.124(6):4572-4578.

[21] Sangermano M, Messori M, Galleco MM, Rizza G, Voit B. Scratch resistant tough nanocomposite epoxy coatings based on hyperbranched polyesters. Polymer. 2009;50(24):5647-5652.

[22] Sangermano M, Priola A, Malucelli G, Bongiovanni R, Quaglia A, Voit B, et al. Phenolic hyperbranched polymers as additives in cationic photopolymerization of epoxy systems. Macromolecular Materials and Engineering. 2004;289(5):442-446.

[23] Flores M, Fernández-Francos X, Ferrando F, Ramis X, Serra A. Efficient impact resistance improvement of epoxy/anhydride thermosets by adding hyperbranched polyesters partially modified with undecenoyl chains. Polymer. 2012;53:5232-5241.

[24] Sunder A, Bauer T, Mulhaupt R, Frey H. Synthesis and thermal behavior of esterified aliphatic hyperbranched polyether polyols. Macromolecules. 2000;33(4):1330-1337.

[25] Karger-Kocsis J, Frohlich J, Gryshchuk O, Kautz H, Frey H, Mülhaupt R. Synthesis of reactive hyperbranched and star-like polyethers and their use for toughening of vinylester-urethane hybrid resins. Polymer. 2004;45(4):1185-1195.

[26] Morell M, Ramis X, Ferrando F, Serra A. Effect of polymer topology on the curing process and mechanical characteristics of epoxy thermosets modified with linear or multiarm star poly(-caprolactone). Polymer.52(21):4694-4702.

[27] Sunder A, Hanselmann R, Frey H, Mulhaupt R. Controlled synthesis of hyperbranched polyglycerols by ring-opening multibranching polymerization. Macromolecules. 1999;32(13):4240-4246.

[28] Sunder A, Mülhaupt R, Frey H. Hyperbranched polyether-polyols based on polyglycerol: Polarity design by block copolymerization with propylene oxide. Macromolecules. 2000;33(2):309-314.

[29] Wilms D, Stiriba S-E, Frey H. Hyperbranched Polyglycerols: From the Controlled Synthesis of Biocompatible Polyether Polyols to Multipurpose Applications. Accounts of Chemical Research. 2009;43(1):129-141.

[30] Sunder A, Krämer M, Hanselmann R, Mülhaupt R, Frey H. Molecular Nanocapsules Based on Amphiphilic Hyperbranched Polyglycerols. Angewandte Chemie International Edition. 1999;38(23):3552-3555.

[31] Gao C, Yan D. Hyperbranched Polymers: from Synthesis to Applications. Progress in Polymer Science. 2004;29(3):183-275.

[32] Fernández-Francos X, Foix D, Serra À, Salla JM, Ramis X. Novel thermosets based on DGEBA and hyperbranched polymers modified with vinyl and epoxy end groups. Reactive and Functional Polymers. 2010;70(10):798-806.

[33] Zhang X. Modifications and applications of hyperbranched aliphatic polyesters based on dimethylolpropionic acid. Polymer International. 2011;60(2):153-166.

[34] Luciani A, Plummer CJG, Nguyen T, Garamszegi L, Manson J-AE. Rheological and Physical Properties of Aliphatic Hyperbranched Polyesters. Journal of Polymer Science, Part B: Polymer Physics. 2004;42(7):1218-1225.

[35] Reina JA, Cádiz V, Mantecón A, Serra À. Chemical modification of poly(epichlorohydrin) with unsaturated potassium carboxylates. Angewandte Makromolekulare Chemie. 1993;209:95-109.

[36] Mas C, Mantecón A, Serra À, Ramis X, Salla JM. Improved thermosets obtained from cycloaliphatic epoxy resins and γ-butyrolactone with lanthanide triflates as initiators. I. Study of curing by differential scanning calorimetry and fourier transform infrared. Journal of Polymer Science, Part A: Polymer Chemistry. 2005;43(11):2337-2347.

[37] Fernàndez X, Salla JM, Serra À, Mantecón A, Ramis X. Cationic copolymerization of cycloaliphatic epoxy resin with a spirobislactone with lanthanum triflate as initiator: I. Characterization and shrinkage. Journal of Polymer Science, Part A: Polymer Chemistry. 2005;43(15):3421-3432.

[38] Kubisa P, Penczek S. Cationic activated monomer polymerization of heterocyclic monomers. Progress in Polymer Science. 1999;24(10):1409-1437.

[39] Santiago D, Morell M, Fernández-Francos X, Serra À, Salla JM, Ramis X. Influence of the end groups of hyperbranched poly(glycidol) on the cationic curing and morphology of diglycidylether of bisfenol A thermosets. Reactive and Functional Polymers. 2011;71(4):380-389.

[40] Crivello JV. Cationic photopolymerization of alkyl glycidyl ethers. Journal of Polymer Science, Part A: Polymer Chemistry. 2006;44(9):3036-3052.

[41] Matejka L, Chabanne P, Tighzert L, Pascault JP. Cationic polymerization of diglycidyl ether of bisphenol a. Journal of Polymer Science, Part A: Polymer Chemistry. 1994;32(8):1447-1458.

[42] Foix D, Fernández-Francos X, Ramis X, Serra À, Sangermano M. New pegylated hyperbranched polyester as chemical modifier of epoxy resins in UV cationic photocuring. Reactive and Functional Polymers. 2011;71(4):417-424.

[43] Renukappa RNM, Chikkakuntappa R, Kunigal NS. Montmorillonite Nanoclay Filler Effects on Electrical Conductivity, Thermal and Mechanical Properties of Epoxy-Based Nanocomposites. Polymer Engineering and Science. 2011;51(9):1827-1836.

[44] Akesson D, Skrifvars M, Walkenstrom P. Preparation of thermoset composites from natural fibres and acrylate modified soybean oil resins. Journal of Applied Polymer Science. 2009;114(4):2502-2508.

[45] Yang P, Wang G, Xia X, Takezawa Y, Wang H, Yamada S, Du Q, Zhong W. Preparation and thermo-mechanical properties of heat-resistant epoxy/silica hybrid materials. Polymer Engineering & Science. 2008;48(6):1214-1221.

[46] Fernández-Francos X, Santiago D, Ferrando F, Ramis X, Salla JM, Serra À, et al. Network structure and thermomechanical properties of hybrid DGEBA networks cured with 1-methylimidazole and hyperbranched poly(ethyleneimine)s. Journal of Polymer Science Part B: Polymer Physics. 2012;50(21):1489-1503.

[47] Lange J, Toll S, Manson JAE, Hult A. Residual stress build-up in thermoset films cured above their ultimate glass transition temperature. Polymer. 1995;36(16):3135.

[48] González L, Ramis X, Salla JM, Mantecón A, Serra À. The degradation of new thermally degradable thermosets obtained by cationic curing of mixtures of DGEBA and 6,6-dimethyl (4,8-dioxaspiro[2.5]octane-5,7-dione). Polymer Degradation and Stability. 2007;92(4):596-604.

[49] Lazzeri A, Bucknall CB. Dilatational bands in rubber-toughened polymers. Journal of Materials Science. 1993;28(24):6799-6808.

[50] Pearson RA, Yee AF. Influence of particle size and particle size distribution on toughening mechanisms in rubber-modified epoxies. Journal of Materials Science. 1991;26(14):3828-3844.

Effect of molecular weight of polyesters with multiarm star topology used as additives in cycloaliphatic epoxy thermosets cured by ytterbium triflate

Marjorie Flores,[1] Xavier Fernández-Francos,[1] Xavier Ramis,[2] Francesc Ferrando,[3] Àngels Serra[1*]

[1] Department of Analytical and Organic Chemistry, Universitat Rovira i Virgili, C/ Marcel·lí Domingo s/n, 43007, Tarragona, Spain.
[2] Thermodynamics Laboratory, ETSEIB Universitat Politècnica de Catalunya, Av. Diagonal 647, 08028, Barcelona, Spain.
[3] Department of Mechanical Engineering, Universitat Rovira i Virgili, C/ Països Catalans, 26, 43007, Tarragona, Spain.

Abstract

A series of well-defined multiarm star polyesters (HX-PCL), obtained by growing poly(*ε*-caprolactone) arms with a degree of polymerization of approximately 10 from commercially available Boltorn polyesters of different molecular weight were characterized and used as thermoplastic modifiers in epoxy thermosets. The increase of the molecular weight of the core led to an increased number of arms per molecule, but the degree of polymerization of the arms remained similar. The multiarm stars were used in different proportions in formulations of cycloaliphatic epoxy resin (CE) cured by ytterbium triflate as cationic initiator. The effect of the molecular weight of the stars and their proportion on the curing and in the viscosity of the reactive mixture was studied by dynamic scanning calorimetry (DSC) and rheometry. The addition of star-shaped modifiers to the epoxy resin led to homogeneous materials with a slight reduction in thermomechanical characteristics. The modified thermosets can be considered to be thermally reworkable, due to their low initial degradation temperatures. The effect of the addition of star-like structures on the impact energy dissipation and microhardness was also studied.

Keywords: *Star polymers, hyperbranched, epoxy resin, cationic polymerization, thermosets.*

Introduction

Cycloaliphatic epoxy resins show a marked superiority over Bisphenol A resins in electrical and electronic applications due to their high arc resistance, since diglycidylether of bisphenol A (DGEBA) thermosets decompose in the presence of the high-temperature arc to produce carbon, which can act as conductor, leading to insulation failure. In addition, they have low viscosity, high heat deflection temperatures and excellent weatherability [1]. However, cycloaliphatic epoxy matrices are usually brittle, due to their high crosslinking densities, but especially if they are cured by cationic homopolymerization. This cationic curing can be performed by the use of thermal curing agents or by UV initiated photoirradiation. Crivello et aI. [2,3,4] reported the photoinitiated cationic homopolymerization of epoxy resins using sulfonium and iodonium salts, among others. Although photoinduced epoxy curing is advantageous from the point of view of the reduction in the waste of energy, there are some significant drawbacks: light absorption and scattering inhibit efficient irradiation and the irradiation source and shape and thickness of the sample makes difficult to reach a homogeneous material. As an alternative, thermal cationic curing seems to be easier for some practical applications and allows the use of such materials as adhesive for non-transparent substrates and the formation of thicker or filled films. Among thermal cationic initiators, benzyl sulfonium, ammonium and phosphonium salts have been described [5]. Also boron trifluoride complexes [6] have a broad industrial application and in the last decade lanthanide triflates have been proposed [7].

Most of the work published in toughness improvement in cycloaliphatic epoxy thermosets by adding dendritic structures as modifiers has been reported in photoinitiated systems by Sangermano et al. [8,9] but scarce references have been published in thermally cured materials [10,11].

In the field of toughness improvement by addition of hyperbranched polymers (HBPs), it seems that the most successful results were achieved when phase separation occurred. Usually, phase separation may be promoted during processing by a chemically induced phase separation mechanism, which is strongly influenced by the relationship between the reaction kinetics of the curing process and the reactivity of the HBP modifier. The initial miscibility, which is a key point for processing and stability of the blend in the uncured state, is strongly dependent on the chemical design of the HBP final groups [12]. According to that, the selection of the HBP, a suitable curing mechanism and the control of the curing kinetics are of utmost importance in order to achieve a significant toughness enhancement.

Among dendritic polymers, multiarm stars can be regarded as potential modifiers for epoxy thermosets. As dendritic structures, they present lower viscosities than linear analogs which make them valuable to maintain processability characteristics, which are critical in the applicability of their formulations as coatings and adhesives [13]. Another advantage is the easy preparation of multiarm stars by various synthetic strategies and the possibility to tailor the structure to get the adequate properties. Their use as toughness modifiers of thermally cured epoxy thermosets has been recently reported, but most of the published works are based on DGEBA resins [14,15,16].

Multiarm poly(*ε*-caprolactone) star copolymers have been synthesized by ring-opening polymerization of *ε*-caprolactone using hyperbranched poly(glycidol) (PGOH-PCL) [17] or poly(styrene) (PS-PCL) [16] as macroinitiators and $Sn(oct)_2$ as the catalyst. Poly(*ε*-caprolactone) (PCL) is a hydrophobic, semi-crystalline polyester with a high chain flexibility which is miscible in most epoxy systems [18,19,20]. The effect of PCL-stars as modifiers of epoxy thermosets and their high processability in reference to linear analogs has been reported [21]. Mechanical characteristics such as impact resistance and microhardness were better for the multiarm star modified materials. When PCL-stars were used in anionically cured epoxy thermosets, the best results in processability and thermomechanical characteristics were obtained when the arms had a degree of polymerization of 10 [14].

Because of the possible technological applications of multiarm stars with PCL arms as modifiers in thermosetting materials, in the present paper we describe the preparation of a series of star-like structures using as the core commercially available hyperbranched polyester, known as Boltorn, with different molecular weights. This allows the preparation of well-defined polyester-PCL star-like structures with different molecular weights and number of arms, but maintaining the arm length to a value close to 10 repeating units (Scheme 1). The presence of PCL arms in the structure helps to compatibilize Boltorn type polyesters with the epoxy resins, which is a requirement to get uniform materials. The multiarm stars synthesized have been added in different proportions as modifiers of cycloaliphatic epoxy thermosets obtained by curing CE with ytterbium triflate as the initiator. The properties of the materials and the evolution of the curing process of these formulations are discussed in this paper.

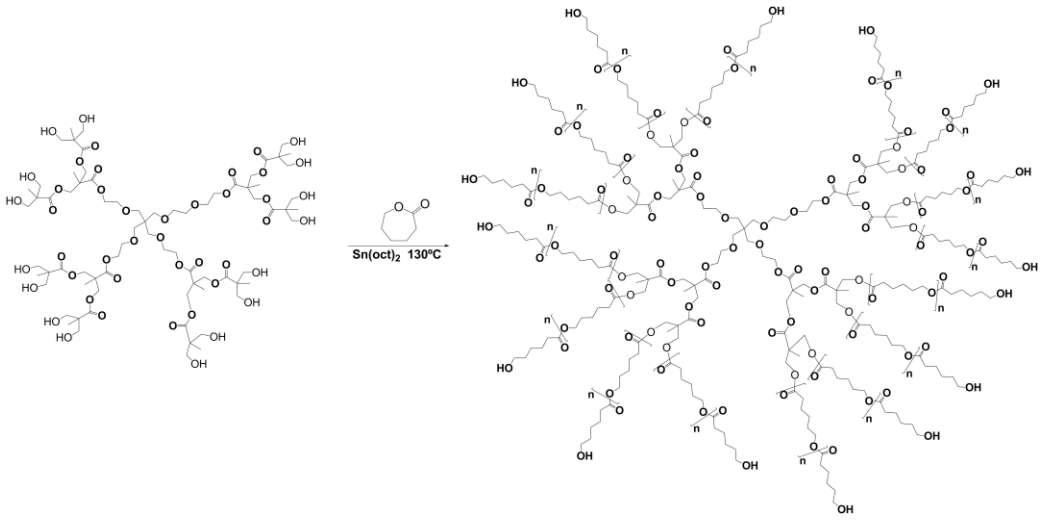

Scheme 1. Synthetic route to multiarm stars HX-PCL (X accounts for the Boltorn HX used as the core molecule and can be 20, 30 and 40)

Experimental section

Materials

Hyperbranched polymers: Boltorn H20 (Mw = 1747 g/mol, 16 OH), Boltorn H30 (Mw = 3500 g/mol, 32 OH) and Boltorn H40 (Mw = 7316 g/mol, 64 OH) were donated by Perstorp and were used as received. ε-Caprolactone (CL) was distilled under vacuum, tin (II) 2-ethylhexanoate ($Sn(oct)_2$), 3,4-epoxycyclohexylmethyl 3,4-epoxycyclohexyl carboxylate (CE, 126 g/eq) and ytterbium triflate ($Yb(OTf)_3$) were purchased from Sigma-Aldrich. All solvents were purchased from Scharlau and used after conventional purification.

Synthesis of multiarm stars (H20-PCL, H30-PCL, H40-PCL) (Scheme 1)

5 g of the selected hyperbranched polyester and the required amount of ε-CL (10 mol of ε-CL/eq OH in the HBP) (Table 1) were introduced at room temperature in a two-necked flask with stirring under inert atmosphere. Afterwards, two drops of $Sn(oct)_2$ were added to the solution mixture and the flask was maintained during 24 h in an oil bath thermostatized at 130 ºC. The product was precipitated in diethyl ether. Finally, the polymer was filtered and dried under vacuum at 45 ºC for 2 days. The proportions of the reactants used and some of the characteristics of the multiarm star are collected in Table 1. ^{1}H NMR (400 MHz, $CDCl_3$, ppm) (Figure 1, H20-PCL multiarm star polymer): 4.20 (-CH_2-O-CO-,(A)), 4.0 (-CH_2-OCO-, 5), 3.5 (-CH_2-OH, 5'), 3.30–3.70 (-CH_2-O- and -CH_2-OH, (B)), 2.20 (-CH_2-COO-, 1 and 1'), 1.60–1.40 (-CH_2-, 3, 3' and 4, 4'), 1.30 (-CH_2-, 2 and 2') and 1.05–1.15 (-CH_3, (C)).

Table 1. Preparation data, molecular weight and structural characteristics of the multiarm stars.

Star	*Mol OH*	*Mol CL*	DP_{arm} [a]	PCL_{arms} [b]	*Mn*[c] g/mol)
H20-PCL	0.0464	0.464	15	11	20600
H30-PCL	0.0457	0.457	11	29	38700
H40-PCL	0.0438	0.4381	16	41	73630

[a] Degree of polymerization of the PCL arms (DP_{arm}) determined by ^{1}H NMR spectroscopy
[b] Average number of PCL arms per molecule determined by ^{1}H NMR spectroscopy
[c] Average number molecular weight of the obtained stars calculated by ^{1}H-NMR spectroscopy.

Preparation of epoxy formulations

The mixtures were prepared by adding the required amount of the selected HX-PCL into the CE epoxy resin and gently heating (60 ºC) until it was dissolved and the solution became clear. Then, 0.5 phr (part of initiator per hundred parts of CE/HX-PCL mixture) of ytterbium triflate was added and the resulting solution was stirred and cooled down to -10 ºC to prevent polymerization. Mixtures containing 3 or 5 wt% (by weight) of HX-PCL and a neat formulation with CE and 0.5 phr of ytterbium triflate were prepared. The compositions of the formulations studied are detailed in Table 2. It can be observed that the equivalent amount of added hydroxyl groups is very similar in all cases, increasing slightly with increasing the molecular weight of the core.

Table 2. Composition of the formulations with different weight percentages of HX-PCL. In percentage by total weight (%wt) of the mixture and equivalent ratio (Xeq) in eq/g of mixture of the relevant species: the epoxy group for EC, the active species for $Yb(OTf)_3$ and the OH group for HX-PCL.

Formulation	EC		$Yb(OTf)_3$		OH in HX-PCL	
	X_{eq} (eq/g)	wt%	$X_{eq}\cdot10^{06}$ (eq/g)	wt%	$X_{eq}\cdot10^{06}$ (eq/g)	wt%
Neat	0.0079	99.5	8.0	0.50	0.0	0.0
3% H20-PCL	0.0077	96.5	8.0	0.50	2.3	3.0
5% H20-PCL	0.0075	94.5	8.0	0.50	3.9	5.0
3% H30-PCL	0.0077	96.5	8.0	0.50	2.5	3.0
5% H30-PCL	0.0075	94.5	8.0	0.50	4.1	5.0
3% H40-PCL	0.0077	96.5	8.0	0.50	2.6	3.0
5% H40-PCL	0.0075	94.5	8.0	0.50	4.3	5.0

Characterization

Differential scanning calorimetry

The samples were analyzed on a Mettler-Toledo DSC822e with sample robot, liquid nitrogen cooling and calibrated with indium standards. The samples of the multiarm stars were

analyzed according to the following temperature schedule: 10 min at 100 ºC, cooling at 5 ºC/min from 100 ºC to -100 ºC, 10 min at -100 ºC and heating at 10 ºC/min from -100 ºC to 100 ºC. All the thermal data were determined from the second heating scan. The glass transition temperature (T_g) was determined as the midpoint in the heat capacity jump (ΔC_p) during the glass transition of the polymers, the error in the evaluation is estimated to be approximately ± 1 °C. The melting temperature (T_m) was determined as the temperature peak during melting of the polymers. The fusion enthalpy (Δh_m) was measured using an integral tangential baseline accounting for the changes in heat capacity during the melting transition. The degree of crystallinity was calculated using the fusion enthalpy and taking into account the fraction of PCL in the polymer and the theoretical fusion enthalpy of pure PCL [22].

Non-isothermal curing experiments were performed from 30 to 250 ºC at heating rate of 10 ºC/min to determine the reaction heat. In non-isothermal curing process the degree of conversion by DSC (α_{DSC}) was calculated as follows:

$$\alpha_{DSC} = \frac{\Delta h_t}{\Delta h_{dyn}} \qquad (1)$$

where Δh_T is the heat released up to a temperature T, obtained by integration of the calorimetric signal up to this temperature and Δh_{dyn} is the total reaction heat associated with the complete conversion of all reactive groups obtained dynamically.

Thermogravimetry

Thermogravimetric analyses were carried out in a Mettler TGA/SDTA851e/LF/1100 thermobalance. Samples with an approximate mass of 8 mg were degraded between 30 and 800 ºC at a heating rate of 10 ºC/min in N_2 (100 cm^3/min measured in normal conditions).

Dynamic mechanical analysis

Dynamic mechanical analyses were carried out with a TA Instruments DMA Q800. The samples were cured isothermally in a mould at 80 ºC for 2 h, 2 h at 150 ºC and then post-cured for 1 h at 180 ºC. Single cantilever bending at 1 Hz was performed at 3 ºC/min from 30 to 220 ºC on prismatic rectangular samples (1.5 x 10 x 5 mm^3).

Rheometric analysis

Rheometric measurements were carried out in the parallel plates (geometry of 25 mm) mode with an ARG2 rheometer (TA Instruments, UK, equipped with electrical heated plates, EHP). Complex viscosity (η^*) of the pure multiarm stars was recorded as function of angular frequency (0.05 – 100 rad/s) with a constant deformation of 50% at different temperatures (60, 70 and 80 ºC).

Microhardness

Microhardness was measured with a Wilson Wolpert (Micro-Knoop 401MAV) device following the ASTM D1474-98 (2002) standard procedure. For each material 10 determinations were made with a confidence level of 95%. The Knoop microhardness (*HKN*) was calculated from the following equation:

$$HKN = \frac{L}{A_p} = \frac{L}{l^2 C_p} \qquad (2)$$

where, L is the load applied to the indenter (0.025 Kg), A_p is the projected area of indentation in mm^2, l is the measured length of long diagonal of indentation in mm, C_p is the indenter constant (7.028×10^{-2}) relating l^2 to A_p. The values were obtained from 10 determinations with the calculated precision (95% of confidence level).

Impact resistance

Impact tests were performed at room temperature by means of a Zwick 5110 impact tester according to ASTM D 4508-05 using rectangular samples (25 x 12 x 2.5 mm^3). The pendulum employed had a kinetic energy of 1 J. For each material, 9 determinations were made. The impact strength (*IS*) was calculated from the energy absorbed by the sample upon fracture as:

$$IS = \frac{E - E_0}{S} \qquad (3)$$

where E and E_0 are the energy loss of the pendulum with and without sample respectively, and S is the cross-section of the samples.

Scanning electron microscopy

The fracture area of impacted samples was metalized with gold and observed with a scanning electron microscope (SEM) Jeol JSM 6400 with a resolution of 3.5 nm.

Results and discussion

Synthesis and characterization of HX-PCL multiarm star polymers

The multiarm star polymers synthesized in this work were prepared by the so-called "core first" strategy using Boltorn type polyesters of different weight as the core, which consequently lead to stars with different number of arms. The well-known cationic ring-opening polymerization of ε-CL catalyzed by $Sn(Oct)_2$ was used to grow the arms from the OH terminal groups of the core molecule, as reported previously [23]. The proportion of ε-CL to OH groups in the polymerization reaction was fixed at 10 for all the polymers with the aim to obtain stars with similar arm lengths.

H40-PCL polymers were previously synthesized by the same methodology [24] and it was determined that not all the OH were able to initiate the polymerization of ε-CL and therefore, the number of arms was lower than expected.

To fully characterize the synthesized stars, we determined the degree of polymerization of the arms by ^1H NMR spectroscopy. Figure 1 shows as an example the spectrum of one of the HX-PCL synthesized with the corresponding assignments.

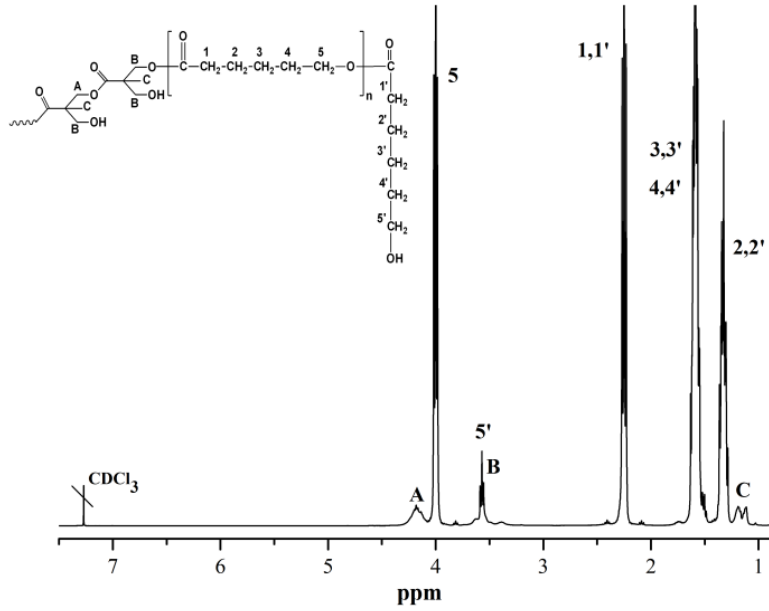

Figure 1. ^{1}H-NMR spectrum in $CDCl_3$ of H20-PCL multiarm star polymer.

Usually, in PCL stars the intensity of the signals **5** and **5'** are used to determine the DP of the arms [14], but in our case the overlapping of signal **5'** with methylene signals of the core molecule (**B**) did not allow to perform in this way the calculation. Thus, we selected the signal at 2.3 ppm, assigned to the methylene protons **1** and **1'** of the repeating and final CL units and the signal at 4 ppm, assigned to the methylene **5** of the repeating unit. The difference between the former and the latter allowed calculating the intensity contribution of the final CL unit. Dividing this value by the intensity of signal **5** and adding the final unit, the *DP* of the PCL arms was calculated for each multiarm star. The results obtained are collected in Table 1. As we can see, although this polymerization has a living character and the feed molar ratio PCL/OH was 10 in all cases, a higher degree of polymerization than expected was achieved. Thus, it can be concluded that some OH groups were not able to initiate the polymerization of ε-CL, which could be attributed to the interaction between OH groups by hydrogen bonding or to topological restrictions which rendered some hydroxyl groups inactive. Thus, the following step was the calculation of the number of arms in each multiarm star. In order to do so, we used the global intensity of the broad signals corresponding to methyl groups of the core molecule (**C**) at 1-1.3 ppm divided by 3 and the intensity of the signal **5**, which corresponds to a methylene in the arms, divided by 2 and by the number of these methylene units in the arm (DP_{arms}-1) and we related them to the number of OH and CH_3 in the core molecule given in the data sheet of Boltorn polyesters. All these calculations are only approximate because the large and highly branched structure of these molecules disturbs the relaxation times of the protons and broadens the signals corresponding to the core structure, but they were comparable to the values obtained by ^{13}C-NMR spectroscopy registered in quantitative conditions. As we can see, the number of arms was lower than the predicted by the number of OH in the HBP core. The number of arms reached a maximum for H30-PCL (29 of 32 possible) and therefore, the arms had a lower *DP*. From the molecular weight of the core and the number of arms and their *DP*, average molecular weights in number were calculated for all the synthesized structures and reported in Table 1.

Table 3 summarizes the most relevant thermal properties of the multiarm stars, determined by calorimetry and thermogravimetry. The values of T_g and T_m were in the range of linear PCL. No T_g attributable to the core structure was evidenced. As we can see, the PCL in the arms maintained its semicrystalline character, even when the DP_{arm} was the lowest. No significant differences were observed between the different multiarm stars giving similar values to those measured for PCL multiarm star with hyperbranched poly(glycidol) as the core and arms of a DP_{arm} near to 10 [14]. Thus, the influence of the core in the crystalline character of the stars seems to be negligible. The low value of the heat capacity jump during the glass transition, indicating a smaller amount of amorphous component than expected, could be explained by the influence of the crystalline domains on the neighboring amorphous regions.

Table 3. Thermal characteristics of HX-PCL multiarm stars determined by DSC and TGA.

Star	T_g (ºC)	ΔC_p (J/g·K)	T_m (ºC)	Δh_m (J/g)	X_c (%)	$T_{5\%}$ [a] (ºC)	T_{max} [b] (ºC)
H20-PCL	-54.5	0.103	50.7	67.5	49.7	302	344
H30-PCL	-57.6	0.099	49.5	65.6	48.3	288	347
H40-PCL	-55.2	0.100	51.8	68.2	50.2	287	352

[a] Temperature of a 5% of weight loss calculated by thermogravimetry.
[b] Temperature of the maximum rate of weight loss.

The results of the thermogravimetric analysis are summarized in Table 3. On increasing the core size, the onset temperature of the decomposition process decreased, but the temperature of the peak of the maximum degradation increased. Figure 2 shows a two-step degradation pattern of the multiarm stars. As we can see, the stars with longer arms present a quicker degradation in the first step. The ester groups in the arms and core structure experiment degradation by a β-elimination process, giving rise to different fragments that are lost in two different processes. The first one would correspond to the degradation of the arms and the second could be related to the degradation of the core molecule. We verified that the thermal degradation of the HBP core occurred at a temperature similar to the second degradation peak of the multiarm star.

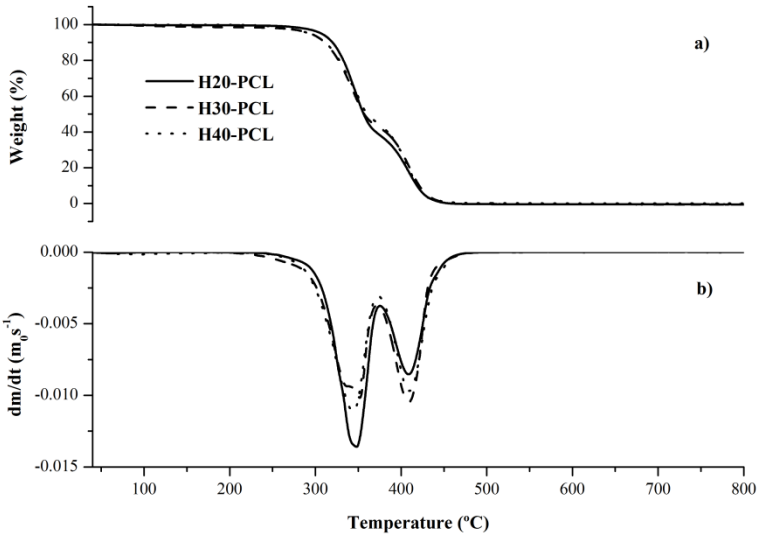

Figure 2. TGA curves of the pure multiarm stars synthesized in N_2 atmosphere

The complex viscosity of the multiarm stars was determined at different temperatures on varying the frequency. All formulations showed a Newtonian behavior, with a constant value of complex viscosity in the selected frequency range. Table 4 collects the complex viscosity value of the HX-PCL stars at temperatures of 60, 70 and 80 ºC. As expected, the viscosity decreased on increasing the temperature. However, there was not a clear dependence on the molecular weight of the star. Thus, although H30-PCL star had an intermediate molecular weight, the viscosity of this star resulted to be the lowest. This fact can be rationalized by its more globular structure, given by its shorter arms in comparison with the other stars. Thus, the more influencing factor seems to be the length of the arms that causes entanglements when the arm length is long enough. The dependence of the viscosity on the arm length was put into evidence in a previous study [25].

Table 4. Viscosities of the multiarm star polymers synthesized measured at different temperatures

Temperature (ºC)	***η**** **(Pa·s)**		
	H20-PCL	**H30-PCL**	**H40-PCL**
60	5.64	5.07	6.78
70	3.78	3.31	4.65
80	2.59	2.26	3.09

Curing of CE resin with different proportions of HX-PCL

Cycloaliphatic epoxy resins can be thermally cured by cationic curing agents, one of the most promising being lanthanide triflates [7]. In a previous work, it was proved that 0.5 phr of lanthanide triflate was enough to assure the complete cure of CE resin [7]. Therefore, 0.5 phr of

$Yb(OTf)_3$ was selected to prepare the formulations studied, which contained a 3 or a 5% of the multiarm star modifiers. Figure 3 shows the effect of the addition of H30-PCL on the curing kinetics determined with DSC.

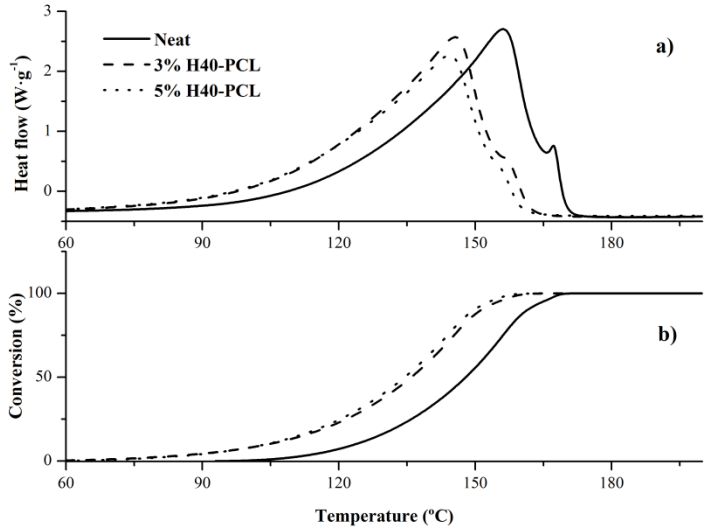

Figure 3. Calorimetric non-isothermal curves and degree of conversion against temperature of CE/H30-PCL mixtures initiated by 0.5 phr of $Yb(OTf)_3$ at 10 ºC/min.

In the figure we can see that the progressive addition of HX-PCL shifted the curves at lower temperature. However, this behavior was not general for all the formulations studied and the addition of a 5% of H20-PCL to the formulation decelerated the curing process in comparison to the mixture with a 3%. A shift of the curves to lower temperatures was previously observed on adding HBPs and multiarm stars with OH groups as chain ends to epoxy formulations [26], which was attributed to the contribution of the AM mechanism to the cationic curing process, favored when hydroxyl groups were present in the reactive mixture [27]. However, in other studies a delaying effect was observed which could be explained on the basis of the higher viscosities of the modified formulations [28].

Calorimetric data of the curing process for all the formulations studied are collected in Table 5. The heat released on curing is mainly due to the opening of epoxy groups because of the ring strain. Thus, the enthalpy per gram of mixture decreased on increasing the proportion of modifier. However, the enthalpy per epoxy equivalent for all the formulations exhibited a value of 70-80 kJ/ee which was similar to that described in the curing of cycloaliphatic epoxy resin [7].

Table 5. Thermal and thermomechanical data of neat and modified formulations with different amounts of HX-PCL.

Formulation	Δh (J/g)	Δh[a] (kJ/ee)	T_{max}[b] (ºC)	$T_{tan\delta,DMA}$[c] (ºC)	E_r[d] (MPa)	$T_{5\%}$[e] (ºC)	T_{max}[f] (ºC)
Neat	576	73	156	150	23.9	255	274
3% H20-PCL	626	82	143	135	15.9	244	273
5% H20-PCL	610	81	147	138	16.7	243	274
3% H30-PCL	567	74	148	146	21.9	247	267
5% H30-PCL	547	73	144	138	16.3	242	262
3% H40-PCL	576	75	145	137	15.6	245	271
5% H40-PCL	558	74	144	132	14.6	244	271

[a] Enthalpies per equivalent of epoxy group.
[b] Temperature of the maximum of the curing exotherm.
[c] Temperature of the maximum of the tan δ.
[d] Storage modulus in the rubbery state at the temperature of tan δ+ 40 ºC
[e] Temperature of a 5% of weight loss calculated by thermogravimetry.
[f] Temperature of the maximum rate of weight loss.

Thermal and thermomechanical properties of the thermosets

The T_g of the cured materials obtained could not be detected by DSC and thus, they were measured by DMTA, which is a more adequate technique for highly crosslinked materials. The effect of the addition of the modifiers in the *tan* δ plot against temperature is represented in Figure 4 and the temperatures of the maximum and storage modulus are collected in Table 5.

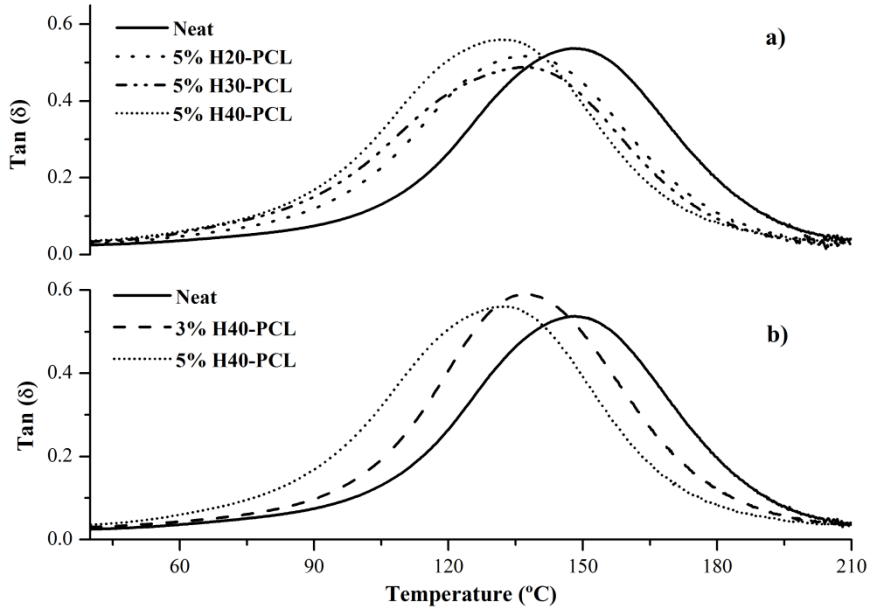

Figure 4. *Tan δ* against temperature at 1 Hz for some of the thermosets obtained.

As we can see, the *tan* δ curves are unimodal and no relaxations were observed at low temperature. Both facts evidenced the homogeneous character of the modified thermosets. The high solubility of PCL in epoxy matrices and the covalent linkage of terminal hydroxyl groups to the polyether structure due to the concurrence of the AM mechanism were responsible for this homogeneity, which will be further confirmed by SEM inspection.

On increasing the molecular weight of the multiarm star in the material (Figure 4a) the *tan* δ curve shifted to slightly lower temperatures as a consequence of the increase in the flexibility of the structure on increasing the size of the molecule. Moreover, on increasing the proportion of modifier in the thermoset, the T_g generally decreased, and this decrease was greater for the H40-PCL modified formulations, as it can be seen in Figure 4b. The reduction in the *tan* δ temperature could be related to the presence of hydroxyl groups as chain ends in the star, which led to a higher contribution of the AM mechanism and therefore to chain transfer processes that finally reduced the crosslinking density. Indeed, in Table 5 it is shown that the addition of the modifier decreased the modulus after relaxation, which was related to the effective crosslinking density. Also, the interpenetration of the arms of the star in the epoxy network increased the plasticization of the material, which also contributed to reduce the T_g. There was no much effect on changing the molecular weight of the star, but the rubbery modulus was generally reduced on increasing the proportion of the modifier.

The thermal stability of the materials obtained was tested by thermogravimetry and the most significant data are collected in Table 5. The complex shape of the curves is represented as an example in Figure 5 for the formulations containing a 5% of HX-PCL.

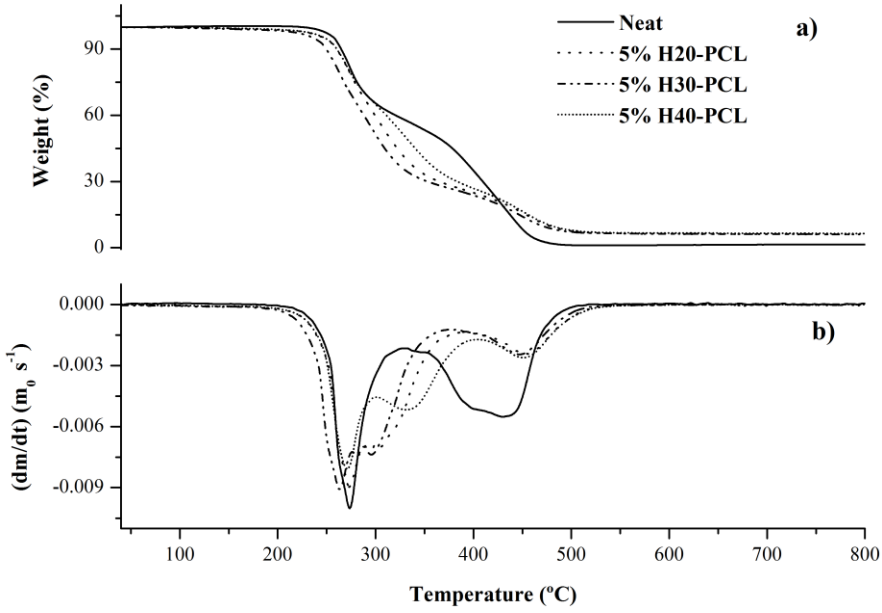

Figure 5. TGA and derivative curves of the thermosets modified with a 5% of HX-PCL

The neat and modified thermosets show highly complex degradation processes, with three different degradation steps. First, it can be observed that the presence of the multiarm stars decreases the onset of the degradation process because of the breakage of polyester structures

in the multiarm star through a *β*-elimination process. Comparable results were obtained in the modification of DGEBA with PGOH-PCL, although the use in the present case of a cycloaliphatic epoxy resin with an ester group in the structure leads to lower $T_{5\%}$ temperatures and a more notable effect than in the previous study [21]. The materials prepared fall on the definition of reworkable thermosets, proposed by Ober et al. [29]. The term "reworkable" applied to epoxy thermosets does not mean that they can be recycled but it refers to the ability of the network structure to break-down under controlled conditions in order to remove it from the substrate. The reworkability in thermosets is usually accomplished by the introduction of ester groups in the network. In our case, both the resin and the multiarm stars contained a great number of ester groups, which helped to reduce the initial degradation temperature. However, if we compare the $T_{5\%}$ of the thermosets and pure HX-PCL stars we can observe that the initial degradation temperature was lower for thermosets contrary to that expected. The explanation to this unexpected behavior could be found in the presence of $Yb(OTf)_3$ in the thermoset that catalyzed the *β*-elimination process as demonstrated previously [30]. In a previous study on the modification of thermally cationic cured CE resins initiated by benzyl tetrahydro thiophenium hexafluoroantimonate, higher thermal stability was observed for the unmodified formulation and for the material containing a 31% of linear PCL with a molecular weight of 4000 [31]. Thus, it is clear that the use of $Yb(OTf)_3$ is the most adequate initiator to get reworkable epoxy thermosets, but it is detrimental for materials with higher thermal stability requirements.

Mechanical properties of the HX-PCL modified thermosets

Several authors reported a toughness improvement of cationically cured epoxy resins modified with diols [32], some of them being poly(ε-caprolactone) diols [31]. Usually, they reported a softening of the polymer with the subsequent reduction of the T_g. The use of hydroxyl terminated PCL multiarm stars was proposed in order to improve toughness without compromising hardness and T_g of the final material, due to the multifunctionality of hydroxyl terminated dendritic structures. Up to now there are no reported data on the effect of the use of PCL stars with different molecular weight and different number of arms in impact strength values.

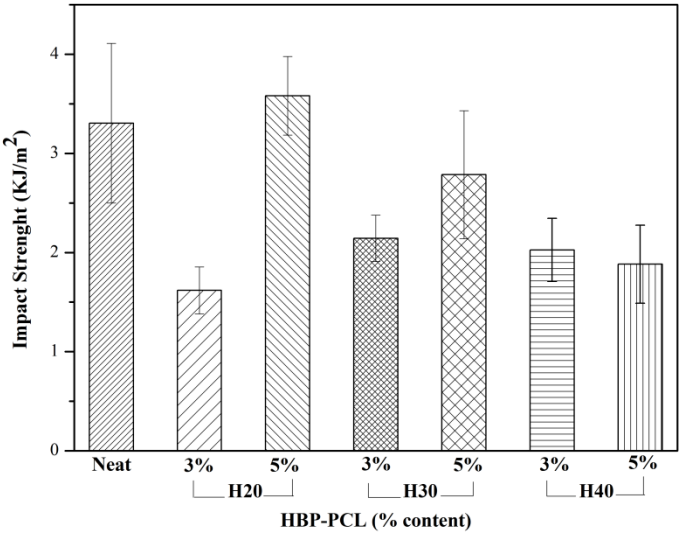

Figure 6. Impact strength values for the thermosets obtained.

The effect of adding HX-PCL in different proportions to the formulations in the impact strength is shown in Figure 6. It was possible to observe that the modification of CE with star topologies did not improve this value in comparison to the neat material and only a 5% of H20-PCL seems to be slightly advantageous. In a previous work, we compared the effect of a linear or star PCL in the impact resistance of DGEBA thermosets cured by $Yb(OTf)_3$ [21]. In that case the addition of the PGOH-PCL star was advantageous, leading to higher improvements and a 75% increase in the impact resistance, in reference to the neat material, was obtained for the modified thermoset containing a 10 wt.% of the PCL star. This was attributed to the high capacity of the arms of the star to interpenetrate into the epoxy network which increased the number of flexible points capable of undergoing plastic deformation. However, in that case the number of arms was about 100, the molecular weight was higher, the core of the molecule was more flexible, constituted by aliphatic polyether structures and the proportion of modifier was higher.

Indentation hardness measurements have proven to be useful in rating coatings on rigid substrates for their resistance to mechanical abuse, such as that produced by blows, gouging and scratching. As we can see in Figure 7, the addition of HX-PCL decreased the hardness but without any regular trend. Probably, the plasticizing effect exerted by the flexible stars added could justify this behavior. The final microhardness of the materials is a compromise between different factors such as: degree of crosslinking, molecular weight and length of the arms. However, it can be said that the addition of a 3% of H30-PCL or a 5% of H40-PCL to the formulation did not worsen significantly the hardness of the material.

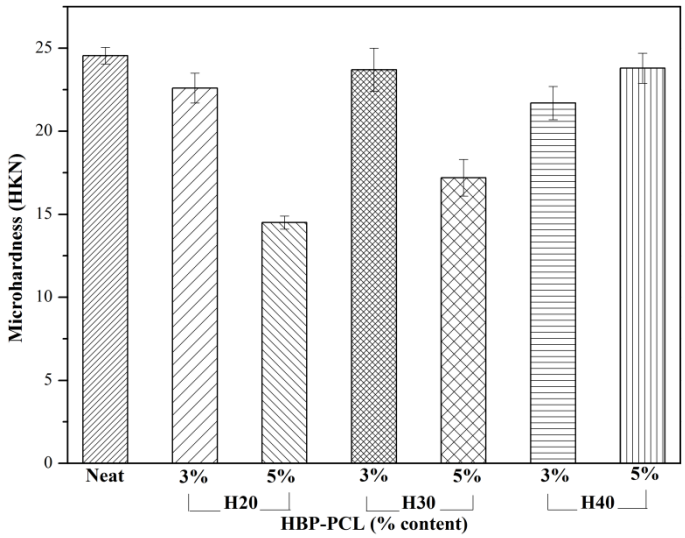

Figure 7. Knoop microhardness values for the thermosets obtained.

Fractography by SEM

The fracture surfaces after impact tests were examined by SEM to further investigate the morphology of the materials and the most representative micrographs are shown in Figure 8.

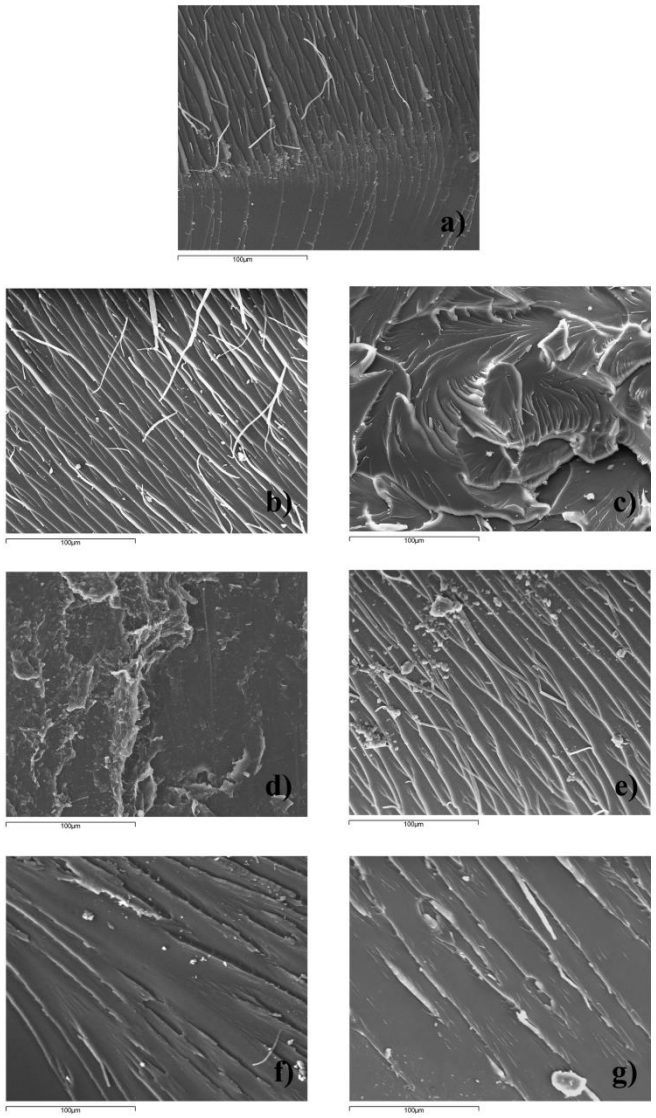

Figure 8. SEM micrographs of the fracture surface of the materials obtained from ECH formulations: a) Neat (x 500) and modified (x 500) with b) 3% H20-PCL; c) 5% H20-PCL; d) 3% H30-PCL; e) 5% H30-PCL; f) 3% H40-PCL; g) 5% H40-PCL.

As can be seen, all the micrographs presented a homogeneous appearance without any sign of phase separation, according to DMTA results, due to the good compatibility of HX-PCL and the epoxy matrix. The smooth glassy fractured surface, with little cracks, of the materials modified with H40-PCL (Figure 8 f and g) accounts for its low impact strength. In contrast, the fracture surface of the materials with a 5 wt% of H20-PCL (Figure 8 c) was much rougher than that of the unmodified thermoset, suggesting that the impact specimens broke more yieldingly as it occurred. This toughness improvement could be explained in terms of *in situ* reinforcing and toughening mechanism.

Conclusions

Following a “core-first” strategy, multiarm star copolymers were obtained by a cationic ring-opening polymerization of *ε*-caprolactone from hyperbranched Boltorn type polyesters of different molecular weight. ^{1}H-NMR spectroscopy allowed us to determine the number and length of the PCL arms. Viscosity and thermal characteristics of these polymers were also determined.

The multiarm star polymers obtained were added as modifiers in the curing of cycloaliphatic epoxy resin using $Yb(OTf)_3$ as cationic initiator. The addition of these modifiers to the reactive mixture slightly accelerated the curing.

The *tan* δ of the modified materials was lower than that of the neat thermosets but higher than 130 ºC and the shape of these curves demonstrated their homogeneous character as proved by SEM inspection of the fracture surfaces.

The thermal degradation curves of the materials containing HX-PCL stars were quite complex and the materials were more degradable than pure multiarm-stars due to the presence of $Yb(OTf)_3$, which catalyzed the *β*-elimination process. These modified thermosets can be regarded as reworkable.

Impact strength was only slightly improved in the materials with a 5% of H20-PCL. The inspection by SEM of these materials confirmed its more yielding fracture.

Acknowledgements

The authors would like to thank MINECO (MAT2011-27039-C03-01 and MAT2011-27039-C03-02) and to the Comissionat per a Universitat i Recerca de la Generalitat de Catalunya (2009-SGR-1512) for the financial support. M.F. acknowledges the grant BES-2009-025226. Perstorp is acknowledged for kindly providing Boltorn HBPs.

References

[1] Lee SM (1988) In: May CA (ed) Epoxy Resins. Chemistry and Technology, 2on edn. Marcel Dekker Inc, New York

[2] Crivello JV, Lam JHW (1977) Macromolecules 10:1307-1315

[3] Crivello JV (1983) Ann Rev Mater Sci 13:173-190

[4] Crivello JV (1999) J Polym Sci Part A: Polym Chem 37:4241-4254

[5] Endo T, Sanda F (1996) Macromol Symp 107:237-242

[6] Cervellera R, Ramis X, Salla JM, Mantecón A, Serra A (2006) J Appl Polym Sci 102:2086-2093

[7] Mas C, Serra A, Mantecón A, Salla JM, Ramis X (2001) Macromol Chem Phys 202:2554-2564

[8] Sangermano M, Malucelli G, Bongiovanni R, Priola A, Harden A (2005) Polym Int 54:917-921

[9] Sangermano M, Priola A, Malucelli G, Bongiovanni R, Quaglia A, Voit B, Ziemer A (2004) Macromol Mater Eng 289:442-446

[10] Däbritz F, Voit B, Naguib M, Sangermano M (2011) Polymer 52:5723-5731

[11] Foix D, Ramis X, Sangermano M, Serra A (2012) J Polym Sci Part A: Polym Chem 50:1133-1142

[12] Liu Y, Wang Y, Jing X (2005) J Polym Mater 22:159-168

[13] Voit B, Lederer A (2009) Chem Rev 109:5924-5973

[14] Morell M, Lederer A, Ramis X, Voit B, Serra A (2011) J Polym Sci Part A: Polym Chem 49:2395-2406

[15] Meng Y, Zhang XH, Du BY, Zhou BX, Zhou X, Qi GR (2011) Polymer 52:391-399

[16] Morell M, Foix D, Lederer A, Ramis X, Voit B, Serra A (2011) J Polym Sci Part A: Polym Chem 49:4639-4649

[17] Burgath A, Sunder A, Neuner I, Mülhaupt R, Frey H (2000) Macromol Chem Phys 201:792-797

[18] Guo Q, Groeninckx G (2001) Polymer 42:8647-8655

[19] Fan W, Wang L, Zheng S (2009) Macromolecules 42:327-336

[20] Hameed N, Guo Q, Hanley T, Mai YW (2010) J Polym Sci Part B: Polym Phys 48:790-800

[21] Morell M, Ramis X, Ferrando F, Serra A (2011) Polymer 52:4694-4702

[22] Van Krevelen DW (1994) Properties of Polymers, 3rd edn. Elsevier, Amsterdam

[23] Trollsås M, Hedrick JL, Mecerreyes D, Dubois Ph, Jerome R, Ihre H, Hult A (1997) Macromolecules 30:8508-8511

[24] Chen S, Zhang X-Z, Cheng S-X, Zhuo R-X, Gu Z-W (2008) Biomacromolecules 9:2578-2585

[25] Acebo C, Fernández-Francos X, Ferrando F, Serra A, Salla JM, Ramis X (2013) React Funct Polym 73:431-441

[26] Morancho JM, Cadenato A, Ramis X, Fernández-Francos X, Salla JM (2010) Thermochim Act, 510:1-8

[27] Kubisa P, Penczek S, (2000) Prog Polym Sci 24:1409-1437

[28] Foix D, Khalyavina A, Morell M, Voit B, Lederer A, Ramis X, Serra A (2012) Macromol Mater Eng 297:85-94

[29] Chen J-S, Ober CK, Poliks MD, Zhang Y, Wiesner U, Cohen C (2004) Polymer 45:1939-1950

[30] González L, Ramis X, Salla JM, Mantecón A, Serra A (2007) Polym Degrad Stab 92:596-604

[31] Lützen H, Bitomsky P, Rezwan K, Hartwig A (2013) Eur Polym J 49:167-176

[32] Hartwig A, Koschek K, Lühring A, Schorsch O (2003) Polymer 44:2853-2858

Photocuring of cycloaliphatic epoxy formulations using polyesters with mutiarm star topology as additives

Marjorie Flores,[1] Xavier Fernández-Francos,[1*] Xavier Ramis,[2] Marco Sangermano,[3] Francesc Ferrando,[4] Àngels Serra[1]

[1] Department of Analytical and Organic Chemistry, Universitat Rovira i Virgili, C/ Marcel·lí Domingo s/n, 43007, Tarragona, Spain.
[2] Thermodynamics Laboratory, ETSEIB Universitat Politècnica de Catalunya, Av. Diagonal 647, 08028, Barcelona, Spain.
[3] Dept. of Material Science and Chemical Engineering, Politecnico di Torino, C.so Duca degli Abruzzi 24, 10129 Torino, Italy
[4] Department of Mechanical Engineering, Universitat Rovira i Virgili, C/ Països Catalans, 26, 43007, Tarragona, Spain.

Abstract

Multiarm star polyesters have been synthesized by growing poly(ε-caprolactone) arms from hyperbranched polyesters cores of different molecular weight and used as polymeric modifiers in UV-curable cationic formulations based on a biscycloaliphatic epoxy resin. The effect of the multiarm stars on the curing kinetics has been investigated by real-time FTIR. The thermal-mechanical properties of the photocured thermosets have been studied with calorimetry and dynamomechanical and thermogravimetric analysis. Impact strength tests have been performed to assess their effect on the toughness of the cured materials. An accelerative effect of these modifiers has been observed as a consequence of the participation of the hydroxyl groups in the cationic curing of epoxides. A decrease in the glass transition is observed, as a consequence of the incorporation of the modifiers into the network structure, leading to homogeneous materials.

Keywords: *Star polymers, hyperbranched, epoxy resin, photocuring, thermosets.*

Introduction

The widespread use of thermosetting epoxy resins in many industrial applications such as coatings, adhesives, moulding compounds or composites, can be explained by a combination of attractive properties, such as their thermomechanical behaviour, their chemical and environmental stability and their good processability [1]. In addition, they are highly versatile because of the great variety of available curing agents and organic and inorganic modifiers and fillers that can be used to improve their properties [2]. Bisphenol A resins are by far the most widely used epoxy resins, but cycloaliphatic epoxy resins possess some superior properties such as high arc resistance, low viscosity, high heat deflection temperatures and excellent weatherability [1], which make them a better choice depending on the application, such as photocurable cationic formulations [3-6]. However, a major drawback of cycloaliphatic epoxy resins is their brittleness, caused to their high crosslinking density and the rigidity of the polymeric backbone, which may place strong restrictions and design constraints in their application [7].

Liquid rubbers and thermoplastics were firstly used as additives to increase the fracture toughness of thermosets but the thermomechanical properties and the processability is greatly compromised [8]. Recently, hyperbranched polymers (HBP) have been proposed as alternative polymeric modifiers for thermosetting formulations [9-13]. The dendritic structure of HBPs makes these modifiers very promising in terms of processability because of the low entanglement that leads to low viscosities in comparison to linear polymers [14]. By partial or complete modification of their numerous hydroxyl terminal groups, it is possible to tune their interaction with the matrix

or facilitate their covalent linkage to the epoxy matrix, which can lead to phase-separated or homogeneous morphologies [15, 16]. The presence of non-modified reactive groups in the HBP shell can improve the interaction in the interphase between the separated particles and the matrix.

The reports on the toughening of cycloaliphatic epoxides are scarce and the field is still open for research. A variety of modifiers such as high viscosity CTBN rubbers [17, 18], poly(ethylenephtalate) [19], inorganic fillers such as nanosize silicon dioxide [20] or carbon nanotubes [21], oligofluorosiloxanes [22], reactive copolymers [23] or multiarm hyperstars [24] have been tried with different degrees of success. We recently reported a two-fold increase in the impact strength of thermally cured cycloaliphatic epoxides using a hyperbranched poly(glycidol) partially modified with end undecenoyl chains [16]. The use of reactive hyperbranched polymers in the UV-curing of cycloaliphatic epoxides has also been reported [12, 25-27], producing in most cases a toughness increase at the expense of reducing the glass transition temperature T_g and the elastic modulus.

Multiarm stars are another class of dendritic polymers that can be used as polymeric modifiers for epoxy thermosets, with similar advantages to those of hyperbranched polymers, because of their compact dendritic structures. Karger-Kocsis et al. [28] reported a significant toughness increase in vinyl ester-urethane hybrid formulations using hyperbranched star-like polyethers as modifiers. Morell et al. synthesized multiarm stars with poly(ε-caprolactone) arms and hyperbranched poly(glycidol) core and used them in cationic epoxy formulations, which resulted in a significant increase in toughness [29]. Acebo et al. [30] reported the synthesis of multiarm stars with poly(ε-caprolactone) arms and hyperbranched poly(ethyleneimine) core and their use in anionic epoxy formulations, showing a complex effect on the impact strength depending on the arm length and core size. Multiarm stars with hyperbranched aromatic-aliphatic polyester core and poly(methyl methacrylate-*b*-hydroxyethyl methacrylate) arms with different copolymeric sequence and composition have been used as polymeric modifiers in UV-cured and thermally cured biscycloaliphatic formulations [24], but a decrease in both the strain at break and elongation at break were reported.

Recently, we modified Boltorn^{TM} type hyperbranched polyesters of different core size by growing poly(ε-caprolactone) arms (HX-PCL) [31], and used them as polymeric modifiers in thermal cationic biscycloaliphatic diepoxide formulations. It was shown that the curing kinetics was accelerated by the modifiers because of the participation of reactive hydroxyl groups in the curing, but the mechanical properties could not be improved. In the present paper, we report the use of these modifiers in cationic UV-curable formulations based on a biscycloaliphatic epoxy resins (CE). The photocuring of these formulations has been monitored by real-time FTIR. The thermal and dynamomechanical properties have been measured using differential scanning calorimetry (DSC), thermogravimetric analysis (TGA), and dynamic-mechanic thermal analysis (DMTA). Mechanical tests have been performed to determine the impact strength of the resulting thermosets. The morphology of the materials has also been investigated by electron microscopy (SEM).

Experimental section

Materials

The hyperbranched polymers Boltorn H20 (Mw = 1747 g/mol, 16 OH), Boltorn H30 (Mw = 3500 g/mol, 32 OH) and Boltorn H40 (Mw = 7316 g/mol, 64 OH) were donated by Perstorp and were used as received. ε-Caprolactone (ε-CL), distilled under vacuum, tin (II) 2-ethylhexanoate ($Sn(oct)_2$), bis-cycloaliphatic diepoxy resin 3,4-epoxycyclohexylmethyl 3,4-epoxycyclohexyl carboxylate (CE, 126 g/eq) and triphenylsulfonium hexafluoroantimonate (PI, $[Ph_3S]^+$ $[SbF_6]^-$) were purchased from Sigma-Aldrich.

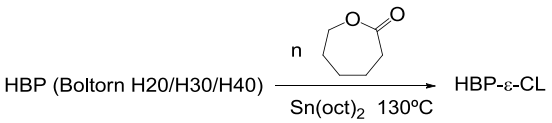

Scheme 1. Synthesis of multiarm stars with Boltorn cores and poly(ε-caprolactone) arms.

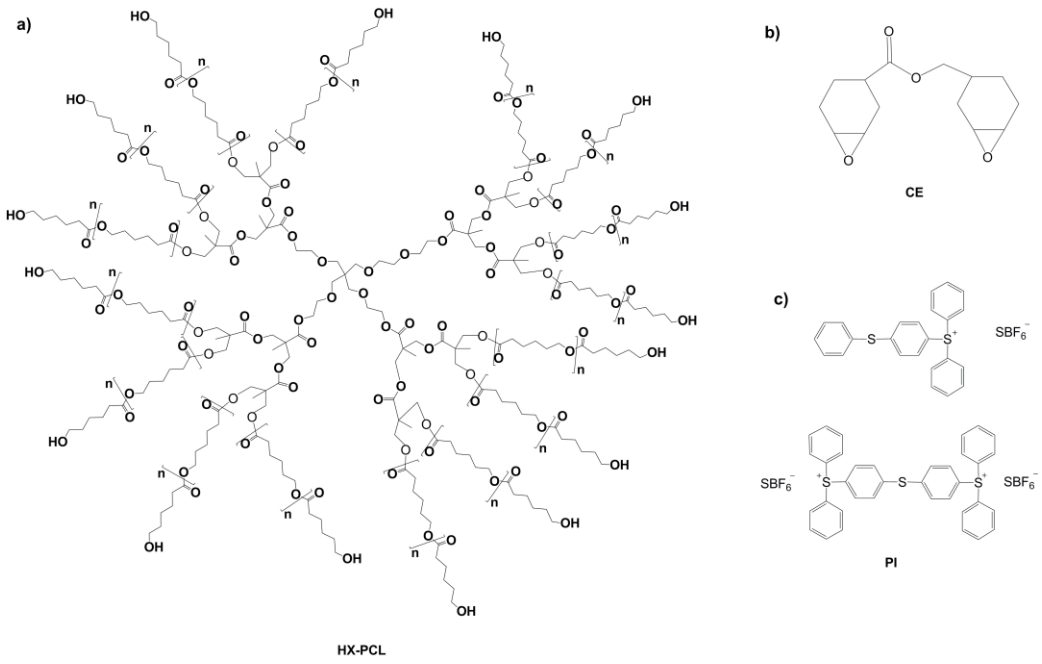

Scheme 2. Chemical structures of a) Idealized multiarm star, b) bis-cycloaliphatic diepoxy resin (CE) and c) triphenylsulfonium hexafluoroantimonate (PI).

Synthesis of multiarm stars (H20-PCL, H30-PCL, H40-PCL) (Scheme 1)

5 g of the HBP and the required proportion of ε-CL in order to obtain 10 eq ε-CL per each eq OH of HBP (ratio 1:10 eqOH:ε-CL) (Table 1) were mixed at room temperature in a two-necked flask with stirring under inert atmosphere. Afterwards, the initiator, ($Sn(oct)_2$), was added to the solution mixture and the flask was immersed in an oil bath thermostatized at 130 ºC during

24 h. Later, the product was precipitated in ethyl ether. Finally, the polymer was filtered and dried under vacuum at 45 ºC for 2 days. ^{1}H NMR (400 MHz, $CDCl_3$, ppm) (Fig. 1): 4.20 (-CH_2-O-CO-,(A)), 4.0 (-CH_2-OCO-, 5), 3.5 (-CH_2-OH, 5'), 3.30–3.70 (-CH_2-O- and -CH_2-OH, (B)), 2.20 (-CH_2-COO-, 1 and 1'), 1.60–1.40 (-CH_2-, 3, 3' and 4, 4'), 1.30 (-CH_2-, 2 and 2') and 1.05–1.15 (-CH_3, (C)).

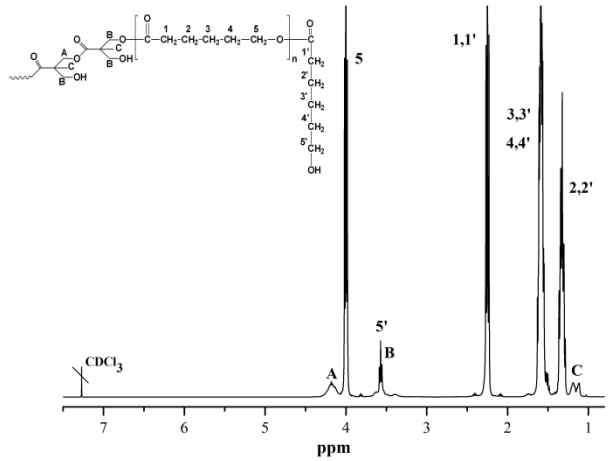

Figure 1. ^{1}H RMN spectrum of Boltorn H20 core modified with poly(ε-caprolactone) arms (H20-PCL) in $CDCl_3$.

Sample preparation

Mixtures were prepared by adding the required amount of HBP (5, 10 and 15 parts per hundred parts of resin, phr) into the epoxy resin (CE) and gently heating (*ca.* 80 ºC) until it was dissolved and the solution became clear. Then, 1 phr of the PI were added in reference to the CE resin (see Table 1) and the solution was homogeneized by mechanical stirring.

Table 1. Composition of the formulations. In percentage by total weight (%wt) of the mixture and equivalent ratio (Xeq) in eq/g of mixture of the relevant species.

Formulation	*CE*		*HX-PCL*		*PI*	
	X_{eq} ($x10^{-3}$)	*Wt%*	X_{eq} ($x10^{-4}$)	*Wt%*	X_{eq} ($x10^{-5}$)	*Wt%*
Neat	7.86	99.01	0.00	0.00	1.78	0.99
H20-PCL (%)						
5%	7.49	94.34	0.37	4.72	1.69	0.94
10%	7.15	90.09	0.70	9.01	1.62	0.90
20%	6.56	82.64	1.28	16.53	1.49	0.83
H30-PCL (%)						
5%	7.49	94.34	0.39	4.72	1.69	0.94
10%	7.15	90.09	0.75	9.01	1.62	0.90
20%	6.56	82.64	1.37	16.53	1.49	0.83
H40-PCL (%)						
5%	7.49	94.34	0.41	4.72	1.69	0.94
10%	7.15	90.09	0.78	9.01	1.62	0.90
20%	6.56	82.64	1.44	16.53	1.49	0.83

The samples were photocured by exposing to UV radiation in a UV oven (Vilber Lourmat Bio-Link Crosslinker) equipped with 6 lamps of 8 W each emitting 365 nm wavelength UV radiation.

The samples for dynamic-mechanical thermal analyses (DMTA) (30 x 8 x 1 mm^3) were prepared by pouring the liquid formulation into a polypropylene mold with a 1 mm Teflon spacer. A dose of 12 J/cm^2 was applied on both sides of the samples in order to ensure complete activation of the photoinitiator.

The samples for impact strength tests (25 x 12 x 2.5 mm^3) were photocured in a polypropylene mold with a 2.5 mm Teflon spacer. A dose of 36 J/cm^2 on each side of the samples was used in this particular case.

After demoulding, the samples were subsequently postcured during 2 hours at 180 ºC. Afterwards, the samples were polished to prismatic rectangular shape before the analyses.

Characterization

^{1}H NMR 400 MHz spectra were obtained using a Varian Gemini 400 spectrometer with Fourier Transformed. ^{1}H-NMR spectra were acquired in 1 min and 16 scans with a 1.0 s relaxation delay (D1). $CDCl_3$ was used as solvent and TMS as internal standard.

The kinetics of photopolymerization was determined by real-time (RT) FT-IR spectroscopy, employing a Thermo-Nicolet 5700 FTIR device. Epoxy group conversion was followed in real-time upon UV exposure, by monitoring the decrease in the absorbance due to epoxy groups in the region 760–780 cm^{-1}. A medium pressure mercury lamp equipped with an optical guide was used to induce the photopolymerization (light intensity on the surface of the sample was about 5 mW/cm^{-2}). Variation in the experimental conditions (light intensity, humidity and temperature) caused slight differences in the kinetic curves. For this reason all the conversion curves contained in the figures were performed on the same day and under the same conditions and thus good reproducibility was obtained. All the polymerization reactions were performed at room temperature at constant humidity (25–30%). The conversion during photocuring ($\alpha_{UV,FT\text{-}IR}$) was calculated using the following equation:

$$\alpha_{UV,FT-IR} = 1 - \frac{\overline{A^t}}{\overline{A^0}} \qquad (1)$$

where A^t is the normalized absorbance of the epoxy band at a given time and A^0 is the initial absorbance.

DMTA analyses were carried out with a TA Instruments DMA Q800. Single cantilever bending was performed on prismatic rectangular samples. The apparatus was operated dynamically, at 2 ºC/min, from 40 to 250 ºC. The frequency of application of the force was 1 Hz and the amplitude of the deformation 10 μm. The T_g value was assumed as the maximum of the loss factor curve ($tan\ \delta$).

Rheometric measurements were carried out in the parallel plates (geometry of 25 mm) mode with an ARG2 rheometer (TA Instruments, UK, equipped with electrical heated plates, EHP). Complex viscosity (η^*) of the pure multiarm stars was recorded as function of angular frequency (0.05 – 100 rad/s) with a constant deformation of 50 % at 60 ºC.

Thermogravimetric analysis (TGA) was performed with a METTLER TGA/SDTA 851 instrument between 30 and 800 ºC at a heating rate of 10 ºC/min in air.

The cryofracture of the specimens were done under liquid nitrogen. Afterwards, the samples were metalized with gold and observed by SEM using a scanning electron microscopy Jeol JSM 6400.

The impact test was performed at room temperature by means of a Zwick 5110 impact tester, according to ASTM D4508-10 using rectangular samples. The pendulum employed had a kinetic energy of 1 J.

Results and discussion

Synthesis and characterization of HX-PCL multiarm star polymers

Although the synthesis and characterization of the multiarm star polymers used in this work have already been described in detail [31], a short summary of their relevant characteristics is shown in Table 2. As observed, H20-PCL and H40-PCL stars have a lower number of arms than expected from the number of OH terminal groups in the HBP, resulting in a longer arm length than that of H30-PCL. Table 2 also shows that, in spite of the different arm length and molecular weight, all the stars are semicrystalline solids at room temperature, with a T_g about -55 ºC, a degree of crystallinity X_C of *ca*. 50% and a melting peak temperature T_m of *ca*. 50 ºC. The viscosity of the multiarm stars depends on both the degree of polymerization of the poly(ε-caprolactone) arms and the molecular weight, being the former the most relevant factor.

Table 2. Summary of structural characteristics and properties of the multiarm stars [31].

Star	DP_{arm} [a]	PCL_{arms} [b]	*Mn*[c] (g/mol)	$\eta^*_{60ºC}$ (Pa·s)	T_g (ºC)	T_m (ºC)	X_c (%)
H20-PCL	15	11	20600	5.64	-54.5	50.7	49.7
H30-PCL	11	29	38700	5.07	-57.6	49.5	48.3
H40-PCL	16	41	73630	6.78	-55.2	51.8	50.2

[a] Degree of polymerization of the PCL arms (DP_{arm}) determined by ^{1}H NMR spectroscopy
[b] Average number of PCL arms per molecule determined by ^{1}H NMR spectroscopy
[c] Average number molecular weight of the obtained stars calculated by ^{1}H-NMR spectroscopy.

Photocuring kinetics of CE resin with different proportions of HX-PCL

Cationic photocuring and thermal curing of CE resin with a variety of polymeric modifiers has been studied in the past [12, 16, 24, 26, 27, 32, 33]. The presence of reactive hydroxyl groups in the mixture accelerates the photocuring process because of their participation in the cationic ring-opening of epoxides by the activated monomer (AM) mechanism [34, 35]. Even the

absorbed environmental moisture is capable of accelerating the curing process, making it possible to reach complete cure even at room temperature in dark conditions after photoirradiation [3]. However, one must take into account the concurrence of other factors that have the opposite effect, such as 1) the availability of the reactive hydroxyl groups, depending on the modifier composition, topology, structure and molecular weight, 2) the mobility of the reactive species formed by reaction of the polymeric modifiers and 3) the presence of ether groups in the modifier structure. Therefore, some possibilities arise: a clear accelerative effect can been observed [12, 26], a clearly decelerative effect [24, 32] or a complex combined effect depending on the amount of polymeric modifier [33].

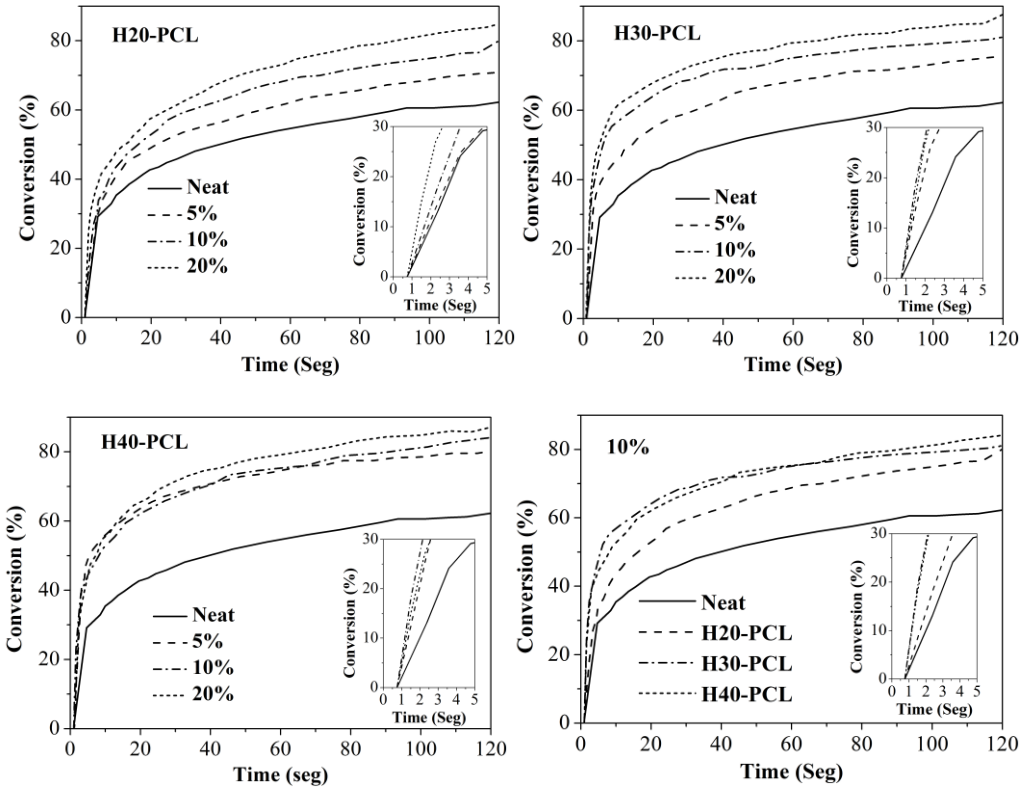

Figure 2. FTIR curves representing conversion as function of irradiation time for neat CE resins and modified formulations with different proportions of H20-PCL, H30-PCL and H40-PCL and the comparison for the formulations containing a 10% of all the modifiers

Figure 2 show that the addition of H20-PCL produces a gradual accelerative effect on the photocuring of the CE resin. This accelerative effect was also observed in the cationic thermal curing of CE with ytterbium triflate [31]. It is hypothesized that the catalytic effect of reactive hydroxyl groups is predominant over other structural and composition factors. The addition of H30-PCL and H40-PCL also produces an accelerative effect, but the effect is less gradual as the molecular weight of the modifier increases. If the effect of the different modifiers is compared, it is observed that H40-PCL and H30-PCL produce a stronger effect than H20-PCL, which can be rationalized by 1) the higher amount of available hydroxyl groups of H40-PCL in comparison with H20-PCL in the former case and 2) the shorter arm length of H30-PCL in comparison with H20-PCL in the latter case, leading to lower mobility restrictions.

Table 3 compares the extent of the photocuring process of the different formulations. It is observed how on increasing the amount of modifier, the degree of conversion achieved increases. This effect is more gradual and pronounced with H20-PCL, in agreement with the effect in the curing kinetics, as discussed above. The samples are not able to reach complete curing because of the occurrence of vitrification, which makes it necessary a subsequent thermal postcuring to complete the polymerization. Decker et al. showed that a dark postcuring at room temperature under high relative humidity conditions could lead to complete conversion of epoxy groups [3], because of the absorption of water and its participation via the AM mechanism, resulting in significant chain termination and transfer processes and a reduction in the crosslinking density of the cured material. In this case, though, the samples for DMA and TGA analysis were postcured shortly after photoirradiation, following the cure schedule described in section 0, in order to overcome vitrification and achieve complete curing, and to maximize the crosslinking density and the T_g.

Table 3. Conversion of epoxy groups from FTIR spectra after photocuring ($\alpha_{UV,FTIR}$), thermo mechanical data and temperature of initial degradation of the prepared thermosets.

Sample	$\alpha_{UV,FTIR}$ *(%)*	$T_{tan\ \delta}$ *(ºC)*	$T_{5\%}$ *(ºC)*
Neat	63	186	324
H20-PCL (%)			
5	72	168	298
10	80	162	301
20	85	145	324
H30-PCL (%)			
5	75	152	309
10	80	151	292
20	88	150	291
H40-PCL (%)			
5	80	173	265
10	84	153	302
20	87	146	298

Thermal and thermomechanical properties of the thermosets

The glass transition temperature of the cured materials was determined by DMTA, as the peak temperature of *tan* δ. The plot of *tan* δ against temperature is represented in Figure 3 and the peak temperature is reported in Table 3**.**

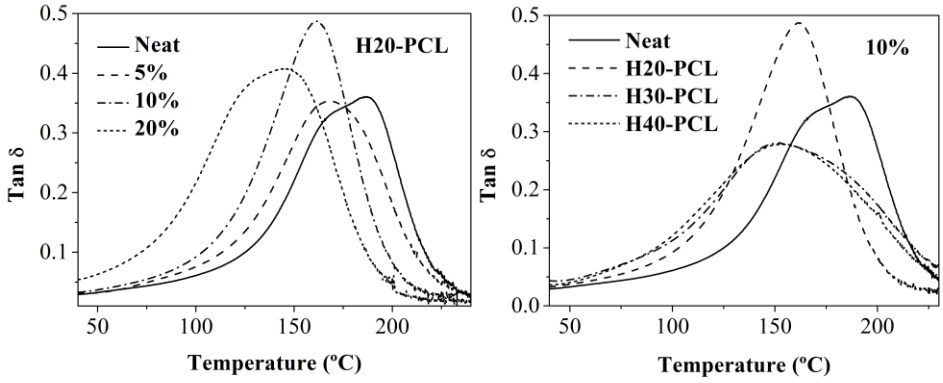

Figure 3. Tan δ against temperature for the neat and modified materials with different proportions of H20-PCL (left) and 10 % of all the modifiers (right).

The addition of either modifier produces a gradual decrease in glass transition temperature, as illustrated for H20-PCL in Figure 3. It is observed a shift down to lower temperatures of the *tan δ* peak, which is an indicative of the mechanical relaxation of the network and is closely related with the glass transition. This is not as clearly deduced from the data shown in Table 3. Indeed, the *tan* δ curves broadens with the addition of the modifiers, especially H30-PCL and H40-PCL, which makes it difficult to determine a nominal value of T_g and puts into evidence a somewhat heterogeneous network structure with a disperse distribution of crosslinking density that may be caused by the covalent incorporation of the modifier into the network structure.

A reduction in glass transition temperature had already been observed in a previous work on the modification of CE with smaller amounts of H20-PCL, H30-PCL and H40-PCL cured with ytterbium triflate [31]. Also similar results were obtained for cationic cured DGEBA formulations using a multiarm star with a hyperbranched poly(glycidol) core [29], and using H30 as modifier [36]. First of all, one must take into account the high solubility of PCL in epoxy matrices, especially in cycloaliphatic formulations, which makes it possible to obtain homogeneous materials. Second, the terminal hydroxyl groups of the PCL arms can form covalent linkages with the network structure due to their participation in the cationic curing of epoxides by the AM mechanism [34]. When a hydroxyl group reacts with a tertiary oxonium cation, the chain growth is stopped and a proton is transferred to a monomer, which turns into a secondary oxonium cation that can propagate the polymerization, generating in turn another hydroxyl group. In consequence, the participation of the end hydroxyl groups of the PCL arms in the curing may result in a decrease in crosslinking density and a loosening of the network structure, thus resulting in a decrease in glass transition temperature.

However, the calculated T_g values using a standard rule of mixtures such as the Fox equation (results not shown) are significantly lower than the experimental ones. Such deviations are commonly observed in phase-separated modified thermosets [15] but they are also present in homogeneous materials, as we recently reported [37]. The materials are homogeneous, as will be confirmed later by SEM microscopy and, indeed, no secondary relaxation corresponding to the appearance of a second phase at low temperatures was observed. It can be hypothesized that the incorporation of the modifiers into the network structure can produce significant mobility restrictions arising from the highly crosslinked hyperbranched core and the presence of physical

entanglements between the poly(ε-caprolactone) arms and the crosslinked thermosetting network, as reported previously for poly(ethyleneimine) modified hybrid epoxy networks [37].

Figure 4 compares the thermal stability of the obtained materials and the characteristic temperatures of 5% weight, $T_{5\%}$, are reported in Table 3. It was expected a certain decrease in thermal stability on increasing the proportion of star in the formulation, caused by the growing amount of ester groups in the modifier. However, Table 3 shows no well-defined trend in $T_{5\%}$. In Figure 4 it is observed, overall, that the use of the different modifiers somewhat increases the thermal stability of the cured materials, especially on increasing the molecular weight of the modifier. Indeed, with H20-PCL only the material with a proportion of 20% of the modifier has a higher thermal stability, whereas with H40-PCL a 5% of the modifier is sufficient to increase the thermal stability. In our previous work, we observed that the use of these modifiers decreased the thermal stability of CE formulations cured with ytterbium triflate [31]. However, in that case there was a concurrent effect of the introduction of more ester groups coming from the PCL arms and the hyperbranched aliphatic polyester core, and the catalytic role of ytterbium triflate in the degradation [38], because ytterbium triflate is a Lewis acid and *β*-elimination of ester groups is promoted in the presence of acid species [39]. If one compares the thermal stability of the UV-cured materials with that of the ones cured with ytterbium triflate [31], there is a great difference arising from the catalytic role of lanthanide triflates in thermal degradation. Similar differences have been previously observed between UV-cured and thermally cured epoxy formulations [40].

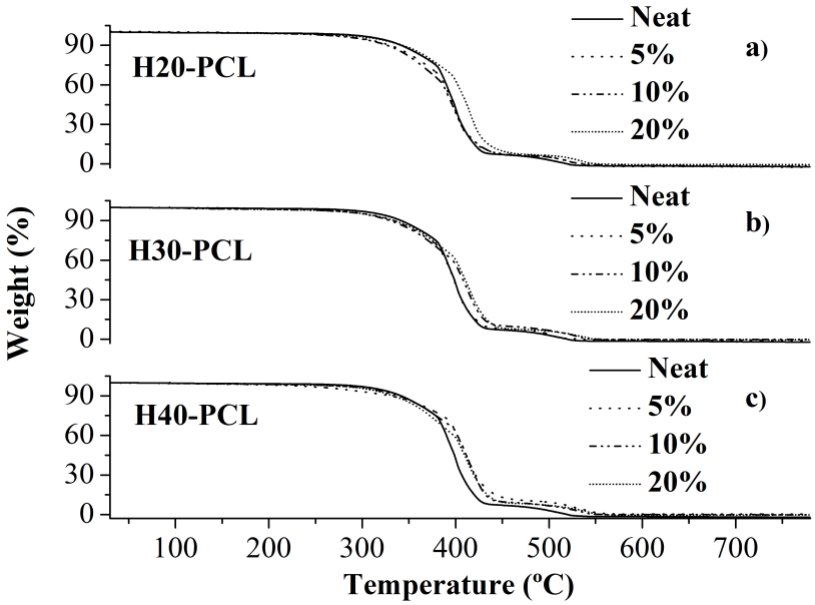

Figure 4. TGA curves for the different materials obtained at 10 ºC/min under air atmosphere.

Mechanical properties of the HX-PCL modified thermosets

We recently demonstrated that multiarm PCL stars with hyperbranched poly(glycidol) core could improve the impact strength of cationic epoxy thermosets to a higher extent than linear PCL, while retaining better thermomechanical properties [29]. Multiarm PCL stars with hyperbranched poly(ethyleneimine) core have also been synthesized and used in anionic epoxy

formulations, with a positive effect on impact strength depending on the arm length and hyperbranched core size [30]. However, in our previous work on the modification of cationic CE formulations with PCL multiarm stars we reported a significant decrease in impact strength upon addition of the modifier [31].

Figure 5 shows the results of the impact strength measurements of the neat and modified formulations. In contrast with our previous results [31], no decrease in impact strength has taken place but the opposite, achieving an optimum effect with 10 % of H20-PCL.

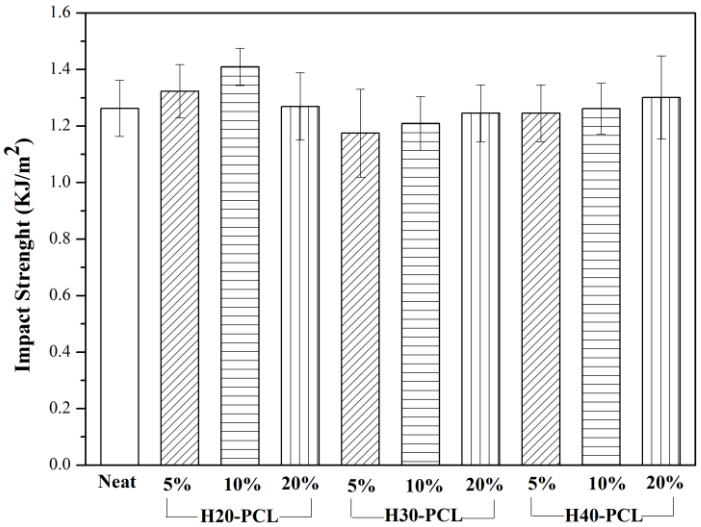

Figure 5. Impact strength dependence of thermosets containing different amounts of the modifiers.

It is acknowledged that hyperbranched polymers that undergo phase separation during curing are capable of producing a significant enhancement in impact strength [9, 11, 15, 16] due to the stress concentration in the area surrounding the particles and an effective stress transfer to the particles, leading to the activation of several energy absorption mechanisms such as shear yielding of the matrix in the vicinity of the particles and cavitation of the particles. In homogenoeus systems, an *in-situ* reinforcing mechanism caused by a loosening and flexibilization of the network structure is held accountable for, most of the times, a discrete enhancement in impact strength [41]. An enhancement in impact strength has been reported for UV-cured cationic epoxy formulations modified with hyperbranched polymers undergoing phase separation during curing [27] but a certain improvement has also been observed in homogeneous materials [12, 26]. In previous works [15, 16] we observed that an excessive compatibility between the resin and the polymeric modifier prevented phase separation and therefore the toughening effect was very limited. In the present case it seems that we have obtained homogeneous materials, of which it can be deduced that the toughening effect can only be discrete, because only an *in-situ* reinforcement may take place.

In Figure 6 the SEM micrographs of the fracture surfaces of the neat and modified material with H20-PCL after impact tests are shown. As suggested previously in the thermomechanical study, homogeneous materials have been obtained, without evident traces of phase separation From the smooth fracture surfaces it can also be inferred that all the materials

have a similar brittle fracture, which was to be expected taking into account the above reported values of impact strength. The fracture surfaces appear to be only slightly rougher in the case of the modified materials, indicating a somewhat enhanced matrix shear yielding in agreement with the discrete enhancement in toughness discussed above.

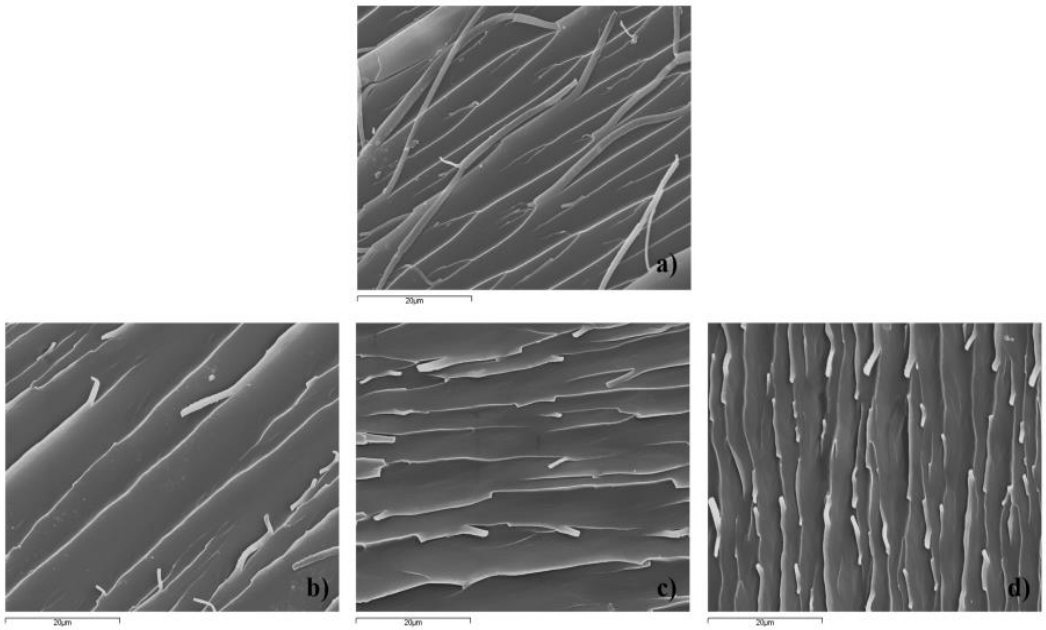

Figure 6. SEM micrographs of the fracture surface of the neat material (a) and modified materials with 5% (b), 10% (c) and 20% (d) of H20-PCL.

Conclusions

Multiarm star copolymers have been synthesized by cationic ring-opening polymerization of *ε*-caprolactone from hyperbranched aliphatic polyesters of different molecular weight as a core. These multiarm star polymers obtained have been used as polymeric modifiers of UV-cured cycloaliphatic epoxy resin.

The presence of these modifiers accelerated the photocuring process because of the participation of the end hydroxyl groups of the poly(*ε*-caprolactone) arms in the cationic curing of epoxides by the activated monomer (AM) mechanism. The effect is more significant with the higher molecular weight modifier (H40-PCL) than with the lower molecular weight modifier (H20-PCL).

Homogeneous materials have been obtained, with a modest decrease of the glass transition temperature because of the incorporation of the modifiers into the network structure and the subsequent loosening and flexibilization of the network structure. The materials have a higher thermal stability than those cured with lanthanide triflates and even a slight increase in thermal stability upon addition of the modifiers has also been observed.

Only H20-PCL had a measurable positive effect on the impact strength of the modified thermosets, while the others did not produce a clear decrease or increase in this property. This discrete effect arises from the fact that the materials are homogeneous and only an *in-situ* reinforcement of the matrix may take place.

Acknowledgements

The authors would like to thank MINECO (MAT2011-27039-C03-01, MAT2011-27039-C03-02) and Generalitat de Catalunya (2009-SGR-1512) for giving financial support. M.F. acknowledges the grant BES-2009-025226 and X.F.-F. Acknowledges the contract JCI-2010-06187. Perstorp is acknowledged for kindly providing Boltorn HBPs.

References

[1] May CA. Epoxy Resins: Chemistry and Technology. 2nd ed. New York: Marcel Dekker; 1988.

[2] Petrie EM. Epoxy Adhesive Formulations. New York: McGraw-Hill; 2006.

[3] Decker C, Nguyen T, Viet T, Thi HP. Photoinitiated cationic polymerization of epoxides. Polymer International. 2001;50(9):986-997.

[4] Decker C, Nguyen Thi Viet T, Decker D, Weber-Koehl E. UV-radiation curing of acrylate/epoxide systems. Polymer. 2001;42(13):5531-5541.

[5] Crivello JV, Acosta Ortiz R. Design and synthesis of highly reactive photopolymerizable epoxy monomers. Journal of Polymer Science Part A: Polymer Chemistry. 2001;39(14):2385-2395.

[6] Crivello JV. Discovery and development of onium salt cationic photoinitiators. Journal of Polymer Science, Part A: Polymer Chemistry. 1999;37(23):4241-4254.

[7] Bagheri R, Marouf BT, Pearson RA. Rubber-toughened epoxies: A critical review. Polymer Reviews. 2009;49(3):201-225.

[8] Zheng S. Epoxy Polymers: New Materials and Innovations. In: Pascault J-P, Williams RJJ, editors. Epoxy Polymers: New Materials and Innovations. Weinheim: Wiley-VCH; 2010.

[9] Boogh L, Pettersson B, Manson J-AE. Dendritic hyperbranched polymers as toughеners for epoxy resins. Polymer. 1999;40(9):2249-2261.

[10] Ratna D, Simon GP. Thermomechanical properties and morphology of blends of a hydroxy-functionalized hyperbranched polymer and epoxy resin. Polymer. 2001;42(21):8833-8839.

[11] Ratna D, Varley R, Simon GP. Toughening of trifunctional epoxy using an epoxy-functionalized hyperbranched polymer. Journal of Applied Polymer Science. 2003;89(9):2339-2345.

[12] Sangermano M, Malucelli G, Bongiovanni R, Priola A, Harden A. Investigation on the effect of the presence of hyperbranched polymers on thermal and mechanical properties of an epoxy UV-cured system. Polymer International. 2005;54(6):917-921.

[13] Zhang D, Jia D. Toughness and strength improvement of diglycidyl ether of bisphenol-A by low viscosity liquid hyperbranched epoxy resin. Journal of Applied Polymer Science. 2006;101(4):2504-2511.

[14] Voit B, Lederer A. Hyperbranched and highly branched polymer architectures-synthetic strategies and major characterization aspects. Chemical Reviews. 2009;109(11):5924-5973.

[15] Flores M, Fernández-Francos X, Ferrando F, Ramis X, Serra A. Efficient impact resistance improvement of epoxy/anhydride thermosets by adding hyperbranched polyesters partially modified with undecenoyl chains. Polymer. 2012;53:5232-5241.

[16] Flores M, Morell M, Fernández-Francos X, Ferrando F, Ramis X, Serra À. Enhancement of the impact strength of cationically cured cycloaliphatic diepoxide by adding hyperbranched poly(glycidol) partially modified with 10-undecenoyl chains. European Polymer Journal. 2013;49(6):1610-1620.

[17] Tripathi G, Srivastava D. Effect of carboxyl-terminated butadiene acrylonitrile copolymer concentration on mechanical and morphological features of binary blends of nonglycidyl-type epoxy resins. Advances in Polymer Technology. 2007;26(4):258-271.

[18] Tripathi G, Srivastava D. Toughened Cycloaliphatic Epoxy Resin for Demanding Thermal Applications and Surface Coatings. Journal of Applied Polymer Science. 2009;114(5):2769-2776.

[19] Lijima T, Fujimoto KI, Tomoi M. Toughening of cycloaliphatic epoxy resins by poly(ethylene phthalate) and related copolyesters. Journal of Applied Polymer Science. 2002;84(2):388-399.

[20] Zhang X, Xu W, Xia X, Zhang Z, Yu R. Toughening of cycloaliphatic epoxy resin by nanosize silicon dioxide. Materials Letters. 2006;60(28):3319-3323.

[21] Zhang X-H, Zhang Z-H, Xu W-J, Chen F-C, Deng J-R, Deng X. Toughening of cycloaliphatic epoxy resin by multiwalled carbon nanotubes. Journal of Applied Polymer Science. 2008;110(3):1351-1357.

[22] Gao N, Liu W, Ma S, Tang C, Yan Z. Cycloaliphatic epoxy resin modified by two kinds of oligo-fluorosiloxanes for potential application in light-emitting diode (LED) encapsulation. Journal of Polymer Research. 2012;19(8):9923-9923.

[23] Ochi M, Ichikawa N, Harada M, Hara M, Uchida H. Toughening of cycloaliphatic epoxy resin improved by reactive copolymers with flexible alkyl side chains. Journal of Applied Polymer Science. 2012;124(6):4572-4578.

[24] Dabritz F, Voit B, Naguib M, Sangermano M. Hyperstar poly(ester-methacrylate)s as additives in thermally and photocured epoxy resins. Polymer. 2011;52(25):5723-5731.

[25] Sangermano M, Messori M, Galleco MM, Rizza G, Voit B. Scratch resistant tough nanocomposite epoxy coatings based on hyperbranched polyesters. Polymer. 2009;50(24):5647-5652.

[26] Sangermano M, Priola A, Malucelli G, Bongiovanni R, Quaglia A, Voit B, Ziemer A. Phenolic hyperbranched polymers as additives in cationic photopolymerization of epoxy systems. Macromolecular Materials and Engineering. 2004;289(5):442-446.

[27] Sangermano M, Malucelli G, Bongiovanni R, Priola A, Harden A, Rehnberg N. Hyperbranched Polymers in cationic photopolymerization of epoxy systems. Polymer Engineering and Science. 2003;43(8):1460-1465.

[28] Karger-Kocsis J, Frohlich J, Gryshchuk O, Kautz H, Frey H, Mülhaupt R. Synthesis of reactive hyperbranched and star-like polyethers and their use for toughening of vinylester-urethane hybrid resins. Polymer. 2004;45(4):1185-1195.

[29] Morell M, Ramis X, Ferrando F, Serra A. Effect of polymer topology on the curing process and mechanical characteristics of epoxy thermosets modified with linear or multiarm star poly(ε-caprolactone). Polymer. 2011;52(21):4694-4702.

[30] Acebo C, Fernandez-Francos X, Ferrando F, Serra A, Salla JM, Ramis X. Multiarm star with poly(ethyleneimine) core and poly(ε-caprolactone) arms as modifiers of diglycidylether of bisphenol A thermosets cured by 1-methylimidazole. Reactive & Functional Polymers. 2013;73(3):431-441.

[31] Flores M, Fernàndez-Francos X, Ramis X, Ferrando F, Serra À. Effect of Molecular Weight of Polyesters with Multiarm Star Topology used as Additives in Cycloaliphatic Epoxy Thermosets Cured by Ytterbium Triflate. Journal of Polymer Research. 2013 (submitted).

[32] Foix D, Fernández-Francos X, Ramis X, Serra À, Sangermano M. New pegylated hyperbranched polyester as chemical modifier of epoxy resins in UV cationic photocuring. Reactive and Functional Polymers. 2011;71(4):417-424.

[33] Morancho JM, Cadenato A, Ramis X, Fernandez-Francos X, Flores M, Salla JM. Effect of a hyperbranched polymer over the thermal curing and the photocuring of an epoxy resin. Journal of Thermal Analysis and Calorimetry. 2011;105(2):479-488.

[34] Kubisa P, Penczek S. Cationic activated monomer polymerization of heterocyclic monomers. Progress in Polymer Science. 1999;24(10):1409-1437.

[35] Crivello JV, Liu S. Photoinitiated cationic polymerization of epoxy alcohol monomers. Journal of Polymer Science, Part A: Polymer Chemistry. 2000;38(3):389-401.

[36] Fernández-Francos X, Salla JM, Cadenato A, Morancho JM, Serra A, Mantecón A, Ramis X. A new strategy for controlling shrinkage of DGEBA resins cured by cationic copolymerization with hydroxyl-terminated hyperbranched polymers and ytterbium triflate as an initiator. Journal of Applied Polymer Science. 2009;111(6):2822-2929.

[37] Fernández-Francos X, Santiago D, Ferrando F, Ramis X, Salla JM, Serra À, Sangermano M. Network structure and thermomechanical properties of hybrid DGEBA networks cured with 1-methylimidazole and hyperbranched poly(ethyleneimine)s. Journal of Polymer Science Part B: Polymer Physics. 2012;50(21):1489-1503.

[38] González L, Ramis X, Salla JM, Mantecón A, Serra À. The degradation of new thermally degradable thermosets obtained by cationic curing of mixtures of DGEBA and 6,6-dimethyl-(4,8-dioxaspiro[2.5]octane-5,7-dione). Polymer Degradation and Stability. 2007;92(4):596-604.

[39] Shirai M, Kawaue A, Okamura H, Tsunooka M. Photo-cross-linkable polymers having degradable properties on heating. chemistry of Materials. 2003;15(21):4075-4081.

[40] Fernandez-Francos X, Salla JM, Cadenato A, Morancho JM, Mantecon A, Serra A, Ramis X. Novel thermosets obtained by UV-induced cationic copolymerization of DGEBA with an spirobislactone. Journal of Polymer Science, Part A: Polymer Chemistry. 2007;45(23):5446-5458.

[41] Fu J-F, Shi L-Y, Yuan S, Zhong Q-D, Zhang D-S, Chen Y, Wu J. Morphology, toughness mechanism, and thermal properties of hyperbranched epoxy modified diglycidyl ether of bisphenol A (DGEBA) interpenetrating polymer networks. Polymers for Advanced Technologies. 2008;19(11):1597-1607.

A new two-stage curing system: thiol-ene/epoxy homopolymerization using an allyl terminated hyperbranched polyester as reactive modifier

Marjorie Flores,[1] Adrian M. Tomuta,[1] Xavier Fernández-Francos,[1] Xavier Ramis,[2] Marco Sangermano,[3] Angels Serra[1*]

[1.] Dept. of Analytical and Organic Chemistry, University Rovira i Virgili, C/ Marcel·lí Domingo s/n, 43007, Tarragona, Spain
[2.] Thermodynamics Laboratory, ETSEIB University Politècnica de Catalunya, C/ Av. Diagonal 647, 08028, Barcelona, Spain
[3.] Dept. of Material Science and Chemical Engineering, Politecnico di Torino, C.so Duca degli Abruzzi 24, 10129 Torino, Italy

Abstract

An allyl terminated hyperbranched polyester (HBP) was added to an epoxy formulation containing a trithiol compound to perform a thiol-ene click reaction. By this procedure a flexible thioether network was formed. The photoirradiation of the reactive mixture, which contained a cationic photoinitiator, converted the thioether network in a multifunctional thermal macroinitiator, capable to initiate the cure of the cycloaliphatic epoxy resin (CE) in a second thermal stage. Depending on the proportion of HBP, thermal or photocuring of the epoxy resin took place in different extent, leading to networks with different structures. The photocuring procedure was followed by FTIR and the thermal second stage by DSC. The materials obtained were characterized by DMTA, TGA and SEM. The addition of HBP-Allyl and the trithiol to the formulation allowed increasing the T_g on comparison with the neat epoxy thermoset. The system proposed constitutes a new two-stage dual photo-thermal curing procedure for cycloaliphatic epoxy resins with a thermal latent character.

Keywords: *epoxy resin, hyperbranched, thiol-ene reaction, photocuring, thermoset.*

Introduction

It has been reported that click reactions are characterized by a high thermodynamic driving force. They are quantitative, rapid, without the occurrence of by-products or side-reactions and possible in mild conditions. However, the most remarkable characteristics are based on the concepts of modularity and orthogonality [1]. This modular approach is often more efficient than a conventional synthetic strategy involving sequential reactions and the orthogonality allows to access a large number of structures as the individual building blocks can be combined in different ways. In polymer chemistry, the orthogonality allows in conjunction with one or more polymerization methods to access a broad range of polymeric materials that would be difficult to prepare otherwise [2]. Click reactions have been employed in combination with living polymerization techniques, such as ring-opening polymerization (ROP), [3,4] ring-opening metathesis polymerization (ROMP), [5] cationic polymerization [6] or controlled radical vinyl polymerization [7].

Among other click reactions, thiol-ene has been proved to be particularly useful for polymer synthesis under extremely mild conditions [8]. It is advantageous over Huisgen's 1,3-dipolar cycloaddition by the possibility of photoinitiation without copper catalyst, which is believed to be cytotoxic and produce other neurological illnesses. Moreover, azide groups are also often associated with potential toxic side effects, and certain azides have a real explosive potential.

Thiol-ene reactions were used in one of our previous studies to prepare a hyperbranched polymer with thioether and ester groups in its structure [9]. This polymer was used as a modifier in the cure formulation of a cycloaliphatic epoxy resin (CE) leading to a dual latent curing system, promoted by the use of UV irradiation. By this irradiation in the presence of a photoinitiator, thioether groups were transformed into trialkylsulfonium moieties, able to initiate the thermal cationic homopolymerization of CE resin in the second stage of curing. This system led to thermosets with T_gs higher than 200 ºC and storage moduli in the rubbery state which increased with the amount of HBP. This fact was related to the multifunctionality of the HBP acting as initiator, which became covalently linked to the epoxy matrix. However, the drawback of this method was the tedious synthesis of the HBP structure, performed by a five-step iterative methodology based on that proposed by Hawker et al [10]. For thioether-ester dendrimers.

To overpass this drawback, in the present paper we generate *in situ* thioether groups by a thiol-ene reaction on allyl terminated hyperbranched polyester. This reaction takes place at room temperature by photoirradiation at the very beginning of the curing process and generates a primary network with thioether moieties, which are transformed into trialkylsulfonium groups by reacting with activated epoxy groups. The activation of these epoxy groups occurs with UV light by the presence of a cationic photoinitiator. However, thioether groups inhibit the photopolymerization of epoxides by forming trialkylsulfonium sites. These sulfonium salts are inactive under UV irradiation but are able to initiate the thermal curing of epoxide CE resin, leading to highly crosslinked networks [11]. The curing system proposed in the present study has a dual photo-thermal curing characteristic and therefore it is suitable for two-stage curing processes.

The use of the allylic terminated HBP as reactive modifier has two different aims: firstly, the participation in the thiol-ene process with the subsequent formation of a macroinitiator with multiple initiating sites, which can lead to high T_g thermosets and secondly, the introduction of a certain flexibility and structural inhomogeneities in the final network, which should help to increase mechanical characteristics as reported previously by several authors [12,13,14]. It should be said that the adequate tailoring of the HBP structure is crucial to reach the thermal and mechanical properties desired. Thus, we have selected an aromatic polyester structure to maintain the thermal stability and rigidity of the thermoset. The short aliphatic structures in the HBP increase mobility without much plasticization of the cured material.

Experimental part

Materials

4,4-Bis(4-hydroxyphenyl) valeric acid, N,N'-dicyclohexylcarbodiimide (DCC) and allyl bromide were purchased from Aldrich and used without further purification. Methanol, N,N-dimethylformamide (DMF), acetone and tetrahydrofurane (THF) were purchased from Scharlab and purified by standard procedures. Inorganic salts were purchased from Panreac. 4-(N,N-dimethylamino) pyridinium p-toluenesulfonate (DPTS) was prepared as described in the literature [15].

The bis-cycloaliphatic diepoxide 3,4-epoxycyclohexymethyl 3'4'-epoxycyclohexyl carboxylate, (CE, 126 g/eq), triphenylsulfonium hexafluoroantimonate (PI, $Ph_3{}^+SbF_6{}^-$) and trimethylolpropane tris-(3-mercaptopropionate) (TMP) were purchased from Aldrich and used without further purification.

Hyperbranched polyester synthesis (HBP-OH)

The HBP-OH was synthesized following a previously described procedure proposed by Schallausky et al [16]. From 4,4-bis(4-hydroxyphenyl) valeric acid, as AB_2 monomer, and DPTS and DCC in anhydrous DMF. The ^{1}H and ^{13}C NMR data were in accordance with those published [17]. M_n: 8700 g/mol, M_w: 12300 g/mol. T_g 121 ºC (by DSC).

Allyl modification of HBP-OH (HBP-Allyl)

The modification was performed by nucleophylic substitution on allyl bromide by the phenolate end groups, formed by treating HBP-OH with K_2CO_3 in a mixture of THF and acetone, as previously reported [18]. HBP-Allyl was obtained by precipitating the solution in THF in water. The polymer was dried in a vacuum oven at 50 °C overnight and a white powder was obtained. Yield: 90%. T_g 81 ºC (by DSC). NMR data were in accordance to the previously reported by us [18].

Samples preparation

Mixtures were prepared by adding the required amount of HBP-Allyl (5, 10 and 15 parts per hundred parts of resin, phr) into the epoxy resin (CE) and gently heating (100 ºC) until it was dissolved and the solution became clear. Then, 1 phr of PI in reference to the resin and the required amount of TMP (see Table 1) were added and the mixture was homogenized. The structures of the monomers and HBP-Allyl are shown in Scheme 1.

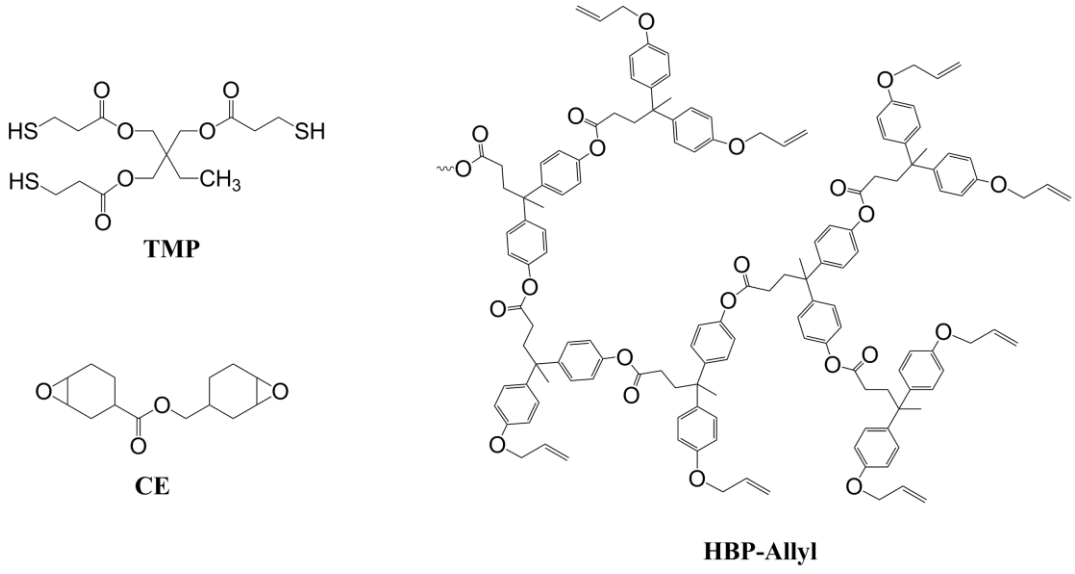

Scheme 1. Components of the curing mixture.

For DMTA analyses, formulations were coated, by means of a wirewound applicator onto a glass substrate and photocured by exposing to UV radiation with a fusion lamp (H-bulb) in air at a conveyor speed of 5 m min^{-1}, with radiation intensity on the surface of the sample of 280 mW cm^{-2}. After that, they were placed in an oven for 4 h at 150 ºC.

DSC analyses were carried out on 8-10 mg samples previously exposed to UV irradiation using an UV oven (Vilber Lourmat Bio-Link Crosslinker) equipped with 6 lamps of 8 W each emitting 365 nm wavelength UV radiation.

Table 1. Composition of the formulations. In percentage by total weight (%wt) of the mixture and equivalent ratio (Xeq) in eq/g of mixture of the relevant species.

Formulation	CE		HBP-Allyl		TMP		PI	
	X_{eq} ($x10^{-3}$)	wt%	X_{eq} ($x10^{-4}$)	wt%	X_{eq} ($x10^{-4}$)	wt%	X_{eq} ($x10^{-6}$)	wt%
Neat	7.86	99.00	0.00	0.00	0.00	0.00	8.92	1.00
HBP-Allyl								
5%	3.96	92.82	0.66	4.64	0.66	1.62	8.29	0.93
10%	3.96	87.35	1.31	8.74	1.31	3.04	7.76	0.87
15%	3.96	82.49	1.97	12.37	1.97	4.31	7.31	0.82

Characterization

A Bruker Vertex 70 FTIR spectrometer equipped with an attenuated total reflection (ATR) accessory (Golden GateTM, Specac Ltd.) which is temperature controlled (heated single-reflection diamond ATR crystal) and equipped with a liquid nitrogen-cooled mercury-cadmium-telluride (MCT) detector was used to monitor the evolution of functional groups during isothermal photocuring of the formulations. Spectra were collected at 40, 60 and 80 ºC in absorbance mode with resolution of 4 cm^{-1} in the wavelength range from 600 to 4000 cm^{-1} being 20 scans for each spectrum. A Hamamatsu Lightningcure LC5 (Hg-Xe lamp) with one beam conveniently adapted to the ATR accessory was used to irradiate the samples. A wire-wound rod was used to set a sample thickness of 25 μm. The OPUS^{TM} software was used for the analysis of the spectra. The spectra were corrected taking into account the dependence of the penetration depth on the wavelength and normalized using the area of the aliphatic ester band at 1727 cm^{-1}. The bands at 789 and 748 cm^{-1} were used for the monitoring of epoxy groups. The following expression was used to determine the conversion of epoxy groups:

$$x_{epoxy} = 1 - \frac{A'_{epoxy,t}}{A'_{epoxy,0}} \qquad (1)$$

where, A'_{epoxy}, is the normalized area of the epoxy bands, and the subindexes *t* and *0* indicate the photocuring time and the beginning of the photocuring, respectively.

Dynamic postcuring experiments were carried out on a Mettler DSC-822e cooled with liquid nitrogen and equipped with a TSO801RO robotic arm. The samples deposited in open DSC pans were irradiated in the UV oven up to a dose level of 6 J/cm^2. The samples were covered with a pierced lid and thermally postcured at heating rates of 2, 5, 10 and 15 ºC/min. The relative conversion *x* during the postcuring stage was calculated based on the heat evolved during the postcuring as follows:

$$x = \frac{\Delta h_T}{\Delta h_{total}} \qquad (2)$$

where, Δh_T is the heat evolved up to a given temperature and Δh_{total} is the total reaction heat evolved during postcuring. The degree of conversion of epoxy groups achieved during the photocuring stage can be calculated as:

$$x_{UV,epoxy} = 1 - \frac{\Delta h_{total}}{\Delta h_{theor}} \qquad (3)$$

where Δh_{theor} is the theoretical reaction heat released by complete conversion of epoxy groups taking into account the composition of the mixture and an experimental reaction heat of 70-75 kJ [19,20] per epoxy group determined previously.

The apparent activation energy throughout the thermal postcuring was determined using the isoconversional kinetics analysis method of Kissinger-Akahira-Sunose, which is based on the following expression:

$$\ln\left(\frac{\beta}{T^2}\right) = \ln\left(\frac{k_0 \cdot R}{g(x) E}\right) - \frac{E}{R \cdot T} \qquad (4)$$

where β is the heating rate, k_0 is the pre-exponential factor of the Arrhenius kinetic constant, E is the apparent activation energy and $g(x)$ is the integral expression of the kinetic model governing the curing process. The representation $ln(\beta/T^2)$ against $-1/R \cdot T$ for all the heating rates at a fixed degree of conversion produces a straight line. From the slope one can determine the apparent activation energy E and from the intercept at the origin one can obtain, after some rearrangement, a factor including both the kinetic model and the pre-exponential factor, $ln(g(x)/k_0)$.

The isothermal curing at different temperatures was simulated from the isoconversional data, without needing to know the kinetic model governing the process. For a given degree of conversion, the time needed to reach this conversion at a given temperature is given by the following expression:

$$\ln t = \ln\left(\frac{g(x)}{k_0}\right) + \frac{E}{R \cdot T} \qquad (5)$$

where the parameters $ln(g(x)/k_0)$ and E have been previously determined. Further details on the kinetic methods can be found elsewhere [21].

Dynamic-mechanical thermal analyses (DMTA) were performed using a Triton Technology DMA from Mettler-Toledo dynamic analyzer operating in single cantilever mode at 1 Hz. *Tan δ* were measured from 50 to the temperature at which the rubbery state was observed. The T_g value was assumed as the maximum of the loss factor curve (*tan δ*). Specimens with dimensions ca. 2 x 0.5 x 0.1 cm were used.

Thermogravimetric analysis (TGA) was performed with a Mettler TGA/SDTA 851 instrument between 30 and 800 °C at a heating rate of 10 °C/min in air.

The cryofractures of the specimens were performed under liquid nitrogen. Afterwards, the samples were metalized with gold and observed by SEM using a scanning electron microscopy Jeol JSM 6400.

Results and discussion

Although thiol-ene click reactions have the potential to be applied in thermosetting materials, usually low T_g values and low stiffness and strength are obtained, due to the formation of flexible thioether linkages, low crosslink density and to the limited availability of rigid thiol monomers [22]. To overcome these limitations hyperbranched polymers with thiol or vinyl-terminal groups have been used, because of their multifunctionality [23,24]. Other authors reported the combination of thiol-ene and other curing reactions to reach high T_g thermosets [4]. Recently, the curing by combination of a thiol-ene reaction with DGEBA cationic photopolymerization has been reported, but T_gs below 0 ºC were always obtained [25]. In a similar way, mixtures of DGEBA and triallyl-1,3,5-triazine-2,4,6-trione reacting with a tetrathiol by two different competitive ways, thiol-epoxy and thiol-ene processes, conduced to thermosets with T_gs in the range of 70-77 ºC [26]. In this second study a more rigid structure of the allyl monomer and a higher functionality of thiol are the responsible of the higher T_g value reached.

Our proposed alternative to prepare high T_g thermosets is the incorporation of vinyl terminated hyperbranched polymers and trifunctional thiol monomers into photocurable cycloaliphatic epoxy formulations. It has been proved that thiols inhibit cationic photopolymerization of epoxy resins by the protonation of epoxy groups by the photoinitiator and subsequent reaction with thiol groups [27] (Scheme 2.a.). However, the orthogonality of thiol-ene reaction allows that UV curing of thiol-ene formulations will not be affected by the presence of epoxy monomers, and an almost complete conversion of thiol and ene reactive groups will be achieved in a very short irradiation time, such as was previously demonstrated (Scheme 2.b.) [25]. By this reaction thioethers are formed in a primary network because of the high functionality of HBP-Allyl and the trifunctionality of TMP. Scheme 2.c depicts the formation of trialkylsulfonium salts, which are efficient thermal initiators, during UV irradiation after the first thiol-ene coupling. These salts have excellent room temperature stability and are capable of initiating rapid epoxy polymerization at temperatures above 100 ºC [28] and can act as a multifunctional initiator similarly than described previously by us [9].

It should be commented that thiols can also react with epoxy groups in the presence of tertiary amines, but in the present study this process is suppressed because of the lack of amines and the low reactivity of cycloaliphatic epoxies towards nucleophiles.

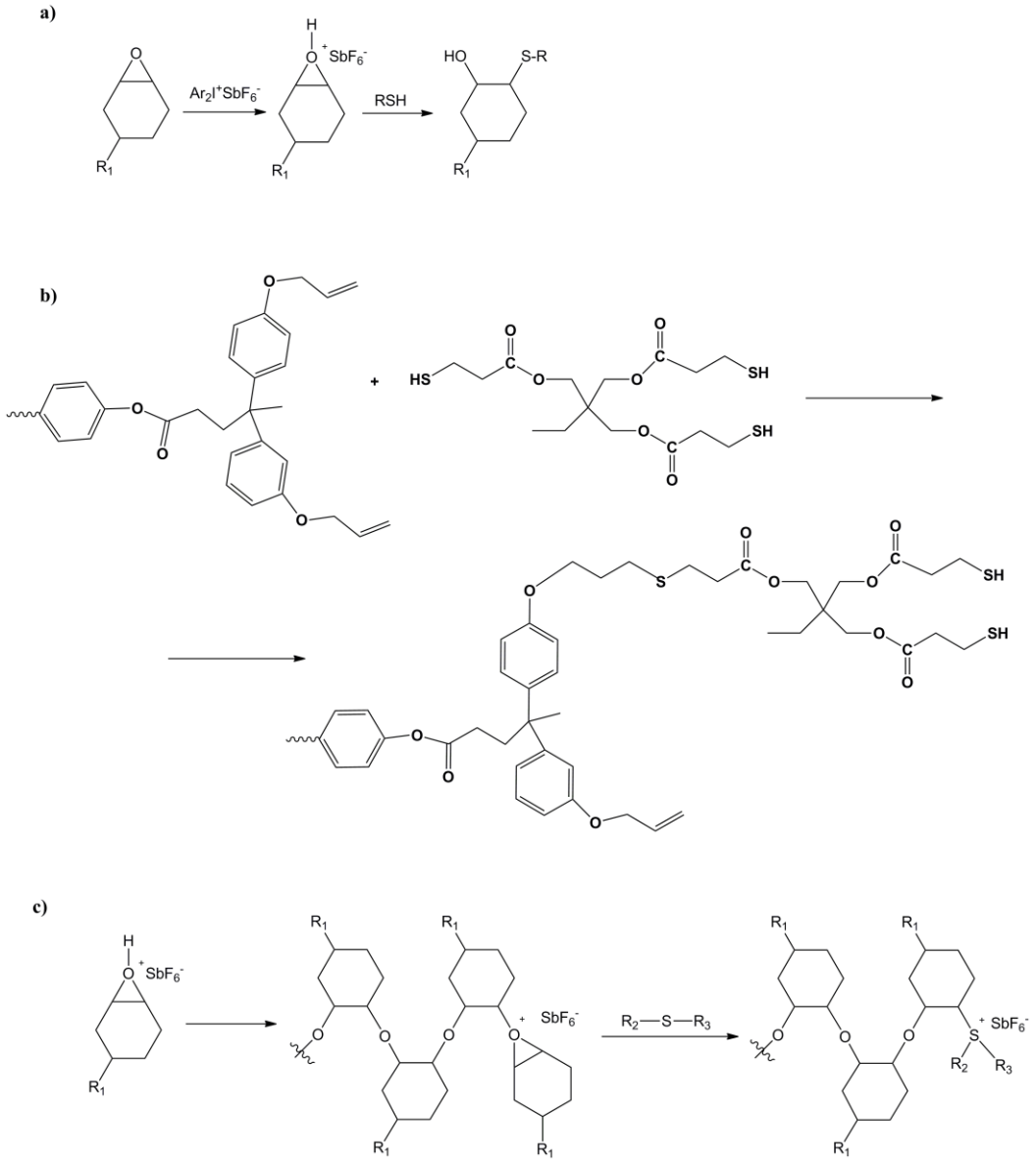

Scheme 2. Photopolymerization inhibition by thiols (a) thiol-ene reaction (b) and formation of sulfonium salts during photoirradiation (c).

Study of the UV photocuring process

Real time ATR-FTIR analyses were made on the formulations collected in Table 1 named 5, 10 and 15% HBP-Allyl. The structures of the components of the formulations are depicted in Scheme 1.

Figure 1 shows the evolution of the bands during 600 s of photoirradiation. As we can see there is a notable increase of the C-O absorptions at 1170 cm^{-1} and reduction of the epoxy

bands at 790 and 748 cm^{-1}, corresponding to the epoxy homopolymerization, up to the first 40 seconds of irradiation. However, the process slows down later on and only small changes are observed after 600 seconds of irradiation. The bands corresponding to C=C st. of allyl groups and S-H st. of thiols cannot be easily observed because of the low intensity and their low proportion in the formulation.

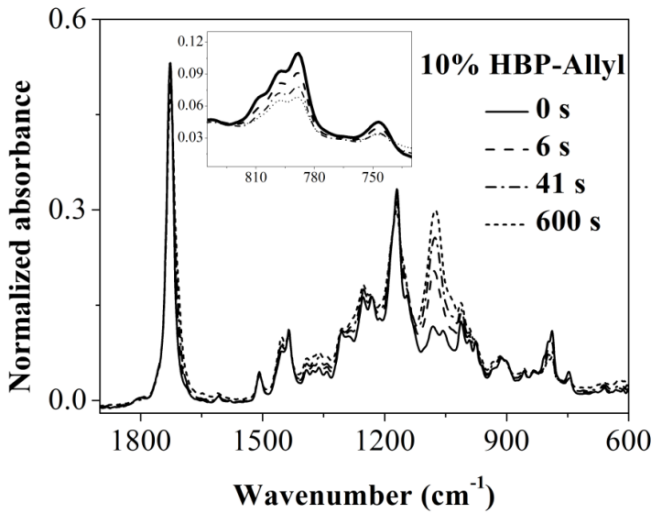

Figure 1. Zones of the FTIR spectra during UV-irradiation of the formulation containing a 10 % of HBP-Allyl at 40 ºC.

We calculated the conversion of epoxy groups with the photoirradiation time using the bands at 790 and 748 cm^{-1} and equation 1 of the experimental part. Figure 2 shows the plot of conversion as a function of irradiation time of the neat CE formulation and the other modified formulations containing HBP-Allyl and the stoichiometric amount of thiol at different temperatures.

As can be seen in the figure, whereas the neat formulation reached the complete conversion of epoxy groups at 80 ºC (up to vitrification), the conversion in the formulations containing HBP-Allyl is lower, and in the formulation 15%-HBP-Allyl it is reduced to only 50%. High temperatures are usually needed to overpass the vitrification process as seen in the plot of the neat formulation, but in the HBP-Allyl containing formulations even at 80 ºC the evolution of the epoxide is limited. It is also noticeable that on changing the temperature of photocuring in the HBP-Allyl modified formulations takes place a cross between conversion lines. It can be observed that in the first seconds of photoirradiation a fast conversion of epoxide groups occurs but then it slows down. Therefore, it seems that in the early stages, the curing is controlled by the generation of active species by UV irradiation, but the occurrence of different reactions such as those shown in Scheme 2 produces a complex change from UV irradiation to temperature control of the reaction, depending on the relative rates of 1) thiol and allyl groups reaction to form thioether bonds, 2) reaction of thiol and thioether groups with oxonium cations to produce less active species, 3) propagation of epoxy homopolymerization.

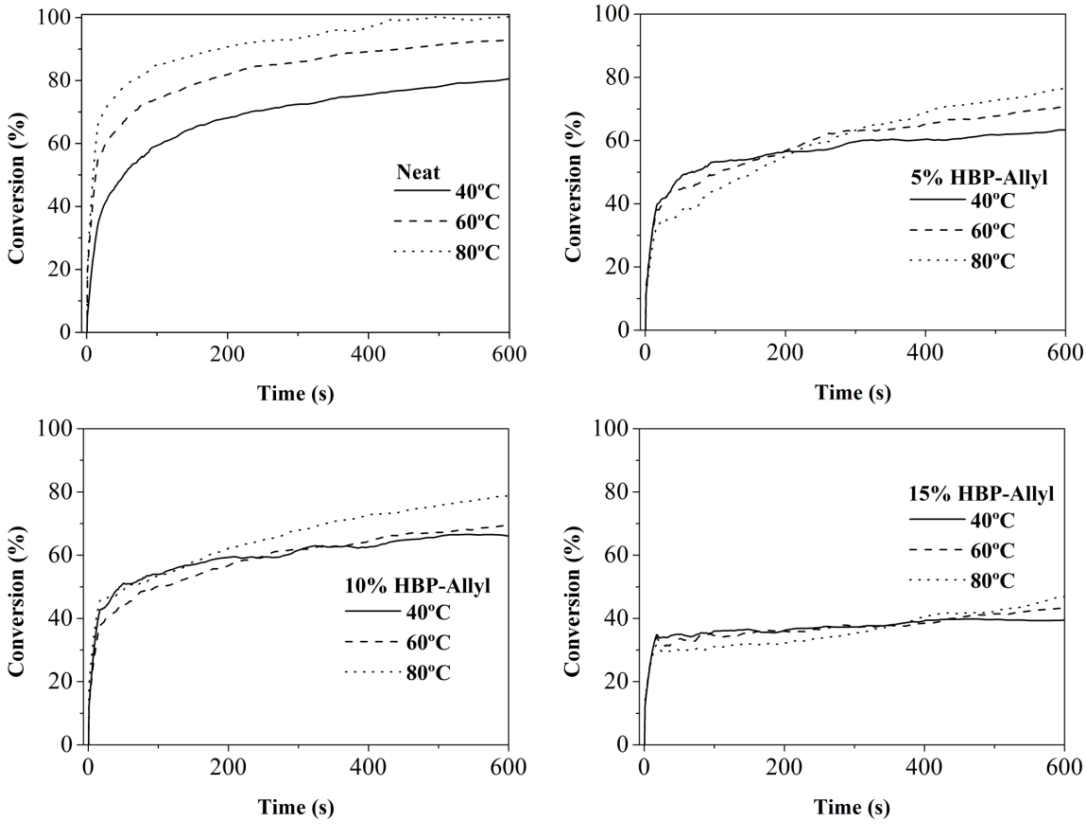

Figure 2. Conversion curves obtained by FTIR for the curing by UV-irradiation of the neat formulation and the modified formulations containing 5, 10 and 15% of HBP-Allyl at 40, 60 and 80 ºC.

It should be said that the lower the proportion of HBP-Allyl and TMP in the formulation the higher the conversion of epoxide reached. This can be explained on the basis of the competition between homopolymerization and thiol-ene reaction as depicted in Scheme 2. The higher the proportion of allyl and thiol groups in the formulation the higher the proportion of thioether formed, which are transformed into sulfonium salts, inhibiting the photoinitiated homopolymerization of epoxides. The formed sulfonium salts are not active to initiate the thermal cationic curing of the remaining epoxide groups up to temperatures higher than 100 ºC and therefore the curing stops. In a previous work [25] it was proved that allyl and thiol groups reacted simultaneously reaching a 100% conversion after a few seconds of irradiation. It should be remembered that in the present case, the relatively low amount of allyl and thiol groups in the formulation did not allow to monitor their disappearance by FTIR spectroscopy.

Study of the thermal curing process

The second stage of the curing, that takes place in thermal conditions was studied by non-isothermal DSC. Figure 3 shows the calorimetric curves and the conversion plot for the formulations studied after photoirradiation at room temperature.

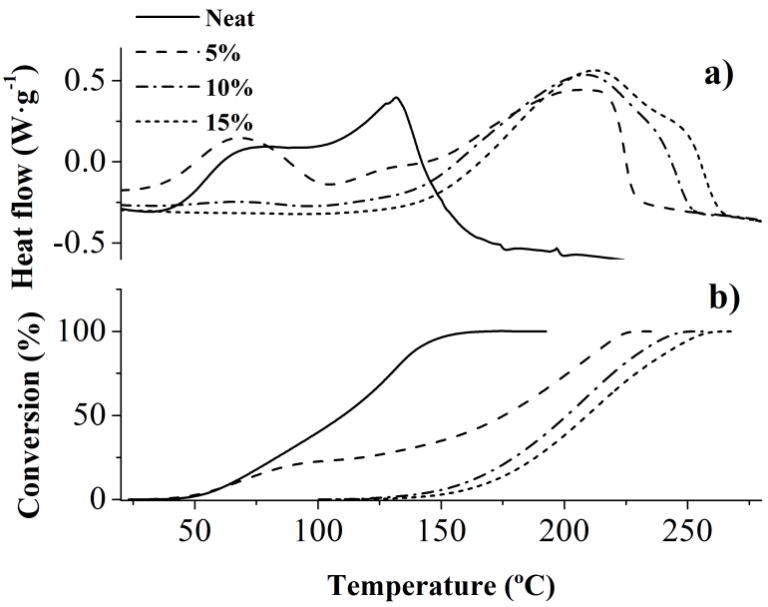

Figure 3. Calorimetric and conversion curves for the curing of the formulations studied at 10 ºC/min in N_2 atmosphere after UV-irradiation at room temperature.

As can be seen, the neat formulation and the formulation 5% HBP-Allyl begin to react as soon as the samples undergo devitrification and the trapped oxonium cations can rapidly resume the epoxy polymerization. Formulations containing 10 and 15% of HBP-Allyl are only able to react above 100 ºC, because of the reactivation of the less active alkyl sulfonium salts formed during the photoirradiation stage. Moreover, the formulation containing 5% HBP-Allyl also shows a noticeable exothermicity in this temperature region because of the previous formation of alkyl sulfonium salts. These observations indicate that these curing systems have the potential to be two-stageable, being the first stage photoinitiated and the second stage thermal. Only the formulations 10 and 15% HBP-Allyl can be considered as true two-stageable with a thermal latent character, because only a single exotherm above 100 ºC is observed.

Table 2 collects some data extracted from thermal studies of the curing process. It should be noted that it was not possible to determine by DSC the T_gs after photoirradiation of all the formulations. From the enthalpies of the table we can see that the addition of the HBP-Allyl and TMP to the formulation increases the proportion of thermal curing, due to the inhibition of the photocuring caused by the formation of thioether groups by the thiol-ene process. The results are in close agreement with the above discussion on the FTIR monitoring of the photocuring process. The higher HBP-allyl and TMP content, the higher the extent of thiol-ene process and the lower the epoxy conversion in the photoirradiation stage at room temperature.

Table 2. Thermal and thermomechanical data of neat and modified formulations. Δh_{total} and $x_{UVepoxy}$ have been defined in characterization section, $T_{tan\delta}$ is the peak temperature of the *tan* δ trace from the DMA analysis, $T_{5\%}$ is the temperature of 5% weight loss during thermogravimetric analysis and T_{max} is the temperature of maximum rate of degradation.

Sample	Δh_{res} *(J/g)*	$x_{UVepoxy}$	$T_{tan\ \delta}$ *(ºC)*	$T_{5\%}$ *(ºC)*	T_{max} *(ºC)*
Neat	333	0.44	177	304	412
HBP-Allyl (%)					
5	334	0.41	198	328	415
10	362	0.32	186	317	412
15	401	0.21	163	314	409

The kinetics of the reactive processes was studied for the neat formulation and the pure two-stage 10 and 15% HBP-Allyl formulations by performing calorimetric scans at different heating rates on the previously photoirradiated samples in the UV chamber at room temperature. The dependence of the apparent activation energy on the degree of conversion was calculated by the isoconversional method and it is presented in Figure 4.

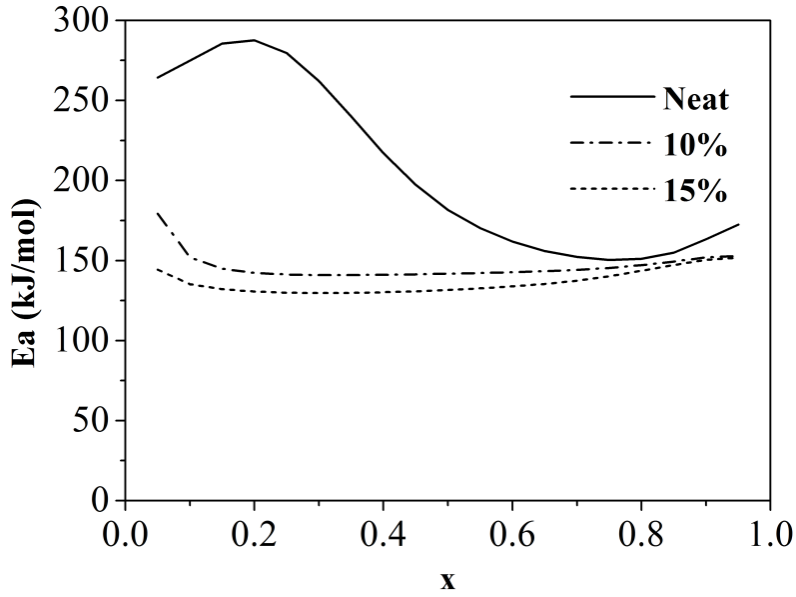

Figure 4. Dependence of the activation energy on the conversion degree of the formulation studied

As we can see in the plot, the initial activation energy for the neat formulation is much higher than the HBP-Allyl containing formulations. This higher value can be attributed to the devitrification process that as it was previously reported has a high activation energy between 200 and 300 kJ/mol [29]. Once the devitrification has been surpassed the activation energy approaches to the values obtained for the HBP-Allyl formulations, which have a constant value of

150 kJ/mol, indicating that the reactive processes occur similarly in both formulations. This indicates that the propagation of the polymerization is similar in all the formulations, but the main difference is the latent character of the sulfonium salt, which triggers the polymerization after reaching temperatures above 100 ºC. After a conversion of 0.8 the activation energy increases due to diffusion phenomena. In a previous work on a similar system, [9] we obtained activation energies of about 130 kJ/mol, typical of thermal curing systems, much higher than those calculated in UV curing [30].

From the kinetic studies, the prediction of the curing behavior at a selected temperature was done. Figure 5 presents the plot of conversion against temperature calculated at 150 ºC for the same formulations.

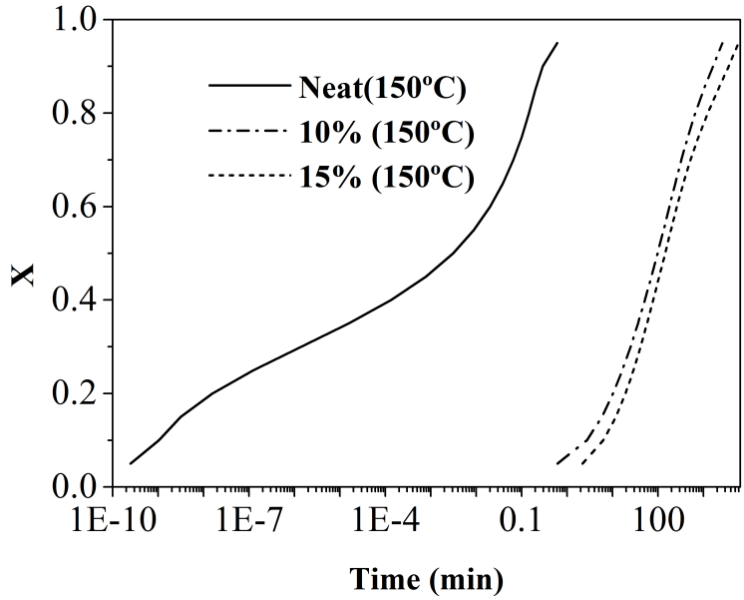

Figure 5. Prediction of the evolution of conversion against time for the thermal stage of curing of the formulations studied at 150 ºC.

As we can observe in the plot, the neat formulation begins to react immediately after devitrification and the thermal postcuring takes place in less than one minute. However, the modified formulations, which are initiated by the sulfonium salts formed in the photoirradiation step, begins later since the sulfonium salts should be thermally activated to produce the homopolymerization of the remaining epoxy groups. The reaction is slow, and the thermal stage of the process should be extended for several hours. If one increases the temperature up to 180 ºC, the postcuring would be shortened to 2-3 hours.

Characterization of the materials

The materials prepared were characterized by thermal mechanical analysis. The *tan* δ curves for all the materials are plotted in Figure 6 and the values of the maximum collected in Table 2.

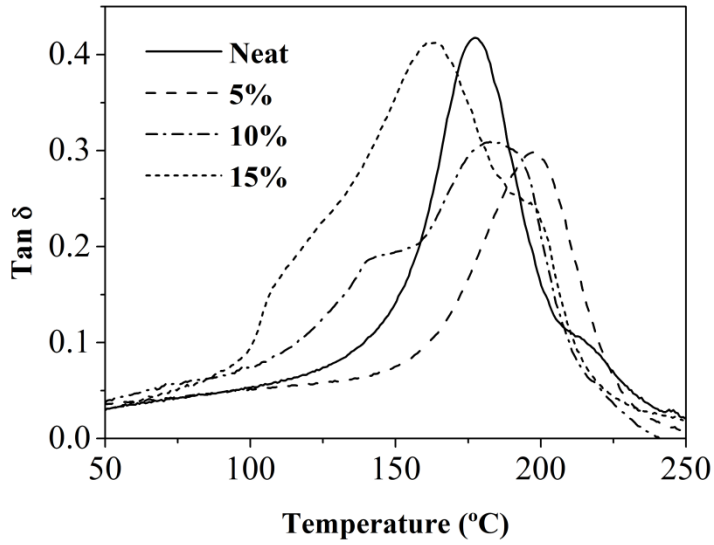

Figure 6. Temperature dependence plot of tan δ against temperature for the obtained materials

As we can see, the neat formulation and the formulation containing 5% HBP-Allyl show a unimodal curve indicating that these materials are homogeneous. The thiol-ene network is still compatible with the epoxy matrix and leads to the increase of the T_g value of the neat material in about 20 ºC. Moreover, the rigidity of the material seems to be higher since the height of the relaxation peak is lowered. This is due to the multifunctionality of the initial formed network with aromatic groups and several initiating sites that leads to highly crosslinked materials.

The curves corresponding to the materials obtained from the 10 and 15%-HBP-Allyl formulations show a more complex shape, broader than the others and with shoulders due to the heterogeneity of chemical composition of the network structure. The higher proportion of hyperbranched reacted with TMP to form a primary networked structure makes difficult the compatibilization with the further formed homopolymerized epoxy structure. Although the addition of a little proportion of HBP-Allyl and TMP to the formulation increased the T_g of the thermoset, a further addition leads to a reduction of the temperature of the maximum of *tan* δ. Thus, it seems that there is a compromise between the multifunctionality of the initially generated thioether network and the proportion of flexible structures of the modifiers added which rends a maximum T_g value and a more homogeneous material for the 5%-HBP-Allyl formulation. The greater area of the *tan* δ curve for the thermoset obtained from 15% HBP-Allyl formulation is indicative of greater damping capability, which seems to increase with the proportion of HBP-Allyl in the modified formulations.

The thermal stability was studied by means of thermogravimetric analysis in air atmosphere. The curves obtained are shown in Figure 7 and the main parameters are collected in Table 2.

The addition of HBP-Allyl and TMP to the formulation leads to an increase in the initial degradation temperature (taken as T5%). As in the tan δ evolution, a further increase of the amount of modifier in the formulation leads to a reduction in this parameter, but the thermal stability of the 15% HBP-Allyl thermoset is higher than the neat material. The addition of a

hyperbranched aromatic polyester structure reduces the proportion of degradable aliphatic ester groups, coming from the CE resin, in the material. There are not great differences in the temperature of maximum degradation rate but the final pyrolysis stage are slightly delayed in the modified formulations.

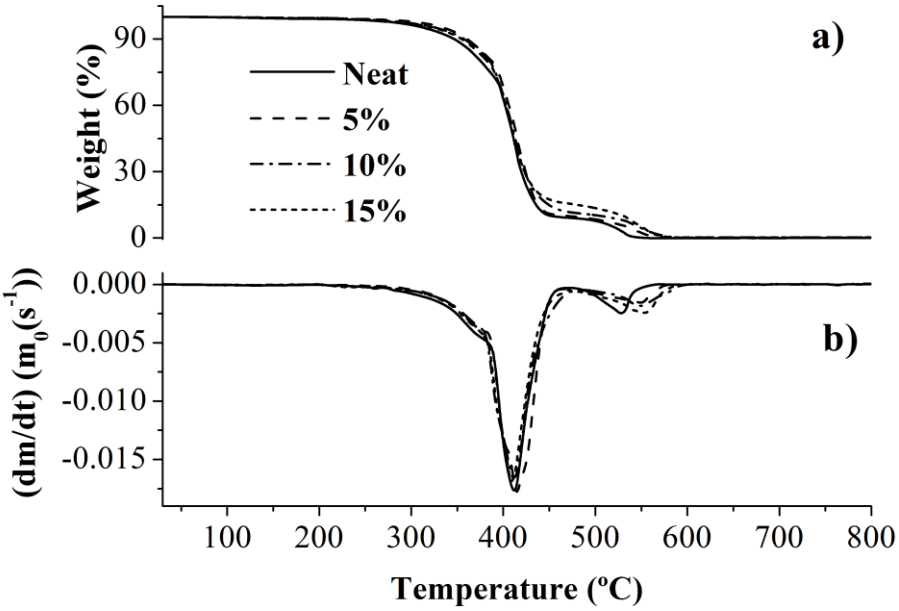

Figure 7. TGA (a) and DTG (b) curves at 10 ºC/min under air atmosphere of the materials obtained.

The materials obtained were cryofractured and observed by electron microscopy to test the type of fracture and to see if some phase separation can be observed. Figure 8 collects some micrographs for all the materials prepared.

The films obtained from the neat formulation show a more fragile fracture than the HBP-Allyl 10 and 15%, which have more deviated cracks and river line structures, which accounts for a higher toughness. The appearance of the fracture surface of the material obtained from HBP-Allyl 5% is much different and a small roughness can be observed. Some spherical particles can be detected in the surfaces of the modified materials but with any regular distribution of size and position, although most of them are in the nanometric size. It is not possible to relate the proportion of HBP-Allyl in the formulation with size or quantity of these separated particles.

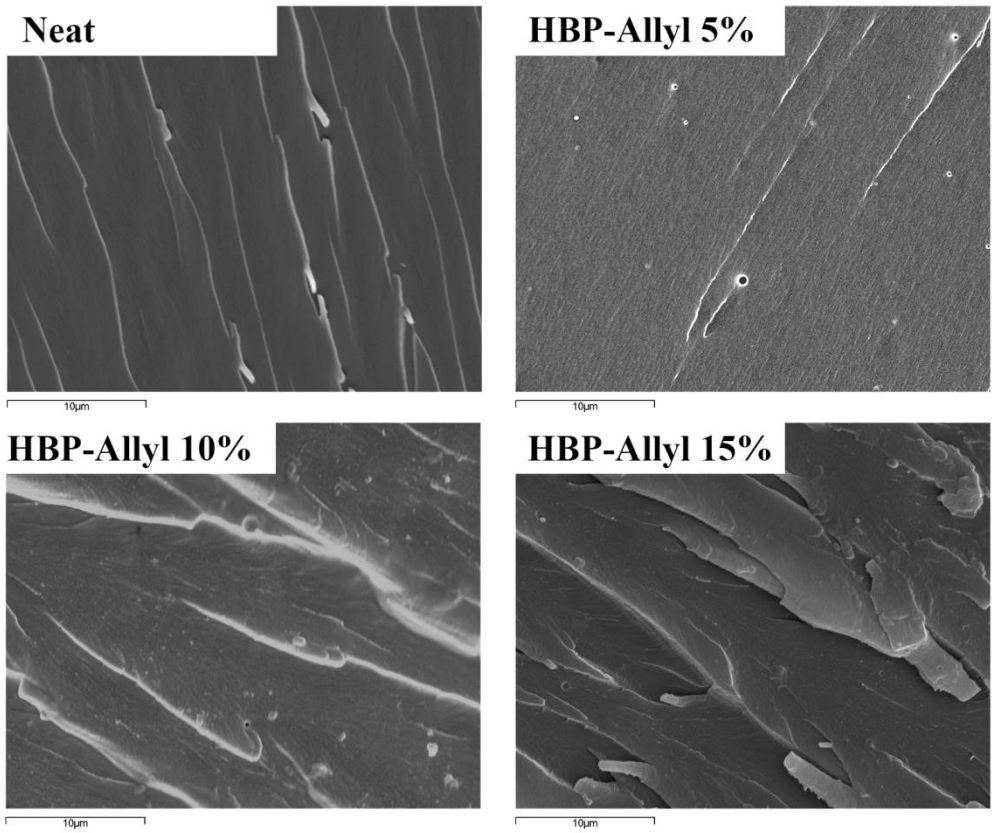

Figure 8. SEM micrographs at 2000 magnifications of the cryofracture surface of the materials obtained from neat, 5% HBP-Allyl, 10% HBP-Allyl and 15% HBP-Allyl formulations.

Conclusions

A new two-stage photoinitiated-thermal dual curing system for a cycloaliphatic epoxy resin has been obtained by the addition of allyl modifed hyperbranched polyester and a trithiol compound to the formulation. This system showed a high latent thermal character.

The first photocuring step included a thiol-ene process and the formation of sulfonium moieties that hindered the homopolymerization reaction of epoxides. These sulfonium salts formed in the primary network were able to activate the epoxy curing at temperatures higher than 100 ºC for the formulations containing 10 and 15% HBP-Allyl, which present a higher proportion of thiol-ene precursors.

The materials obtained showed high T_gs, depending on the content of HBP-Allyl in the formulation, and had slightly higher thermal stabilities than the neat material. By DMTA it was revealed an inhomogeneous structure of the thermosets for 10 and 15% HBP-Allyl formulations, coming from the simultaneous occurrence of different reactive processes. SEM micrographs in all the modified materials showed the existence of small sized particles, without any regular size and position distribution.

Acknowledgements

The authors would like to thank MINECO (MAT2011-27039-C03-01, MAT2011-27039-C03-02) and Generalitat de Catalunya (2009-SGR-1512) for giving financial support. M.F. acknowledges the grant FPI-2009 from the Spanish Government and A.T. the grant FI-DGR 2010 from the Generalitat de Catalunya. X.F-F thanks MINECO for the contract JCI-2010-06187.

References

[1] Kolb HC, Finn MG, Sharpless KB. Click Chemistry: Diverse Chemical Function from a Few Good Reactions. Angew. Chem. Int. Ed. 2001, 40, 2004–2021.

[2] Thomsen AD, Malmstrom E, Hvilsted S. Novel polymers with a high carboxylic acid loading. J. Polym. Sci. Part A: Polym. Chem. 2006, 44, 6360–6377.

[3] Chernykh A, Agag T, Ishida H. Synthesis of linear polymers containing benzoxazine moieties in the main chain with high molecular design versatility via click reaction. Polymer 2009, 50, 382–390.

[4] Beyazkilic Z, Kahveci MU, Aydogan B, Kiskan B, Yagci Y. Synthesis of polybenzoxazine precursors using thiols: simultaneous thiol–ene and ring-opening reactions. J. Polym. Sci. Part A: Polym. Chem. 2012, 50, 4029–4036.

[5] Griesser T, Wolfberger A, Daschiel U, Schmidt V, Fian A, Jerrar A, Teichert C, Kern W. Cross-linking of ROMP derived polymers using the two-photon induced thiol-ene reaction: towards the fabrication of 3D-polymer microstructures. Polym. Chem. 2013, 4, 1708-1714.

[6] Bednarek M. Application of cationic polymerization by activated monomer mechanism and click reactions for the synthesis of functionalized polylactide. Polimery 2012, 57, 501-509.

[7] Liu H, Li S, Zhang M, Shao W, Zhao Y. Facile synthesis of ABCDE-type H-shaped quinto polymers by combination of ATRP, ROP, and click chemistry and their potential applications as drug carriers. J. Polym. Sci. Part A: Polym. Chem. 2012, 50, 4705–4716.

[8] Lutz JF, Schlaad H. Modular chemical tools for advanced macromolecular engineering. Polymer 2008, 49, 817-824.

[9] Foix D, Ramis X, Serra A, Sangermano M. UV generation of a multifunctional hyperbranched thermal crosslinker to cure epoxy resins. Polymer 2011, 52, 3269-3276.

[10] Killops KL, Campos ML, Hawker CJ. Robust, efficient, and orthogonal synthesis of dendrimers via thiol-ene “click” chemistry. J Am Chem Soc 2008, 130, 5062-5064.

[11] Crivello JV. Ring-Opening Polymerization, Mechanisms, Catalysis, Structure and Utility; Brunelle DJ, editor. Munich: Hanser Publishers; 1993; Chapter 5, p. 157.

[12] Boogh L, Pettersson B, Månson J-A E. Dendritic hyperbranched polymers as toughеners for epoxy resins. Polymer 1999, 40, 2249-2261.

[13] Xu G, Shi W, Gong M, Yu F, Feng J. Curing behavior and toughening performance of epoxy resins containing hyperbranched polyester. Polym. Adv. Technol. 2004, 15, 639-644.

[14] Sangermano M, Priola A, Malucelli G, Bongiovanni R, Quaglia A, Voit B, Ziemer A. Phenolic hyperbranched polymers as additives in cationic photopolymerization of epoxy systems. Macromol. Mater. Eng. 2004, 289, 442-446.

[15] Moore JS, Stupp SI. Room temperature polyesterification. Macromolecules 1990, 23, 65-70.

[16] Schallausky F, Erber M, Komber H, Lederer A. An easy strategy for the synthesis of well-defined aliphatic-aromatic hyperbranched polyesters. Macromol. Chem. Phys. 2008, 209, 2331-2338.

[17] Schmaljohann D, Komber H, Voit B. Conversion dependence of the structural units and the degree of branching of a hyperbranched polyester based on 4,4-bis-(4′-hydroxyphenyl) pentanoic acid determined by NMR spectroscopy. Acta Polymerica 1999, 50, 196-204.

[18] Tomuta AM, Ferrando F, Serra A, Ramis X. New aromatic–aliphatic hyperbranched polyesters with vinylic end groups of different length as modifiers of epoxy/anhydride thermosets. React. Funct. Polym. 2012, 72, 556-563.

[19] Fernández X, Salla JM, Serra A, Mantecón A, Ramis X. Cationic copolymerization of cycloaliphatic epoxy resin with a spirobislactone with lanthanum triflate as initiator: I. Characterization and shrinkage. J. Polym. Sci Part A: Polym. Chem. 2005, 43, 3421-3432.

[20] Fernández-Francos X, Salla JM, Cadenato A, Morancho JM, Mantecón A, Serra A, Ramis X. Influence of the initiating mechanism on the cationic photopolymerization of a cycloaliphatic epoxy resin with arylsulphonium salts. J. Polym Sci Part A: Polym. Chem. 2007, 45, 16-25.

[21] Flores M, Fernández-Francos X, Ramis X, Serra A. Novel epoxy-anhydride thermosets modified with a hyperbranched polyester as toughness enhancer. I. Kinetics study. Thermochim Acta 2012, 544, 17-26.

[22] Sangermano M, Colucci G, Fragale M, Rizza G. Hybrid organic–inorganic coatings based on thiol-ene systems. React. Funct. Polym. 2009, 69, 719–723.

[23] Fu Q, Liu J, Shi W. Preparation and photopolymerization behavior of multifunctional thiol–ene systems based on hyperbranched aliphatic polyesters. Prog. Org. Coat. 2008, 63, 100–109.

[24] Trey SM, Nilsson C, Malmström E, Johansson M. Thiol–ene networks and reactive surfaces via photoinduced polymerization of allyl ether functional hyperbranched polymers. Prog. Org. Coat. 2010, 67, 348-355.

[25] Sangermano M, Cerrone M, Colucci G, Roppolo G, Acosta Ortiz R. Preparation and characterization of hybrid thiol-ene/epoxy UV–thermal dual-cured systems. Polym. Int. 2010, 59, 1046–1051.

[26] Carioscia JA, Stansbury JW, Bowman, CN. Evaluation and control of thiol-ene/thiol-epoxy hybrid networks. Polymer 2007, 48, 1526-1532.

[27] Acosta Ortiz R, Puente Urbina BA, Cabello Valdez LV, Berlanga Duarte L, Guerrero Santos R, Garcia Valdez AE, Soucek MD. Effect of introducing a cationic system into a thiol-ene photopolymerizable formulation. J. Polym. Sci. Part A: Polym. Chem. 2007, 45, 4829-4843.

[28] Falk B, Zonca MR, Crivello JV. Modification of photoinitiated cationic epoxide polymerizations by sulfides. J. Polym. Sci. Part A: Polym. Chem. 2005, 43, 2504–2519.

[29] Van Assche G, Swier S, Van Mele B. Modeling and experimental verification of the kinetics of reacting polymer systems. Thermochim. Acta 2002, 388, 327–341.

[30] Fernández-Francos X, Ramis X, Salla JM. Cationic copolymerization of cycloaliphatic epoxy resin with an spirobislactone with lanthanum triflate as initiator. Kinetics of the curing process. Thermochim. Acta 2005, 438, 144-154.

Conclusions

As it was demonstrated along this thesis, not only the selection of the curing agent and curing conditions but also the addition of dendritic polymers as modifiers allows to tuning the properties of epoxy resin based thermosets. Below are described the most important conclusions extracted from this thesis.

1. The copolymerization of mixtures of DGEBA and toluene-2,4-diisocyanate catalysed by tertiary amines yielded materials with oxazolidone, isocyanurate and ether groups in the network structure. The initial composition of the mixtures, the temperature of curing and the catalyst used were the main parameters that defined the final properties of the thermosets. The increase in the initial proportion of isocyanate and the curing at temperatures between 100 and 130 ºC increased the glass transition temperature, the thermal stability and the shrinkage by the amount of isocyanurate ring formed, which was the factor that controlled the gelation. Higher curing temperatures favoured the formation of oxazolidone groups in the network, which increased the thermal stability.

2. Networks containing oxazolidone, isocyanurate, urethane, allophanate and ether groups were prepared by using ytterbium triflate as acidic catalyst of DGEBA and toluene-2,4-diisocyanate mixtures. The use of ytterbium triflate instead of a common tertiary amine strongly increased the pot-life and promoted the formation of urethane and allophanate groups.

3. In the curing of DGEBA/toluene-2,4-diisocyanate mixtures catalysed by benzyl dimethylamine with modified Boltorn H30, the characteristics of the terminal groups of the hyperbranched polymer played an important role. Whereas the addition of epoxidated Boltorn H30 yielded homogeneous materials with high crosslinking density and brittle behaviour, vinyl terminated Boltorn H30 led to phase separated morphologies with tough fracture.

4. Boltorn H30 hyperbranched polyesters modified in different extent with 10-undecenoyl moieties were obtained by a simple acylation procedure. The addition of these modifiers to DGEBA/methyl hexahydrophthalic anhydride formulations in the presence of a tertiary amine as a catalyst allowed to generate phase separated morphologies with a great enhancement on the impact resistance of the obtained thermosets without sacrificing thermal stability, thermomechanical characteristics and processability. The highest toughness enhancement (more than four-fold) was reached by increasing the degree of modification of the H30 up to a 76% but maintaining the presence of reactive hydroxyl groups in the HBP structure to ensure a high interaction between the particles and the matrix. The curing kinetics of these formulations was controlled by the amount of unmodified reactive hydroxyl groups and by the changes in viscosity and mobility that arises from the different degrees of modification.

5. Hyperbranched poly(glycidol) was successfully synthesized and the final hydroxyl groups were partially modified by acylation to obtain hyperbranched polyethers with different proportions of 10-undecenoyl groups as chain ends. The addition of these modifiers to biscycloaliphatic diepoxy resins cured in the presence of ytterbium triflate as cationic initiator produced a notable increase in impact strength of more than 200% with an only 5% in weight of modifier. Furthermore, the thermal stability of the resulting

materials was improved and the glass transition temperature not much decreased. The formation of a well defined morphology consisting of soft rich-modifier microparticles homogeneously distributed within the matrix, with a good compatibility among phases was the responsible of the toughness enhancement.

6. Following a core-first strategy, well-defined multiarm star polyesters were obtained by growing poly(ε-caprolactone) arms from hyperbranched Boltorn type polyesters of different generation number. These multiarm star polymers were added as modifier in the curing of cycloaliphatic epoxy resin using ytterbium triflate as cationic initiator. Although impact strength was not much improved, the effect of molecular weight of the modifier and the thermal reworkable nature of the obtained thermosets were demonstrated. Nevertheless, UV cured materials showed higher thermal stability and toughness enhancement than thermal-cured thermosets, although the proportion of modifiers added were higher in these formulations. All these materials were completely homogeneous.

7. A novel two-stage photoinitiated-thermal dual curing system for cycloaliphatic epoxy resins was obtained by the addition of an allyl terminated aliphatic-aromatic hyperbranched polyester and a trithiol compound to the formulation. During UV irradiation, as consequence of thiol-ene coupling, thioethers moieties were formed. The presence of thioethers in the structure led to the formation of trialkylsulfonium salts that stopped the homopolymerization of epoxy system at room temperature. The sulfonium salts formed in this first stage acted as a latent multifunctional thermal crosslinker being capable of initiating rapid epoxy homopolymerization at temperatures above 100ºC. In general, the modified materials were inhomogeneous with nanometric particles and showed higher glass transition temperature and matrix yielding than the neat material.

List of Abbreviations.

%wt	Weight percentage
α	Degree of conversion
α_{gel}	Conversion at gelation
δ	Chemical shift (ppm) or diphase between tension and deformation
ε	Absorptivity coefficient
ε-CL	ε-Caprolactone
ρ	Density
ρ_0	Density of the uncured formulation
ρ_∞	Density of the fully cured
$\lvert\eta^*\rvert$	Complex viscosity
ΔC_p	Heat capacity jump
Δh_m	Fusion enthalpy
Δh_t	Heat released
Δh_{theor}	Theoretical reaction heat
Δh_{total}	Total reaction heat
A	Absorbance or pre-exponential factor
ACE	Active chain-end mechanism
AM	Monomer activated mechanism
BCDE/CE	3,4-Epoxycyclohexylmethyl-3',4'-epoxycyclohexyl carboxylate
BDMA	*N*, *N*-Benzyldimethylamine
BH30	Boltorn H30
BHMPA	2,2-Bis(hydroxymethyl)propionic acid
C	Concentration

CIPS	Chemical induced phase separation
dα/d*t*	Reaction or conversion rate
DB	Degree of branching
DCC	N,N'-Dicyclohexylcarbodiimide
DGEBA	Diglycidyl ether of bisphenol A
d*h*/d*t*	Heat flow rate
Đ$_M$	Molecular weight dispersity
DMAP	4-(*N*,*N*-dimethylamino)pyridine
DMF	*N*, *N*-dimethylformamide
DMSO	Dimethylsulfoxide
DMTA	Dynamic mechanical thermal analysis
$\overline{DP}$	Degree of polymerization
DPTS	4-(*N*,*N*-dimethylamino)pyridinium p-toluenesulfonate
DSC	Differential scanning calorimetry
E	Energy loss of the pendulum with sample
E'	Storage modulus
E''	Loss modulus
E$_0$	Energy loss of the pendulum without sample
E$_a$	Apparent activation energy
EB	Electron beam
ee	Epoxy equivalent
F	Chain stiffness
FE-SEM	Field emission scanning electron microscopy
FTIR-ATR	Fourier transformed- infrared spectroscopy - Attenuated total reflectance

$g(\alpha)$	Integral conversion function
$H30_{epo}$	Epoxidated Boltorn H30
$H30_{vin}$	Vinylic Boltorn H30
HBP	Hyperbranched polymer
HKN	Hardness Knoop Number
HX-PCL	Multiarm star based on Boltorn core (X can be 20, 30 or 40) and poly(ε-caprolactone) arms
I	Intensity or optical length
IS	Impact strength
k	Rate constant
KAS	Kissinger-Akahira-Sunose
L	Optical pathway
MCPBA	m-Chloroperbenzoic acid
MHHPA	Methylhexahydrophtalic anhydride
MI	1-Methyl imidazole
$\overline{M_n}$	Number average molecular weight
$\overline{M_w}$	Weight average molecular weigh
n	Average crosslinking density
NMR	Nuclear magnetic resonance
PCL	Poly(ε-caprolactone)
PEG	Poly(ethylene glycol)
PEO-b-PS	Poly(ethylene oxide)-b-poly(styrene)
PGOH	Hyperbranched poly(glycidol)
phr	Parts per hundred of resin

PI	Photoinitiator
R	Gas constant
RIMPS	Reaction induced microphase separation
RIPS	Reaction induced phase separation
ROMP	Ring-opening metathesis polymerization
ROP	Ring-opening polymerization
S	Cross-section
SANTONOX	5-tert-Butyl-4-hydroxy-2-methylphenyl sulphide
SEM	Scanning electron microscopy
$Sn(Oct)_2$	Tin (II) 2-ethylhexanoate
T	Temperature
tan δ	Loss tangent
TDI	Toluene -2,4-diisocyanate
TEA	Triethylamine
TEC	Thermal expansion coefficient
TEM	Transmission electron microscopy
T_g	Glass transition temperature
TGA	Thermogravimetric analysis
THF	Tetrahydrofurane
T_m	Melting temperature
TMA	Thermal mechanical analysis
T_{max}	Temperature of the maximum degradation rate
TMP	Trimethylolpropane tris-(3-mercaptopropionate)
TMS	Tetramethylsilane
T_p	Temperature of the peak of the curing exotherm

UV	Ultraviolet
Vs	Volume of the sample
w	Weight
X_{eq}	Equivalent ratio
X_c	Crystallinity
Yb(OTf)$_3$	Ytterbium triflate

List of Publications.

Patents

Flores Guillén, Marjorie; Fernández Francos, Xavier; Mantecón Arranz, Ana; Salla Tarragó, Josep María; Ramis Juan, Xavier; Serra Albet, Maria dels Àngels. "Composicion y procedimiento para el entrecruzamiento de una resina epoxi con un isocianato, y material entrecruzado obtenido". *Spain Pat.,* ES2373276, 2012. Se ha presentado mediante el procedimiento PCT con el número W02012010732 A1 el 11/Julio/2011.

Publications from the thesis

Marjorie Flores, Xavier Fernández–Francos, Josep M. Morancho, Àngels Serra, Xavier Ramis. "Curing and characterization of oxazolidone-isocyanurate-ether networks". *Journal of Applied Polymer Science*, **2012**, 125, 2779.

Marjorie Flores, Xavier Fernández-Francos, Josep M. Morancho, Àngels Serra, Xavier Ramis. "Ytterbium triflate as a new catalyst on the curing of epoxy-isocyanate based thermosets". *Thermochimica Acta*, **2012**, 543, 188.

Marjorie Flores, Xavier Fernández-Francos, Emilio Jiménez Piqué, David Foix, Àngels Serra, Xavier Ramis. "New epoxy thermosets obtained from diglycidylether of bisphenol A and Modified hyperbranched polyesters with long aliphatic chains cured by diisocyanates". *Polymer Engineering and Science,* **2012**, 52, 2597.

Marjorie Flores, Xavier Fernández-Francos, Xavier Ramis, Àngels Serra. "Novel epoxy-anhydride thermosets modified with a hyperbranched polyester as toughness enhancer. I. Kinetics study". *Thermochimica Acta*. **2012**, 544, 17.

Marjorie Flores, Xavier Fernández-Francos, Francesc Ferrando, Xavier Ramis, Àngels Serra. "Efficient impact resistance improvement of epoxy/anhydride thermosets by adding hyperbranched polyesters partially modified with undecenoyl chains". *Polymer,* **2012**, 53, 5232.

Marjorie Flores, Mireia Morell, Xavier Fernández-Francos, Francesc Ferrando, Xavier Ramis, Àngels Serra. "Enhancement of the impact strength of cationically cured cycloaliphatic diepoxide by adding hyperbranched poly(glycidol) partially modified with 10-undecenoyl chains". *European Polymer Journal*, **2013**, 49, 1610.

Marjorie Flores, Xavier Fernández-Francos, Xavier Ramis, Francesc Ferrando, Àngels Serra. "Effect of molecular weight of polyesters with multiarm star topology used as additives in cycloaliphatic epoxy thermosets cured by ytterbium triflate". *Journal of Polymer Research* **2013**, Submitted.

Marjorie Flores, Xavier Fernández-Francos, Xavier Ramis, Marco Sangermano, Francesc Ferrando, Àngels Serra. "Photocuring of Cycloaliphatic Epoxy Formulations using Polyesters with Mutiarm Star Topology as Additives *Journal of Applied Polymer Science*, **2013**, Submitted.

Marjorie Flores, Adrian M. Tomuta, Xavier Fernández-Francos, Xavier Ramis, Marco Sangermano, Àngels Serra. "A new two-stage curing system: thiol-ene/epoxy homopolymerization using an allyl terminated hyperbranched polyester as reactive modifier". *Polymer*, **2013**, under revision.

Collaborations in other publications

Josep M. Morancho, Ana Cadenato, Xavier Ramis, Xavier Fernández-Francos, **Marjorie Flores**, Josep M. Salla, Effect of a Hyperbranched polymer over the thermal curing and the photocuring of an epoxy resin. *Journal of Thermal Analysis and Calorimetry.* **2011**, 105, 479.

Marjorie Flores, David Foix, Angels Serra, Xavier Ramis, Marco Sangermano. "A versatile thiol-ene/sol-gel two-stage curing process based on a hyperbranched polyester with different degrees of 10-undecenoyl modification". Macromolecular Materials and Engineering. In press.

Stages and Meeting Contributions.

Meeting Contributions

Marjorie Flores, Àngels Serra, José M. Salla, José M. Morancho, Xavier Fernández-Francos, Xavier Ramis. "New thermosets based on oxazolidone-isocyanurate-ether polymers and hydroxylated hyperbranched polymers modified with vinyl and epoxy end groups" Macro 2010, 43rd IUPAC World Polymer Congress. Glasgow, UK, July 2010. Poster Presentation.

Marjorie Flores, Xavier Fernández-Francos, José M. Salla, Ana Mantecón, Àngels Serra, Emilio Jiménez-Piqué, Xavier Ramis. "Study of rare earth metal triflates as new catalyst for the formation of Oxazolidone-Isocyanurate-Ether networks from DGEBA and Toluene-2,4-diisocyanate" European Polymer Congress (EPF). Granada, España, June 2011. Poster Presentation.

Marjorie Flores, Xavier Fernández-Francos, Francesc Ferrando, Àngels Serra, Xavier Ramis. "Efecto de la adición de poliesteres hiperramificados con distintas relaciones hidoxilo/undecenoilo terminales en la obtención de termoestables epoxi/anhídrido" VI Congreso de Jóvenes Investigadores en Polímeros. Huelva, España, Abril 2012. Presentación Oral.

Àngels Serra, **Marjorie Flores**, David Foix, Xavier Ramis, Francesc Ferrando, Xavier Fernández Francos. "New epoxy thermosets with improved toughness by adding hyperbranched polymer modifiers" 7th International Conference on Nanostructured Polymers and Nanocomposites. Prague, Czech Republic, April 2012. Oral Presentation.

Marjorie Flores, Àngels Serra, Xavier Ramis, Marco Sangermano, David Foix. "New hybrid materials containing in situ generated silica particles based on thiol-ene crosslinking using hyperbranched polymers as macromonomers" Third International Symposium: Frontiers in Polymer Science. Sitges, Spain, May 2013. Poster Presentation.

Marjorie Flores, Mireia Morell, Xavier Fernández-Francos, Francesc Ferrando, Xavier Ramis, Àngels Serra. "Enhancement of the impact strength of cationically cured cycloaliphatic diepoxide by adding hyperbranched polyglycidol partially modified with undecenoyl chains" Third International Symposium: Frontiers in Polymer Science. Sitges, Spain, May 2013. Poster Presentation.

Stay Abroad

Organization: Politecnico di Torino

Department: Material Science and Chemical Engineering (Dr. Sangermano)

City:	Turin	**Country:**	Italy
Length:	4 months	**Year:**	2012